

THE INTERPLAY BETWEEN MDM2 AND PSMA IN MET- ASTATIC BREAST CANCER CELLS

by

Robyn Bradbury

Cardiff-China Medical Research Collaborative

Cardiff University School of Medicine

Cardiff

December 2016

Thesis submitted to Cardiff University for the degree of Doctor of Philosophy

Acknowledgements

Firstly, I would like to express my sincere gratitude to my supervisors, Professor Wen Jiang and Doctor Yuxin Cui for their continued support and guidance through my Ph.D. study.

Besides this, I would like to thank Miss Fiona Ruge, Doctor Nicola Jordan, Doctor Andrew Sanders and Doctor Tracey Martin, for their help and patience through the good and bad times. Also, thanks to my mum, who always listened, no matter what the hour or subject.

Finally, I want to thank my fellow PhD students, without whom I could never have completed this mammoth task, who have shared the frustrations, the sleepless nights and, of course, the laughter. David Yi Feng, Bethan Frugtniet, Jeyna Resaul, Bruno Bastos, Sarah Koushyar, Emily Telford, Ben Lanning, Ross Collins and Valentina Flamini, I could not have done it without you and I will be forever grateful for your friendship and encouragement.

This thesis is dedicated to my dad, Wayne Bradbury. Who can't be here to see this but for whom this was always for.

Summary

Both mouse double minute (MDM2) and prostate-specific membrane antigen (PSMA) are known to be associated with the progressive properties of cancer. Moreover, overexpression of both molecules has been implicated in an increase in the proliferation, migration and invasion of tumour cells.

MDM2 is a negative regulator of tumour suppressor of p53 but also is known to play multiple p53-independent roles in many cancer types. PSMA was originally thought to be solely expressed in prostate tissues and overexpression prostatic cancers; however, recently its expression was reported in various other solid tumours, including those of the breast.

Our work showed a possible link between these proteins following knockdown of each molecule in breast cancer cell lines, ZR-75.1 and MDA-MB-231, with targeted siRNA molecules. A decrease of MDM2 and PSMA led to a decrease in the proliferative, adhesive, migratory and invasive capacities of the cell lines.

Additionally, knockdown of MDM2 and PSMA led to similar changes in secretion of matrix metalloproteinases (MMPs), with decreases in MMP2 and MMP8 being seen from both breast cell lines investigated.

It was then seen that a link between the two protein could be mediated through the phosphorylation status of serine 473 on protein kinase B (AKT). PSMA knockdown in both breast cancer cell lines led to a decrease of AKT phosphorylation and thus a decrease in MDM2 serine 188. Additionally, it was found that MDM2 siRNA leads to an increase in c-JUN serine 63 phosphorylation, and that PSMA siRNA can lead to an increase at the same site, depending on the cell line.

These results indicate that MDM2, AKT and PSMA may represent a new pathway which could be targeted for therapy for breast tumours and perhaps other types of cancer.

Publications

Bradbury R, Jiang WG and Cui YX (2015). The clinical and therapeutic uses of MDM2 and PSMA and their potential interaction in aggressive cancers. *Biomarkers in Medicine*. 9(12), 1353-70.

Bradbury R & Cui YX (2015). The interplay between mouse double minute 2 (MDM2) and prostate-specific membrane antigen (PSMA) in the progressive properties of breast cancer. *European Journal of Cancer* (published conference abstract).

Bradbury R, Jiang WG & Cui YX (2015). Impeding outgrowth of cancer cells by interfering with the interplay between PSMA and MDM2. *Anticancer Research* (published conference abstract).

Bradbury R, Jiang WG & Cui YX (2016). MDM2 and PSMA play inhibitory roles in metastatic breast cancer cells through regulation of matrix metalloproteinases. *Anticancer Research*. 36(3), 1143-51.

Interplay of MDM2 and PSMA modulates the secretion of the MMPs through AKT phosphorylation in breast cancer cells (submitted conference abstract for ECCO 2017).

Contents

	Page
Chapter I: General Introduction	1
1.1. The breast	2
i. Development of the breast	2
ii. Breast anatomy	3
1.2. Breast cancer	5
i. Pathology and prognostic indicators	7
ii. Hereditary breast cancer	8
iii. Molecular subtypes	9
iv. Treatment	12
1.3. Progressive properties of solid tumours	14
i. Sustaining proliferative signalling	14
ii. Evading growth suppressors	16
iii. Evading apoptosis	17
iv. Enabling replicative immortality	18
v. Inducing angiogenesis	19
vi. Activating invasion and metastasis	21
vii. Enabling characteristics	23
viii. Emerging hallmarks	23
1.4. Mouse double minute 2 (MDM2)	24
i. Clinical relevance of MDM2	24
ii. MDM2 in breast cancer	29
iii. MDM2 as a therapeutic target	30
iv. MDM2 involvement in tumour-associated angiogenesis	36
v. Participation of MDM2 in tumour invasion and metastasis	43
1.5. Prostate-specific membrane antigen (PSMA)	45
i. Clinical relevance of PSMA	45

ii.	PSMA in breast cancer	48
iii.	PSMA as a biomarker for cancer	49
iv.	PSMA as a therapeutic target	53
v.	PSMA involvement in tumour-associated angiogenesis	56
vi.	PSMA involvement in tumour-associated invasion and metastasis	61
1.6.	The matrix metalloproteinases (MMPs)	63
i.	The extracellular matrix	63
ii.	Role of the MMPs	65
iii.	MMPs and cancer	72
1.7.	Protein kinase B (AKT)	76
i.	The role of the PI3K/AKT/mTOR pathway in the cell	76
ii.	The dysregulation of AKT in cancer	77
iii.	Possible links of AKT to MDM2 and PSMA	79
1.8.	The possible interplay between MDM2 and PSMA in cancer	82
1.9.	Aims & objectives	83
	Chapter II: Materials and Methods	85
2.1.	Materials	86
2.1.1.	Cell lines	86
2.1.2.	Collection of human breast cancer tissues	88
2.1.3.	siRNA	88
2.1.4.	Primers	88
2.1.5.	Antibodies	89
2.1.6.	Inhibitors	89
2.2.	Standard reagents and solution	94
2.2.1.	Solutions for use in laboratory	94
2.2.2.	Solutions for use in cell culture	94
2.2.3.	Solutions for use in western blotting	94
2.2.4.	Solutions for use in immunocytochemical staining	96
2.2.5.	Solutions for use in flow cytometric staining	96

2.3. Cell culture, maintenance, storage and transfection	98
2.3.1. Cell maintenance	98
2.3.2. Trypsinisation (detachment of adherent cells and cell counting)	98
2.3.3. Storing cells	99
2.3.4. Resuscitation of cells	99
2.3.5. Transfection of cells with siRNA	99
2.4. Methods for RNA detection	101
2.4.1. RNA isolation	101
2.4.2. Reverse transcription (RT)	102
2.4.3. Quantitative polymerase chain reaction (qPCR)	102
2.5. Methods for protein detection	105
2.5.1. Western blotting	106
2.5.2. Immunocytochemistry	111
2.5.3. Flow cytometric assessment of protein levels	112
2.5.4. RayBio® C-Series human matrix metalloproteinase antibody array C1	115
2.5.5. Enzyme-linked immunosorbent assay (ELISA)	118
2.6. <i>in vitro</i> cell function assays	121
2.6.1. AlamarBlue® cell proliferation assay	121
2.6.2. Tumour-endothelium adhesion assay	121
2.6.3. Transwell migration assay	122
2.6.4. Transwell invasion assay	123
2.6.5. Wound healing (scratch) assay	123
2.6.6. Cell cycle assay	124
2.6.7. Apoptosis assay	124
2.7. Statistical analysis	126
Chapter III: Knockdown of MDM2 and PSMA in breast cancer cell lines and assessment of transcript levels in a breast cancer cohort	127
3.1. Introduction	128
3.2. Materials and methods	130
3.3. Results	133

3.4. Discussion	151
Chapter IV: Knockdown of MDM2 and PSMA in breast cancer cell lines leads to a decrease in proliferative abilities and altered apoptotic ability and cell cycle progression	163
4.1. Introduction	164
4.2. Materials and methods	168
4.3. Results	171
4.4. Discussion	185
Chapter V: Knockdown of MDM2 and PSMA in breast cancer cell lines leads to a decrease in their migratory and invasive capacity	195
5.1. Introduction	196
5.2. Materials and methods	198
5.3. Results	203
5.4. Discussion	229
Chapter VI: Knockdown of MDM2 and PSMA in breast cancer cell lines leads to changes in AKT and c-JUN phosphorylation levels	237
6.1. Introduction	238
6.2. Materials and methods	240
6.3. Results	243
6.4. Discussion	255
Chapter VII: Final Discussion	265
Reference List	275

List of Figures

Figure	Page
1.1. The anatomy of the breast.	4
1.2. Incidence and mortality of breast cancer from 1993 and 2012.	6
1.3. Progressive properties of cancer.	15
1.4. Schematic illustration of mouse double minute 2 (MDM2) structure.	27
1.5. Schematic illustration of prostate-specific membrane antigen (PSMA) structure.	46
2.1. Diagram indicating the principle of how Ampifluor Uniprimer Universal system works during qPCR.	105
2.2. Flow cytometric analysis strategy of protein expression in cell lines	117
3.1. Breast cancer cell line gene expression levels.	134
3.2. Knockdown of MDM2 in MDA-MB-231 cell line.	136
3.3. Knockdown of MDM2 in ZR-75.1 cell line.	138
3.4. Knockdown of PSMA in MDA-MB-231 cell line.	140
3.5. Knockdown of PSMA in ZR-75.1 cell line.	141
3.6. Resultant expression of <i>PSMA</i> transcript following 48 hours of MDM2 siRNA treatment in MDA-MB-231 and ZR-75.1, and <i>vice versa</i> .	143
3.7. 48 hour dual siRNA treatment in MDA-MB-231 and ZR-75.1.	144
3.8. <i>MDM2</i> transcript expression levels in breast tissue.	146
3.9. Survival analysis of breast cancer patients with low	

	or high <i>MDM2</i> transcript expression.	148
3.10	<i>PSMA</i> transcript expression levels in breast tissue.	149
3.11	Survival analysis of breast cancer patients with low or high <i>PSMA</i> transcript expression.	150
4.1.	Proliferation ability of MDA-MB-231 and ZR-75.1 breast cancer cells following 72 hours of MDM2 or <i>PSMA</i> siRNA treatment.	172
4.1.1.	Zoomed in 72 hour cell images Figure 4.1c and d.	173
4.2.	The effect of 72 hours of MDM2 and <i>PSMA</i> siRNA on MDA-MB-231 cell cycle.	175
4.3.	The effect of 72 hours of MDM2 and <i>PSMA</i> siRNA ZR-75.1 cell cycle.	176
4.4	Early and late apoptosis of MDA-MB-231 cells treated with MDM2 and <i>PSMA</i> siRNA.	178
4.5	Early and late apoptosis of ZR-75.1 cells treated with MDM2 and <i>PSMA</i> siRNA.	179
4.6.	Assessment of caspase levels in MDA-MB-231 cells following 72 hours of siRNA treatment and with or without 1.5 hours of staurosporine treatment.	181
4.7.	Assessment of caspase levels in MDA-MB-231 cells following 72 hours of siRNA treatment and with or without 1.5 hours of staurosporine treatment.	183
5.1.	Migration capacity of MDA-MB-231 and ZR-75.1, over a 4 hour period, of siRNA treated cells after 48 and 72 hours of treatment.	204
5.2.	Scratch wound healing assay of siRNA-treated MDA-MB-231 and ZR-75.1 cells.	206
5.3.	Invasion capacity of MDA-MB-231 and ZR-75.1, over a 4 hour period, of siRNA treated cells after 48 and 72 hours of treatment.	208
5.4.	Adhesion capability of MDA-MB-231 and ZR-75.1 cells to an endothelial cell monolayer.	210
5.5.	MDM2 (serine 166) phosphorylation following MDM2 siRNA treatment.	211

5.6.	Gene expression of matrix metalloproteinase (MMPs) and tissue inhibitors of MMPs (TIMPs) in MDA-MB-231 and ZR-751.	215
5.7.	Protein expression of MMPs and TIMPs following siRNA treatment of MDA-MB-231 and ZR-75.1.	216
5.8.	Flow cytometric analysis of MMP2 expression MDA-MB-231.	218
5.9.	Flow cytometric analysis of MMP2 expression in ZR-75.1.	219
5.10.	Flow cytometric analysis of MMP8 expression in MDA-MB-231.	220
5.11.	Flow cytometric analysis of MMP8 expression in ZR-75.1.	221
5.12.	Effect of MMP2 inhibitors on MDA-MB-231 cell proliferation, migration and invasion.	223
5.13.	Effect of MMP2 inhibitors on ZR-75.1 cell proliferation, migration and invasion.	224
5.14.	Effect of MMP8 inhibitor on MDA-MB-231 and ZR-75.1 cell proliferation, migration and invasion.	226
5.15.	Secreted IL-6 and IL-8 levels of MDA-MB-231 and ZR-75.1 following 72 hours of MDM2 or PSMA siRNA treatment, as estimated by ELISA.	227
6.1.	Results of GeneMANIA search with 'MDM2', 'FOLH1/PSMA', 'MMP2' and 'MMP8' outlined as search terms.	244
6.2.	<i>JUN</i> gene and c-JUN protein expression and phosphorylation levels following 72 hours of MDM2 and PSMA siRNA treatment in MDA-MB-231 cells.	245
6.3.	<i>JUN</i> gene and c-JUN protein expression and phosphorylation levels following 72 hours of MDM2 and PSMA siRNA treatment in ZR-75.1 cells.	247
6.4.	AKT gene, protein and phosphorylation levels following 72 hours of MDM2 and PSMA siRNA treatment in MDA-MB-231 cells.	249

6.5.	AKT gene, protein and phosphorylation levels following 72 hours of MDM2 and PSMA siRNA treatment in ZR-75.1 cells.	250
6.6.	Phosphorylation of MDM2 at serines 186 and 188 following 72 hours of MDM2 and PSMA siRNA treatment in MDA-MB-231 and ZR-75.1 cells	253
6.7.	The effect of 50 μ M LY 294002 hydrochloride or LY 303511 on gene levels of MDM2, PSMA and the MMPs in MDA-MB-231 and ZR-75.1 cells.	254
6.8.	Schematic diagram showing the possible interplay between PSMA,	263
7.1.	Hypothesised MDM2 and PSMA interaction through folate metabolism in aggressive tumours.	273
7.2.	Proposed interplay roles of MDM2 and PSMA in tumour invasion and metastasis through multiple signalling pathways.	274

List of Tables

Table		Page
1.1	Common characteristics of molecular subtypes of breast cancer.	10
1.2.	Clinical trials targeting MDM2 for cancer treatment.	35
1.3.	Clinical trials utilising PSMA for cancer imaging and treatment.	57
2.1.	Details of cell lines used in study.	87
2.2.	Primer sequence for all genes assessed through quantitative PCR (qPCR).	89
2.3.	Primary antibodies used in western blotting protocol.	93
2.4.	Components and volumes used in 10% resolving gel.	108
2.5.	Components and volumes used in stacking gel.	108
2.6.	Primary antibodies used in flow cytometric analysis of protein levels.	114

Abbreviations

ADC: antibody drug conjugates
AKT: protein kinase B
ALT: alternative lengthening of telomeres
AP-1: activator protein 1
APS: ammonium Persulphate
AR: androgen receptor
ARF: alternative reading frame
ARK: AMP-activated kinase
ASO: antisense oligonucleotide
BHP: benign hyperplasia prostate
BM: basement membrane
BMI: body mass index
BRCA: breast cancer susceptibility gene
BSA: bovine serum albumin
CAMs: cell-cell adhesion molecules
CAD: C-terminal transactivation domain
CDK: cyclin-dependent kinase
CDS: cell dissociation solution
CT: threshold cycle
DEPC: diethylpyrocarbonate
DHT: dihydrotestosterone
DNA: deoxyribonucleic acid
DMEM: Dulbecco's Modified Eagle's Medium
DMSO: dimethyl sulphoxide
DRE: digital rectal examination

ECM: extracellular matrix

EDTA: ethylenediaminetetraacetic acid

ELISA: enzyme-linked immunosorbent assay

ER: oestrogen receptor

FACs: fluorescent assisted cell-sorting

FAK: focal adhesion kinase

FBS: foetal bovine serum

FGF: fibroblast growth factor

FIH: factor inhibiting HIF1

FISH: fluorescence *in situ* hybridisation

FOLH1: folate hydrolase (another name for PSMA)

GAPDH: glyceraldehyde 3-phosphate dehydrogenase

HER2: human epidermal growth factor receptor

HIF1: hypoxia inducible factor 1

HMVEC: human microvascular endothelial cells

HRP: horse radish peroxidase

HUVEC: human umbilical vein endothelial cells

IDC: invasive ductal carcinoma

IL: interleukin

IGF: insulin growth factor

JNK: c-JUN N-terminal kinase

MDM4/MDMX: mouse double minute 4

MDM2: mouse double minute 2

MEFs: mouse embryonic fibroblasts

MMP: matrix metalloproteinase

miRNA: microRNA

mRNA: messenger RNA

mTOR: mechanistic target of rapamycin

NAAG: N-acetylaspartylglutamic acid
NAALADase: N-acetylated alpha-linked acidic dipeptidase
NES: nuclear export signal
NLS: nuclear localisation signal
NPI: Nottingham prognostic index
NT: non-targeting
OIR: oxygen induced retinopathy
PAGE: polyacrylamide gel electrophoresis
PAK1: p21-activated kinase 1
PBS: phosphate buffer saline
PDK: pyruvate dehydrogenate
PET: positron emission tomography
PI: propidium iodide
PI3K: phosphoinositidine-3-kinase
PIP3: phosphatidylinositol (3,4,5)-triphosphate
PMSF: phenylmethylsulphonyl fluoride
PR: progesterone receptor
PS: phosphatidylserine
PSA: prostate-specific antigen
PSMA: prostate-specific membrane antigen
pTEN: phosphate and tensin homolog
PVDF: polyvinyl fluoride
R²: coefficient of determination
RIPA: radioimmunoprecipitation assay
RING: really interesting new gene
RISC: RNA-induced silencing complex
RFU: relative fluorescent units
RNA: riboxynucleic acid

RPM: revolutions per minute

siRNA: short-interfering RNA

shRNA: short hairpin RNA

SD: standard deviation

SDS: sodium dodecyl sulphate

SERCA: sarcoplasmic/endoplasmic reticulum calcium adenosine triphosphate

STAT3: signal transducer and activator of transcription 3

TBS: tris-buffered saline

TBST: TBS/Tween-20

TCM: tumour conditioned media

TEMED: tetramethylethylenediamine

TGF: transforming growth factor

TIMP: tissue inhibitor of matrix metalloproteinases

TNBC: triple-negative breast cancer

TNF: tumour necrosis factor

TSC: tuberous schlerosis

TSP1: thrombospondin 1

UTR: untranslated region

VEGF: vascular endothelial growth factor

VHL: von Hippel-Lindau

Chapter I

General Introduction

1.1 The breast

i. Development of the breast

Before the onset of puberty, the human breast develops in a similar way in both males and females. However, during puberty in females, the amount of luteinising and follicle-stimulating hormone increase, which causes the ovaries to begin producing oestrogens. The female breasts then begin to develop under the influence of oestrogens and progesterone. Following this, the duct system matures and there is deposition of fat. The onset of ovulation and formation of the corpus luteum then lead to increased levels of oestrogens and progesterone, which results in the further development of the mammary glands and an establishment of the overall breast anatomy.

During each menstrual cycle experienced, the female breasts undergo a proliferative phase, although they do not become fully developed until a pregnancy occurs. During pregnancy, the breast tissue experiences acute proliferative and secretory alterations, with the gradual replacement of the connective and adipose tissue by large, densely packed lobules. During lactation, the alveoli become distended with milk and after pregnancy, when lactation is discontinued, the mammary glands regain their original appearance (Javed and Lteif, 2013, Gusterson and Stein, 2012).

ii. Breast anatomy

The female breast contains adipose tissue embedded with between 15 and 25 lobes. These lobes are radially distributed around the nipple and are interspersed with fibrous septa. The lobes are subdivided into lobules, which are smaller compartments containing alveolar ducts (Figure 1.1a and b). During pregnancy, these ducts develop into a large number of bunches of milk-secreting glands known as alveoli. These alveoli are surrounded by myoepithelial cells and oxytocin-stimulated contractions of these cells aids the transportation of milk towards the nipple (Jesinger, 2014) (Figure 1.1a).

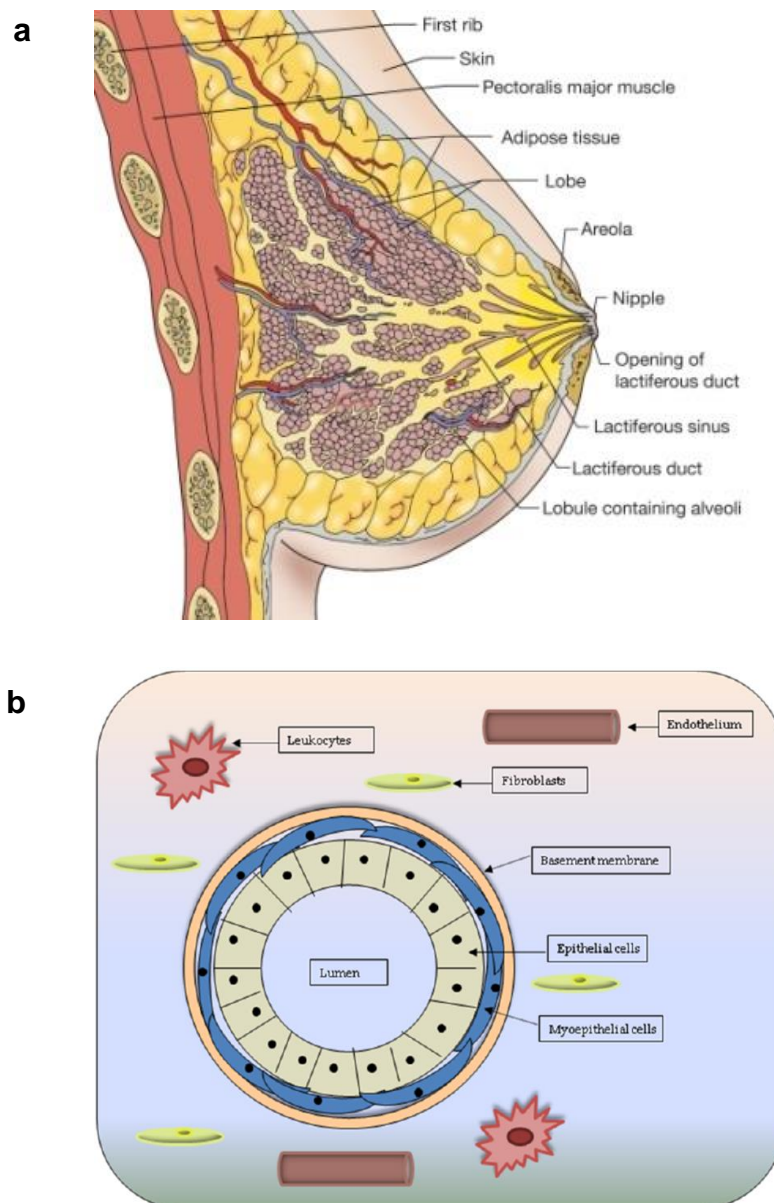


Figure 1.1. The anatomy of the breast. a) Anatomy of the breast, taken from www.aboutcancer.com/breast_anatomy.htm b) Diagram of a normal breast duct and the components of the local microenvironment, taken from Offiah et al., 2011.

1.2. Breast cancer

As the second most common cancer worldwide, breast cancer is the leading cause of cancer-related death in women. Breast cancer exceeds all other cancers in terms of its global burden and has a rising incidence which is extremely high in Northern Europe (Ferlay et al., 2012, Jemal et al., 2011). However, the mortality rates are falling due to earlier diagnosis, as well as improved treatment for those affected by this disease (Figure 1.2). Despite these encouraging improvements, metastasised breast cancer is incurable in many patients (Guth et al., 2009) and is not well understood in terms of molecular drivers and the underlying biological processes (Kimbung et al., 2015).

The complex and heterogeneous nature of breast cancer makes it a fascinating and challenging research field for diagnosis and treatment, with breast cancers representing an array of different disease with both intratumoral and intertumoral genetic and epigenetic mutations (Swanton et al., 2011, Navin et al., 2010).

Alcohol intake (Ellison et al., 2001, Zhang et al., 1999), body mass index (BMI) (Tretli, 1989), hormone replacement therapy (HRT) (Weiss et al., 2002, Nelson et al., 2002), exposure to radiation (Boice et al., 1991, Clemons et al., 2000), early menstruation (Brinton et al., 1988), late menopause (Brinton et al., 1983, Trichopoulos et al., 1972), age of first child birth (Brinton et al., 1983, White, 1987),

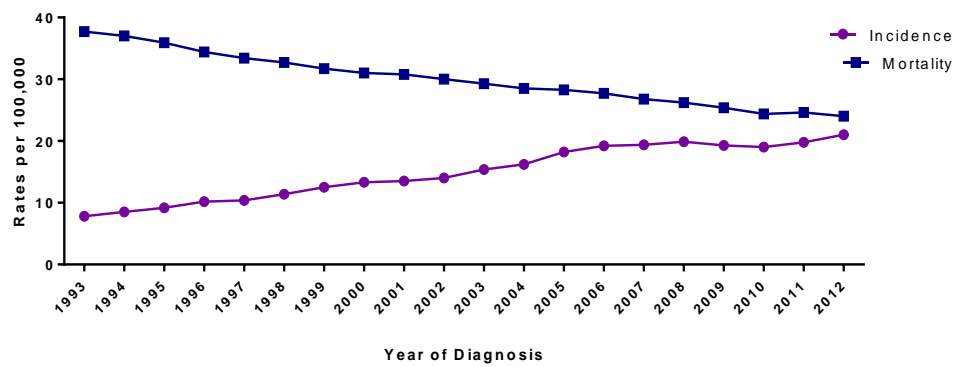


Figure 1.2. Incidence and mortality of breast cancer from 1993 to 2012. Graph is a summarisation of data from Cancer Research UK (www.cancerresearchuk.org), showing the number of incidences and mortalities due to breast cancer over the years 1983-2012.

past history of breast cancer (Page et al., 1982), breast biopsy (Dupont et al., 1993), family history (Pharoah et al., 1997) and germline mutations (Easton et al., 1993), are all known risk factors for the development of breast cancer in females (Singletary, 2003).

i. Pathology and prognostic indicators

Adenocarcinomas are the major type of breast cancer and these originate from the glandular epithelium of the terminal duct lobular unit. Adenocarcinomas are classed as invasive or non-invasive. The term non-invasive refers to cancers which have not penetrated the basement membrane and they are classified as ductal carcinoma *in situ*, lobular carcinoma *in situ* or intraductal papillary carcinoma, with ductal being the most common type. Invasive carcinomas are also designated ductal or lobular, depending on the cell type they resemble. Invasive ductal carcinoma is undeniably the most common form of breast cancer, comprising over three-quarters of cases (Cowell et al., 2013). Besides these common variants, there are more rare or less common breast cancer types; including medullary, mucinous, tubular and metaplastic carcinomas (Yerushalmi et al., 2009).

In order to reach a prognosis, breast cancers are categorised by various classification systems. The most widely applied method is the TNM classification system (Wittekind et al., 2002), which evaluates primary tumour size (T; graded from 1 to 4), the presence of metastasis to the lymph nodes (N; graded from 0 to 3) and distant

metastases occurrence (M; graded as 0 or 1). Another common classification system in use, which is based on histological grade and involves examination of sections using a microscope (Elston and Ellis, 1991). This microscopic analysis involves assessment of mitotic index, nuclear polymorphism and tubule formation. Evaluation of these variables identifies the tumour as being well-differentiated, moderately differentiated or poorly differentiated. The more well-differentiated the cells are the better prognosis for the patient. Finally, Nottingham prognostic index (NPI) can be used to determine the clinical outcome of the patients and whether a patient will benefit from adjuvant therapy. This assessment involves the appraisal of tumour size, lymph node status and histological grade (Albergaria et al., 2011, Hearne et al., 2015).

As well as the use of stage and grade of the breast tumour, expression of oestrogen receptor (ER), progesterone receptor (PR) and human epidermal growth factor receptor (HER2) in the primary tumour is evaluated in order to elect a preferred treatment strategy (Joensuu et al., 2013, Parise and Caggiano, 2014a, Parise and Caggiano, 2014b).

ii. Hereditary breast cancer

Most breast cancers arise sporadically, meaning that patients do not hold a genetic disposition for the disease. However, around 10% of all cases are associated with a family trait (Easton, 2002, Yarden and Papa, 2006). Multiple genetic mutations have been identified to be

responsible for familial breast cancer. The first of these to be detected, and those which are most strongly related to hereditary breast malignancies, were breast cancer susceptibility genes 1 and 2 (BRCA1 and BRCA 2), which give rise to proteins involved in the repair of DNA damage. More recently, more mutations of genes underlying cancer have been found, including p53 and phosphatase and tensin homolog (pTEN) (Easton, 1999a, Easton, 1999b).

iii. Molecular subtypes

Breast cancer is commonly classified into intrinsic molecular subtypes (Table 1.1).

Luminal A

Most breast cancers are luminal tumours and these cells look the most like cells of breast cancers which start in the inner (luminal) cells lining the mammary ducts. Luminal A tumours tend to be ER- and /or PR-positive, HER2-negative and have a tumour grade of 1 or 2. Of the four subtypes of breast cancer, these tumours tend to have the best prognosis, with a high survival rate (Kennecke et al., 2010, Voduc et al., 2010, Falato et al., 2016, Metzger-Filho et al., 2013b). However, recent longer term studies suggest that luminal A breast cancers are more likely to relapse later compared to the other subtypes (Ribelles et al., 2013; Ciriello et al., 2013).

Luminal B

Table 1.1. Common characteristics of molecular subtypes of breast cancer. Table shows the most common profiles for each subtypes. However, not all tumours within the subtype have all of the features listed.

Subtype	Tumour characteristics	Approx. prevalence (%)
Luminal A	<ul style="list-style-type: none"> • ER-positive and/or PR-positive • HER2-negative • Low Ki67 	30-70
Luminal B	<ul style="list-style-type: none"> • ER-positive and/or PR-positive • HER2-positive (or HER2-negative with high Ki67) 	10-20
TNBC/Basal-like	<ul style="list-style-type: none"> • ER-negative • PR-negative • HER-negative 	15-20
HER2 type	<ul style="list-style-type: none"> • ER-negative • PR-negative • HER2-positive 	5-15

Luminal B tumours are another type of luminal tumour. They tend to be ER- and/or PR-positive and highly positive for Ki67, and/or HER2-positive. Patients with luminal B tumours are often diagnosed at a younger age than those with luminal A (Metzger-Filho et al., 2013b, Lund et al., 2010). In comparison to luminal A tumours, luminal B tend to have factors leading to a poorer prognosis: higher tumour grade, larger tumour size and lymph node metastases (Kennecke et al., 2010, Voduc et al., 2010, Metzger-Filho et al., 2013b). However, patients with luminal B tumours have reasonably high survival rates, compared to other subtypes other than luminal A (Falato et al., 2016, Metzger-Filho et al., 2013b).

Triple-negative(TNBC)/basal-like

Triple-negative/basal-like breast cancers are ER-, PR- and HER2-negative. There are several subsets of TNBC. One of these subsets is referred to as basal-like because the tumours have cells with features similar to those of the outer (basal) cells surrounding the mammary ducts. Most basal-like tumours contain p53 gene mutations (Toft and Cryns, 2011).

Most triple-negative breast tumours are basal-like and most basal-like tumours are triple-negative; however, this is not always the case. Around 15-20% of breast cancers are solely triple-negative or basal-like (Fan et al., 2006, Kennecke et al., 2010, Voduc et al., 2010, Falato et al., 2016, Howlader et al., 2014).

Triple-negative/basal-like tumours are often highly aggressive with a poor prognosis compared to the ER-positive subtypes (luminal A and B) (Voduc et al., 2010).

Luminal B tumours are another type of luminal tumour. They tend to be ER- and/or PR-positive and highly positive for Ki67, and/or HER2-positive. Patients with luminal B tumours are often diagnosed at a

HER2 type

These tumours tend to be ER- and PR- negative, lymph node-positive and have a higher tumour grade (Kennecke et al., 2010, Voduc et al., 2010, Falato et al., 2016, Metzger-Filho et al., 2013a).

Around 15% of breast tumours are HER2 type and around 75% of these contain the *p53* gene mutation (Falato et al., 2016, Howlader et al., 2014). The prognosis for HER2 type patients has recently been improved due to the advent of anti-HER2 drugs such as Herceptin (Voduc et al., 2010, Yang et al., 2011).

iv. Treatment

If cancer is limited to the primary breast site upon detection, the primary treatment option is removal of the tumour through surgery. Along with this, a lymph node biopsy, most likely to be the sentinel node, is undertaken in order to determine if the cancer has spread to the lymph ducts or nodes. In cases where metastasis to the lymph node is detected, treatment options are different and can include a wider mastectomy and axilla clearance in order to remove both

primary tumour and lymph nodes likely visited by cancer cells.

Rapidly proliferating cells, like those ones seen in malignancies, are more sensitive to irradiation than non-malignant cells, so surgery is usually combined with radiotherapy of the adjacent breast tissue to eliminate residual tumour cells and so minimise the recurrence risk.

Furthermore, adjuvant therapy is usually undertaken in order to target possible micrometastases (Barker, 2015).

Approximately 70% of breast tumours express hormone receptors such as ER and PR (Lim et al., 2012), and those patients in this category are given anti-hormone therapy five years post-surgery. This approach has been shown to decrease the likelihood of disease recurrence (Konecny et al., 2003, Thurlimann and Senn, 2005).

Chemotherapy, in contrast to radiation, is a systemic treatment option and is used for more aggressive breast cancers or those with distant metastases. The most common chemotherapy types block cell division through varying mechanisms. Alkylating agents cause DNA damage and tumour cell apoptosis; antimetabolites inhibit DNA nucleotide synthesis; anthracyclins interfere with enzymes involved in DNA replication; mitotic inhibitors hinder chromosome segregating proteins. The past few decades have witnessed the increase in the number of available agents for this purpose. Usually, a combination of two or three of these agents is used (Chabner and Murphy, 2005, Chabner and Roberts, 2005).

1.3. Progressive properties of solid tumours

Tumours are more than insular masses of proliferating cells; instead, they are complex tissues comprised of many distinct cell types which partake in heterotypic interactions with one another. Normal cells are thought to be recruited to form tumour-associated stroma and play an active role in tumourigenesis; as such, these stromal cells contribute to the development and expression of certain hallmark capabilities (Hanahan and Weinberg, 2011).

It has been proposed that there are six hallmarks of cancer which, together, constitute an organising principle which provides a logical framework for understanding the remarkable diversity of neoplastic diseases (Hanahan and Weinberg, 2011). These hallmarks hold distinctive and complementary capabilities which enable tumour growth and metastatic dissemination of cells (Figure 1.3).

i. Sustaining proliferative signalling

This is, arguably, the most central and essential trait of cancer cells, allowing them to sustain chronic proliferation. The production and release of growth-promoting signals, which direct entry into and advancement through the cell cycle, by normal tissues. Cancer cells are able to deregulate these signals, with the ability to produce growth factor ligands themselves and then release growth factors, resulting in autocrine proliferative stimulation.

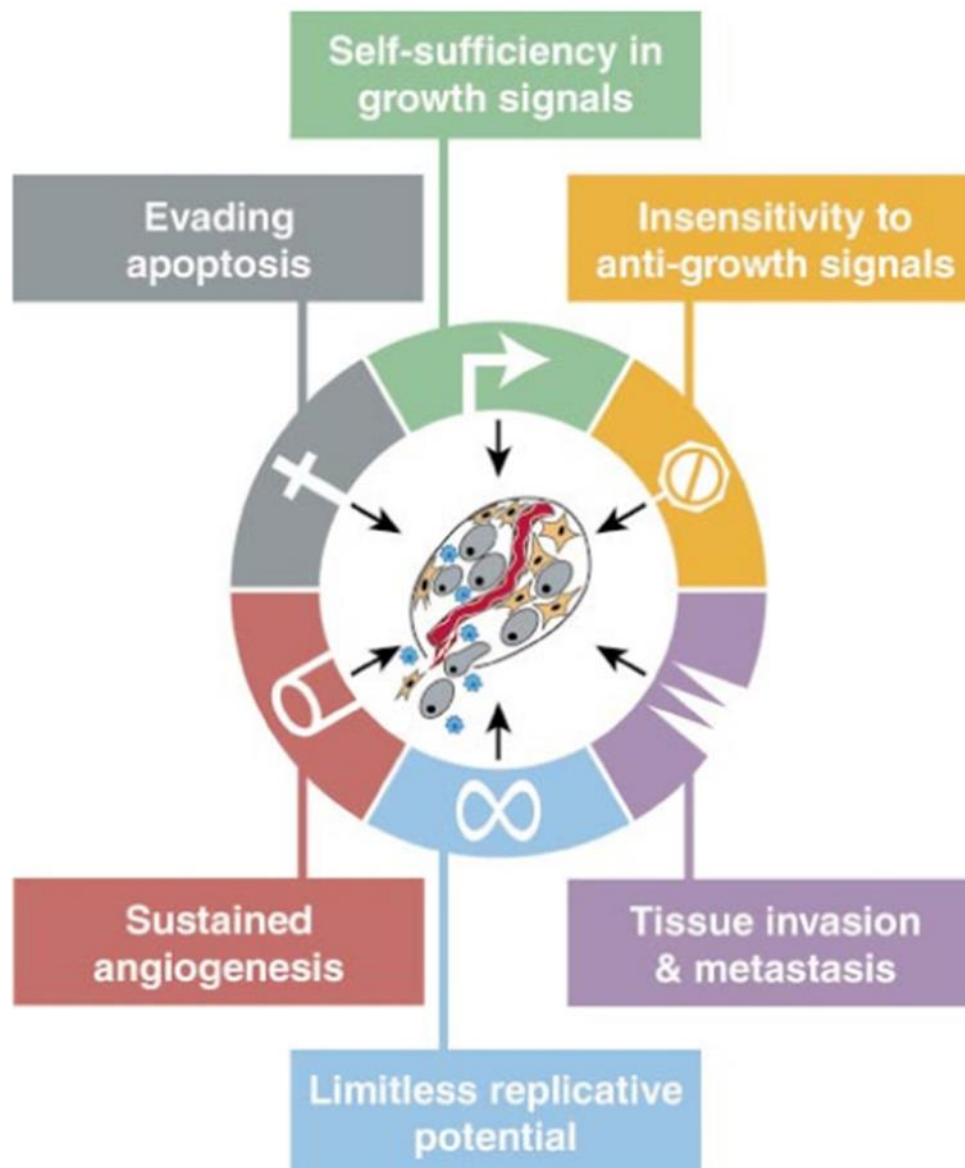


Figure 1.3. Progressive properties of cancer (taken from Hanahan & Weinberg, 2000). There are six properties which a cell has to gain in order to be considered malignant: limitless replicative potential, insensitivity to anti-growth signals, evasion of apoptosis, sustaining angiogenesis, self-sufficiency in growth signals and tissue invasion and metastasis.

Various tumour suppressors which operate to limit cell growth and proliferation have been found due to their inactivation in cancers. The two prototypic tumour suppressors encode the RB (retinoblastoma-associated) and TP53 proteins which function as central nodes within two key complementary cellular regulatory circuits which govern the decisions of cells to proliferate or stimulate normal cells in the tumour-associated stroma to release growth factors (Cheng et al., 2008, Bhowmick et al., 2004). Receptor signalling can also be deregulated by the elevation of receptor protein levels displayed at the cancer cell surface, rendering the cells hyperresponsive to the otherwise limiting amounts of growth factor ligand; the same response can be seen from structural changes in the receptor molecules which allow for ligand-independent firing. Ligand independence can also occur from constitutively active components of signalling pathways operating downstream of these receptors, discounting any growth factor stimulatory need of the receptors (Hanahan and Weinberg, 2000, Hanahan and Weinberg, 2011).

ii. Evading growth suppressors

As well as possessing the ability to proliferate uncontrollably, cancer cells need to be able to circumvent the negative regulatory signals which control cell proliferation. Antigrowth signals block cell proliferation through two distinct mechanisms. Cells can be forced out of the active proliferation cycle into a quiescent (G0) state from

which they can re-emerge on some future occasion when extracellular signals permit. Alternatively, cells may be induced to permanently relinquish their proliferative potential by being induced to enter into a post-mitotic state, usually associated with the acquisition of specific differentiation-associated traits (Williams and Stoeber, 2012, Hanahan and Weinberg, 2011).

Normal cells can activate senescence and apoptotic programs (Jones and Thompson, 2009). Cancer cells often contain mutations in the growth suppressor genes, rendering them inactive, and thus they can lose responsiveness to suppression pathways by downregulating receptors or receptors may become mutant or dysfunctional (Fyran and Reiss, 1993, Markowitz et al., 1995)

iii. Evading apoptosis

The ability of tumour cells to expand in population is determined not only by the rate of cell proliferation but also by the rate of attrition. It has been shown that programmed cell death (apoptosis) is present in a latent form in virtually all cell types throughout the body. When triggered through the sensing of a variety of physiological signals, this program progresses in a strictly structured series of steps (Hanahan and Weinberg, 2000).

The apoptotic machinery can be generally divided into two classes of components – sensors and effectors. Sensors are responsible for monitoring both the external and internal environments of the cells for

conditions to assess whether a cell should live or die. These sensors regulate the second class of components, the effectors, which are the initiators of cell death (Norbury and Zivnotovsky, 2004).

Resistance to apoptosis can be acquired by cancer cells through a variety of stages, with the most common loss of pro-apoptotic regulator being a mutated p53 tumour suppressor gene. The resulting functional inactivation of p53 protein occurs in over 50% of human cancers and results in the removal of a key element of the DNA damage sensor which can induce the apoptotic effector cascade (Harris, 1996a, Harris, 1996c, Harris, 1996b). Signals incited by other abnormalities, including hypoxia and oncogene hyper-expression, are also funnelled in part via p53 to the apoptotic machinery; and so these too are compromised when p53 function is lost (Levine, 1997).

iv. Enabling replicative immortality

It is now well-known that the Hayflick limit defines the finite number of divisions a cell can undertake before it becomes senescent (Hayflick, 1997). Interestingly, most types of tumour cells propagated *in vivo* appear to be immortalised, suggesting that this limitless replicative potential is an acquired phenotype during *in vivo* tumour progression and could be essential for the development of a malignant growth state (Hayflick, 1997, Hanahan and Weinberg, 2000).

The ends of chromosomes, known as telomeres, have been shown to be the counting mechanism for cell generations. Throughout each

replication, 50-100 base pairs are lost from telomeres, due to the inability of DNA polymerases to completely replicate the 3' end of chromosomal DNA during S-phase of the cell cycle. Thus, the progressive erosion of the telomeres causes them to lose their ability to perform their function, which is to protect the ends of chromosomes (Counter et al., 1992). Telomere maintenance is evident in virtually all types of malignant cells (Shay and Bacchetti, 1997) and most of this is done through the upregulation of an enzyme, telomerase, which holds the ability to add hexanucleotide repeats to the ends of telomeric DNA and thus repair chromosomes (Bryan and Cech, 1999). Immortalised cells which do not use this mechanism are able to activate a mechanism, termed alternative lengthening of telomeres (ALT), which appears to maintain telomeres through recombination-based interchromosomal exchanges of sequence information (Bryan et al., 1995). Therefore, via one of these mechanisms, telomeres are maintained above a critical threshold and so unlimited multiplication of descendant cells can occur.

v. Inducing angiogenesis

The oxygen and nutrients supplied by the vasculature are crucial for cell function and survival, obligating virtually all cells in a tissue to reside within 100 µm of a capillary blood vessel. There is extensive and compelling evidence towards the importance of induction and

sustenance of angiogenesis in tumours (Bouck, 1996, Folkman and Hanahan, 1991, Hanahan and Weinberg, 2011).

Positive and negative signals which encourage or discourage angiogenesis must be counter-balanced in normal cells in order for angiogenesis to be regulated accordingly. One side of this signalling is communicated through soluble factors and their receptors, the latter being displayed on the surface of endothelial cells. Integrins and adhesion molecules mediating cell-matrix and cell-cell association also play vital roles. The angiogenesis initiating signals are exemplified by vascular endothelial growth factor (VEGF) and acidic and basic fibroblast growth factors (FGF1/2). Each binds to transmembrane tyrosine kinase receptors displayed by endothelial cells (Veikkola and Alitalo, 1999). A prototypical angiogenesis inhibitor is thrombospondin-1 (TSP-1), which is able to bind to CD36, a transmembrane receptor on endothelial cells, couple to intracellular Src-like tyrosine kinases (Bull et al., 1994). Currently, there are more than 25 angiogenic inducing factors known, and a similar number of inhibitors (Hanahan and Weinberg, 2000).

Also contributing to this regulatory balance is integrin signalling. Quiescent vessels express a class of integrins, whereas sprouting capillaries express another. Intervening signalling from the latter class of integrins can inhibit angiogenesis (Giancotti and Ruoslahti, 1999), highlighting the importance of cell adhesion to angiogenesis (Hynes and Wagner, 1996).

It has emerged that tumours possess the ability to activate the angiogenic switch by altering the balance of inducers and inhibitors (Hanahan and Folkman, 1996, Hanahan and Weinberg, 2000). A common strategy used by cancer cells to modify this balance involves an alteration to gene transcription. Many tumours show increased expression of VEGF or FGFs compared to their normal tissue counterparts. In others, expression of endogenous inhibitors such as TSP-1 or β -interferon are downregulated. Moreover, both transitions may occur in some tumours (Volpert et al., 1997). The tumour cell's ability to induce and sustain angiogenesis appears to be attained in one or more discrete steps during tumour development, via an 'angiogenic switch' from vascular quiescence. The mechanisms fundamental to this angiogenic switch remain, thus far, incompletely understood. However, it is apparent that tumour angiogenesis offers a uniquely attractive therapeutic target, as the trait of acquiring a blood supply is common to all tumours (Hanahan and Weinberg, 2011, Hanahan and Weinberg, 2000).

vi. Activating invasion and metastasis

In actuality, the metastasis of a primary tumour to distant locations is the true cause of cancer-related deaths (Sporn, 1996, Hanahan and Weinberg, 2000). Sooner or later, in the development of most cancer types, cancer cells break free from the primary tumour mass and invade adjacent tissues and then colonise distant sites. The capability of cancer cells to invade and metastasise enables them to

escape the primary tumour mass and colonise new terrain in the body where nutrients and space are not limiting.

Invasion and metastasis are highly complex processes and their genetic and biochemical determinants remain incompletely understood. At the mechanistic level, these processes are closely allied; both use similar strategies of operation, involving the changing of the physical coupling of cells to their microenvironment and activation of extracellular proteases.

Several classes of proteins are altered in those cells possessing invasive or metastatic capabilities. Altered proteins include cell-cell adhesion molecules (CAMs) and integrins, which link cells to substrates of the extracellular matrix (Hanahan and Weinberg, 2000).

In cancer, the most commonly observed alteration in cell-to-environment interactions involves E-cadherin, a cell-to-cell interaction molecule which is ubiquitously expressed on epithelial cells.

Coupling between adjacent cells by E-cadherin assimilates the results of anti-growth and other signals through cytoplasmic contact (Christofori and Semb, 1999). E-cadherin is lost in a high proportion of epithelial cancers through mechanisms which may include its mutational inactivation, transcriptional repression or proteolysis of the extracellular region (Christofori and Semb, 1999, Hanahan and Weinberg, 2000)

Another general parameter of invasive and metastatic capability involves extracellular proteases (Coussens and Werb, 1996,

Chambers and Matrisian, 1997). In cancer cells, the genes encoding proteases are upregulated, their inhibitor genes are downregulated and inactive forms are converted to active forms.

vii. Enabling characteristics

Acquisition of these hallmark characteristics is made possible by two enabling characteristics. The first is the development of genomic instability in cancer cells. This leads to the generation of random mutations and rearrangement of chromosomes, amongst which are rare genetic changes which can enable cells to gain these hallmark capabilities. Secondly, the inflammatory state of premalignant and malignant lesions, driven by the cells of the immune system, is Enabling progression (Hanahan and Weinberg, 2011).

viii. Emerging hallmarks

As well as the currently known hallmarks of the progressive properties of cancer, there are two more capabilities which are important for the development of cancer. The first involves reprogramming of the energy metabolism of cells in order to support the continuous growth and proliferation of cancer cells. The second involves evasion of immune cells by cancer cells in order to avoid attack and evasion (Hanahan and Weinberg, 2011).

1.4 Mouse double minute 2 (MDM2)

i. Clinical relevance of MDM2

MDM2 is an evolutionary conserved gene (Fakharzadeh et al., 1991). The murine double minute 2 (*mdm2*) was originally identified as one of three *mdm* genes whose expression is increased more than 50-fold in the spontaneously transformed mouse BALB/c cell line (3T3-DM). These genes are located on small, acentromeric extrachromosomal nuclear bodies, called double minutes (Cahilly-Snyder et al., 1987). The overexpression of the product of the *mdm* gene was later proved to be the reason for the transformation (Fakharzadeh et al., 1991).

The reason for this conveyed transformation potential was shortly discovered, with MDM2 being revealed to bind to the tumour suppressor p53 and thus inhibit its transactivation through its E3 ubiquitin ligase activity (Haupt et al., 1997, Honda et al., 1997, Momand et al., 1992). Since then, *in vivo* experiments have provided compelling evidence towards the importance of the MDM2/p53 interaction (Jones et al., 1995, Mendrysa et al., 2003).

The *p53* gene generates a protein which is involved in the sensing of cell stress and DNA damage, resulting in regulation of the cell cycle and apoptosis (Brown et al., 1998). Mice which do not possess the *mdm2* gene die before embryonic implantation, with a total phenotypic rescue being possible through simultaneous deletion of

the *p53* gene. One study showed genetically modified mice which express just 30% of the normal levels of MDM2 caused decreased body weight and defects in haematopoiesis (Mendrysa et al., 2003). These phenotypes were p53-dependent, emphasising the importance of MDM2 regulation in many cell types. Some tumours contain both high levels of MDM2 and mutations in the *p53* gene. The reason for this is not completely known, although it points towards the involvement of MDM2 in other p53-independent growth-promoting functions (Iwakuma and Lozano, 2003).

The p53 protein transcriptionally activates many genes, including the *mdm2* gene (Lahav, 2008). Therefore, p53 is regulated at protein level by MDM2, but once active, p53 activates the transcription of the *mdm2* gene, locking the proteins into a tight negative feedback loop, vital for cell survival. In conclusion, it is obvious that MDM2 is a critical regulator of p53 activity and its loss leads to an active p53 which has disastrous consequences for the cell or embryo.

The *mdm2* gene consists of 12 exons, which can generate a number of different proteins through alternative splicing. The gene is governed by two promoters, each of which produce a different protein. Alternative splicing of the *mdm2* gene and the generation of short proteins occurs in many tumours. Many short MDM2 proteins encoding just the carboxyl terminus of MDM2 have been identified, meaning that MDM2 does not contain the p53-binding domain (Bartel et al., 2002). The p53-interaction domain is situated at the amino terminus, which in turn binds to the amino transactivation domain of

p53. The really interesting new gene (RING) motif, found at the carboxyl terminus, is known to convey the E3 ubiquitin ligase activity of MDM2, which is vital for the ubiquitination and subsequent degradation of p53 (Haupt et al., 1997, Honda et al., 1997). Other motifs within the MDM2 protein include the nuclear localisation and export signals. The signals are used to move MDM2 to and from the nucleus, another way in which the cell tightly regulates p53 (Roth et al., 1998, Freedman et al., 1997) (Figure 1.4).

MDM4, also known as MDMX, was identified as a critical regulator of p53 also (Riemenschneider et al., 1999, Riemenschneider et al., 2003). Some studies have shown that MDM2 interacts with and stabilised MDM4 through each of their RING domains (Tanimura et al., 1999, Sharp et al., 1999, Jackson and Berberich, 2000, Stad et al., 2001) suggesting a cooperation in order to inhibit p53 function. However, other reports claim that MDM4 works to prevent MDM2 degradation and translocation of p53 (Stad et al., 2001).

Another interaction partner, which works upstream of MDM2 is the tumour suppressor p14^{ARF}. This protein binds to MDM2 and blocks its ubiquitination of p53, as well as export from the nucleus (Weber et al., 2000). Appropriate and accurate control of the ARF-MDM2-p53 pathway is vital for tumour suppression, meaning that this pathway is often targeted for alteration in cancer (Bouska and Eischen, 2009).

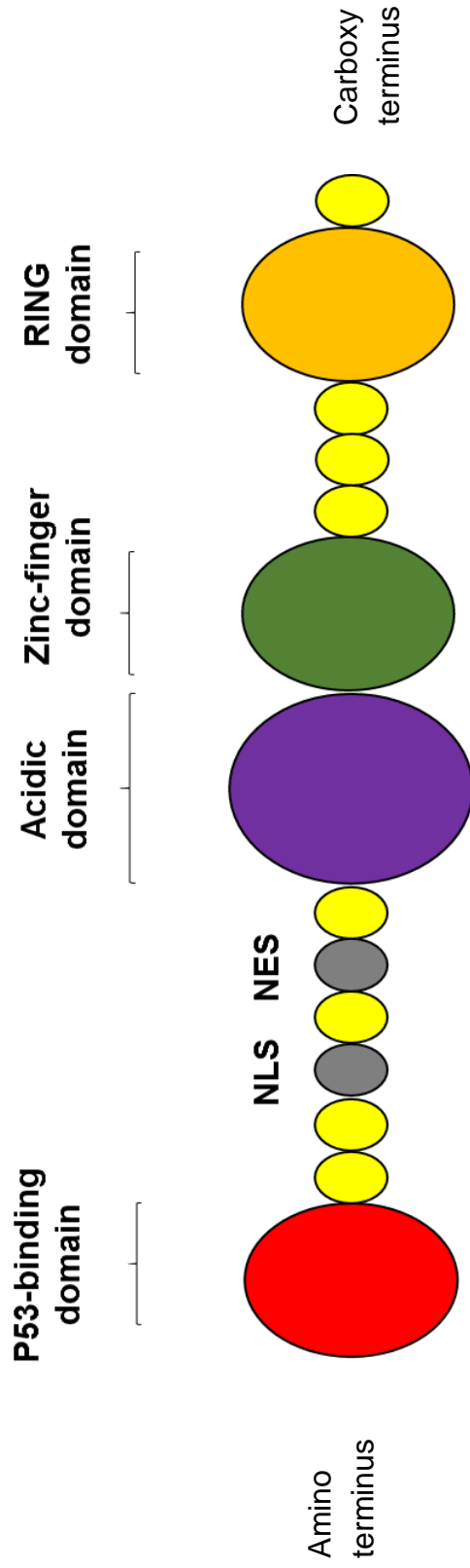


Figure 1.4. Schematic illustration of mouse double minute 2 (MDM2) structure. MDM2 protein is comprised of a p53-binding domain at the amino terminus followed by nuclear localisation (NLS) and export (NES) signals; an acidic domain; a zinc-finger domain; and a RING domain at the carboxy terminus.

Apart from its involvement in p53-dependent activities, it was recently discovered that MDM2 plays a role in p53-independent functions which contribute to tumourigenesis (Lubet et al., 2005). A study of human sarcomas and bladder cancers found tumours which overexpressed MDM2 and mutant p53 and the patients possessing both of these abnormalities had a poorer prognosis than those with just one (Cordon-Cardo et al., 1994). Other studies show that lymphomas arising in transgenic mice with deleted or mutated *p53* also overexpress MDM2 (Alt et al., 2003, Eischen et al., 1999). It has also been indicated that the MDM2 variants which do not possess the p53-binding domain increase cell transformation and tumour development when expressed in mice (Sigalas et al., 1996). These reports suggest that tumours are conveyed an advantage when overexpressing MDM2, even in the absence of functional p53.

It is now known that MDM2 binds and regulates many proteins independent of p53, including proteins involved in DNA repair, DNA replication, cell-cycle control and the apoptosis pathway. These pathways work together to preserve the integrity of genetic information, it has been suggested that MDM2 may act as a central node in the regulation of genome stability and thus transformation (Bouska and Eischen, 2009).

MDM2 is overexpressed due to amplification in around 10% of all human cancers, and overexpression via other mechanisms also occurs in many human malignancies (Rayburn et al., 2005). This means that development of a therapy involving the inhibition of

MDM2 could be used to treat many different patients with various cancer types. Therefore, MDM2 is a major target for drug companies in the development of therapies for cancer patients.

ii. MDM2 in breast cancer

MDM2 protein expression has been shown to be a negative prognostic marker in breast carcinoma (Turbin et al., 2006, Jiang et al., 1997). Other investigators have found that MDM2 overexpression correlates with favourable prognostic parameters i.e. ER overexpression (Hori et al., 2002). Interestingly, amplification of *MDM2* as assessed by fluorescence *in situ* hybridisation (FISH), is not associated with a worse prognosis (Al-Kuraya et al., 2004). Moreover, a study into a breast cell lines (Sheikh et al., 1993) did not show any evidence of aberrant *MDM2* gene copy number. Also, at mRNA level, two studies found increased *MDM2* expression with no apparent alteration in *MDM2* gene copy number (Bueso-Ramos et al., 1993, Sheikh et al., 1993), with a later study backing up these results (McCann et al., 1995).

It is known that oestrogen receptor positive breast cancers often have high levels of MDM2 (Hori et al., 2002). A study into oestrogen-mediated activation of breast cancer cell proliferation showed that oestrogen-treatment of the MCF-7 cell line led to an upregulation of MDM2 protein levels with no effect on p53 protein. MDM2 siRNA treatment also led to an upregulation of basal transcription of p53-target genes, as well as decreased cell growth in 3D Matrigel and

decreased oestrogen-induced cell proliferation in 2D culture. It was also seen that knockdown of p53 protein showed no effect on oestrogen-induced cell proliferation, which led to the conclusion that the activation of MDM2 by oestrogen is independent of p53 (Brekman et al., 2011).

iii. MDM2 as a therapeutic target

The main focus of most therapeutics targeted at MDM2 is to decrease the level of MDM2 protein in cells and therefore allow the reactivation of p53. There are several approaches undertaken to accomplish this: reducing MDM2 levels in cancer cells, inhibiting the E3 ubiquitin ligase complex of MDM2, or the disrupting the interaction between p53 and MDM2 (Wade et al., 2013).

A basic strategy to decreasing MDM2 protein expression is to specifically target the gene using small interfering RNA (siRNA), short hairpin RNA (shRNA) or microRNA (miRNA) approaches. The downregulation of MDM2 using antisense oligonucleotides has led to the stabilisation and activation of the p53 pathway in cancer cells growing in culture and in tumour xenograft mice. Interestingly, mutant p53 cells have responded equally as well as those harbouring wild-type p53. This result supports the notion that MDM2 has other p53-independent activities involved in its contribution to tumour growth and progression (Zhang et al., 2004).

Another way to reactivate p53 activity is to inhibit the ubiquitin ligase activity of MDM2 (Brooks and Gu, 2003). Recently, small-molecule inhibitors have been discovered which specifically target the E3 ligase activity of MDM2. Numerous compounds from this group of inhibitors have been shown to inhibit *in vitro* p53 ubiquitination (Yang et al., 2005). Studies using cancer cells reported that these molecules activate p53 signalling and thus induced apoptosis. However, these compounds have shown low potency and selectivity, with more optimisation being vital before assessment of the therapy's potential (Yang et al., 2005, Vassilev, 2007).

Small molecule inhibitors of the MDM2-p53 interaction have been identified, with the logic that disruption of binding will lead to a degradation of p53. In the past decade, much effort has been invested in this approach, with a recent yield of the first potent and selective pharmacological activators of wild-type p53. A few of these small molecules do represent viable leads for the development of therapeutic agents. The first of these MDM2 antagonists, the nutlins, were identified from a class of compounds named cis-imidazoles (Vassilev, 2007, Vu et al., 2013). The nutlins displace p53 from MDM2 *in vitro* and crystal structures have shown that they bind to the p53 pocket of MDM2 in a way which remarkably mimics the molecular interactions between the two proteins. Proliferating cancer cells have been shown to be effectively blocked in the G1 and G2 phases and undergo apoptosis following treatment with these inhibitors (Vassilev, 2007). The nutlins were the first molecules to

prove that activation of wild-type p53 using pharmacological inhibitors of the MDM2-p53 interaction was a feasible therapeutic concept. As predicted by the molecular mechanism, it seems that only cells with wild-type p53 are sensitive to these compounds, so the p53 status of tumours would need to be determined before any therapeutic approach is undertaken. *In vitro* and *in vivo* studies conducted using the nutlins have verified their anti-tumour effect (Tovar et al., 2006).

Recently, there has been an influx of small molecule MDM2 inhibitors undergoing clinical trials, with seven currently in Phase 1, all of which target the interaction between MDM2 and p53 (Zhao et al., 2015).

The first of these, AM 232 was discovered through studies into AM 8553, a compound produced using *de novo* design strategy based on the structure of MDM2. AM 232 targets a shallow cleft on the surface of MDM2; has been found to be potent and selective; and has shown notable anti-tumoural activity *in vivo* (Bernard et al., 2012, Sun et al., 2014). Roche currently have two compounds in trials, R05045337 (RG7112) and R05503781 (RG7388), with R05045337 being based on the original Nutlin family of inhibitors (Vu et al., 2013).

R05503781 is the second generation of R05045337, with superior potency and selectivity (Ding et al., 2013). Novartis have developed a drug named CGM097 which has been optimised and moved to clinical trials, with analogs currently being developed and their efficacy assessed *in vivo* (Parks et al., 2005). A fifth inhibitor, named DS-3032b was developed by Daiichi Sankyo following a miniaturised

thermal denaturation assay used to screen chemical libraries, leading to a unique series of benzodiazepinedione antagonists of the MDM2-p53 interaction being discovered (Grasberger et al., 2005).

SAR4058383 was developed by the University of Michigan and Sanofi, with promising early studies showing that a single optimised oral dose of the compounds leading to complete tumour regression in the SJSA-1 cell line model (Wang et al., 2014). Finally, MK-8242 was developed by Merck Sharp & Dohme Corp and a clinical trial of patients with solid tumours was recently completed (Zhao et al., 2015).

It is well known that, following DNA damage, p53 is activated and this leads to arrest of the cell cycle and apoptosis in sensitive tissues (Gudkov and Komarova, 2003). Therefore, a main concern of using therapeutics to activate p53 is the effect of this act in normal tissues. Mice with MDM2 reduced to around 30% of its normal level show increased p53 in all tissues tested. Apart from slight disturbances in haematopoiesis and an increase in apoptosis in the small intestine, these mice developed normally (Mendrysa et al., 2003, Vassilev, 2007). Further, nude mice can tolerate nutlin-3 for three weeks at doses that cause inhibition and regression of tumours (Tovar et al., 2013). It seems that these studies suggest that perhaps activation of p53 through MDM2 inhibition may be a promising therapeutic option and can be well tolerated *in vivo* (Vassilev, 2007).

Although use of these inhibitors can be extremely useful for cancer therapeutic development, their effectiveness depends on multiple

factors. Firstly, as already mentioned, the therapeutic effect of p53 activation could be abolished through the potential cell cycle arrest or cell death caused by p53 activation. Secondly, MDM2 is not the only regulator of p53 in cells, so other interactors may hinder the cellular response to MDM2 antagonists. For example, MDM4 another p53-binding protein, cannot be displaced by nutlin-3, so the effectiveness of nutlins can be compromised in tumour cells which overexpress MDM4 (Vassilev, 2007).

Therefore, although MDM2 represents a useful and potent target for inhibitors in the impedance of cancer progression, an ideal therapeutic has not yet been identified. However, with our new understanding of the functions of p53-dependent and -independent MDM2 and accelerating speed of drug development, it is possible that an MDM2-targeted therapy could be effectively applied to halt tumour outgrowth in patients (clinical trials of MDM2-targeted therapeutics summarised in Table 1.2.).

Table 1.2. Clinical trials targeting MDM2 for cancer treatments.
Table modified from Bradbury *et al.* (Bradbury *et al.*, 2015).

Intervention	Target	Cancer type targeted	Affiliates	Trials stage	Current status
Biological: CD105/Yb-1/ SOX2/CDH3/MDM2 multiphasmid vaccine	MDM2- expressing tumor cells	Advanced solid tumors, lymphomas	University of Washington	Phase I	Not yet recruiting
Drug: RO6839921	MDM2-p53 interaction	Neoplasms, leukemia, myelodysplastic syndrome	Hoffman-La Roche	Phase I	Recruiting
Drug: DS-3032	MDM2-p53 interaction	HER2-negative stage III-IV	Daiichi Sankyo Inc.	Phase I	Recruiting
Drug: RO5045337	MDM2-p53 interaction	Soft tissue sarcoma, neoplasms, leukemia	Hoffman-La Roche	Phase Ib	Active, not recruiting/ Completed
Drug: RO5503781	MDM2-p53 interaction	Neoplasms	Hoffman-La Roche	Phase I	Completed
Drug: thioureidobutyronitrile	p53 activator	Solid Tumors	Cellceutix Corporation	Phase I	Recruiting
Drug: HDM201	MDM2-p53 interaction	Advanced tumors (TP53wt) liposarcoma	Novartis Pharmaceuticals	Phase I	Recruiting
Drug: CGM097	MDM2-p53 interaction	Solid tumors with p53 wt states	Novartis Pharmaceuticals	Phase I	Recruiting
Drug: SAR405838	MDM2-p53 interaction	Neoplasm malignant	Sanofi	Phase I	Ongoing
Drug: MK-8242	MDM2-p53 interaction	Solid tumors	Merck Sharp & Dohme Corp.	Phase I	Completed
Drug: AM 232	MDM2-p53 interaction	Advanced solid tumors, multiple myeloma	Amgen	Phase I	Recruiting

vi. MDM2 involvement in tumour-associated angiogenesis

VEGF is a potent angiogenic factor which plays an important role in regulating normal physiological and pathological angiogenesis.

Correctly timed expression of VEGF at appropriate levels is crucial for normal development of vasculature and homeostasis, but also vital for solid tumour growth. VEGF is highly expressed in solid tumours and is required for the development and maintenance of blood vessels within the tumour, which is a prerequisite for successful tumour growth and metastasis.

A co-expression study was undertaken to evaluate the correlated expression of MDM2 and VEGF, finding that, over eight different cancer cell lines, higher MDM2 expression meant higher VEGF mRNA, with the cell lines with lost p53 function showing highest VEGF levels (Narasimhan et al., 2007). They verified their findings further by inhibiting MDM2 using a specific MDM2-specific antisense oligonucleotide (HDMAS5) and saw a significant decrease in VEGF mRNA and protein levels. Finally, they proved that transfecting the MDM2 gene in the prostate cancer cell line, LNCaP, produced a cell line overexpressing MDM2 and VEGF. The same group then identified MDM2 as a regulator of VEGF expression in cancer cells. Human umbilical vein endothelial cells (HUVECs) were treated with tumour-conditioned media (TCM) from HMAS5-treated cancer cells. They found that VEGF release from cells and VEGF-dependent

angiogenesis were significantly reduced *in vitro* (Narasimhan et al., 2008).

Hypoxia-inducible factor 1 (HIF-1) is a heterodimeric transcription factor which generates a response to oxygen deprivation due to hypoxic conditions. Active HIF-1 is comprised of two subunits: HIF-1 β is constitutively expressed in the cell, however, under normoxic conditions HIF-1 α is covalently modified by prolyl hydroxylases, allowing von Hippel-Lindau tumour suppressor (VHL) E3 ubiquitin ligase to polyubiquitinate and thus targets HIF-1 α for degradation (Ivan et al., 2001, Jaakkola et al., 2001). Factor inhibiting HIF-1 (FIH-1) can also hydroxylate HIF-1 α , preventing coactivator binding and so inhibiting transcription of target genes (Mahon et al., 2001). Following a decrease in cellular oxygen levels, the rates of hydroxylation are decreased, VHL does not bind, HIF-1 α is stabilised and the HIF-1 the heterodimer can form (Joshi et al., 2014). Overexpression of HIF-1 α has been linked to angiogenesis, tumour invasion and a poor prognosis in many types of cancer (Bos et al., 2005, Nakanishi et al., 2005, Theodoropoulos et al., 2004, Zagzag et al., 2000). The HIF-1 transcription factor binds to the 5' flanking sequence of *vegf* and is essential for the transactivation of *vegf* during hypoxia.

It has been known for some time that hypoxia is a physiological inducer of tumour suppressor p53, with p53 protein levels increasing under hypoxic conditions (Graeber et al., 1996). Since MDM2 is the most important negative regulator of p53, many groups began to look

into the precise mechanism of the interaction between hypoxia and p53, and whether MDM2 was involved (Nieminen et al., 2005, Lau et al., 2006, Secchiero et al., 2007, LaRusch et al., 2007, Binder, 2007, Lee et al., 2009, Mahon et al., 2001, Zhou et al., 2011, Muthumani et al., 2014, Xiong et al., 2014).

In 2005, a study showed that MDM2 positively activates HIF-1 α in hypoxic tumour cells. Co-immunoprecipitation showed that MDM2 precipitates with HIF-1 α , completely independently of p53 (Nieminen et al., 2005). Evidence towards the involvement of MDM2 in the regulation HIF-1 α expression under hypoxic conditions came from Lau *et al.* (Lau *et al.*, 2006), who found that inhibitory effects on HIF-1 α by the anti-cancer drug 3-(5'-hydroxymethyl-2'-furyl)-1-benzyl indazole (YC-1), was MDM2-dependent and that overexpression of MDM2 reversed its inhibitory effects. A very recent study also suggested that, under hypoxic conditions, MDM2 is capable of ubiquitinating HIF-1 α with its E3 ubiquitin ligase domain in a PTEN/phosphoinositide 3-kinase (PI3K)-dependent manner. The group's results suggested that the PI3K-protein kinase B (AKT) signalling axis is a requirement for the preservation of HIF-1 α stability during hypoxia (Joshi et al., 2014).

Another study showed that nutlin-3 conferred anti-angiogenic activity. It was found that nutlin-3 dose-dependently suppressed the total tube length and the number of capillary connections developed from HUVECs. Also, the migration of endothelial cells was shown to be significantly inhibited by nutlin-3 in response to various

chemoattractants (Secchiero et al., 2007). In the same year, two more reports were published demonstrating the inhibition of HIF-1 α by nutlin-3, leading to inhibited VEGF production and thus angiogenesis in tumours (LaRusch et al., 2007, Binder, 2007). Lee *et al.* (Lee et al., 2009) then suggested a mechanism through which this occurred after finding that nutlin-3 downregulated HIF-1 α in p53-positive cells but also functionally inactivated HIF-1 α in p53-negative cells. Of these two occurrences, they found that the second mainly contributed to VEGF suppression by nutlin-3. It was reported that MDM2 competes with FIH which is a regulator of HIF-1 α , by binding its C-terminal transactivation domain (CAD). FIH hydroxylates Asn803 in the CAD domain under normoxic conditions. However, when conditions are hypoxic, this hydroxylation is inhibited due to the limited oxygen and so HIF-1 α becomes stable and active (Mahon et al., 2001, Lando et al., 2002). When MDM2 competes for binding of the CAD of HIF-1 α , this hydroxylation is inhibited and so p300 is recruited. They found that nutlin-3 reinforced the FIH-mediated inactivation of HIF-1 α through inhibiting any interaction between CAD and MDM2 (Lee et al., 2009). This theory is in direct contrast to the report by LaRusch *et al.* (LaRusch et al., 2007), who reported that the N-terminal domain of HIF-1 α was needed for binding of MDM2. This could imply that each domain of HIF-1 α interacts individually in different ways with MDM2 or they cooperate to bind MDM2. Therefore, it is widely accepted that hypoxia induces VEGF transcription through induction of HIF-1 α . However, in 2011, a group

set out to investigate the posttranscriptional regulation occurring, in which HIF-1 α does not seem to be important (Zhou et al., 2011). Their work followed on from a study which showed that in rat cardiac myocytes hypoxia can induce VEGF steady-state mRNA 25-fold, however the hypoxia-mediated transcription rate of VEGF increases just 3.1-fold (Levy et al., 1996). Their results showed that the RING domain of MDM2 can bind to AU-rich elements of the VEGF 3' untranslated region (UTR) and regulate VEGF mRNA stability and thus its translation. Interestingly, they also demonstrated that during hypoxia, MDM2 was dephosphorylated and translocated to the cytoplasm from the nucleus, where it was able to induce high levels of VEGF in cancer cells (Zhou et al., 2011). The same group then undertook a study to elucidate whether p53 played a role in the interaction between MDM2 and VEGF. They did this through the use of two cell lines, MCF-7 which expresses wild-type p53 and MDA-MB-468, which expresses mutant p53. They studied the effect of nutlin-3 and anti-MDM2 antisense oligonucleotide (ASO), on these cell lines and saw that ASO significantly inhibited the VEGF transcript and protein levels in a dose- and time-dependent manner, whereas nutlin-3 had no effect. The effect of hypoxia was also studied, and it was observed that ASO treatment significantly inhibited HIF-1 α expression at 3, 6 and 12 hours of hypoxia in both cell lines. An inhibitory effect on HIF-1 α was also seen in the nutlin-3 treated MCF-7 (wild-type p53) but not in MDA-MB-468 (mutant p53). The group used siRNA targeted at HIF-1 α as well as ASO treatment and found

that HIF-1 α only seems to have a role in VEGF production in early hypoxia (at 6 hours, but not at 48 hours). HIF-1 α siRNA did not reverse the inhibitory effect of ASO on VEGF production. Therefore, the group surmised that ASO downregulates hypoxia-induced VEGF production via a HIF-1 α -independent mechanism. When the same experiment was undertaken using nutlin-3, it was seen that nutlin-3 significantly inhibited the level of secreted VEGF from the MCF-7 cells at early hypoxia. When the cells were transfected with HIF-1 α siRNA, nutlin-3 failed to inhibit VEGF production. This exhibits that the effect of nutlin-3 on VEGF regulation in early hypoxia is HIF-1 α -dependent. ASO treatment of mice with tumours of each cell type showed a substantial decrease in serum VEGF levels, measured by ELISA. On the other hand, nutlin-3 treatment produced little effect on VEGF production (Xiong et al., 2014).

A very recent study investigated the precise mechanism supporting the induction of VEGF transcription by MDM2. They used prostate cancer cell lines LNCaP and MDM2 transfected LNCaP (LNCaP-MST). As expected, they found that VEGF transcription was significantly higher in the LNCaP-MST cells compared to the non-transfected LNCaP (Muthumani et al., 2014). Activation of the PI3K-mTOR pathway has previously been reported upon increase of VEGF expression in normoxic and hypoxic conditions (Narasimhan et al., 2008). Since HIF-1 α is required as a primary member of this pathway, it is generally assumed that activation of the pathway is more effective under hypoxic conditions, in terms of induction of

VEGF transcription. Yet, this study showed that in the LNCaP-MST cells, the PI3K-mechanistic target of rapamycin (mTOR) pathway seems to be activated and the basal HIF-1 α appear high. They reported that MDM2 seemed to be triggering an elevated level of HIF-1 α , in line with increasing expression of VEGF in normoxic cells, even when hypoxic conditions are lacking. The data presented also suggested that signal transducer and activator of transcription 3 (STAT3) and nuclear factor κ B (NF- κ B) may play important roles in MDM2-mediated activation of VEGF transcription since their levels were increased in the LNCaP-MST cells compared to the non-transfected LNCaP cells (Muthumani et al., 2014).

It has also been suggested that p53 can negatively regulate VEGF expression. In 2000, Ravi *et al.* (Ravi et al., 2000) claimed that homozygous deletion of p53 in human colon cancer cells promoted neovascularisation and growth of xenograft tumours in nude mice. They showed that upon loss of p53, HIF-1 protein levels are enhanced and so VEGF expression is augmented. It was also demonstrated that forced HIF-1 α expression in p53-expressing cancer cells promotes the expression of VEGF and this leads to neovascularisation of tumour xenografts. Therefore, the group concluded that p53 acts as a molecular chaperone to HIF-1 α , facilitating its recognition by MDM2 for ubiquitination. This work was disputed by a later study (Nieminen et al., 2005) which suggests that the group's results may be due to the use of hypoxia-mimicking

agents such as cobalt and thus the proteins in complex could change.

In conclusion, despite the great amount of studies undertaken in order to elucidate the role of MDM2 in both angiogenesis and hypoxia, the precise mechanisms are yet to be exposed. It is widely accepted that MDM2 and VEGF levels are coordinated in cancer and that HIF-1 α increase can upregulate VEGF transcription during hypoxia. It has been proved many times that MDM2 and HIF-1 α interact during hypoxia, although whether this is a direct or indirect interaction, and whether it involves p53 tumour suppressor is under scrutiny. It has also been suggested that a second layer of regulation occurs between MDM2 and VEGF, at post-transcriptional level, independent of HIF-1 α . Therefore, perhaps there are different points of regulation of VEGF levels by MDM2 during hypoxia and HIF-1 α and p53 may play a role in some, but not others.

v. Participation of MDM2 in tumour invasion and metastasis

Due to the high expression of MDM2 in a number of cancer types, its roles in the invasion and subsequent metastasis of tumours have been studied. Migration and invasion through the extracellular matrix are reliant on the matrix metalloproteinases (MMPs) which are zinc-dependent remodelling endopeptidases implicated in many pivotal roles in tumour growth and the multistep processes of invasion and

metastasis. Different members of the MMP family exert contradicting roles at various stages of cancer progression (Gialeli et al., 2011).

The most obvious feature of MDM2 involvement in the progressive properties of cancer is its interaction with p53. The ability of MDM2 to block p53 activity is exploited by tumour cells. However, there are other ways in which MDM2 contributes to the progression of cancer. It was shown that in breast cancer cells MDM2 can decrease E-cadherin protein level through ubiquitination and ectopic expression of MDM2 increases cell-cell dissociation, invasion and cell motility (Yang et al., 2006). A study into patients with malignant melanoma showed that MDM2 expression level was directly associated with the thickness of a tumour and weakly with invasion level (Rajabi et al., 2012).

Immunohistochemical staining of invasive ductal breast carcinoma (IDC) showed a significant correlation between MDM2 and MMP9 expression. *In vitro* studies in MDA-MB-231 and MCF-7 breast cancer cell lines have shown that siRNA targeted at MDM2-targeted siRNA significantly decreased cell invasion, migration and proteolysis, with the opposite seen in cells overexpressing MDM2. MDM2 overexpression in these cells was seen to induce MMP9 expression in a dose-dependent manner (Chen et al., 2013). A slightly later study also linked the expression of MDM2 and MMP9 in the oncogenesis of lung cancer in rats (Zhang et al., 2014).

1.5 Prostate-specific membrane antigen (PSMA)

i. Clinical relevance of PSMA

PSMA is a type II membrane protein with a unique three-part structure: a 19 amino acid internal region, a 24 amino acid transmembrane region and a 707 amino acid external portion (Chang, 2004, Leek et al., 1995) (Figure 1.5). It has recently been demonstrated that PSMA has an internalisation signal which allows internalisation of the protein on the cell surface into an endosomal compartment (Rajasekaran et al., 2005). The PSMA gene is located on the chromosome 11p in a region that is not currently deleted in prostate cancer (O'Keefe et al., 1998).

PSMA has only a few sites of expression in normal tissues: the prostate epithelium, the kidney proximal tubules, the nervous system glial cells and the small bowel jejunal brush border (Mhaweche-Fauceglia et al., 2007, Sacha et al., 2007) . At the jejunal brush border the protein is better known as FOLH1 and here it converts dietary folate (pteroylpolyglutamate) to monoglutamated folate (Halsted et al., 1998, Ristau et al., 2014). In the nervous system, however, PSMA carries out its N-Acetylated alpha-linked acidic dipeptidase (NAALADase) function and hydrolyses N-Acetylaspartylglutamic acid (NAAG), the most abundant peptide neurotransmitter in the mammalian nervous system

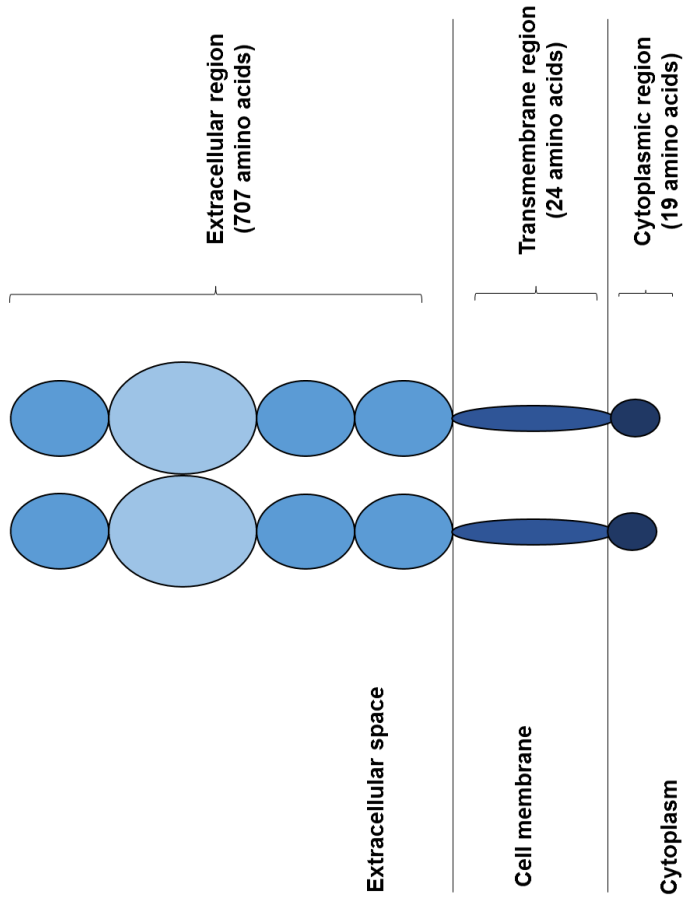


Figure 1.5. Schematic illustration of prostate-specific membrane antigen (PSMA) structure. PSMA protein is comprised of three regions: a large extracellular region of 707 amino acids; a transmembrane region of 24 amino acids; and a cytoplasmic region of 19 amino acids. Diagram adapted from (Rajasekaran et al., 2005) and (Chang, 2004)

(Neale et al., 2000, Ristau et al., 2014). The presence of PSMA in the prostate and proximal tubules of the kidneys is not yet understood but it has been suggested that this could be due to the reuptake of folate in the kidneys and the release of monoglutamated folates into the seminal fluid (Ristau et al., 2014).

The cell surface expression of PSMA has been shown to increase directly in cancers of higher-grade, metastases, prostate cancer which is castration-resistant and cancers giving an adverse clinical outcome (Ross et al., 2003, Perner et al., 2007). Furthermore, PSMA expression was observed to decrease in the prostate cancer cell line, LNCaP, when incubated with androgen dihydrotestosterone (DHT) and, conversely, cells grown in androgen-stripped media displayed increased PSMA expression (Liu et al., 2012b). It is clear that increased expression and enzymatic activity of PSMA in aggressive tumours are telling of a selective advantage bestowed by PSMA upon tumour cells and this contributes to prostate carcinogenesis.

PSMA has also been reported to be expressed in the neovasculature of a considerable majority of malignant solid tumours (bladder, breast, kidney pancreas, lung and melanoma), but not in the corresponding normal vasculature (Chang and Heston, 2002).

PSMA has been identified as an excellent target for imaging and therapy of cancer for several reasons. The specificity of its expression is a key factor, with only a limited number of normal tissue types expressing the protein, along with PSMA's large

extracellular region allowing therapeutics to be exclusively targeted to the tumour region and malignant cells. The fact that PSMA is a transmembrane protein is also important, as its extracellular region can be easily targeted by therapeutics. Also, the presence of an internalisation sequence within the protein means that therapeutics targeted at PSMA could be internalised through binding. Finally, PSMA's peptidase activities means that it could be involved in the processing of a pro-drug targeted at tumour cells (Rajasekaran et al., 2005, Chang and Heston, 2002, Akhtar et al., 2012). Therefore, there is a very strong case for the use of PSMA as a biomarker and therapeutic target in the fight against cancer.

ii. PSMA in breast cancer

PSMA was originally thought to be solely expressed in prostate cancer (Horoszewicz et al., 1987, Troyer et al., 1995, Pinto et al., 1996); however, later it was shown to be highly expressed in both the cells and neovasculature of many other tumour types, including breast, gastric, colorectal, renal and bladder cancers (Chang et al., 1999, Silver et al., 1997a, Silver et al., 1997b, Haffner et al., 2009).

Recently, the expression of PSMA in breast cancer has been studied in the hope that targeting the molecule may give rise to a new therapy for this type of tumour. One group investigated the expression of PSMA in breast neovasculature and found that 98% of the vasculature primary carcinoma shown PSMA positivity through immunohistochemical staining. Further, it was seen that all breast

metastases which were secondary to invasive breast carcinoma showed PSMA expression. Interestingly, this group reported that when the metastasised and primary tumour staining scores from the same patient were compared, the same score was seen, which is opposing to other reports claiming that PSMA expression increases with metastasis (Ross et al., 2003, Perner et al., 2007). They saw that patients with a higher PSMA staining score had a bigger median tumour size, a higher Ki-67 proliferation index, a higher nuclear grade and compared to those of a lower staining score (Wernicke et al., 2014). Another group showed that PSMA is expressed in the blood vessels of breast cancer brain metastases, as well as the primary tumours (Nomura et al., 2014). Further, a recent report found that tumour-conditioned media (TCM) from metastatic, highly invasive cell lines MDA-MB-231 results in an increased expression of PSMA in HUVECs, compared to MCF-7 TCM or VEGF treatment (Liu et al., 2012a).

iii. PSMA as a biomarker for cancer

Since prostate cancer tissues shows high PSMA expression and increased enzymatic activity of PSMA compared to normal and benign hyperplasia prostate (BHP) tissues (Lapidus et al., 2000, Burger et al., 2002) the use of PSMA as a biomarker for prostate cancer is under investigation. A direct correlation has been identified in adenocarcinomas between the expression of PSMA and Gleason score, which is used to stage prostate cancer (Burger et al., 2002). A

study by Ross *et al.* suggests that PSMA could act as a biomarker for prognosis as it shows a significant correlation with adverse prognostic factors such as tumour grade, aneuploidy, biochemical recurrence and pathological stage (Ross et al., 2003).

The current standard for early detection of prostate cancer involves a digital rectal examination (DRE) and a serum test for prostate-specific antigen (PSA). Despite its use, there is no definite level of PSA which can actively distinguish between men with prostate cancer and those with a benign hyperplasia, leading to false positive results and overtreatment of men with limited disease (Perner et al., 2007).

PSA is different from PSMA in a number of ways: PSA is a secretory protein, whereas PSMA is an integral membrane protein. PSMA is a liquefaction in semen, whereas PSA holds several enzymatic functions. PSA is decreased with androgen deprivation, whereas the inverse is true of PSMA (Chang, 2004).

PSMA immunohistochemistry was seen to have a higher (84%) sensitivity than PSA (58%) in staining of tissues from metastatic sites. Strong, diffuse staining was seen in 17 of 19 cases of metastatic prostate cancers, compared to 13 from PSA staining. Positivity for either of the molecules was seen in 89% of metastatic prostate cancer and this combination immunohistochemistry was slightly more sensitive than that of PSMA alone, indicating that a

combination of PSMA and PSA immunohistochemistry could be a beneficial prognostic assessment for patients (Bernacki et al., 2014).

Quantification of PSMA and PSA levels in peripheral blood showed significant differences among BPH, locally confined prostate cancer and metastasised prostate cancer in expression of PSA and PSMA.

It was found that one cancer cell could be detected in 2×10^7 mononuclear cells (Zhang et al., 2008).

The first clinical agent targeting PSMA in prostate cancer was the monoclonal antibody 7E11/CYT-356, which was labelled with Indium-111 and known as ^{111}In -capromab or ProstaScint (Wynant et al., 1991, Elsasser-Beile et al., 2009, Ristau et al., 2014). The sensitivity and specificity of the antibody has differed in studies, with an average sensitivity of 60%, a specificity of 70%, a positive predictive value of 60% and a negative predictive value of 70% (Apolo et al., 2008, Rosenthal et al., 2001). These poor results could be a consequence of ^{111}In -capromab recognising an intracellular epitope, and therefore only binding molecules in cells with a damaged cell membrane (Ristau et al., 2014).

This led to the development of second-generation antibodies which can bind to the extracellular region of PSMA and thus could be superior to the capromab pendetide. One of these developed antibodies, J591, has shown potential in imaging primary prostate cancer, as well as bone metastases. Clinical trials with $^{99\text{m}}\text{Tc}$ -labelled J591 established detection of primary prostate cancer, as

well as prostate bed recurrence and distant metastases, again, including metastasis to bone (Ristau et al., 2014, Nargund et al., 2005). Several other developed monoclonal antibodies (3/A12, 3/E7 and 3/F11) bind to different epitopes of PSMA (Ristau et al., 2014). A study using ^{64}Cu -3/A12 for positron emission tomography (PET) imaging of prostate cancer xenograft showed a good tumour-to-background ratio (Elsasser-Beile et al., 2009). A fourth monoclonal antibody targeting PSMA, 3C6, has been labelled with ^{111}In for imaging in prostate cancer (Regino et al., 2009).

Radiolabelled PSMA inhibitor N-[N-[(S)-1,3-dicarboxypropyl]carbonyl]-S-[^{11}C]methyl-L-cysteine (DCFBC) has been successfully used in PET imaging of xenografts expressing PSMA (Foss et al., 2005). The molecule was labelled with ^{18}F , with studies into its biodistribution and imaging showing a high uptake of ^{18}F -DCFBC in PSMA-positive tumours but slight or no uptake in tumours negative for PSMA (Mease et al., 2008). Urea-based compounds have also been identified as possible targets for imaging of prostate cancer with PET and SPECT (Chen et al., 2009). MIP-1095 and MIP-1072, which are small-molecule inhibitors targeting PSMA, have shown a high affinity for PSMA and their uptake when labelled with ^{123}I has been successfully imaged by SPECT (Hillier et al., 2009, Osborne et al., 2013).

iv. PSMA as a therapeutic target

PSMA has been exposed as an attractive therapeutic target due to its expression being 100- to 1000-fold less in normal cells in comparison to prostate carcinoma cells (Sokoloff et al., 2000). So far, antibody-based radiotherapy, antibody-drug conjugates (ADC), PSMA-targeted prodrug therapy and PSMA-based immunotherapy have been investigated (Ristau et al., 2014).

The leading PSMA antibody-based radiotherapeutic is Lutetium-177 J591, which showed acceptable toxicity and excellent metastatic site targeting in a phase I clinical trial (Bander et al., 2005). A recent phase II clinical trial utilised Lutetium-177 J591 in patients with metastatic castration-resistant prostate cancer (Tagawa et al., 2013). Just less than 60% of patients showed a decrease in PSA levels with 1/10 showing a reduction of more than half and the therapeutic showed accurate targeting of metastatic sites (Akhtar et al., 2012). The higher concentration used in the trials (70 mCi/m²) led to longer survival of patients (almost 22 months, compared to 12), but resulted in increased grade 4 hematologic toxicity and platelet transfusions (Tagawa et al., 2013, Ristau et al., 2014) .

J591 antibody has also been utilised in the production of ADC, which involves the linking of a drug or toxin to an antibody (Akhtar et al., 2012). MLN2704 is an antimicrotubule agent which has been conjugated to J591. Phase 1 studies in over 20 patients showed >50% decrease in PSA levels dropped by more than half in 2

patients, although grade 3 toxicities occurred in 3 patients³ of the patients (Galsky et al., 2008, Ristau et al., 2014). A multicentre phase II/III clinical trial undertaken in 62 men with metastatic castration-resistant prostate cancer showed stabilisation or decline in PSA in a majority of patients; however, limitation of treatment occurred due to toxic effects of the compound (Ristau et al., 2014, Akhtar et al., 2012).

Work has been undertaken in xenograft LNCaP mice, using an immunotoxin consisting of the anti-PSMA mAb E6 and deglycosylated ricin A, showing reduced tumour growth (Ristau et al., 2014). Another group coupled melittin-like peptide 101 to J591 and also saw a significant tumour growth inhibition in mice (Russell et al., 2004, Akhtar et al., 2012). Monomethylauristatin E (MMAE) has also been conjugated to a mAb which recognised the PSMA external domain (Ma et al., 2006).

Recently, a group engineered a prodrug for tumour endothelial cells in prostate cancer therapy (Denmeade et al., 2012). Their work involved the coupling of a PSMA-specific peptide to thapsigargin (inhibitor) of the sarcoplasmic/endoplasmic reticulum calcium adenosine triphosphate (SERCA) pump. SERCA is a vital cellular protein which is essential for the viability of all cell types. Before cleavage of the PSMA-specific molecule, the conjugate is inactive. However, post-cleavage, local SERCA inhibition ensues (Ristau et al., 2014). Preclinical xenograft models treated with thapsigargin

showed significant prostate cancer tumour regression at doses which were modestly toxic to the host (Denmeade et al., 2012).

The use of immunotherapy in oncology has been long utilised, but only recently has work on PSMA as a target begun to be investigated (Akhtar et al., 2012). This type of therapy is based on the concept that IL-2 stimulates natural killer cells, thus enhancing antibody-dependent cellular cytotoxicity. A phase II trial of the anti-PSMA monoclonal antibody J591 was undertaken in patients with recurrent prostate cancer for 8 weeks, with patients receiving continuous low-dose subcutaneous interleukin-2 (IL-2) every day, with infusions of J591 weekly. Of 176 patients, nine had stable PSA, with declines of up to 34%. The therapy was well tolerated and the toxicity was low, with non-progressors showing a trend with significant natural killer (NK) cell expansion (Akhtar et al., 2012, Ristau et al., 2014).

Thus, although PSMA-targeted therapy is yet to yield clinically important effects on the survival of patients without severe side effects ensuing, several fields are currently under study and as our molecular techniques and our understanding of tumour biology become more advanced, PSMA-therapeutics are likely to play an important role in the development of treatment for cancer patients (Ristau et al., 2014) (clinical trials of PSMA as a biomarker and therapeutic target summarised in Table 1.3.).

v. PSMA involvement in tumour-associated angiogenesis

In terms of links of PSMA to VEGF, there are differing views. A report by Tsui *et al.* (Tsui et al., 2005) claimed that there was a correlation between PSMA and VEGF expression in the tumours of xenograft mice, when immunohistological analysis was undertaken.

Forced PSMA expression in a prostate cancer cell line, RM-1, and quantification of secretion of VEGF by cells led to the conclusion that stable transfection of PSMA promoted VEGF release. When these cells were injected into mice, immunohistochemistry was performed and VEGF levels were seen to be significantly higher in the mice injected with the cells expressing PSMA (Zhao et al., 2012).

Since it is found in the neovasculature of many tumours, PSMA is thought to regulate angiogenesis. In 2006, a group demonstrated that PSMA is required for angiogenesis *in vivo* and invasion of endothelial cells *in vitro*, where it was exhibited to be involved in laminin-specific signalling and regulation of the dynamics of the cytoskeleton through the Rho GTPase effector molecule p21-activated kinase 1 (PAK-1). The group hypothesised that PSMA partakes in an autoregulatory feedback loop where, in its active state, it increases integrin signal transduction, PAK activation, followed by endothelial cell adhesion and invasion. This process leads to the dissociation the PSMA/filamin complex and a decrease in PSMA activity and therefore integrin- β 1 activity is held in check (Conway et al., 2006).

Table 1.3. Clinical trials utilising PSMA for cancer imaging and treatment. Table taken from (Bradbury et al., 2015).

Intervention	Use	Cancer type targeted	Affiliates	Trials stage	Current status
Drug: 68Ga-PSMA	Imaging/diagnosis	Prostate cancer	Ebrahim Delpassand	Phase II	Recruiting
Drug: PSMA ADC 2301	Treatment	mCRPC	Progenics Pharmaceuticals, Inc.	Phase II	Completed
Drug: PSMA ADC BrUOG 263	Treatment	Glioblastoma multiforme, gliosarcoma	Heinrich Elinzano, MD	Phase II	Active, not recruiting
Drug: PSMA ADC 1301	Treatment	mCRPC	Progenics Pharmaceuticals, Inc.	Phase I	Completed
Biological: peptide vaccine/ drug: poly IC-LC	Vaccine treatment	Prostate cancer	H. Lee Moffitt Cancer Center and Research Institute	Phase I	Active, not recruiting (has results)
Drug: Anti-PSMA designer T cells	Treatment	Prostate cancer	Roger Williams Medical Centre	Phase II	Active, not recruiting
Biological: rsPSMA protein plus alhydrogel vaccine	Vaccine treatment	Prostate cancer	Memorial Sloan–Kettering Cancer Centre	Phase I	Completed
Biological: anti-PSMA monoclonal antibody MDX1201-A488	Imaging/diagnosis	Prostate cancer	City of Hope Medical Centre	Phase I	Recruiting
Biological: gene modified T cells	Treatment	Prostate cancer	Roger Williams Medical Centre	Phase I	Active, not recruiting
Biological: engineered autologous T cells/drug: cyclophosphamide	Treatment	Prostate cancer	Memorial Sloan–Kettering Cancer Centre	Phase I	Recruiting
Biological: human PSMA plasmid DNA vaccine	Treatment	Kidneycancer	Memorial Sloan–Kettering Cancer Centre	Phase I	Active, not recruiting
Drug: 18F-DCFBC	Imaging/diagnosis	Prostate cancer	Sidney Kimmel Comprehensive Cancer Center	Phase II	Active, not recruiting
Device: ProxiScan (scintigraphic rectal probe)	Imaging/diagnosis	Prostate cancer	Sidney Kimmel Comprehensive Cancer Center	Phase I	Completed
Biological: PSMA prostate cancer vaccine/IL-12	Treatment	Prostate cancer	University of Chicago	Phase II	Completed
Biological: PSMA/PRAME (MKC1106-PP)	Treatment	Advanced cancer	Mannkind Corporation	Phase I	Completed
Drug: 123I-MIP-1072	Imaging/diagnosis	Prostate cancer	Molecular Insight Pharmaceuticals, Inc.	Phase I	Terminated
Drug: 89Zr-J591	Imaging/diagnosis	Glioblastoma multiforme, gliosarcoma	Memorial Sloan–Kettering Cancer Centre	Phase I	Recruiting
Drug: 111-In capromab pendetide	Imaging/diagnosis	Prostate cancer	Molecular Insight Pharmaceuticals, Inc.	Phase I	Completed
Biological: androgen ablation/dendritic cell vaccine	Treatment	Prostate cancer	Pawel Kanlinski	Phase I	Recruiting
Drug: 89Zr-DFO-huJ591	Imaging/diagnosis	Prostate cancer	Memorial Sloan–Kettering Cancer Centre	Phase II	Active, not recruiting

Data taken from [63].

1. General Introduction

Intervention	Use	Cancer type targeted	Affiliates	Trials stage	Current status
Drug: G-202	Imaging/diagnosis	Glioblastoma multiforme, advanced hepatocellular carcinoma	GenSpera, Inc.	Phase II	Recruiting Phase II
Drug: ^{99m} Tc MIP 1404	Imaging/diagnosis	Prostate cancer	Molecular Insight Pharmaceuticals, Inc.	Phase I	Active, not recruiting
Radiation: [⁸⁹ Zr]Df-IAB2M	Treatment	Prostate cancer	ImaginAb, Inc.	Phase II	Recruiting
Drug: EC1169	Treatment	Prostate cancer	Endocyte	Phase I	Recruiting
Drug: GVAX and ipilimumab	Treatment	mCRPC	VU University Medical Center	Phase I	Terminated

In a subsequent study, the same group then went on to assess the role of PSMA in ocular neovascularisation. To do this they used an oxygen induced retinopathy model (OIR) and it was observed that, after an initial decrease in retinal PSMA mRNA, transcript levels were progressively increased over the time of the relative hypoxia. Vessel formation was then assessed in the retina of PSMA null mice under these conditions of relative hypoxia. Again, it was seen that the loss of PSMA in these mice did not affect the development of normal retinal vasculature. However, mice undergoing OIR showed a remarkable difference between PSMA null and wild-type. The capillaries in the mid-periphery formed a dense, honeycomb of close vessels. In comparison, retinas from PSMA null animals after OIR showed a vascular pattern which closely resembled the normal structure, with less avascular area in the central region and more highly branched capillaries in the periphery. It was also seen that, in comparison to the wild-type, PSMA null mice vessels were better perfused and more functional. Finally, the study evaluated the use of 2-(phosphonomethyl)pentanedioic acid (2-PMPA) PSMA inhibitor in wild-type mice and obtained similar results. Therefore, the absence of PSMA seems to lead to a less pathogenic phenotype in the retina. The involvement of PSMA in angiogenesis through this mechanism was seen to be independent of VEGF (Grant et al., 2012).

In 2011, a group undertook a study analysing the result of TCM from breast cancer cell lines, MDA-MB-231 (oestrogen receptor negative) and MCF-7 (oestrogen receptor positive), on human umbilical vein

endothelial cells (HUVECs). They found that the aggressive MDA-MB-231 breast cell line TCM induced tube formation of the HUVECs, however, TCM from MCF-7, PC3, LNCap, VEGF-containing Vasculife medium, or without Matrigel led to the HUVECs forming only incomplete, short tube-like structures. In the tubules formed following treatment with TCM from MDA-MB-231, the high level of PSMA expression compared to HUVECs treated with the other TCM or VEGF-containing media, was demonstrated using both qRT-PCR and fluorescent inhibitor-affinity labelling. Subsequently, to elucidate which factors in the TCM from MDA-MB-231 may cause the tubule formation and expression of PSMA, they fractionated the TCM and found that one factor above 30 kDa and another below 3 kDa were essential for formation. This study needs to be extended and more ER+ and ER- cell line TCMs used, but if the results are confirmed in more cell lines, this model could be easily used to assess tumour-vasculature targeting agents for imaging and therapeutic applications (Liu et al., 2011).

It is certain that PSMA is involved in angiogenesis; however, the precise mechanism by which PSMA exerts its effect is unknown. PSMA has been linked to VEGF levels in some reports, with increased and decreased PSMA levels being reflected in VEGF expression. However, a group who have released a number of related papers on the subject of PSMA in angiogenesis claim that the involvement of this protein is VEGF-independent. This suggests that

PSMA may also play a number of roles in angiogenesis, some involving VEGF, others not.

vi. PSMA involvement in tumour-associated invasion and metastasis

A paper by Ghosh *et al.* (Ghosh et al., 2005) showed that, surprisingly, in prostate cancer cells, ectopic expression of PSMA in the PSMA-negative cell line PC-3 cells reduced their invasiveness. On the other hand, they found that knockdown of PSMA in the PSMA-positive cell line, LNCaP, increased their invasiveness five-fold. PSMA mutants lacking the carboxypeptidase activity of the protein were produced and showed that this reduced the impact of PSMA expression on invasiveness. Another study involving the injection of the mouse prostate cancer cell line RM-1 with stable expression of PSMA into mice showed the formation of lytic bone lesions and distinct MMP9 expression compared to the control (Zhao et al., 2012).

It was found that the sequential digestion of laminin, a predominant component of the extracellular matrix (ECM), occurs through PSMA working downstream of MMP2, generating small peptides which enhance the invasive and adhesive abilities of HUVECs *in vitro*, providing evidence that these peptides activate adhesion through integrin $\alpha_6\beta_1$ and focal adhesion kinase (FAK). It was suggested that since PSMA is a glutamate-specific peptidase, cleavage of a laminin-

derived peptide substrate could modify the overall charge of the peptide and so facilitate integrin binding (Conway et al., 2006).

1.6 The matrix metalloproteinases (MMPs)

i. The extracellular matrix

The extracellular matrix (ECM) is a structural support network, involved in the maintenance of all cells (Hynes, 2009). It is known that the ECM plays a role in many cellular processes including cell proliferation (Hynes, 2009), differentiation (Discher et al., 2005) and migration (Pelham and Wang, 1997). The ECM is the non-cellular element of tissues, sometimes likened to the 'glue' that links cells together, where it is a principal constituent of tissues (Rolfe and Grobbelaar, 2012). The ECM is composed of proteins, such as collagens (Kim et al., 2011b), elastins (Eckes et al., 2010), fibronectin (Tanzer, 2006), laminins (Tanzer, 2006), tenascins (Eckes et al., 2010), growth factors (Eckes et al., 2010, Kim et al., 2011b) and MMPs (Streuli, 1999, Page-McCaw, 2008).

The multiple components of the ECM are organised into a distinguishable three-dimensional (3D) structure, which can be separated into two components, the basement membrane (BM) and interstitial matrix.

The ECM is recognised as an active environment, constantly experiencing changes in composition and structure. These changes occur in response to actions and signals from the surrounding cells. As a consequence, the communication between cells and the ECM is

vital to understanding how these two components of tissues respond and learn to adapt to one another (Kular et al., 2014).

The basement membrane

The main components of the BM include fibronectins, laminins and collagen type IV. The latter provides the tissue with tensile strength. The BM is known to be more dense and 'less porous' than the interstitial matrix (Lu et al., 2012). The BM is found in blood vessels, epithelial and endothelial tissues, forming an extremely orderly network, with the epithelial tissues being highly dependent on the BM in order to conduct its expected role (Kim et al., 2011b). Integrin between the BM and the cells lying above convey messages regarding cell shape and motility (Tanzer, 2006).

The interstitial matrix

The interstitial matrix occurs in the same places as the BM; however, it is also found between connective tissue cells, such as those within the tendon. The major elements which form this component of the ECM are collagens, elastin and fibronectin, creating a '3D amorphous 'gel'. Despite collagen composing the majority of the fibrous proteins within this matrix, it is fibronectin which dictates the organisation of the matrix structure. Every tissue within the body exhibits its own characteristic ECM, fit for the purpose needed (Frantz et al., 2010).

ii. Role of the MMPs

The MMPs are members of the large metzincin superfamily. In a classical sense, MMPs work together to degrade all components of the ECM and the BM. Recently, substrate identification studies have shown that MMPs can regulate the release or activation of antibiotics factors, chemokines, cytokines, growth factors and other bioactive molecules, and therefore are able to participate in physiological processes such as angiogenesis, bone remodelling, innate and adaptive immunity, inflammation and neurite growth (Loffek et al., 2011).

High sequence similarity in the MMP catalytic domains is found in almost all species tested. At least 25 different vertebrate MMPs have been characterised up to now and 24 different MMPs are found in humans. The diversity of the current mammalian MMP gene family is thought to be due to extensive gene tandem duplication and exon shuffling during evolution in the tetrapod lineages. Taking this into account, some of the MMP members are most likely derivatives from a single gene resulting in an MMP gene cluster, whose organisation is preserved from amphibians to mammals. The cluster in the human genome is located on chromosome 11q22 and contains MMP1, MMP3, MMP7, MMP8, MMP10, MMP12, MMP13, MMP20 and MMP27. In contrast, most of the other human MMPs are located on other chromosomes, resulting in a total of 10 distinct chromosomal

locations for all 24 human MMP genes (Loffek et al., 2011, Fanjul-Fernandez et al., 2010).

Though MMP activity has been shown to be essential in many cell biological processes and various fundamental physiological events involving tissues remodelling, such as angiogenesis, wound healing, bone development and mammary involution (Page-McCaw et al., 2007), the real interest in MMPs comes from their role in several pathological conditions, such as cancer and chronic inflammatory diseases (Lopez-Otin and Matrisian, 2007).

Regulation of the MMPs

Due to their wide substrate spectrum, MMPs are integrated as important regulators of tissue homeostasis and immunity in the networks of multidirectional communication within tissues and cells. Uncontrolled MMP activity can easily become destructive to cells and tissues and so their action must be tightly regulated.

The catalytic activity of the MMPs is highly controlled at four different levels:

- 1) Gene expression with transcriptional and post-transcriptional regulation
- 2) Compartmentalisation of the MMPs
- 3) Pro-enzyme activation by removal of the pro-domain

- 4) Inhibition by specific inhibitors e.g. tissue inhibitors of matrix metalloproteinases (TIMPs) and by non-specific proteinase inhibitors e.g. α_2 -macroglobulin.

Once active, MMPs can modulate the global proteolytic potential in the extracellular milieu through zymogen (pro-form MMP) activator and inhibitor degradation (Overall and Lopez-Otin, 2002, Ra and Parks, 2007, Loffek et al., 2011).

Control of MMPs at gene level

Although MMP gene expression is chiefly regulated at transcriptional level, post-transcriptional control of mRNA stability also occurs, through the action of cytokines, nitric oxide or miRNA.

Despite the low expression of most MMPs under quiescent conditions, their transcription is tightly controlled and individually regulated. No solitary chemokine, cytokine, oncogene growth factor has been found which is solely responsible for the overexpression of MMPs in certain tumours, though tumour necrosis factor (TNF)- α and IL-1 are often implicated. The signal transduction pathway which modulates MMP promoter activities are also diverse. Several of the MMP promoters share multiple cis-elements in their promoters regions, consistent with observations that some MMPs are co-regulated by various inductive stimuli (Vincenti and Brinckerhoff, 2007).

Interestingly, it has been exhibited that promoters of functionally related MMPs such as MMP2/MMP9 (gelatinases) or MMP1/MMP8 (collagenases) are distinct, indicating different activation pathways. Based on their cis-elements, MMP promoters are categorised into three groups (Yan and Boyd, 2007). The first represents the vast majority of MMP promoters and contains a TATA box and AP-1-binding site close to the transcription start site and is very often combined with an upstream PEA3-binding site, for the control of MMP transcription via several cytokines and growth factors, such as VEGF, keratinocyte growth factor or TNF- α . The second group (promoters for MMP8, MMP11 and MMP21) also contain a TATA box but lack the proximal activator protein (AP-1) site. The regulation of these promoters is fairly simple and distinct from the first type of promoter. The final group of promoters (including MMP2, MMP14 and MMP28) does not comprise a TATA box and, therefore, transcription from these promoters begins at multiple sites. Additionally, expression of MMPs in this group is mainly determined by the ubiquitous Sp-1 family of transcription factors which bind to a proximal GC box. Expression of these MMPs is usually constitutive, which is only slightly sensitive to induction by growth factors or cytokines (Chakraborti et al., 2003).

Transcriptional control of the MMPs is also most likely to be additionally influenced by epigenetic mechanisms such as DNA methylation and/or chromatin remodelling with histone

acetylation. DNA methylation of cytosines within CpG islands in the promoter region represses chromatin state and thus inhibits gene expression. Therefore, hypomethylation of MMP promoters can lead to increased enzyme expression in cancers (Loffek et al., 2011).

Post-transcriptional gene regulation has also been shown to be important in the regulating the expression of MMPs, with MMP2, MMP9 and MMP13 also being shown to be regulated through mRNA stability (Yan and Boyd, 2007, Clark et al., 2008).

Pro-MMP activation

MMPs are initially produced as inactive pro-forms (zymogens) which are inactivated through removal of a pro-domain. The pro-domains holds a conserved “cysteine switch” sequence motif which sits close to the catalytic domain, whose free cysteine residue interacts with the catalytic zinc ion to maintain enzyme latency and prevent binding and cleavage of the substrate (Van Wart & Birkedal-Hansen, 1990). A conformational activation of the MMP zymogen in the pro-domain leads to a conformational activation, which removes the cysteine residue from the site, allowing water to interact with the zinc ion in the active site. This event can be initiated by three mechanisms:

- 1) Direct cleavage of another endopeptidase through removal of the pro-domain
- 2) Allosteric reformation of the pro-domain

- 3) Chemical modification of the free cysteine by reaction oxygen species or non-physiological agents

Later events, allosteric control and reduction of the free cysteine also enables the enzyme to remove its own pro-domain by autoproteolysis (Ra and Parks, 2007).

Eleven of the 24 MMPs in human, including all of the membrane-bound MMPs, are activated through an intracellular process via pro-protein convertases or furins. Furins are transmembranous subtilisin-like serine proteinases in the trans-Golgi network which is responsible for sorting secretory pathway proteins to their final destination, including the cell surface and secretory granules. Consequentially, all these members of the MMP family can instantly begin their catalytic action either on the cell surface or when secreted into the pericellular environment.

The remaining MMP members are expressed and secreted as inactive pro-forms, which must be activated. The activation of pro-MMPs is thought to be a stepwise process which takes place in the immediate pericellular space. The first step involves an initial conformational change within the pro-peptide, leading to a disruption of the cysteine switch-zinc interaction. Successively, the pro-domain is removed by intra- or intermolecular processing of partially activate MMP intermediates or other active MMPs (Van Wart and Birkedal-Hansen, 1990).

An alternative method by which the zymogens are activated is probably initiated by the intrinsic allostery of the MMP molecule. Consequently, domain flexibility of the modular domain of the MMP can contribute through promotion of long-range conformational transitions induced by protein binding via exosites (Sela-Passwell et al., 2010).

Tissue Inhibitors of MMPs (TIMPs)

It is a recognised view that the balance between the production of active enzymes and their inhibition is critical to avoid the conditions of uncontrolled ECM turnover, inflammation and dysregulated cell growth and migration, which would result in disease (Loffek et al., 2011).

The naturally occurring inhibitors of human MMP activity are the four TIMPs. Each TIMP molecule consists of around 190 amino acids with two distinct domains: a large N-terminal and a smaller C-terminal domain, each one stabilised by three conserved disulphide bonds. The N-terminal can fold independently and is fully functional to inhibit MMPs by chelated their catalytic zinc atom with a 1:1 molar ratio. The function of the C-terminal is not fully understand but has been shown to bind tightly to the haemopexin domain of latent MMPs. TIMP2, TIMP3 and TIMP4 have been described to interact with MMP2 and TIMP1 and TIMP3 with MMP9 (Murphy and Nagase, 2008, Loffek et al., 2011).

In general, all TIMPs are broad spectrum inhibitors of MMPs, but there are difference in their specificity. For example, TIMP1 has been shown to have low inhibitory activity against MMP19 and MMP14 while it is more potent against MMP3 and MMP7 than the other TIMPs. TIMP2 inhibits the activity of all of the MMPs and its expression of constitutive, in contrast to the other TIMP family members, which are inducible (Loffek et al., 2011).

iii. MMPs and cancer

The MMPs have been considered as a potential diagnostic and prognostic biomarker in many forms of cancer (Roy et al., 2009) and the notion of these enzymes being used as therapeutic targets was introduced many years ago due to their involvement in the metastatic potential of various cancer (Noel et al., 2008, Murphy and Nagase, 2008).

During the development to malignancy, tumour cells are involved in several interactions with the tumour microenvironment, involving the ECM, growth factors and cytokines, as well as surrounding cells such as macrophages, neutrophils, endothelial cells and fibroblasts (Kessenbrock et al., 2010, Murphy and Nagase, 2008). Four of the hallmarks of progressive cancer (migration, invasion, angiogenesis and metastasis) are dependent on the surrounding environment. MMPs are critical to these processes as they degrade adhesion molecules and thus modulate cell-cell and cell-ECM interactions (Gialeli et al., 2011).

MMP and cancer cell invasion

The ECM is a dynamic structure which can orchestrate cell behaviour by interacting with them. MMP proteolytic activity is required for cancer cell degradation of the physical barriers during local expansion as well as intravasation at nearby blood vessels, extravasation and invasion at a distant location. During this invasive process, localisation of MMPs to specialised cell surface structures, called invadopodia, is requisite for their ability to promote cancer cell invasion. Invadopodia are where ECM degradation takes place and they utilise transmembrane invadopodia-related proteinases such as MMP14, as well as secreted and activated MMPs at the site, such as MMP2 and MMP9 (Weaver et al., 2006, Gialeli et al., 2011).

MMPs and cancer cell proliferation

MMPs can modulate the bioavailability of growth factors and function of cell-surface receptors. Moreover, several MMPs (MMP1,2,3,7,9,11 and 19) cleave insulin growth factor (IGF)-binding proteins which also regulate growth factor availability (Nakamura et al., 2005, Gialeli et al., 2011).

MMPs and cancer cell apoptosis

Enzymes which degrade matrices confer both apoptotic and anti-apoptotic activities. MMPs confers anti-apoptotic signals to cancer

cells by cleaving Fas ligand, a transmembrane stimulator of Fas death receptor, from the cell surface. This activity inactivates this receptor and, in cancer cells, induces a resistance to apoptosis and chemoresistance. It can also promote apoptosis in the neighbouring cells (Strand et al., 2004, Mitsiades et al., 2001, Kirkin et al., 2007). It is also thought that MMPs may show an anti-apoptotic effect through indirectly activating AKT (Gialeli et al., 2011, Kulik et al., 1997). However, MMPs are also known to promote apoptosis, usually through change of the ECM composition e.g. cleavage of laminin, which affects integrin signalling (Sympson et al., 1994, Gialeli et al., 2011).

MMPs and tumour angiogenesis and vasculogenesis

The MMPs play a double role in the tumour vasculature as they can act to both positively and negatively regulate angiogenesis depending on the time points of expression during tumour angiogenesis and vasculogenesis, as well as the bioavailability of substrates. Key players in tumour angiogenesis are MMP2, 9 and 19 (Rundhaug, 2003, Gialeli et al., 2011).

In order for new vessels to form, it is vital that ECM degradation occurs and, subsequently, to generate pro-angiogenic factors. MMP9 participates in the angiogenic switch due to the increase in the availability of important factors in this process, such as VEGF (Xu et al., 2001, Gialeli et al., 2011).

However, the angiogenic balance is highly regulated by MMPs since they can also downregulate the formation of new blood vessels through generation of degradation fragments which can inhibit angiogenesis (Iozzo et al., 2009, Gialeli et al., 2011).

MMPs and cell adhesion and migration

Movement of cells is related to the proteolytic activity of MMPs, regulating the dynamic ECM-cell and cell-cell interactions during migration. In the beginning, degradation of the ECM leads to cryptic peptide generation which promote the migration of cancer cells (Xu et al., 2001, Koshikawa et al., 2000). Several integrins also play a role in the regulation of cell migration as they can serve as MMP substrates (Baciu et al., 2003, Gialeli et al., 2011).

1.7 Protein kinase B (AKT)

i. The role of the PI3K/AKT/mTOR pathway in the cell

Various cytokines and growth factors can not only promote cell proliferation but also maintain the viability of cells. The binding of these factors to receptors initiates a signalling cascade leading to the activation of the lipid kinase PI3K, and the generation of the second messengers phosphatidylinositol (3,4,5)-triphosphate PIP3 recruits protein kinases, including AKT (also known as protein kinase B) and its upstream activators pyruvate dehydrogenase kinases (PDK1 and PDK2) (Martini et al., 2014).

AKT is a serine/threonine kinase which has emerged as a vital central node of signalling within all cells of higher eukaryotes and thus is one of the most important and versatile protein kinases at the core of human physiology and disease (Manning and Cantley, 2007). This pathway is a key component of growth factor-induced cell survival and has been implicated in the suppression of apoptosis in a number of cell types, through a variety of stimuli, including growth factor withdrawal, cell cycle discordance, loss of cell adhesion, DNA damage and treatment with anti-Fas antibody or transforming growth factor β (TGF β) (Brunet et al., 2001, Feng et al., 2004a). The PI3K/AKT pathway is highly conserved and its activation is tightly controlled through a multistep process (Hemmings and Restuccia,

2015). Phosphorylation of AKT at serines 308 and 473 activates the kinase and allows its release from the membrane, leading to an interaction with a range of cytoplasmic and nuclear substrates (Feng et al., 2004a). AKT-mediated phosphorylation is involved in many cell processes, including survival, growth, proliferation, glucose uptake, metabolism and angiogenesis. *AKT* is now known to include a family of three closely related, highly conserved cellular homologs, terms *AKT1*, *AKT2* and *AKT3*. The encoded proteins are serine/threonine kinases which belong to the protein kinase B (PKB) family (Testa and Bellacosa, 2001, Testa and Tsihchlis, 2005).

Akt activates the downstream mTOR kinase through inhibition of a complex formed by tumour suppressor proteins tuberous sclerosis 1 and 2 (TSC1 and TSC2), also known as hamartin and tuberin (Altomare and Testa, 2005). mTOR generally mediates cell growth and proliferation through regulation of ribosomal biogenesis and protein translation (Ruggero and Sonenberg, 2005) and has the ability to regulate nutrient response by restriction of progression through the cell cycle in the presence of suboptimal growth conditions (Plas and Thompson, 2005).

ii. The dysregulation of AKT in cancer

Studies have shown that the PI3K/AKT signalling pathway components are frequently altered in cancer. This pathway regulates cell proliferation and survival, cell growth (size), glucose metabolism, cell motility and angiogenesis (Testa and Tsihchlis, 2005).

Following the identification of AKT activation as an important contributor to tumourigenesis, intense research began into the regulation of this pathway. In recent years, it has been shown that this pathway plays a role not only in tumour development but also in the tumour's response to cancer treatment (Hemmings and Restuccia, 2015).

AKT has been shown to be a central node in many cellular processes which are dysregulated in the development of progression of cancer and aberrant AKT signalling is implicated in many sporadic human cancers (Altomare and Testa, 2005, Bellacosa et al., 2005).

In addition, AKT is known to phosphorylate and inactivate the FOXO transcription factors, which mediate the expression of genes for apoptosis, such as the Fas ligand gene (Pommier et al., 2004, Altomare and Testa, 2005).

AKT has also been shown to mediate cell cycle progression through the phosphorylation and consequent inhibition of glycogen synthase kinase 3 β to avert cyclin D1 degradation (Liang and Slingerland, 2003). Additionally, AKT directly antagonises the action of cell cycle inhibitors by phosphorylating a site located near their NLS to induce cytoplasmic retention of these inhibitors (Bellacosa et al., 2005, Testa and Bellacosa, 2001). Moreover, phosphorylation of the AKT/mTOR kinases also results in an increase in translation of cycle D1, D4 and E transcripts (Muisse-Helmericks et al., 1998, Altomare and Testa, 2005).

Recently, the involvement of the PI3K-AKT pathways in MMP regulation has been studied more thoroughly and AKT has been found to stimulate cell migration through its upregulation the secretion of MMP9 in fibrosarcomas (Kim et al., 2011b). In addition, two other studies found that the MMPs are regulated by AKT, with one showing that AKT activation was correlated with MMP2 induction (Park et al., 2006) and another showing that, in ovarian cancer cells, PI3K-Akt mediates the fibronectin-dependent secretion of MMP9 (Thant et al., 2000). A study by Zhang and Brodt in lung carcinoma cells (Zhang and Brodt, 2003) extended our knowledge of its mechanism, finding that PI3K-AKT plays an important role in the regulation of membrane type 1 matrix metalloproteinase (MT1-MMP) activation by the receptor for insulin-like growth factor (IGF-IR) and its ligands (IGFI and II). MT1-MMP activates MMP2 and contributes directly to the invasive capacity of cells through degradation of collagen 1 and the adhesion molecule CD44 (Kohn and Liotta, 1995, Liotta and Kohn, 2001). Another study presented a novel AMP-activated protein kinase (ARK5) as a downstream effector of AKT-induced tumour cell invasion which is also involved in MMP2 and MMP9 production (Suzuki et al., 2004).

iii. Possible links of AKT to MDM2 and PSMA

Several recent studies have also shown that p53-mediated apoptosis is inhibited under conditions in which the PI3K-AKT pathway is activated (Sabbatini and McCormick, 1999, Yamaguchi et al., 2001,

Mazzoni et al., 1999, Hong et al., 1999, Gottlieb et al., 2002). It is thought that AKT may inhibit p21 (a cyclin-dependent kinase inhibitor) expression through its phosphorylation and subsequent activation of MDM2, leading to a downregulation of p53-mediated transcription of p21 (Mayo and Donner, 2001, Zhou et al., 2001). It could be that PI3-AKT signalling is required but perhaps is not sufficient, to wholly account for the role of MDM2 in p53 protein level regulation (Mayo and Donner, 2001).

Around 20% the amino acids comprising MDM2 are either serine or threonine residues and MDM2 is thus phosphorylated at multiple sites *in vivo* (Meek and Knippschild, 2003). Two clusters of phosphorylation sites occur on MDM2, one at the amino terminal (amino acids 1-193) and the other in the central domain (amino acids 194-293) (Hay and Meek, 2000). It has been shown that AKT and MDM2 can interact directly and that human MDM2 contains putative AKT phosphorylation sites (serine 166, 186 and 188). These motifs are proximal to the NLS and NES of MDM2 and are conserved in human, mouse, hamster and zebrafish, indicating a functional importance of these sites. Downstream of the phospho-acceptor serine or threonine is a structural amino acid (serine, threonine), glycine or proline, which induces a tight turn in the peptide, providing the optimal structure for AKT recognition. It was also suggested that MDM2 nuclear entry is reliant on PI3-kinase/AKT signalling and this signalling plays a role in p53 functional suppressor and degradation (Mayo and Donner, 2001, Zhou et al., 2001). Although AKT is best

known for promoting cell survival and growth, it can also stimulate proliferation through multiple downstream targets impinging on cell-cycle regulation.

Moreover, a study by Feng *et al.* (Feng *et al.*, 2004b), showed that AKT phosphorylation of sites serine 166 and 188 (no phosphorylation was seen at serine 186) inhibits MDM2 self-ubiquitination and thus stabilises the protein. This self-ubiquitination feature of MDM2 is important for the regulation of protein levels in cells (Honda *et al.*, 1997, Honda and Yasuda, 1999, Fang *et al.*, 2000). Similar data were gained from another group (Ashcroft *et al.*, 2002), who indicated that phosphorylation of MDM2 by AKT increased the ability of MDM2 to target p53 for ubiquitin-dependent degradation. The group also showed a correlation of AKT phosphorylation with MDM2 protein stability. Furthermore, a third study suggested that AKT enhances the ubiquitination-promoting function of MDM2 by phosphorylating ser186, which results in a reduction of p53 protein (Ogawara *et al.*, 2002). This work is backed up by data from human tumour cells where overexpression of AKT correlated with elevated levels of MDM2 phosphorylation (Feng *et al.*, 2004b).

PSMA has also been linked to phosphorylation of AKT at serine 473, with Guo *et al.* (Guo *et al.*, 2014) showing that, following knockdown of PSMA, the levels of phospho-AKT decreased, but total AKT levels remained the same. Therefore, the group surmised that AKT phosphorylation at serine 473 may play a critical role as a downstream signalling target effector of PSMA.

1.8 The possible interplay between MDM2 and PSMA in cancer

Recently, a paper was published which links the expression levels of PSMA and MDM2. Xu *et al.* (Xu *et al.*, 2013) used the LNCaP (PSMA positive) and PC3 (PSMA negative) prostate cancer cell lines to assess metastasis-related genes which were downregulated in cells with silenced PSMA. It was found that MDM2 decreased over 80 fold. The paper also indicated that the treatment of the LNCaP cell line with PSMA-targeted siRNA led to an upregulation of MMP3 and 13, and a downregulation of MMP2. Since the degradation of the extracellular matrix and basement membrane by MMPs is pivotal to whether a tumour infiltrates and metastases, it may be deduced that PSMA and MDM2 are involved in the regulation of MMP secretion and they may interplay in order to modify their levels. This theory is supported by the many reports linking both proteins to a number of MMPs (Conway *et al.*, 2006, Yang *et al.*, 2006, Rajabi *et al.*, 2012, Chen *et al.*, 2013) and we hypothesise that this interplay may be mediated by AKT.

1.9 Aims & objectives

Although scientists now understand the general principles of the progressive properties of cancer, the molecular mechanisms behind how early cancer becomes metastasis is still not well understood. It is vital that we gain an understanding of the underlying processes in order to design specific therapeutics targeting the molecular dysregulation occurring.

It was recently seen that a decrease in *MDM2* gene expression followed PSMA knockdown. Also, MDM2 and PSMA are implicated in similar pathways, including the PI3K/AKT pathway. It has been shown that AKT and MDM2 can interact directly through phosphorylation and that human MDM2 contains putative AKT phosphorylation sites (serines 166, 186 and 188). PSMA has also been linked to AKT serine 473 phosphorylation, with knockdown of PSMA leading to a decrease in the phosphorylation levels at this site. MDM2, PSMA and the AKT have also been linked to various MMPs (-2, -9).

Additionally we identified c-JUN as a potential link of MDM2 and PSMA using GeneMANIA, an online gene function prediction tool.

We hypothesise that there is a link between MDM2 and PSMA in breast cancer cell lines, through AKT or c-JUN phosphorylation, which may lead to a change in MMP secretion levels.

The aims of this study were:

1. To screen and identify the expression profile of MDM2 and PSMA in breast cancer cell lines in order to select cell models for knockdown.
2. To induce siRNA-mediated knockdown of MDM2 and PSMA in both of these molecules.
3. To identify the roles of each of the molecules in the functionality of breast cancer cells.
4. To assess the underlying signalling pathways of these functional changes and the involvement of the MMPs.
5. To evaluate the role of AKT and c-JUN phosphorylation in the downstream signalling pathways of both MDM2 and PSMA.

Chapter II

Materials & Methods

Statement of undertaking

All experiments in this thesis were undertaken by Robyn Bradbury, apart from collection of breast cancer tissue and subsequent RNA isolation and quantitative PCR. Statistical analysis of breast cancer cohort data was done by Professor Wen Jiang.

2.1. Materials

2.1.1. Cell lines

The current study used eight breast cancer cell lines (BT-20, MCF-7, ZR-75.1, SK-Br-3, BT-483, MDA-MB-468, BT-549 and MDA-MB-231) and one immortalised normal breast cell line (MCF-10A), all purchased from American Type Culture Collection (ATCC; Middlesex, UK). Human microvascular endothelial cells from adult dermis (HMVECad) were purchased from ThermoFisher (Waltham, MA, USA). All cancer cells were maintained in Dulbecco's Modified Eagle's Medium (DMEM; ThermoFisher); apart from BT-483 and BT-549 which were maintained in RPMI-1640 media (ThermoFisher). Both media were supplemented with 10% foetal bovine serum (FBS) and 1 x antibiotic cocktail mix (penicillin/streptomycin). MCF-10A cell line was maintained in MEBM media supplemented with MEGM kit (Lonza, Tewkesbury, UK) and 100 ng/ml cholera toxin (Sigma-Aldrich, Poole, Dorset, UK). The HMVECad cell line was maintained in 131 Media (ThermoFisher) with microvascular growth supplements (all MVGS; Gibco, Paisley, UK) (The cell lines used in the current study are outlined in Table 2.1).

Table 2.1. Details of cell lines used in study. Alphabetical list of those cells lines used throughout study, with those chosen for usage in further experiments shown in **bold**.

Cell Line	Origin	Cell morphology	Site
BT-20	74 year old Caucasian female	Epithelial	Primary tumour
BT-483	23 year old Caucasian female	Epithelial	Primary tumour
BT-549	72 year old Caucasian female	Epithelial	Primary tumour
HMVECad	Unknown	Endothelial	Skin vasculature
MCF-10A	36 year old Caucasian female	Epithelial	Primary
MCF-7	69 year old Caucasian female	Epithelial	Pleural effusion
MDA-MB-231	51 year old Caucasian female	Epithelial	Pleural effusion
MDA-MB-468	51 year old Black female	Epithelial	Pleural effusion
SK-Br-3	43 year old Caucasian female	Epithelial	Pleural effusion
ZR-75.1	64 year old Caucasian female	Epithelial	Ascites

2.1.1. Collection of human breast cancer tissues

148 fresh breast tissue samples were collected immediately after surgery and stored at -80°C until use, with approval of the Bro Taf Health Authority local research ethics committee (01/4304; approval letter in Appendix). The cohort contained 30 normal background breast tissue and 112 breast cancer tissue samples. All patients provided written consent.

Specimens were verified by a consultant pathologist and a routine follow-up was carried out after surgery and details were stored in a database. The median follow-up period was 120 months.

Section stored Samples were prepared in 1 ml TRI reagent and homogenised for 2 minutes. RNA extraction could then be undertaken as normal.

2.1.2. siRNA

MDM2-, FOLH1- and Non-Targeting ON-TARGETplus siRNA reagents were obtained from Dharmacon (Layfayette, CO, USA). Dry siRNA pellet was diluted to a 20 µM stock using 1 x siRNA buffer (Dharmacon). 20 µl aliquots were produced to prevent degradation through freeze-thaw and stored at -20 °C for long-term storage.

2.1.3. Primers

All primers used in the study were synthesised by Sigma-Aldrich and diluted upon receipt according to data sheet from the company.

Primers were stored at -20 °C. Details of primers used for quantitative polymerase chain reaction (qPCR) are detailed in Table 2.2.

2.1.4. Antibodies

Primary Antibodies

Details of primary antibodies used in the study are given in Table 2.3.

Secondary Antibodies

The secondary antibodies used in the western blotting procedure in this study were horseradish peroxidase (HRP) conjugated anti-mouse (A9044) and anti-rabbit (A0545) IgG antibodies, both purchased from Sigma-Aldrich.

2.1.5. Inhibitors

Marimastat (CAS 154039-60-8; Santa Cruz Biotechnology, Dallas, TX, USA) and ARP100 (CAS 704888-90-4; Santa Cruz Biotechnology) were used to inhibit MMP2 protein activity.

Marimastat was diluted in dimethylsulphoxide (DMSO; Sigma-Aldrich) to a 1 mM stock concentration, whilst ARP100 was diluted in DMSO to a 10 mM stock concentration. MMP8 inhibitor I (CAS 236403-25-1; Santa Cruz Biotechnology) was used to inhibit MMP8 activity and was diluted in DMSO to a 1 mM stock concentration. LY 294002 hydrochloride (TOCRIS Bioscience, Bristol, UK) was used to

inhibit PI3-kinase activity and indirect phosphorylation of AKT (serine 473) and was controlled by LY 303511, an inactive analogue (TOCRIS Bioscience). Both compounds were diluted to 25 mM in DMSO. All diluted inhibitors were stored at -20 °C. When being further diluted for experimental purposes, the inhibitors were diluted in DMEM media (with or without serum, depending on experiment), and used alongside a DMSO control containing an equal volume of DMSO as present in the inhibitor treatment. All inhibitors were used at concentration suggested by manufacturer.

Table 2.2. Primer sequences for all genes assessed through quantitative PCR (qPCR). zReverse indicates those primers with the addition of a Z-sequence (**ACTGAACCTGACCGTACA**) to the 5' end of the respective primers.

Target Gene	Direction	Sequence
AKT	Forward	CTACTACGCCATGAAGATCC
AKT	zReverse	GGTCTGGAAAGAGTACTTCAG
Caspase 3	Forward	GGCGTGTCATAAAATACCAG
Caspase 3	zReverse	ACAAAGCGACTGGATGAA
Caspase 7	Forward	ACTTTTGTTCGCTTTCGC
Caspase 7	zReverse	TGATCATCTGCCATCGTTC
Caspase 8	Forward	AGAAAGGAGGAGATGGAAAG
Caspase 8	zReverse	GACCTCAATTCTGATCTGCT
Caspase 9	Forward	AAGCCCAAGCTCTTTTC
Caspase 9	zReverse	GTTACTGCCAGGGGACTC
GAPDH	Forward	AAGGTCATCCATGACAACCTT
GAPDH	zReverse	GCCATCCACAGTCTTCTG
JUN	Forward	AAGATCCTGAAACAGAGCAT
JUN	zReverse	GCTGGACTGGATTATCAGG
MDM2	Forward	GTTATCTCAGTGCCTTTTGC
MDM2	zReverse	AACAGACACATGTTCTACCC
MMP1	Forward	GGATGCTCATTTTGATGAAG
MMP1	zReverse	TAGAATGGGAGAGTCCAACA
MMP2	Forward	CAGGGAATGAGTACTGGGTCTATT
MMP2	zReverse	ACTCCAGTTAAAGGCAGCATCTAC
MMP3	Forward	TCTGAGGGGAGAAATCCTGA
MMP3	zReverse	GGAAGAGATGGCCAAAATGA
MMP7	Forward	AAATGGACTTCCAAAGTGGT
MMP7	zReverse	TTCCCATACAACTTTCTCTG
MMP8	Forward	AAACTGTTTCAGGACTACCT
MMP8	zReverse	ATCGCTGCATTTCTTTAAGC
MMP9	Forward	AACTACGACCGGGACAAG
MMP9	zReverse	GGAAAGTGAAGGGGAAGA

MMP10	Forward	CATTCAGTCTCTCTACGGAC
MMP10	zReverse	CCGAAGGAACAGATTTTGTG
MMP11	Forward	GTGCCCTCTGAGATCGAC
MMP11	zReverse	CAGGGTCAAACCTCCAGTAG
MMP12	Forward	ACCCACGTTTTTATAGGACC
MMP12	zReverse	GATAACCAGGGTCCATCATC
MMP13	Forward	TCCCAGGAATTGGTGATAAAGTAGA
MMP13	zReverse	CTGGCATGACGCGAACAATA
PSMA	Forward	ATTGCTCTGGGAAAATTGTA
PSMA	zReverse	AGGAGCAAAGTAGTCAGCAG
TIMP1	Forward	CTTCACCAAGACCTACACTG
TIMP1	zReverse	TTTGCAGGGGATGGATGGATAAAC
TIMP2	Forward	ATGCAGATCTAGTGATCAGG
TIMP2	zReverse	TATATCCTTCTCAGGCCCTT

Table 2.3. Primary antibodies used in western blotting protocol.

Antibody	Code	Company	Species	Dilution
AKT	sc 5298	Santa Cruz	Mouse	1:200
Phospho-AKT (ser473)	sc 81433	Santa Cruz	Mouse	1:200
Caspase-3	sc 7148	Santa Cruz	Rabbit	1:200
Caspase-8	sc 70501	Santa Cruz	Mouse	1:200
Caspase-9	sc 17784	Santa Cruz	Mouse	1:200
GAPDH	sc 32233	Santa Cruz	Mouse	1:10,000
MDM2 (SMP14)	sc 965	Santa Cruz	Mouse	1:200
Phospho-MDM2 (ser166)	3521	Cell Signalling	Rabbit	1:1000
Phospho-MDM2 (ser186)	Ab22710	Abcam	Mouse	1:500
Phospho-MDM2 (ser186/188)	Ab111617	Abcam	Rabbit	1:200
PSMA (D718E)	12815	Cell Signalling	Rabbit	1:1000

2.2. Standard reagents and solutions

2.2.1. Solutions for use in laboratory

Diethylpyrocarbonate (DEPC) Water

500 µl Diethylpyrocarbonate (DEPC; Sigma-Aldrich) was made up to 500 ml using deionised H₂O. The solution was left overnight and then autoclaved.

2.2.2. Solutions for use in cell culture

Phosphate buffered saline (PBS)

50 ml of 10x stock of PBS (Sigma-Aldrich) was diluted with 450ml of distilled water, and then autoclaved.

100x Antibiotic Cocktail Mix

5 g streptomycin, 3.3 g penicillin and 12.5 g amphotericin B in DMSO were dissolved in PBS and filtered. 5 ml was then added to a 500 ml bottle of media.

2.2.3. Solutions for use in western blotting

RIPA Buffer

0.61 g Tris base was added to 75 ml distilled H₂O. 0.88 g of NaCl and 0.19 g EGTA were then added to the solution and stirred until all solids were dissolved. The pH value was adjusted to 7.5 using HCl. 1ml of Triton x100 was then added and stirred until dissolved. Finally

2. Materials & Methods

250ml of 400 mM EDTA solution was added and the volume was adjusted to 100 ml using distilled H₂O. The RIPA buffer was stored at 2-8 °C until ready to use. Upon requirement of cell lysis, protease inhibitors were added to the basic RIPA. For each 1 ml needed, 10 µl aprotinin (1 mg/ml), 10 µl leupeptin (1mg/ml), 10 µl sodium vanadate (1 mg/ml) and 20 µl of sodium fluoride (1 mg/ml) (all bought as powder from Sigma-Aldrich) was added to 940 µl of basic RIPA buffer. Just before use on cells, 10 µl phenylmethylsulfonyl fluoride (PMSF; 10 mg/ml) (Sigma-Aldrich) was added to the solution. 50 µl of RIPA buffer was used to lyse cells covering one well of a six-well plate.

10% w/v Ammonium Persulphate (APS)

1 g APS (Melford Laboratories Ltd, Suffolk, UK) was dissolved in 10 ml distilled water and then stored at 4 °C for further use.

Tris Buffered Saline (TBS)

10% w/v TBS (0.5M Tris, 1.38 M NaCl, pH7.4) stock solution was prepared by dissolving 606 g of Tris (Sigma-Aldrich) and 765 g of NaCl (Melford Laboratories Ltd) in 10 litres distilled water. The pH was adjusted to 7.4 using HCl (Sigma-Aldrich) and stored at room temperature.

0.1% v/v TBS/Tween (TBST)

1ml of Tween 20 (Sigma-Aldrich) was added to 1 litre of TBS, prepared as detailed above.

Running Buffer

1 litre of 10 x TRIS/glycine/SDS (T7777) (Sigma-Aldrich) was added to 9 litres of distilled H₂O.

Transfer Buffer

1 litre of 10 x TRIS/glycine concentrate (Sigma-Aldrich) was added to 2 litres of methanol (ThermoFisher) and 7 litres of distilled H₂O.

2.2.4. Solutions for use in immunocytochemical staining

Diaminobenzidine (DAB) chromogen

2 drops (approximately 50 µl) of wash buffer, 4 drops of DAB (Vector Laboratories, Inc., Burlingame, CA, USA) and 2 drops of H₂O₂ were added to 5 ml of distilled water and mixed well before use.

ABC Complex

The ABC complex was prepared by using a kit provided by Vector Laboratories Inc. 4 drops of each reagent A and B were added to 20ml of wash buffer before being mixed thoroughly and left at room temperature for 30 minutes before use.

2.2.5. Solutions for use in flow cytometric staining

Wash buffer

The wash buffer was produced through dissolving 2 mM EDTA (Sigma-Aldrich) in PBS.

FACS Buffer

FACS buffer was created through adding 5% v/v FCS to wash buffer.

Blocking Buffer

Blocking buffer was prepared by adding 1% v/v bovine serum albumin (BSA) (Sigma-Aldrich) to PBS-Tween (PBS with 0.05% Tween-20).

2.3. Cell culture, maintenance, storage and transfection

2.3.1. Cell maintenance

Cell lines were routinely split once a week and maintained in 25 cm² culture flasks (Grenier Bio-One Ltd, Kremunster, Austria) with a loosened cap and incubated at 37 °C, 95% humidification and 5% CO₂. Medium on cells was changed every 2-3 days. Mycoplasma contamination in cell cultures was estimated on a monthly basis using the EZ-PCR Mycoplasma Test Kit (Biological Industries, Israel).

2.3.2. Trypsinisation (detachment) of adherent cells and cell counting

Following the cells reaching a confluency of 80-90%, the medium was aspirated and the cells were washed briefly with sterile PBS. Adherent cells were then detached using 1-2ml of Trypsin/EDTA (Sigma Aldrich), then incubated at 37°C for approximately 5 minutes until detachment can be seen under a light microscope. At this point, an equal volume of serum-containing media was added to the cell suspension in order to quench the trypsin, and solution was added to a universal container. The suspension was centrifuged at 1700 x g for 5 minutes in order to collect the cell pellet. The supernatant was aspirated from the universal container and the pellet was resuspended in an appropriate volume of serum-free media (if being used for siRNA treatment), or in normal culture media to be reseeded

into tissue culture flasks. Cells were counted using Counter II FL Automated Cell Counter (ThermoFisher) and then seeded at an appropriate concentration for experimental needs.

2.3.3. Storing cells

Cell stocks with low passage number were stored in liquid nitrogen. To do this, cells were trypsinised as detailed in 2.3.2 and resuspended in medium containing 10% v/v DMSO at a cell density of 1×10^6 cells/ml. The cell suspension was then divided into 1ml aliquots and added to CRYO.S tubes (Grenier Bio-One), the tubes were wrapped in protective tissue paper, stored overnight at -80°C and then transferred to liquid nitrogen tanks for long-term storage.

2.3.4. Resuscitation of cells

In order to resuscitate cells, they were removed from liquid nitrogen and rapidly thawed in warm water, before being transferred into a universal container containing 10 ml of pre-warmed medium and centrifuged at $1,000 \times g$ for 7 minutes. The supernatant was aspirated and the pellet was resuspended in 5 ml of serum-containing media. The cell suspension was then transferred into a fresh 25 cm^2 culture flask and transferred to the incubator.

2.3.5. Transfection of cells with siRNA

1 ml of MDA-MB-231 or ZR-75.1 cells added per well of a six-well plate at a concentration 1.5×10^6 cells/ml in serum-free media, then allowed to attach overnight at 37°C . Cells were then transfected

with siRNA using 2 μ l/ml DharmaFECT1 (ZR-75.1) or 1 μ l/ml DharmaFECT4 (MDA-MB-231) according to manufacturer's instructions (Dharmacon). Cells were used for experiments 72 hours post-transfection.

2.4. Methods for RNA detection

2.4.1. RNA isolation

Medium on cells was aspirated and the monolayer was then washed twice with PBS. 0.5 ml of TRI reagent (Sigma-Aldrich) was added per well of a six-well plate. Cells were scraped into an Eppendorf and either stored at -20 °C for future use or, for continuation of the protocol, allowed to stand at room temperature for 5 minutes. 0.05 ml of 1-bromo-3-chloropropane (Sigma-Aldrich) was then added to the solution, shaken vigorously for 5 minutes and then allowed to stand for 15 minutes at room temperature. Following this, the suspension was centrifuged at 4 °C, for 15 minutes at 12,000 x g in the Hettich MIKRO 200R (DJB Labcare Ltd., Buckinghamshire, UK). The solution separated into three phases: a red organic phase (protein), a white interphase (DNA) and a colourless upper aqueous phase (RNA). The upper phase was carefully removed and put into a fresh tube. 0.25 ml of isopropanol (Sigma-Aldrich) was then added, shaken and allowed to stand for 10 minutes at room temperature. The solution was then centrifuged at 4 °C, for 10 minutes at 12,000 x g and the supernatant discarded. The pellet was washed with 1 ml of 75 % v/v ethanol (made with DEPC water) and vortexed. This suspension was centrifuged at 7,500 X G for 5 minutes and then ethanol removed, avoiding pellet. The RNA pellet was allowed to air dry for around 10 minutes and then dissolved in 15 µl of DEPC water.

The concentration and purity of resultant RNA was measured using the IMPLEN NanoPhotometer (Implen, Schatzbogen, Germany).

2.4.2. Reverse transcription (RT)

The GoScript™ Reverse Transcription System (Promega, Madison, WI, USA) was used to convert RNA into first-strand cDNA. Using concentration gained from the protocol in 2.4.1., 500 ng of RNA was used, along with DEPC H₂O to make up the solution to 4 µl, as well as 1 µl of the Primer Oligo(dT)₁₅. This mix was then heated to 70 °C for 5 minutes, then immediately chilled on ice. The reverse transcription reaction mix with 4 µl GoScript™ 5X Reaction Mix, 1.2 µl MgCl₂, 1 µl PCR Nucleotide Mix, 0.5 µl Recombinant RNasin® Ribonuclease Inhibitor, 1 µl GoScript™ Reverse Transcriptase and 7.2 µl DEPC H₂O. The reverse transcription mix was added to 5 µl of RNA and primer mix. The conditions used for the reverse transcription reaction were:

25 °C for 5 minutes

42 °C for 1 hour

70 °C for 15 minutes

This was undertaken using Applied Biosystems 2720 Thermal Cycler (Life Technologies, Paisley, UK).

2.4.3. Quantitative polymerase chain reaction (qPCR)

cDNA produced in reverse transcription was diluted 1:8 with distilled

H₂O. qPCR performed using Precision FAST 2x qPCR MasterMix (Primer Design, Southampton, UK) and Ampifluor™ Uniprimer™ Universal system (Intergen company®, NY, USA).

The qPCR reaction mix was made as follows:

- 2x qPCR MasterMix – 5 µl.
- Forward primer – 0.3 µl.
- Reverse primer with z-sequence – 0.3 µl.
- PCR H₂O (dH₂O sterilised through UV and autoclaving) – 3 µl.
- cDNA sample – 1 µl.
- Umix – 0.3 µl

The ampifluor probe consists of a 3' region specific to the Z-sequence (ACTGAACCTGACCGTACA) present on the target-specific primers and a 5' hairpin structure labelled with a fluorophore (FAM). When in this hairpin structure, the fluorophore is linked to an acceptor moiety (DABSYL) which acts to quench the fluorescence emitted by the fluorophore, preventing any signal from being detected. During PCR, however, the probe becomes incorporated and acts as a template for DNA polymerisation in which DNA polymerase uses its 5'-3' exonuclease activity to degrade and unfold the hairpin structure, thereby disrupting the energy transfer between fluorophore and quencher, allowing sufficient fluorescence to be detected. The fluorescent signal emitted during each PCR cycle can

then be directly correlated to the amount of DNA that has been amplified. The process is illustrated in Figure 2.1.

Each sample was loaded into a qPCR machine compatible 96-well plate (BioRad Laboratories, Hemel Hempstead, UK) in triplicate, and then covered with optically clear Microseal® (BioRad Laboratories). Quantitative PCR amplification was performed using StepOnePlus™ Real-Time PCR System (ThermoFisher) with the following parameters:

Pre-denaturation for 10 minutes at 95 °C

(70 cycles)

Denaturation 95 °C for 10 seconds

Annealing 55 °C for 30 seconds

Elongation 72 °C for 10 seconds.

The fluorescent signal is detected at the annealing stage by a camera where its geometric increase directly correlates with the exponential increase of product. This is then used to determine a threshold cycle (CT value) for each reaction and the transcript copy number depends on when fluorescence detection reaches a specific threshold. Results were analysed using $\Delta\Delta\text{CT}$ normalisation to housekeeping gene, glyceraldehyde 3-phosphate dehydrogenase (GAPDH) (Livak and Schmittgen, 2001).

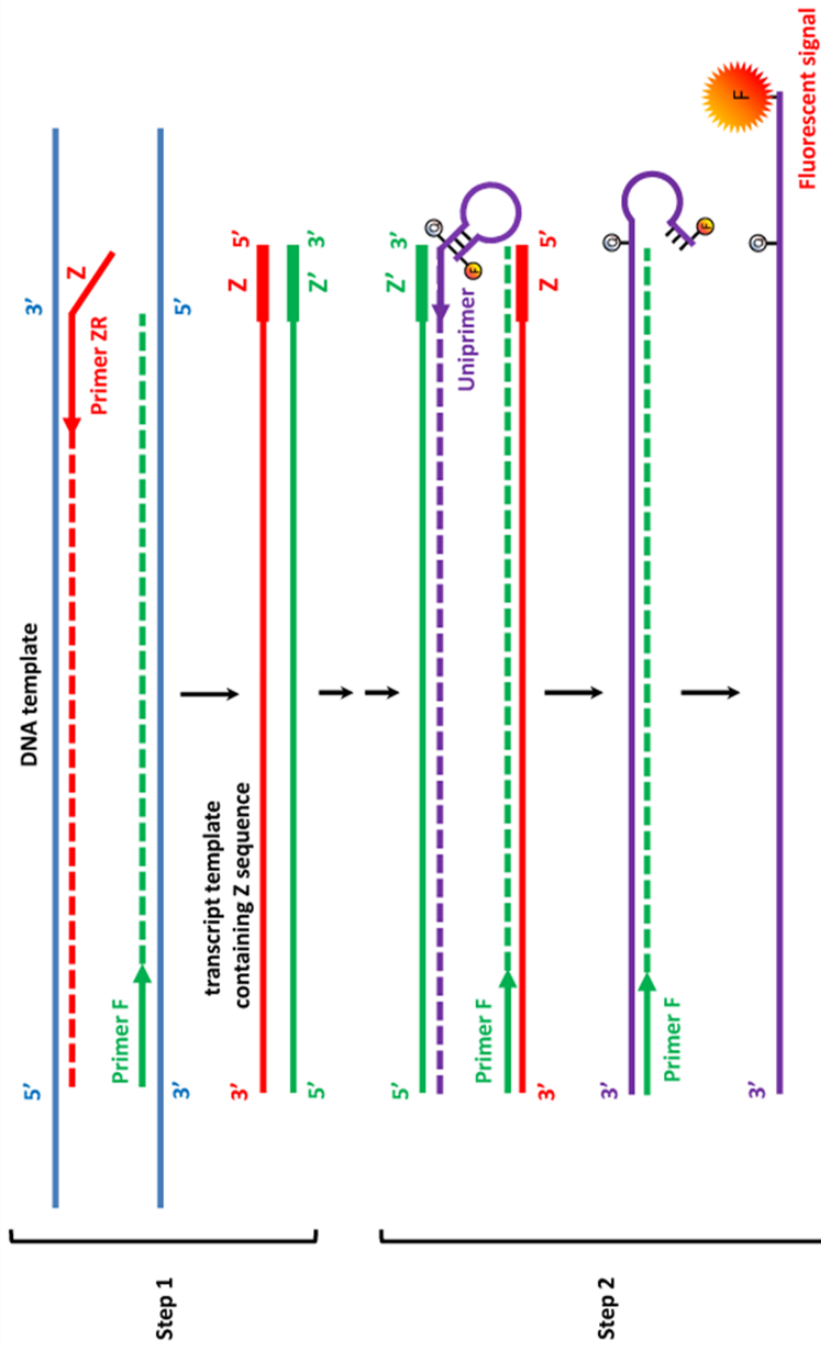


Figure 2.1. Diagram indicating the principle of how Amplifluor Uniprimer Universal system works during qPCR.

.2.5.1. Western blotting

Protein extraction and preparation of cell lysates

When the correct time point was reached, the cell monolayer was washed 2 x with PBS. Following this, 50 µl of radioimmunoprecipitation assay (RIPA) buffer (containing protease inhibitors) was added to each well of a 6-well plate. A scraper was then used to scrape off the cell monolayer and the resultant cell suspension was added to an Eppendorf tube and placed for an hour at 4 °C on a Labinco rotating wheel (Wolf Laboratories, York, UK) to allow cell lysis to take place. Following this, the lysed cells were centrifuged at 13,000 X G for 15 minutes so cell debris formed a pellet. The supernatant was then transferred to a fresh Eppendorf tube and the pellet was discarded. The protein samples were then quantified for Sodium Dodecyl Sulphate (SDS)-polyacrylamide gel electrophoresis (PAGE), as explained below, or stored at -20 °C until further use.

Protein quantification and preparation of samples for SDS-PAGE

For the standardisation of protein samples being loaded on to the SDS-PAGE gel, the concentration of protein in each sample was quantified. This was done using the BioRad DC Protein Assay kit (BioRad Laboratories). In a 96-well plate, 50 mg/ml of bovine serum albumin (BSA) standard (Sigma-Aldrich) was serially diluted in lysis buffer down to a concentration of 0.78 mg/ml and used to set up a standard curve of protein concentration. 5 µl of either protein sample

or standard was added into each test well in triplicate, before 25 µl of 'working reagent A/S' (prepared by adding 20 µl of reagent S per millilitre of reagent A), followed by 200 µl of reagent B. After the samples were mixed, the plate was incubated at room temperature for 10 minutes to allow the colorimetric reaction to occur. Once this was completed, the absorbance of each sample was measured at 620 nm using the ELx800 plate reading spectrophotometer (BioTek, VT, USA). A standard curve could be plotted from these readings, allowing an equation of the line to be produced, allowing protein concentration calculation. The samples were then diluted with an appropriate amount of lysis buffer in order to normalise all of samples to the least concentrated sample. This suspension was then further diluted through addition of 2X Laemmli sample buffer concentration (Sigma-Aldrich) at a ratio of 1:1 before the samples were denatured by boiling at 95 °C for 3 minutes. These samples were allowed to cool and then loaded onto an SDS-PAGE gel.

SDS Polyacrylamide Gel Electrophoresis (SDS-PAGE)

The OmniPAGE CS10 vertical electrophoresis system (Clever Scientific, Rugby, UK) was used to carry out the SDS-PAGE system. Resolving gels of a required percentage (depending on protein size) were prepared in 15 ml aliquots (enough for two gels) by adding volumes of the constituents in Table 2.4. TEMED was added to the

Table 2.4. Components and volumes used in 10% resolving gel.

Chemical	Volume (ml)
H ₂ O	5.9
30% acrylamide (Sigma Aldrich)	5.3
1.5M Tris (pH 8.8) (Sigma Aldrich)	5.0
10% w/v SDS (Melford)	0.2
10 w/v APS (Melford)	0.2
TEMED (Sigma Aldrich)	0.012

Table 2.5. Components and volumes used in stacking gel.

Chemical	Volume (ml)
H ₂ O	3.4
30% acrylamide	0.83
1.0M Tris (pH 6.8) (Sigma Aldrich)	0.6
10% w/v SDS	0.05
10 w/v APS	0.05
TEMED	0.005

mixture just before loading, as this caused the gel to set. The resultant mixture was poured between two glass plates held in place by a loading cassette, until the gel was around 1.5 cm below the top edge of the plate. To prevent gel oxidation, the top of the resolving gel was covered with isopropanol as the gel was left to polymerise at room temperature for around 30 minutes, until set. The excess isopropanol solution was poured away before the stacking gel was added (components and volumes listed in Table 2.5). After the addition of the stacking gel, a well-forming Teflon comb was inserted and the gel was allowed to polymerise for around 20 minutes. Once set, the loading cassette was transferred into an electrophoresis tank and covered with 1 x running buffer, before the well comb was removed. 3 µl of BLUeye Pre-Stained Protein Ladder (Geneflow Ltd, Lichfield, UK), was loaded onto the gel, followed by up to 30 µl of samples (dependent on concentration of protein in sample). The gels were then run at 100V, 50mA and 50 watts for 1.75 hours to allow separation of proteins according to their charge and molecular weight.

Western blot transfer of proteins onto polyvinylidene fluoride (PVDF) membrane

Once the SDS-PAGE was complete, the protein samples were transferred onto Immobilon®-P PVDF membrane (Merck Millipore, MA, USA) by western blotting. The electrophoresis equipment was disassembled and the glass plates were separated. The stacking gel was cut from the resolving and discarded. The resolving gel was

then placed on top of one sponge and three 7.5 cm x 7.5 cm pieces of filter paper (Whatman International Ltd, Maidstone, UK) pre-soaked in transfer buffer. The PVDF membrane was hydrated in methanol (Millipore Merck) and then placed on top of the gel. Following this, three more pre-soaked filter papers and a sponge were added on top of this. This 'sandwich' was then placed in a transfer cassette and placed into a wet transfer tank. The tank was kept cool throughout the blotting process by being allowed to sit in an ice box. Electroblothing was undertaken at 100 V, 300 mA and 50 watts for 1 hour. Once the proteins were transferred, the membranes were blocked for 1 hour in 5% w/v skimmed milk in TBST solution facing upwards in 50ml falcon tubes. This solution blocks the proteins on the membrane, disallowing non-specific binding of the primary antibody. Blocking was undertaken at room temperature on a roller mixer (Wolf Laboratories).

Protein detection using specific immuno-probing

Following blocking, the primary antibody was diluted to appropriate concentration (outlined in Table 2.4) in 5% milk solution and incubated at 4 °C overnight on a roller mixer. The next morning the 5% milk solution containing unbound antibody was poured away and the membrane was washed 3 x in TBST, for 5 minutes per wash. The membranes were further incubated with 5 ml of 1:1000 HRP-conjugated secondary antibody (Sigma-Aldrich; dependent on the species of the primary antibody), diluted in 5% milk solution for 1 hour at room temperature, with continuous rotation. This was

followed by three 5-minute washes using TBST in order to wash off unbound secondary antibody.

Chemiluminescent protein detection

Chemiluminescent protein detection was carried out using EZ-ECL (Biological Industries) which comprises a highly sensitive chemiluminescent substrate which detects the horseradish peroxidase (HRP) used in the western blotting procedure. Solutions A and B of the EZ-ECL were mixed in a 1:1 ratio, allowing 1 ml per membrane. The solution was allowed to develop for 2 minutes and then added to membranes. Excess solution was drained onto a piece of tissue paper and then the chemiluminescent signal was detected using G:Box (Syngene, Cambridge, UK). Semi-quantitative analysis was undertaken using Image J software (National Institutes of Health, NY, USA) in order to assess the levels of protein in the samples.

2.5.2. Immunocytochemistry

Following relevant treatment, 20,000 cells in 200 µl DMEM medium were seeded into each well of an 8-well NUNC Lab Tek® chamber slide (Thermo Scientific), and incubated overnight at 37°C with 5% CO₂. The following morning, the cells were fixed using ice-cold 100% ethanol for 30 minutes at 4°C, before being rehydrated through 30 minutes with PBS at room temperature. Following this, cells were permeabilised using 0.1% v/v TritonX100 in TBS for 5-10 minutes at room temperature. The slide was then blocked using a blocking

solution (1-2 drops of horse serum (Vector Laboratories) added to PBS) for 30 minutes at room temperature. Following blocking, cells were washed three times with PBS before being incubated with primary antibody (1:100, diluted in blocking buffer) for one hour at room temperature. Any unbound antibody was washed off through three washes with PBS, following this incubation period. Cells were then incubated with secondary antibody (1:1000) in blocking buffer for 30 minutes at room temperature. Following this, three washes were undertaken and then cells were incubated with 200µl of working VECTASTAIN® Universal ABC Complex (Vector Laboratories). This solution was subsequently removed through three washes with PBS before a few drops of DAB chromogen (Vector Laboratories) was added and incubated in the dark for 5 minutes. Addition of the DAB causes the solution to turn brown and once this occurs, the DAB was washed off using distilled water before the cells were counterstained with Mayer's haematoxylin for approximately 1 minute. Cells were visualised using a Leica DM 1000 LED microscope (Leica Microsystems, Milton Keynes, UK).

2.5.3. Flow cytometric assessment of protein levels

Following relevant treatment, the cells under assessment were washed using PBS and then HyQTase (GE Healthcare, Chicago, IL, USA) was used to detach cells from the plate. Around 10 minutes were allowed for detachment and then cells were quenched using normal medium. Cells were then transferred, through pipetting, to a 15ml tube and centrifuged at 300 X G for 5 minutes. 2 ml of wash

buffer (PBS + 2mM EDTA) was added to cells and vortexed, before another centrifuge at 300 X G for 5 minutes. Cells were then resuspended in 500 µl of wash buffer using Vortex Genie 2 (Scientific Industries, Inc, NY, USA). Cells were then fixed by adding an equal volume of IC Fixation Buffer (eBioScience, Hatfield, UK). Solutions were then allowed to incubate in the dark at room temperature for 30 minutes. Following this, cells were centrifuged at 600 X G for 5 minutes and the supernatant was discarded. The cells were then resuspended in 1ml of ice cold 100 % methanol (Fisher Scientific, Loughborough, UK) vortexed and incubated on ice for 30 minutes. Cells were then washed using 5 ml of FACS Buffer and then centrifuged again at 600 X G for 5 minutes. Cells were then counted using the Counter II FL Automated Cell Counter (ThermoFisher) and aliquoted to contain 1×10^6 cells per 100 µl in each flow tube, with tubes from each treatment for a negative control, an isotype control and the required antibodies. Cells were then incubated with 1ml of blocking buffer (1% BSA in PBST) for 30 minutes to block the unspecific binding of the antibodies. Following this, another centrifugation at 600 X G for 5 minutes was undergone and primary antibodies produced at 1:100, diluted with blocking buffer (primary antibodies listed in Table 2.6). 100 µl per tube of the diluted primary antibody was added, the cells were vortexed and then incubated for 1 hour at room temperature. Following this, cells were washed twice using PBS and then centrifuged at 600 X G for 5

Table 2.6. Primary antibodies used in flow cytometric analysis of protein levels.

Antibody	Code	Company	Species	Dilution
AKT	sc 5298	Santa Cruz	Mouse	1/200
Phospho-AKT (serine 473)	sc 81433	Santa Cruz	Mouse	1/200
c-JUN	sc 7890	Santa Cruz	Rabbit	1/200
Phospho-c-JUN (serine 63)	sc 1697	Santa Cruz	Rabbit	1/200
MMP2	sc 53630	Santa Cruz	Mouse	1/200
MMP8	sc 137004	Santa Cruz	Mouse	1/200
Normal mouse IgG	sc 5877	Santa Cruz	Mouse	1/200
Normal rabbit IgG	sc 3888	Santa Cruz	Rabbit	1/200

minutes. 100 µl of diluted secondary Alexa Fluor 488 antibody (ThermoFisher Scientific).

(1:500) was added to cells, vortexed and then incubated at room temperature, in the dark for 30 minutes. Finally, cells were washed twice with PBS and then resuspended in 500 µl of FACs buffer. Following this, samples were run on the BD FACSCanto™ II flow cytometer (BD) using the FITC channel.

Data were analysed on FCS Express 4 Cytometry (De Novo Software, Glendale, CA, USA), where side scatter area vs. forward scatter area of cells with Gate 1 around the main cell population (Figure 2.2 a). This gate was then applied to forward scatter area vs. forward scatter height graph, producing Gate 2, which was then applied to each histogram produced (Figure 2.2.b).

2.5.4. RayBio® C-Series Human Matrix Metalloproteinase

Antibody Array C1

Following 24 hours of treatment with siRNA, the cells were washed twice using PBS and then serum-free DMEM added. After a further 48 hours, the tumour-conditioned medium (TCM) was removed from the cells and centrifuged at 2,000 X G for 10 minutes. This medium was then transferred to a fresh Eppendorf tube and frozen at -20 °C until needed. The cells used to produce the TCM were lysed, as outlined in 2.5.1, in order to check knockdown of protein through western blotting. When the TCM was due to be probed for the presence of the MMPs and TIMPs, it was thawed to room

temperature and then centrifuged at 10,000 X G for 5 minutes in order to remove any particulates which may interfere with detection. The membrane was removed from the RayBio® C-Series Human Matrix Metalloproteinase Antibody Array C1 kit (RayBiotech Inc., Georgia, USA) and all components were stabilised to room temperature. Following this, the membranes were placed in a plastic incubation tray and blocked using 2ml of the provided blocking buffer for 30 minutes, with gentle rocking. After this incubation, the blocking buffer was removed and 1 ml of the TCM was added to each membrane. This was incubated at 4 °C overnight. The following morning, the TCM was removed from the wells and the membranes were washed three times with 1X wash buffer 1 and twice with 1 X wash buffer 2, each for 5 minutes. The biotinylated antibody cocktail was produced by pipetting 2 ml of blocking buffer into the vial provided. Following removal of all wash buffer, 1 ml of the biotinylated antibody cocktail was added to each membrane and incubated for 2 hours at room temperature, with gently rocking. After this incubation period, the membranes were washed as previously outlined. The HRP-Streptavidin was then produced through dilution of the provided 1,000X HRP-Streptavidin concentrate with blocking buffer, to produce 2 ml to incubate with each membrane. This incubation was, again, undertaken for 2 hours at room temperature with gentle rocking. The solution was then aspirated from each well

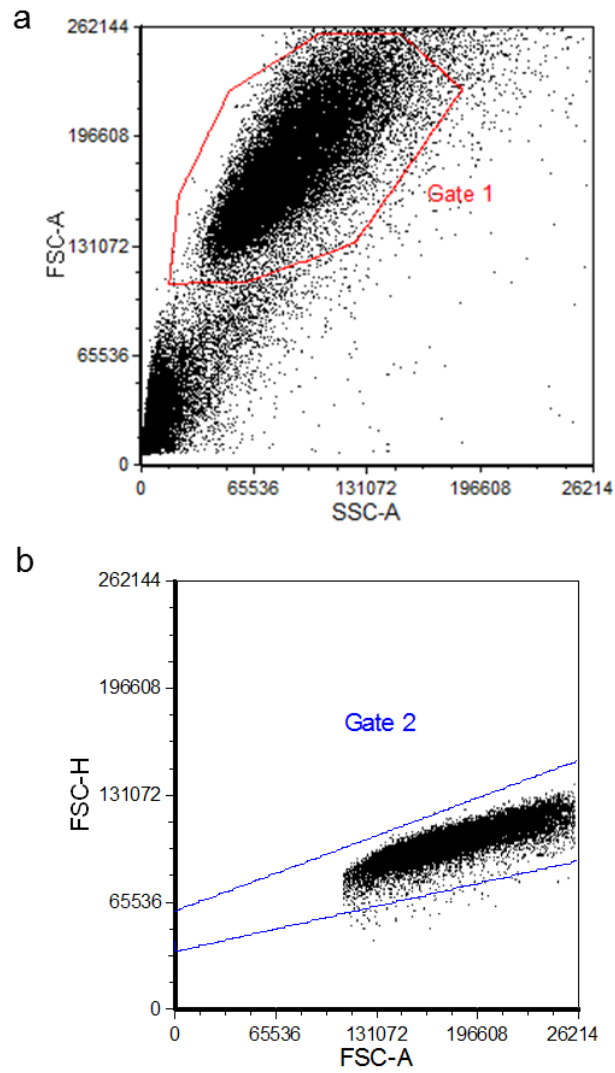


Figure 2.2. Flow cytometric analysis strategy of protein expression in cell lines. a) Side scatter area vs. forward scatter area of cells with Gate 1 around main cell population. b) Forward scatter area vs. forward scatter height of cells, with Gate 1 applied, with Gate 2 around single cell population.

and washes were undertaken as before. During the washing period, the provided Detection Buffers C and D were mixed in a 1:1 ratio, to produce 500 µl per membrane. When washes were complete, the membranes were transferred onto chromatography paper to remove any excess wash buffer and then moved to the provided plastic sheeting. The mixed detection buffers were then added to the membranes and allowed to incubate for 2 minutes. Another plastic sheet was placed on top of the membranes and excess solution removed by gently 'rolling' the plastic sheet and sandwiching the membrane. The membranes were then transferred to the G:Box (Syngene) for chemiluminescent detection. The membranes were imaged, with the resultant image corresponding to Figure 2.3.

Analysis was undertaken using ImageJ software (National Institutes of Health, NY, USA). This was done through measuring the relative intensity of each of the spots, using the same rectangle to measure each area. An average was found for each of the duplicate spots (or six spots for the positive and negative control). From here, the negative average was subtracted from the positive average and this was used to normalise each of the duplicate spots. At this point, the varying intensities of the points on different membranes could be compared.

2.5.5. Enzyme-linked immunosorbent assay (ELISA)

ELISA-Ready-SET-GO® kits were purchased for both interleukin-6 (IL-6) and interleukin-8 (IL-8) from eBioScience. ELISA plates were coated with 100 µl per well of 100 µl 250x capture antibody specific

to IL-6 or IL-8, diluted to 1 x in coating buffer (diluted from 10 x in deionised (DI) water from Sigma-Aldrich). These plates were incubated overnight at 4 °C. The following day, the wells were aspirated and washed 3 x with 250 µl wash buffer (0.05% v/v Tween-20 in PBS). Between each wash step, 1 minute was allowed for soaking and then the plates were blotted on absorbent paper to remove any residual buffer. The 5 x ELISPOT diluent was diluted to 1 x with DI water and wells were blocked with 200 µl of this solution for 1 hour at room temperature. Following this, plates were aspirated and washed once with wash buffer. The lyophilised standards specific to each IL, provided in each kit, were reconstituted through addition of 1 ml of DI water (15 ng/ml), this was allowed to sit for 15 minutes with gentle agitation. Then, further dilution was undertaken in order dilute the standard to the top concentration (250 pg/ml through addition of 5.9 ml 1x ELISPOT diluent to 100 µl of standard). A two-fold serial dilution was undertaken in triplicate in order to produce an eight-point standard curve, with a final volume of 100 µl per well. The samples were diluted to appropriate concentrations with PBS and 100 µl loaded per wells. Three wells were also loaded with just 1x ELISPOT diluent in order for this to serve as a blank. The plate was sealed and incubated for two hours at room temperature. Following this, solutions were aspirated from the wells and 5 washes were undertaken. 100 µl per well of 250x detection antibody was then diluted in 1x ELISPOT diluent and the plates were sealed and incubated at room temperature for 30 minutes. Again, wells were

2. Materials & Methods

aspirated and washed five times. Next, 100 μ l of the 250x avidin-HRP diluted in 1x ELISPOT diluent was added to each well, the plate was sealed and again incubated for 30 minutes at room temperature. After this, wells were aspirated and then washed seven times (this time two minutes soak was allowed between washes. Finally, 100 μ l/well of 1x TMB solution was added and the plate was incubated at room temperature for 15 minutes. Following this 50 μ l, of stop solution (0.16 M sulphuric acid) was added to each well. The plates could then be read at 450 nm. The data were analysed through standard curve production and using the RFU (following subtraction of the blank) gained from the samples to assess the concentration of the sample in pg/ml.

2.6. *In vitro* cell function assays

2.6.1. AlamarBlue® cell proliferation assay

A total of 5×10^3 cells were seeded in 100 μ l of serum-free medium (no antibiotics) per well in a black 96-well plate. Six replicates were undertaken per condition and four identical plates were produced in total. Cells were allowed to attach overnight at 37 °C. Twelve hours later, cells were treated with siRNA and DharmaFECT solutions as specified in section 2.3.5. Six hours post-transfection, all media were changed for 100 μ l of normal DMEM (with antibiotics). At 24-hour intervals from the time of transfection, cell media was changed and 10 μ l of AlamarBlue® Cell Viability Solution (ThermoFisher) was added to each well. The plate was incubated at 37 °C in the dark for four hours and then read on a GLOMAX® MULTI Detection System (Promega) at 570 nm in relative fluorescence units.

2.6.2. Tumour-endothelium adhesion assay

A total of 3×10^5 HMVECs/well were added to a 48-well plate and allowed to form a monolayer overnight. Following 72 hours of siRNA treatment cancer cells were diluted to 1×10^6 cells/ml and 5 μ l of Vybrant DiO cell-labelling solution (Invitrogen, ThermoFisher) were added per millilitre of cell suspension. Cells were incubated for 20 minutes and then washed three times using phosphate buffer solution (PBS). Cells were resuspended at 2×10^5 cells/ml and 200 μ l added to the 48-well plate containing HMVEC monolayer. Cells were allowed to attach for 30 minutes, after which the monolayer was

washed twice with PBS. 350 µl cell dissociation solution was then added to each well and the plates further incubated for 1 hour. The cell suspension was aliquoted into a black 96-well plate and read on a GLOMAX® MULTI Detection System (Promega), at 495 nm excitation and 519 nm emission.

2.6.3. Transwell migration assay

Cells were harvested at the relevant time point using HyQTase cell detachment solution (GE Healthcare). Cells were resuspended in serum-free medium, at a density of 1×10^5 cells/ml. DMEM (1ml) containing 10% v/v FBS (chemoattractant) was added to the receiver wells in triplicate, and 1ml of serum-free DMEM (no chemoattractant) was added to the receiver well of the control transwell. An 8-µm-pore ThinCert™ 24-well plate insert (Grenier Bio-One Ltd.) was placed in each of the receiver wells and 500 µl of cell suspension was added to each transwell insert. Following four hours of incubation, the transwells were washed gently with PBS and then incubated for a further hour in 350 µl cell dissociation solution [CDS (Sigma-Aldrich)/Calcein AM (eBioscience)] at a ratio of 1.2 µl Calcein AM in 1 ml CDS. Following this, the cell suspension was aliquoted into a black 96-well plate and read on a GLOMAX® MULTI Detection System (Promega), at 495 nm excitation and 519 nm emission. To analyse the total directed cell movement, the fluorescence of the well containing no chemoattractant was subtracted from that of the test wells.

2.6.4. Transwell invasion assay

Transwells to be used for the invasion assay were set up the day before the assay was to be undertaken. Defrosted Matrigel (Corning, BD, Oxford, UK) was added to serum-free medium to gain a concentration of 500 µg/ml, then 100 µl of this solution was added to 8-µm-pore ThinCert™ 24-well plate inserts and allowed to dehydrate for 2 hours at 55°C. Forty minutes prior to the experiment, the Matrigel was rehydrated with 100 µl of serum-free media. The rest of the invasion assay was undertaken in the same way as the migration assay (outlined in 2.6.3), except the running time of the experiment was 24 hours.

2.6.5. Wound healing (scratch) assay

Cells were harvested using HyQTase cell detachment solution (GE Healthcare) and seeded into a 24-well plate in 500 µl at a concentration of 7.5×10^5 cells/well in DMEM. Cells were allowed to attach and reach confluence overnight at 37°C. The following morning, a pipette tip was sharpened to form a point, using a sterile scalpel, and the cells were scratched down the centre of the well. Cells were imaged using a Leica DM 1000 LED microscope (Leica Microsystems) each hour in an area determined by blue lines drawn across each well. Images were analysed using ImageJ Software (National Institutes of Health) and the percentage healing of the wound was calculated.

2.6.6. Cell cycle assay

Cells to be analysed were washed 2 x with PBS, then trypsinised. Following detachment of the cells, trypsin was quenched using serum-containing medium. Cells were centrifuged at 1,700 X G for 5 minutes and then resuspended in 5ml of ice cold PBS. Cells were centrifuged again at 1,700 X G for 5 minutes. Cells resuspended in 1ml of ice cold 70% v/v ethanol and left on ice for 2 hours. Following this, cells were again centrifuged using the same conditions and then resuspended in PBS at 1×10^6 cells in 100 μ l for each sample. 150 μ l of 2 μ g/ml propidium iodide (PI; ThermoFisher) was added to each of the samples, apart from the non-stained control. Cells were then incubated at room temperature in the dark for 15 minutes. Following this, samples were run on the BD FACSCanto™ II flow cytometer (BD) using the FL3 channel (575nm).

2.6.7. Apoptosis assay

In order to detect apoptotic cells, the Annexin V Kit (Santa Cruz Biotechnology) was used. This kit contains fluorescent conjugated annexin V (FITC annexin V) and propidium iodide (PI) solution.

The calcium-dependent phospholipid-binding protein annexin V binds to phosphatidylserine (PS), a phospho-lipid component of the cell membrane which is normally located on the cytoplasmic side of the cell membranes in normal live cells. However, when the cells become apoptotic, PS translocates from the inner to the outer leaflet of the cell membrane, resulting in it being exposed to the external

cellular membrane. PI, on the other hand, is a red-fluorescent intercalating dye, capable of permeating only through the cell membranes of non-viable cells and binding to their nucleic acids. Therefore, any cells that have lost their membrane integrity will be stained red by the PI, whereas the apoptotic cells, which are impermeable to PI, will be stained green by the FITC annexin V only. Any live cells present in the solution will show little or no fluorescence. This partial staining allows for easy identification with the BD FACSCanto™ II flow cytometer.

Apoptosis was induced for 2 hours using 1 µl of 1 nM staurosporine (Sigma-Aldrich). Following this, medium was collected and then attached cells trypsinised. Once cells were detached, they were added to the previously collected medium. Cells were centrifuged at 1,500 X G for 5 minutes. The cells were then gently washed with PBS and centrifuged again, under the same conditions. Cells were then resuspended at a concentration of 5×10^5 cells in 200 µl of 1X annexin V binding buffer and aliquoted to suitable flow cytometry tubes, ensuring a control exists for each of the individual stains and no staining. Following this, cells were stained using 3 µl of FITC annexin V (0.01 µg/ml) and 3 µl of PI (100 µg/ml), both provided as part of the annexin V kit.

Following a 30-minute incubation period in the dark, at room temperature, 400 µl of 1X annexin-binding buffer was added and cells were analysed on the BD FACSCanto™ II flow cytometer, reading FITC on FL1 (488 nm) and PI on FL2 (575 nm).

2.7. Statistical analysis

Statistical analysis was performed using GraphPad Prism (GraphPad Software, Inc., CA, USA). Each experiment was performed at least three times and data presented (unless otherwise stated) shows the mean of the three repeats, with error bars shown the standard deviation or standard error. T-test, one-way ANOVA or two-way ANOVA were performed to test for statistical significance, with a *P*-value of <0.05 considered statistically significant. The Mann-Whitney U Test was used to assess significance of clinical samples. Asterisk (*) notation was used to signify significances: * *P*<0.05, ** *P*<0.01, *** *P*<0.001 and **** *P*<0.0001.

Chapter III

Knockdown of MDM2
and PSMA in breast
cancer cell lines and
assessment of
transcript levels in a
breast cancer cohort

3.1. Introduction

Both MDM2 and PSMA expression have been implicated in the progressive properties of breast cancer (Turbin et al., 2006, McCann et al., 1995, Hori et al., 2002, Brekman et al., 2011, Toi et al., 1997, Onel and Cordon-Cardo, 2004, Wernicke et al., 2014, Nomura et al., 2014, Ross et al., 2003, Haffner et al., 2009) and have been shown to be involved in the metastatic abilities of tumours.

MDM2 is known to be a negative prognostic marker for breast cancer (Turbin et al., 2006) and protein overexpression is often seen in studies of human breast cancer (McCann et al., 1995, Onel and Cordon-Cardo, 2004). Meanwhile, PSMA is heavily implicated on the progressive properties of prostate cancer (Chang and Heston, 2002), and has an emerging role in breast tumours (Wernicke et al., 2014, Nomura et al., 2014, Ross et al., 2003, Haffner et al., 2009).

Recently, the expression of PSMA and MDM2 was linked, when Xu *et al.*, (Xu et al., 2013) found that knockdown of PSMA in LNCaP prostate cancer cell lines led to a decrease in the gene expression levels of *MDM2*.

In order to assess the roles of proteins in cells, researchers often decrease their levels using RNA interferences (RNAi). Short interfering RNA (siRNA) is the most commonly used type of RNAi tool for the induction of short-term silencing (2-4 days) of protein coding genes (Elbashir et al., 2001, Reynolds et al., 2004). A great

amount of effort has been used with the hope of using siRNA-based therapies to tackle genetic or viral diseases (Wilson and Doudna, 2013).

siRNA is a synthetic RNA duplex which is designed to target a specific messenger RNA (mRNA) for degradation. This duplex comprises two strands of RNA, a guide (or antisense) strand and a passenger (or sense) strand. These form a duplex which is 19 to 25 base pairs in length with 3' dinucleotide overhangs. Following transfection of these duplexes into cells, the guide strand is loaded into an RNA-induced silencing complex (RISC). This activated complex of protein and nucleic acid can then cause gene silencing through perfectly complementary binding to a single target mRNA sequence and thus targeting it for cleavage and degradation (Carthew and Sontheimer, 2009, Wilson and Doudna, 2013).

Therefore in this chapter we attempted to select two breast cancer cell lines which would be best for the study being undertaken. We then induced siRNA-mediated knockdown of both MDM2 and PSMA in each of these cell lines in order to verify the findings of Xu *et al.*, (2013) in breast cancer cell lines. In addition, a breast cancer cohort was screened for transcript expression levels of both *MDM2* and *PSMA* (Xu *et al.*, 2013).

3.2. Materials and methods

Cell lines and treatments

MDA-MB-231 and ZR-75.1 metastatic breast cancer cell lines, maintained in DMEM media with 10% FBS and antibiotics, were used in this chapter (further details of how cell lines used for screening were maintained given in Section 2.1.1). These cell lines were transiently transfected with MDM2-, PSMA- or non-targeting siRNA using Fect4 or Fect1 transfection reagents, respectively. All treatments were undertaken in a 6-well plate and a total volume of 1ml of treatment was used in each case. Treatments were undertaken for 48 or 72 hours, dependent on the experiment.

siRNA transfection

1 ml of MDA-MB-231 or ZR-75.1 cells added per well of a six-well plate at a concentration 1.5×10^6 cells/ml in serum-free media, then allowed to attach overnight at 37 °C. Cells were then transfected with siRNA using 2 µl/ml DharmaFECT1 (ZR-75.1) or 1 µl/ml DharmaFECT4 (MDA-MB-231) according to manufacturer's instructions (Dharmacon). Doses of 0, 10, 25, 50 and 100 nM siRNA were used and then the optimised dose was repeated for the RNA isolation at time points 0, 6, 12, 24, 48, 72 and 96 hours.

RNA isolation and RT-PCR

Following treatment of MDA-MB-231 and ZR-75.1 cells with MDM2-, PSMA- and non-targeting siRNA for time points 0, 6, 12, 24, 48, 72 and 96 hours in a 6-well plate, TRI reagent was added to cells. RNA

isolation and RT-PCR were then undertaken according to sections 2.4.1 and 2.4.2.

Quantitative PCR (qPCR)

qPCR was undertaken using cDNA produced in reverse transcription detailed above, using primers for MDM2, PSMA and GAPDH (listed in Table 2.3), following the procedure outlined in 2.4.3. CT values gained from these processes were analysed using $2^{-\Delta\Delta CT}$ normalisation to GAPDH. Each qPCR sample was set up in triplicate, with the experiment being independently set up three times. Analysis was undertaken using unpaired t-test Welch's correction of MDM2- and PSMA-targeting siRNA compared to NT.

Western blotting

Following 72 hours of treatment of MDA-MB-231 and ZR-75.1 with MDM2, PSMA and NT siRNA, cells were scraped from the 6-well plate into 50 μ l RIPA buffer (with added inhibitors), left on a blood wheel for 1 hour at 4°C, then centrifuge for 15 minutes at 13,000 X G. Following this an equal amount of 2 x Laemmli and SDS-PAGE, western blotting and immune-probing using MDM2, PSMA and GAPDH (antibody list in Table 2.4) was undertaken as outlined in 2.5.1.

Collection of human breast tissue

148 fresh breast tissue samples were collected immediately after surgery and stored at -80°C until use, with approval of the Bro Taf

Health Authority local research ethics committee. The cohort contained normal background breast tissue and breast cancer tissue samples. RNA isolation and RT-qPCR were undertaken according to procedure outlined above.

Statistical analysis

Data was statistically analysed using unpaired t-test Welch's correction, with a P -value of <0.05 considered statistically significant. Asterisk (*) notation was used to signify significances: * $P<0.05$, ** $P<0.01$, *** $P<0.001$ and **** $P<0.0001$.

3.3. Results

Gene expression of MDM2 and PSMA in breast cancer cell lines

Many breast cancer cell lines are currently available for use, all with varying ER, PR and HER2 statuses; some are from metastatic sites, whilst some are from primary tumours; there are cell lines from the majority of the different subtypes; and some have wild-type p53, with others being mutant. Before embarking on this study, it was important to select the correct cell lines in order to gain the most relevant and novel information concerning the role of both MDM2 and PSMA in breast cancer cell lines. Screening of transcript levels of MDM2 in breast cancer cell lines BT-20, MCF-7, ZR-75.1, SK-Br-3, BT-483, MDA-MB-468, BT-549 and MDA-MB-231, as well as the normal breast epithelium cell line MCF-10A, was undertaken in order to decide upon cell lines to use. This screening showed negligible expression of MDM2 was picked up in the normal MCF-10A cell line. Interestingly, those cell lines which were not reported to be triple-negative breast cancer (TNBC) type showed higher expression of MDM2 than TNBC. Of the non-TNBC cells, ZR-75.1 cells showed the highest expression levels; whilst MDA-MB-231 showed the highest expression of MDM2 in TNBC lines (Figure 3.1a). Following assessment of PSMA gene expression in each of the same cell lines, some similar trends were seen. Again, very low expression of PSMA was seen in the normal epithelial breast cell line, MCF-10A. Also, the non-TNBC lines again showed higher expression than the TNBC. In this case, SK-Br-3 showed the highest expression of PSMA

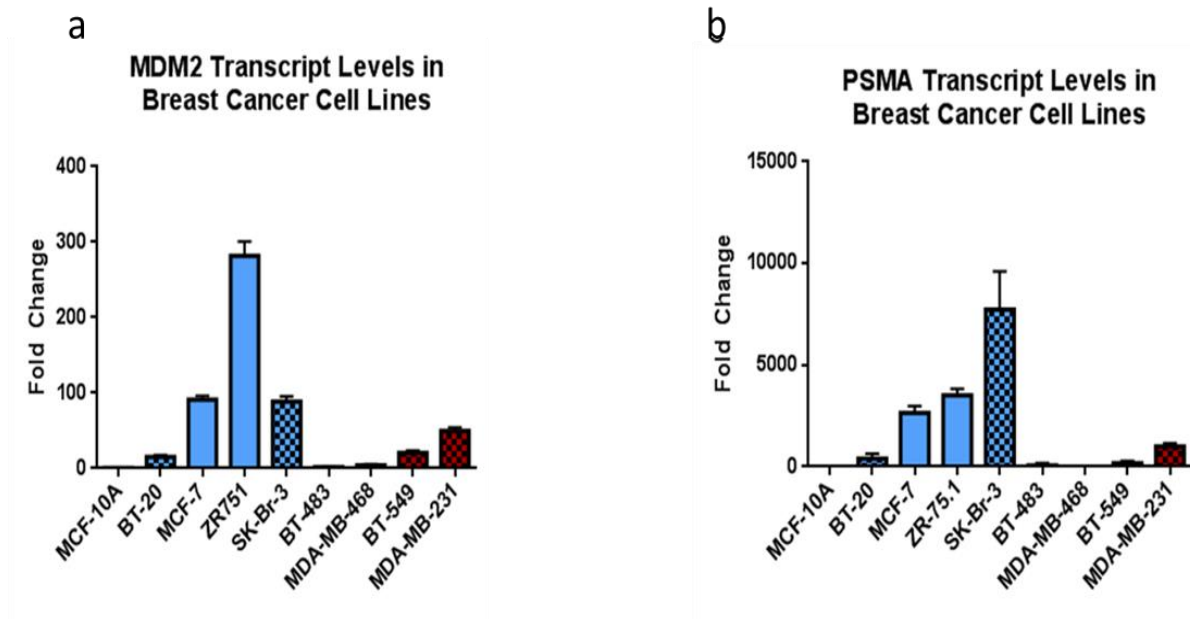


Figure 3.1. Breast cancer cell line gene expression levels a) Screening of MDM2 transcript expression levels from cell lines MCF-10A, BT-20, MCF-7, ZR-75.1, SK-Br-3, BT-483, MDA-MB-468, BT-549 and MDA-MB-231. b) Screening of PSMA transcript expression levels from cell lines MCF-10A, BT-20, MCF-7, ZR-75.1, SK-Br-3, BT-483, MDA-MB-468, BT-549 and MDA-MB-231. (Blue shows cells which are non-TNBC and red shows cells which are TNBC. Patterned bars show cells which have a mutated p53 gene).

in the TNBC lines (Figure 3.1b). However, SK-Br-3 cells grow extremely slowly and are not particularly amenable to the kind of functional work which is intended for this study and so cell lines ZR-75.1 and MDA-MB-231 were chosen to continue the work.

Knockdown of MDM2 in breast cancer cell lines

In order to achieve knockdown of MDM2 protein in breast cancer cells, MDM2-targeting siRNA, along with a NT control siRNA, was transfected into cells using Dharmacon Fect4 (MDA-MB-231) or Fect1 (ZR-75.1) transfection reagents. All gene expression data was normalised to NT control siRNA, following checks that there is no significant effect on cells by NT control at any time or dose.

In MDA-MB-231 cells, at a time-point of 48 hours, four concentrations of the siRNA were assessed, along with one treatment solely transfection reagent. It was shown that 10nM MDM2 siRNA gave no significant change from NT control; but 25 ($p=0.0206$), 50 ($p=0.0313$) and 100 nM ($p=0.0041$) siRNA all showed a significant decrease in *MDM2* gene expression levels (Figure 3.2a). Since a gene-level knockdown of over 50% was hoped to be achieved, 100 nM MDM2 siRNA was chosen as the concentration to achieve knockdown in further work. Following this, a time-course was undertaken using the chosen concentration of 100 nM of MDM2 siRNA at 0, 6, 12, 24, 48, 72 and 96 hours (Figure 3.2b). It was seen that only from 24 hours does gene knockdown occur; with 24 ($p=0.0021$), 48 ($p=0.0020$), 72

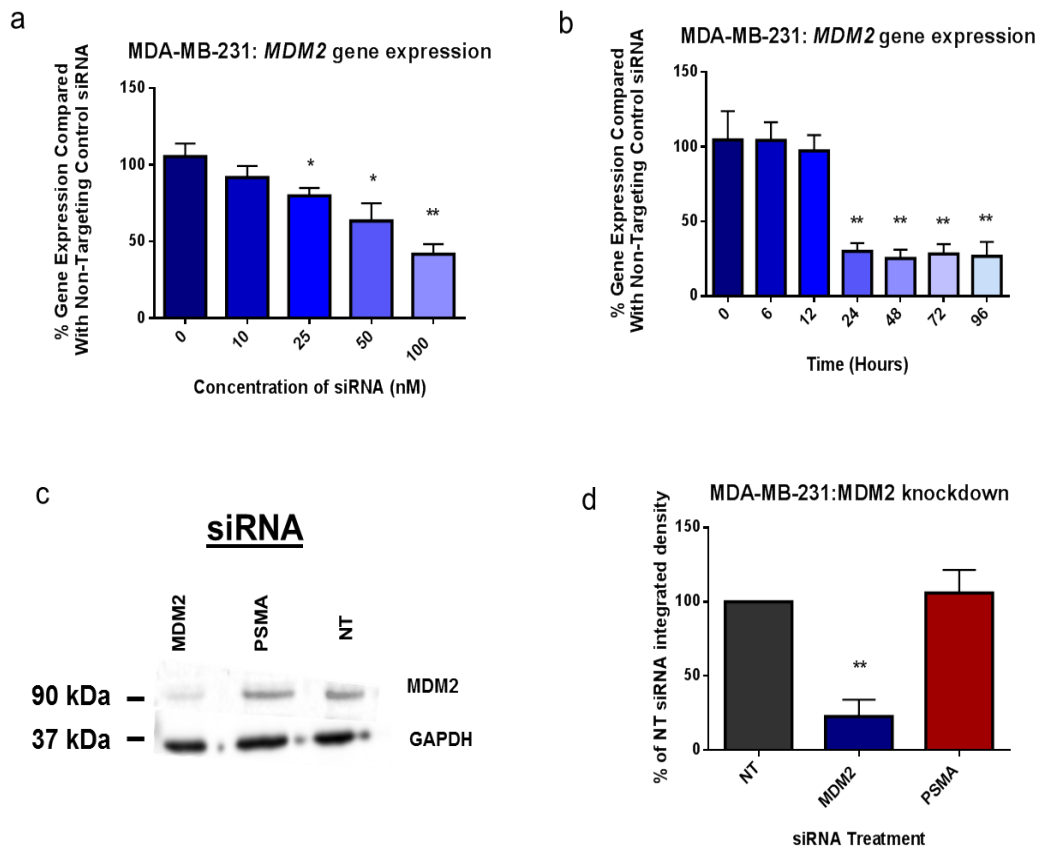


Figure 3.2. Knockdown of MDM2 in MDA-MB-231 cell line. a) Dose-dependent knockdown of *MDM2* gene at 0, 10, 25, 50 and 100 nM MDM2 siRNA concentrations (graph shows mean+SD; individual experiments carried out in triplicate; n=3). b) Time-course expression of *MDM2* gene at 0, 6, 12, 24, 48 and 72 hours following 100nM MDM2 siRNA treatment (graph shows mean+SD; individual experiments carried out in triplicate; n=3). c) MDM2 protein expression following 72 hours of MDM2, PSMA or NT siRNA treatment (blot show representative data; n=3). d) Percentage integrated density of NT control siRNA over three western blots (graph shows mean+SD; n=3). (Statistical significance assessed through unpaired t-test with Welch's correction between targeting siRNA and NT control expression levels, with * $p < 0.05$, ** $p < 0.01$).

($p=0.0027$) and 96 hours ($p=0.0034$) showing a significant decrease in *MDM2* gene expression compared to the NT control siRNA

Following this, MDM2 protein expression was assessed following MDM2, PSMA and NT siRNA treatment, with 65% protein knockdown being achieved in MDM2 siRNA treated cells, compared to the NT control siRNA treated cells (Figure 3.2c and d).

In ZR-75.1 cells, the same set of experiments was carried out in order to determine the optimal dose and which time points showed knockdown. *MDM2* gene expression was seen to begin to significantly decrease at 25 nM ($p=0.0106$), but gene levels are only more than 50% decreased at 50 ($p=0.0003$) and 100 nM ($p=0.0013$) (Figure 3.3a). Therefore, 50 nM MDM2 and NT siRNA were used to treat ZR-75.1 at time points 0, 6, 12, 24, 48, 72 and 96 hours (Figure 3.3b). A significant decrease in *MDM2* gene expression in MDM2 siRNA treated cells, compared to NT control siRNA, only occurs at 24 hours ($p=0.0053$). This knockdown continues at 48 ($p=0.0005$), 72 ($p=0.0004$) and 96 hours ($p=0.0017$). MDM2 protein knockdown was assessed in MDM2, PSMA and NT siRNA treated cells, after 72 hours of treatment, with 73% knockdown being achieved (Figure 3.3c and d).

Knockdown of PSMA in breast cancer cell lines

Once again, these experiments were carried out in order to optimise the knockdown of PSMA in MDA-MB-231 and ZR-75.1 breast cancer cell lines.

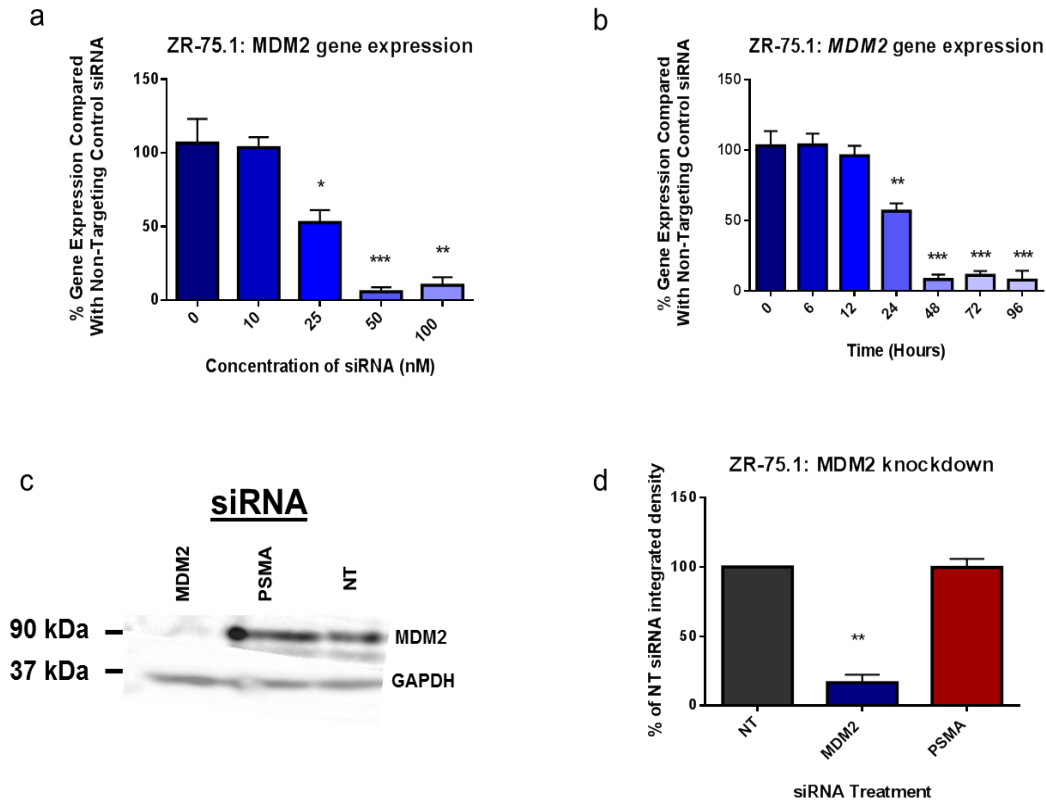


Figure 3.3. Knockdown of MDM2 in ZR-75.1 cell line. a) Dose-dependent knockdown of *MDM2* gene at 0, 10, 25, 50 and 100 nM MDM2 siRNA concentrations (graph shows mean+SD; individual experiments carried out in triplicate; n=3). b) Time-course expression of *MDM2* gene at 0, 6, 12, 24, 48 and 72 hours following 100nM MDM2 siRNA treatment (graph shows mean+SD; individual experiments carried out in triplicate; n=3). c) MDM2 protein expression following 72 hours of MDM2, PSMA or NT siRNA treatment (blot show representative data; n=3). d) Percentage integrated density of NT control siRNA over three western blots (graph shows mean+SD; n=3). (Statistical significance assessed through unpaired t-test with Welch's correction between targeting siRNA and NT control expression levels, with * $p < 0.05$, ** $p < 0.01$ and *** $p < 0.001$).

Firstly, in MDA-MB-231, varying doses of PSMA siRNA were used, along with NT siRNA in order to assess the level of knockdown at 10, 25, 50 and 100 nM concentrations. The data showed that only at 50 ($p=0.0228$) and 100 nM ($p=0.0033$) did the siRNA show a significant level of knockdown compared to the NT control (Figure 3.4a).

However, since only at 100 nM was over 50% gene knockdown achieved, this concentration was again used in order to complete other PSMA siRNA treatments in MDA-MB-231. Next, the level of knockdown at varying time points was assessed (Figure 3.4b). This showed that knockdown was only seen at gene levels from 24 hours ($p=0.0234$) onwards, right through to 96 hours ($p=0.0177$). Protein levels were then assessed following 72 hours of treatment and it was shown that PSMA siRNA at 100 nM leads to a 45% knockdown of PSMA protein from MDA-MB-231 cells (Figure 3.4c and d).

Similarly, assessment of PSMA gene expression levels in ZR-75.1 using varying concentrations of PSMA-targeted siRNA showed a significant decrease at 25 ($p=0.0438$), 50 ($p=0.0036$) and 100 nM ($p=0.0107$). However, the decrease at 25nM was only 26% and so 50 nM was chosen as the concentration of siRNA to be used for further experiments (Figure 3.5a). Following this, a time course assessment was undertaken over a 96 hour period post-siRNA treatment at 50nM. This work showed that PSMA gene expression was significantly decreased following 24 hours of siRNA treatment but only by around 48% ($p=0.0161$); whereas at 48 ($p=0.0043$), 72 ($p=0.0030$) and 96 ($p=0.0008$) hours, all knockdown in gene

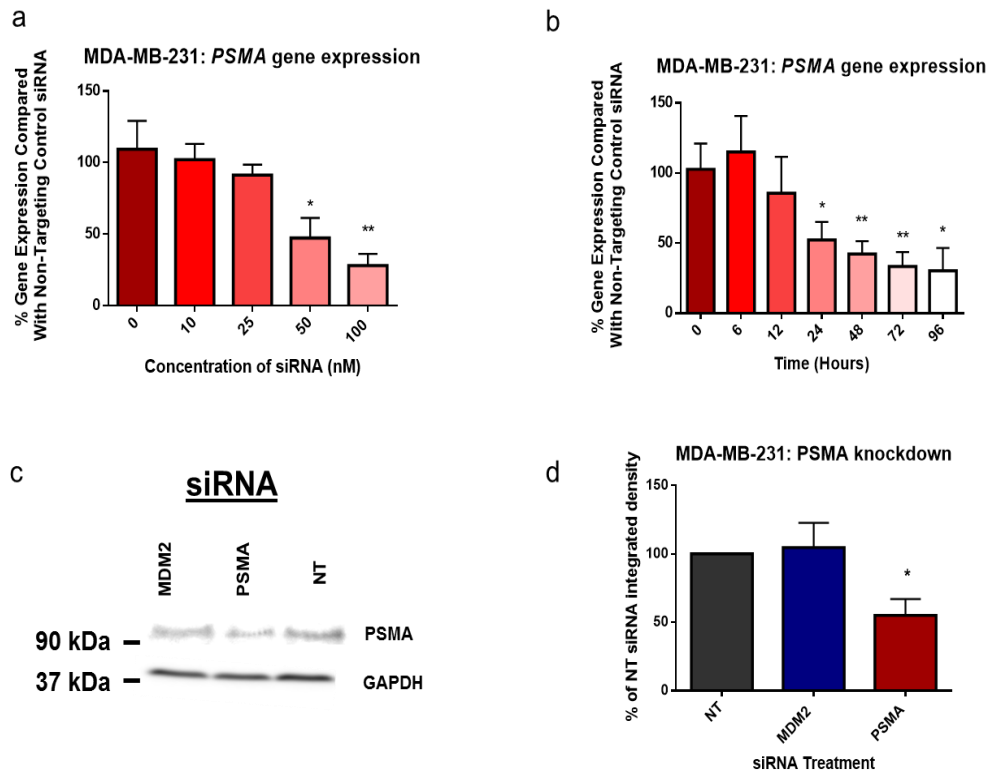


Figure 3.4. Knockdown of PSMA in MDA-MB-231 cell line. a) Dose-dependent knockdown of *PSMA* gene at 0, 10, 25, 50 and 100 nM PSMA siRNA concentrations (graph shows mean+SD; individual experiments carried out in triplicate; n=3). b) Time-course expression of *PSMA* gene at 0, 6, 12, 24, 48 and 72 hours following 100nM PSMA siRNA treatment (graph shows mean+SD; individual experiments carried out in triplicate; n=3). c) PSMA protein expression following 72 hours of MDM2, PSMA or NT siRNA treatment (blot show representative data; n=3). d) Percentage integrated density of NT control siRNA over three western blots (graph shows mean+SD; n=3). (Statistical significance assessed through unpaired t-test with Welch's correction between targeting siRNA and NT control expression levels, with * $p < 0.05$, ** $p < 0.01$).

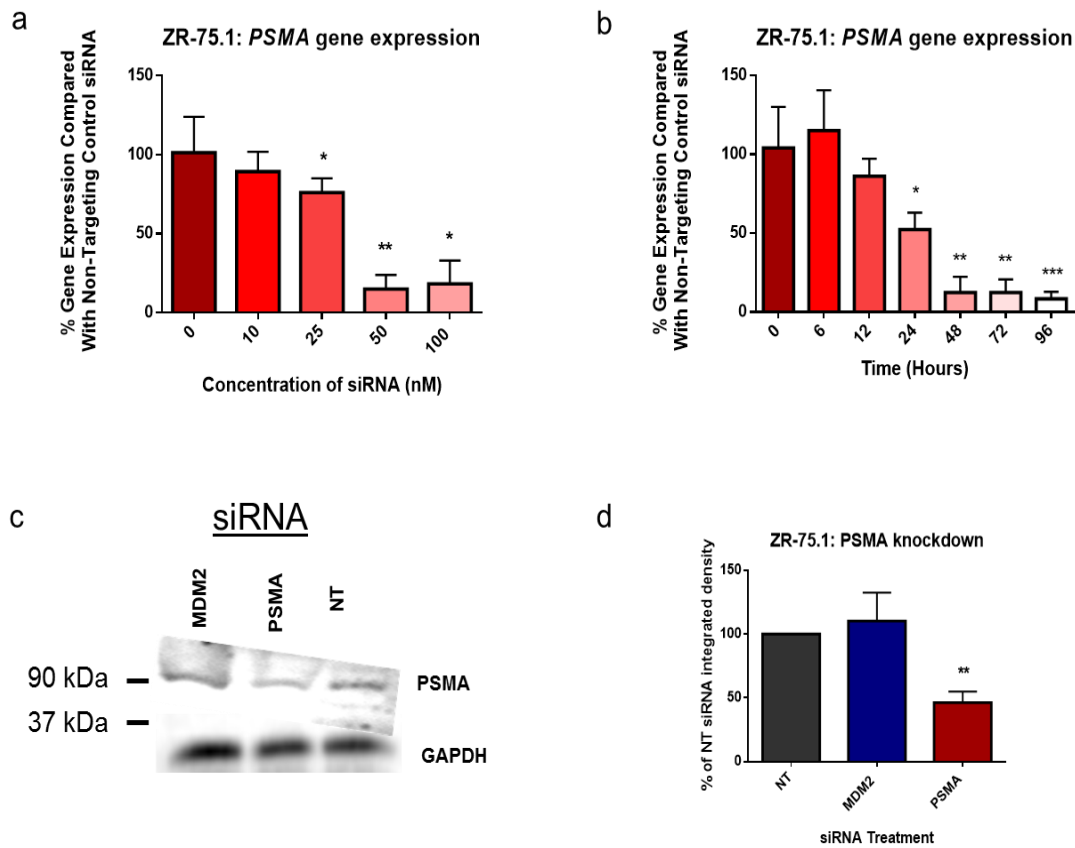


Figure 3.5. Knockdown of PSMA in ZR-75.1 cell line. a) Dose-dependent knockdown of *PSMA* gene at 0, 10, 25, 50 and 100 nM PSMA siRNA concentrations (graph shows mean+SD; individual experiments carried out in triplicate; n=3). b) Time-course expression of *PSMA* gene at 0, 6, 12, 24, 48 and 72 hours following 100nM PSMA siRNA treatment (graph shows mean+SD; individual experiments carried out in triplicate; n=3). c) PSMA protein expression following 72 hours of MDM2, PSMA or NT siRNA treatment (blot show representative data; n=3). d) Percentage integrated density of NT control siRNA over three western blots (graph shows mean+SD; n=3). (Statistical significance assessed through unpaired t-test with Welch's correction between targeting siRNA and NT control expression levels, with * $p < 0.05$, ** $p < 0.01$, $p < 0.001$).

expression were greater than 50% compared to the NT control (Figure 3.5b). Finally, protein expression following knockdown was assessed, with a 54% knockdown in PSMA expression following targeted siRNA treatment ($p=0.0085$) (Figure 3.5c and d).

MDM2 knockdown leads to a decrease in PSMA gene expression and vice versa

After 48 hours post-transfection of MDM2 siRNA into MDA-MB-231 and ZR-75.1, mRNA levels of *PSMA* were assessed. Interestingly, a significant decrease in *PSMA* levels were seen following MDM2 siRNA (MDA-MB-231: $p=0.0058$; ZR-75.1: $p=0.0021$) (Figure 3.6a and b), as well as a significant decrease in *MDM2* gene expression being seen following PSMA siRNA treatment (MDA-MB-231: $p=0.0037$; ZR-75.1: $p=0.0129$) (Figure 3.6c and d).

In addition, dual treatment was undertaken in MDA-MB-231 cells with 50 nM of each MDM2/PSMA, MDM2/NT or PSMA/NT siRNAs and was compared to 100nM of NT, giving an equal concentration of siRNA for each comparative experiment. This experiment showed a highly significant decrease in both *MDM2* and *PSMA* expression, compared to NT siRNA ($p<0.0001$) (Figure 3.7a and b).

Assessment of *MDM2* gene expression showed a greater decrease in transcript levels in the cells treated with MDM2/PSMA and MDM2/PSMA than PSMA/NT siRNAs. On the other hand, *PSMA* gene expression showed a greater decrease when cells were treated with MDM2/PSMA or PSMA/NT siRNA, compared to those treated

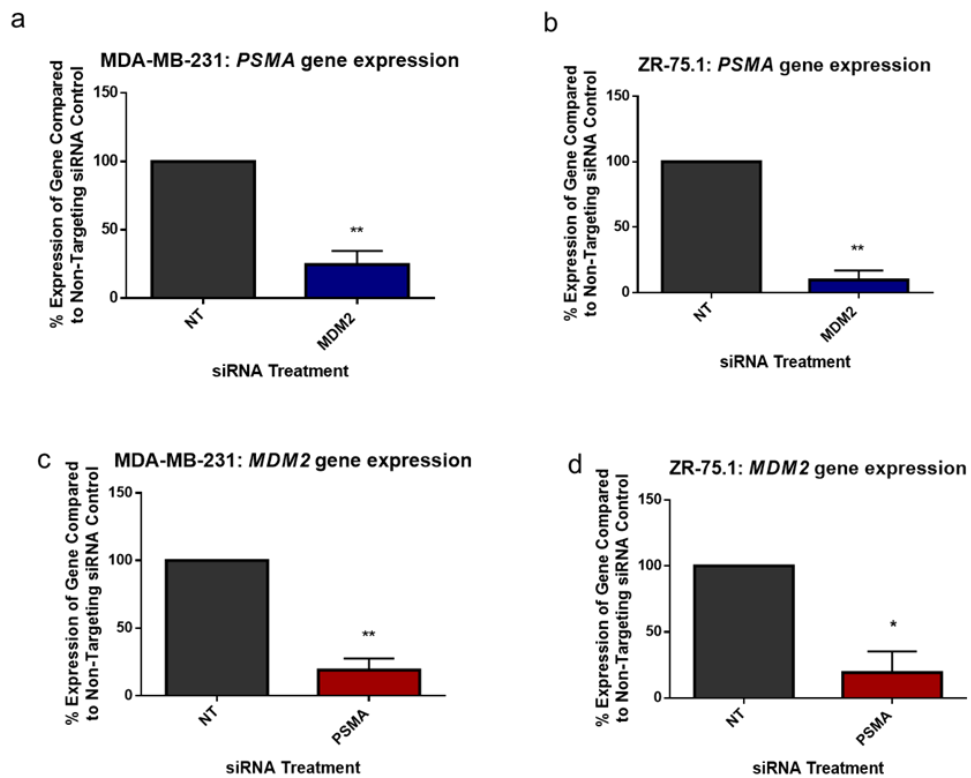


Figure 3.6. Resultant expression of *PSMA* transcript following 48 hours of *MDM2* siRNA treatment in MDA-MB-231 and ZR-75.1, and vice versa. a) % *PSMA* gene expression following *MDM2* siRNA treatment in MDA-MB-231 cells. b) % *PSMA* gene expression following *MDM2* siRNA treatment in ZR-75.1 cells. c) % *MDM2* gene expression following *PSMA* siRNA treatment in ZR-75.1 cells. D) % *MDM2* gene expression following *PSMA* siRNA treatment in ZR-75.1 cells. (Graphs show % expression compared to NT control siRNA treated cells +SD). (Statistical significance assessed using unpaired t-test with Welch's correction with * $p < 0.05$ and ** $p < 0.01$).

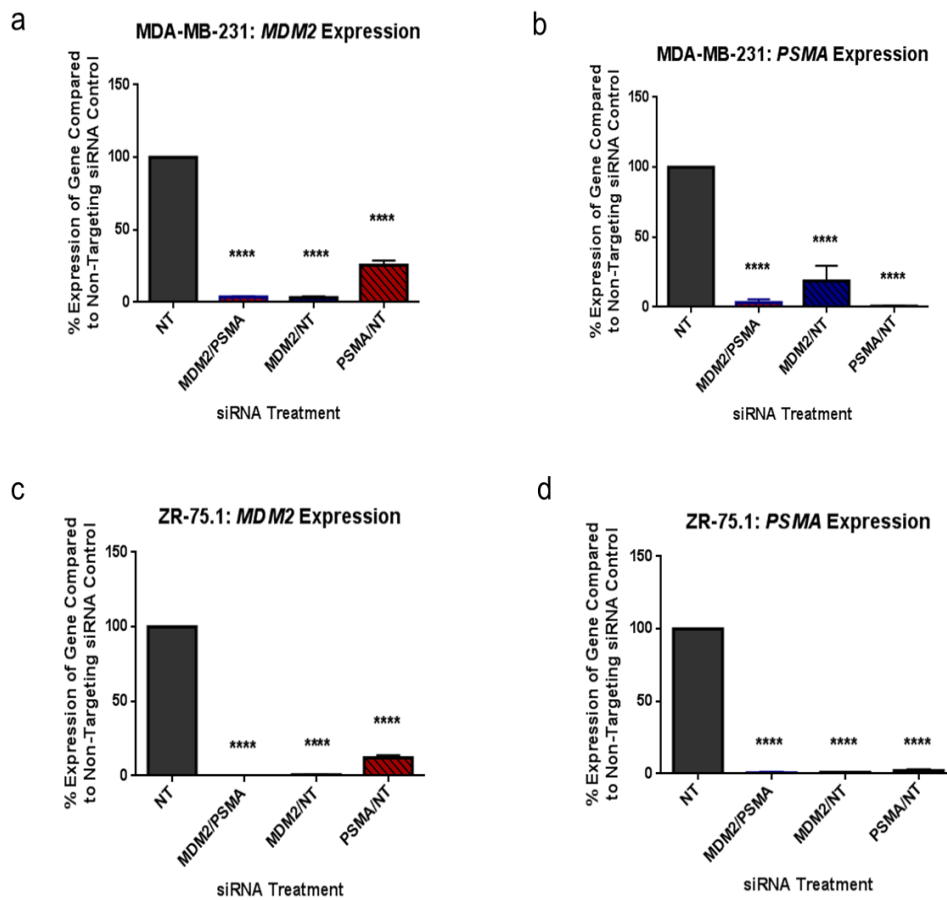


Figure 3.7. 48 hour dual siRNA treatment in MDA-MB-231 and ZR-75.1 cell lines. a) Percentage expression of *MDM2* transcript following treatment with NT, MDM2/PSMA, MDM2/NT or PSMA/NT siRNA in MDA-MB-231 cells. b) Percentage expression of *PSMA* transcript following treatment with NT, MDM2/PSMA, MDM2/NT or PSMA/NT siRNA in MDA-MB-231 cells. c) Percentage expression of *MDM2* transcript following treatment with NT, MDM2/PSMA, MDM2/NT or PSMA/NT siRNA in ZR-75.1 cells. d) Percentage expression of *PSMA* transcript following treatment with NT, MDM2/PSMA, MDM2/NT or PSMA/NT siRNA in ZR-75.1 cells. (Graphs show % expression compared to NT control siRNA treated cells +SD) (Statistical significance assessed using one way ANOVA with **** $p < 0.0001$).

with MDM2/NT siRNA alone. Analysis of the resultant effect on ZR-75.1 cells treated with the same dual siRNAs showed similarly significant results, compared to NT siRNA ($p < 0.0001$) (Figure 3.7c and d). Again, the decrease in *MDM2* transcript levels was most striking in those cells treated with MDM2/PSMA and MDM2/NT siRNA compared to PSMA/NT siRNA.

Assessment of MDM2 and PSMA transcript levels in breast tissue

Analysis of breast tissue samples containing 30 normal background breast tissue and 112 breast cancer tissues samples was undertaken. When *MDM2* transcript levels were assessed, no significant difference was seen between the normal and tumour tissue expression levels ($p = 0.536$) (Figure 3.7a). *MDM2* gene expression levels were shown to increase from tumours of grade 1 to grade 2 ($p = 0.010$) and to grade 3 ($p = 0.009$); although no significant difference was seen between grade 2 and 3 ($p = 0.825$). No significant difference was seen between the different values of Nottingham Prognostic Index (NPI). TNM stage 1 exhibited significantly higher than stage 2 ($p = 0.029$) and stage 3 ($p = 0.001$); but no significance was seen between any stage and stage 4. Moreover, stage 3 was significantly decreased from stage 2 ($p = 0.0268$). There was no significant trend in the relation of *MDM2* and clinical outcome, whether those patients were disease free at follow up or had a poor outcome. There was also no significant difference in *MDM2* expression whether the tumour was ductal, lobular or other. A

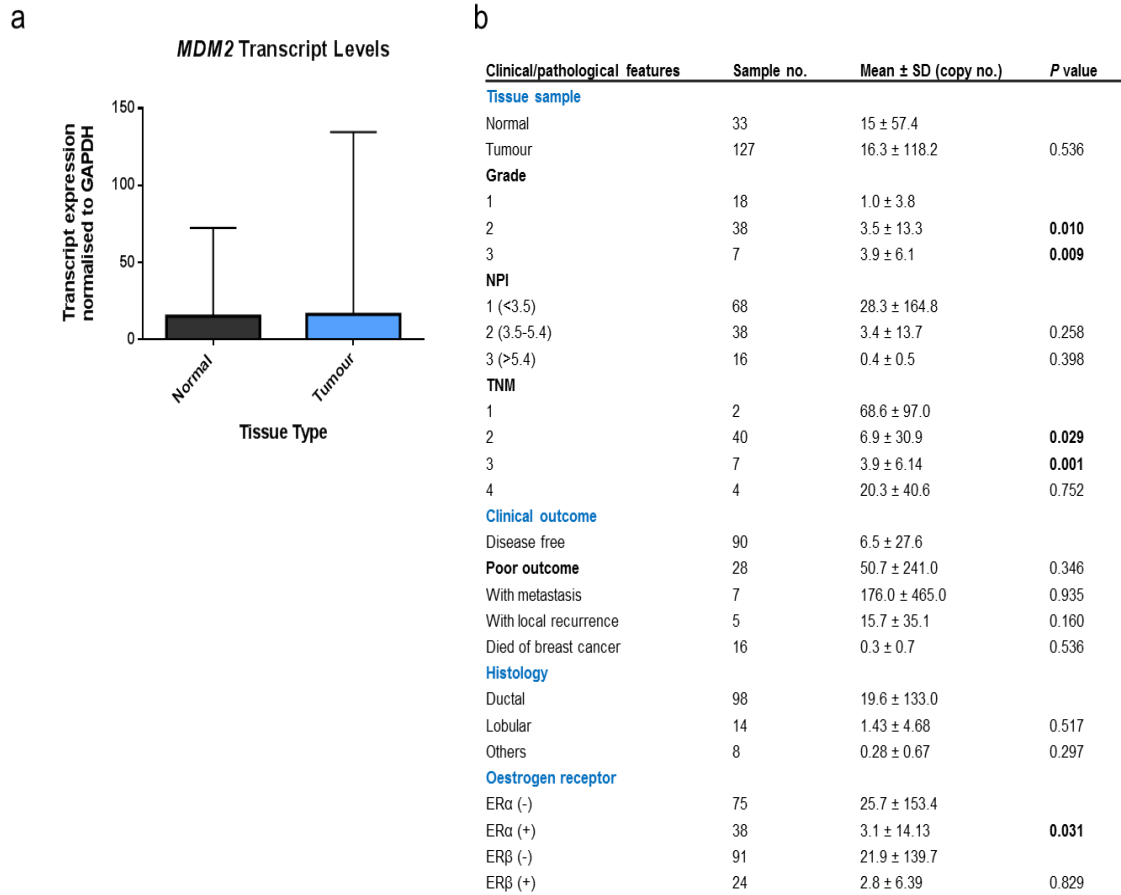


Figure 3.8. *MDM2* transcript expression levels in breast tissue. a) Fold change in transcript expression of *MDM2* in both normal and tumour breast tissue (Graph shows transcript no. + SD). b) Clinical/pathological features of normal and tumour breast tissues with mean copy number, SD and *p*-value (Significances assessed using Mann-Whitney U Test; **bold numbers represent those with a significant difference**).

significant difference was seen between patients with negative and positive oestrogen receptor α (ER α), with ER α (-) showing a significantly higher mean than those which are ER α (+) ($p=0.031$). On the other hand, no significance was seen between patients who were ER β negative and positive. When survival analyses were carried out, it was noted that patients with higher levels of MDM2 tend to have shorter overall (Figure 3.9a) and disease-free survival (Figure 3.9b), although the difference was not significant.

When *PSMA* transcript levels were assessed in the same breast cancer cohort, no significant difference was seen in expression between the normal and tumour breast tissues ($p=0.744$) (Figure 3.10a). Analysis of *PSMA* transcript levels following the division of the tissues into their clinical features also showed no striking or significant differences in expression. However, comparison of ductal and lobular tumours showed a trend of very low *PSMA* transcript expression the lobules, compared to the ducts, although this did not reach significance ($p=0.544$) and neither reached significance when compared to other histological forms. The one significant difference seen in this data was between the ER β (-) and ER β (+) patients, with those who were negative showing a significantly lower *PSMA* transcript level than those who were positive ($p=0.028$) (Figure 3.10b). In addition, there were no significant differences between patients with high and low *PSMA* levels in overall survival ($p=0.359$)(Figure 3.11a) or disease-free survival ($p=0.079$)(Figure 3.11b).

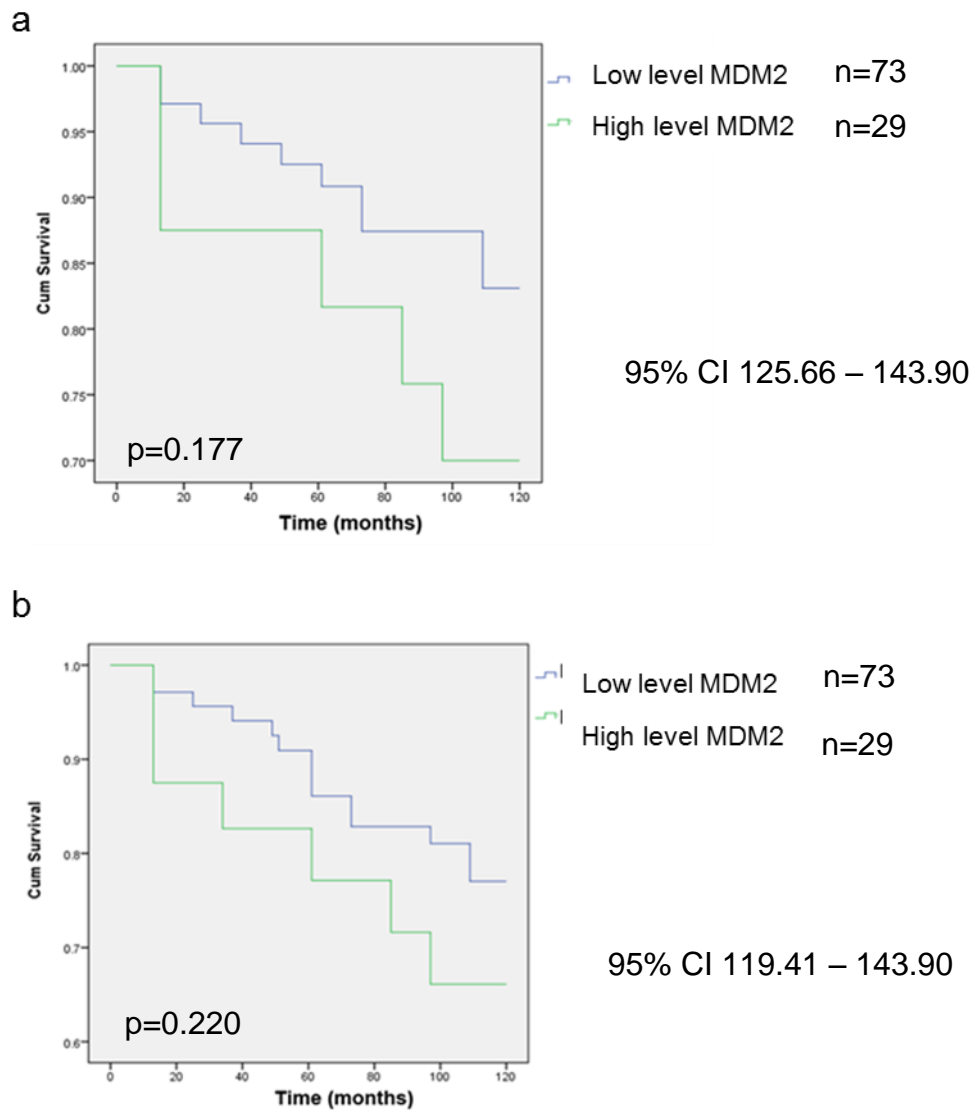


Figure 3.9. Survival analysis of breast cancer patients with low or high *MDM2* transcript expression. a) Overall survival (high level MDM2 median 138.12 and low level MDM2 median 116.30). b) Disease-free survival (high level MDM2 median 132.53 and low level MDM2 median 111.53). (NPI2 used to dichotomise data; graphs show cumulative survival against survival time in months).

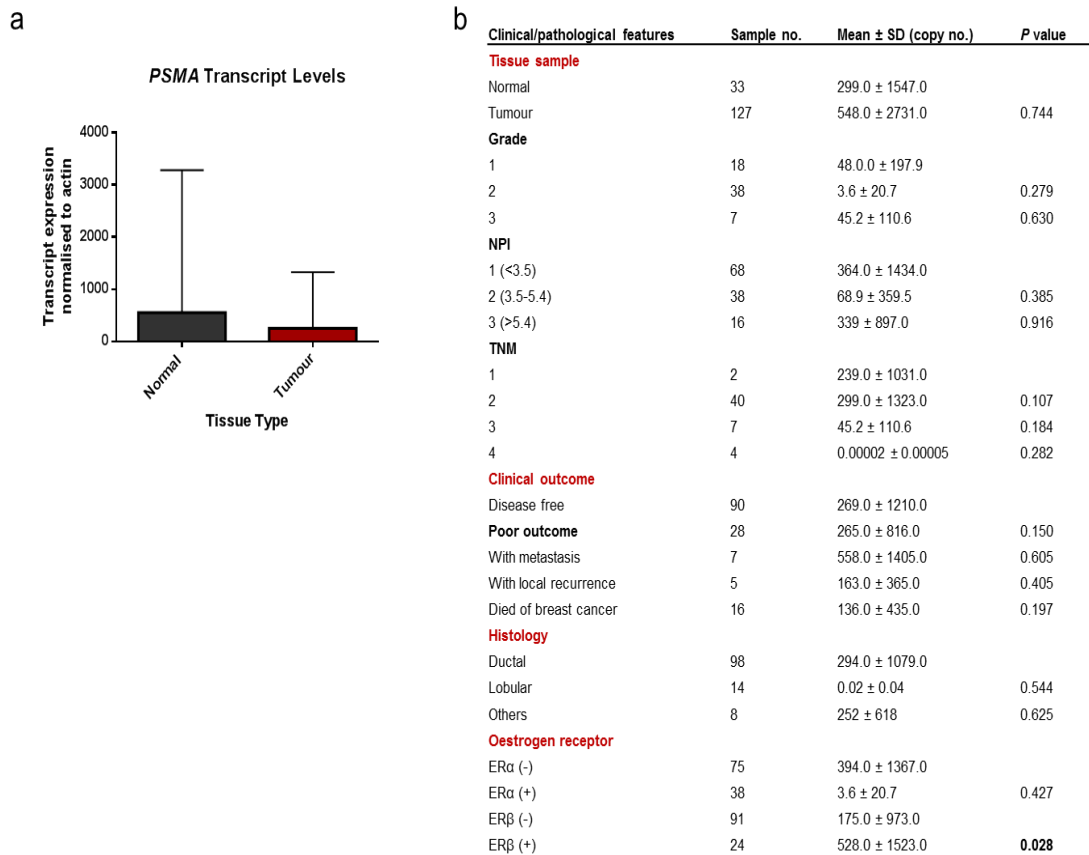


Figure 3.10. PSMA transcript expression levels in breast tissue. a) Fold change in transcript expression of *PSMA* in both normal and tumour breast tissue (Graph shows transcript no. + SD). b) Clinical/pathological features of normal and tumour breast tissues with mean copy number, SD and *p*-value (Significances assessed using Mann-Whitney U Test; **bold numbers represent those with a significant difference**).

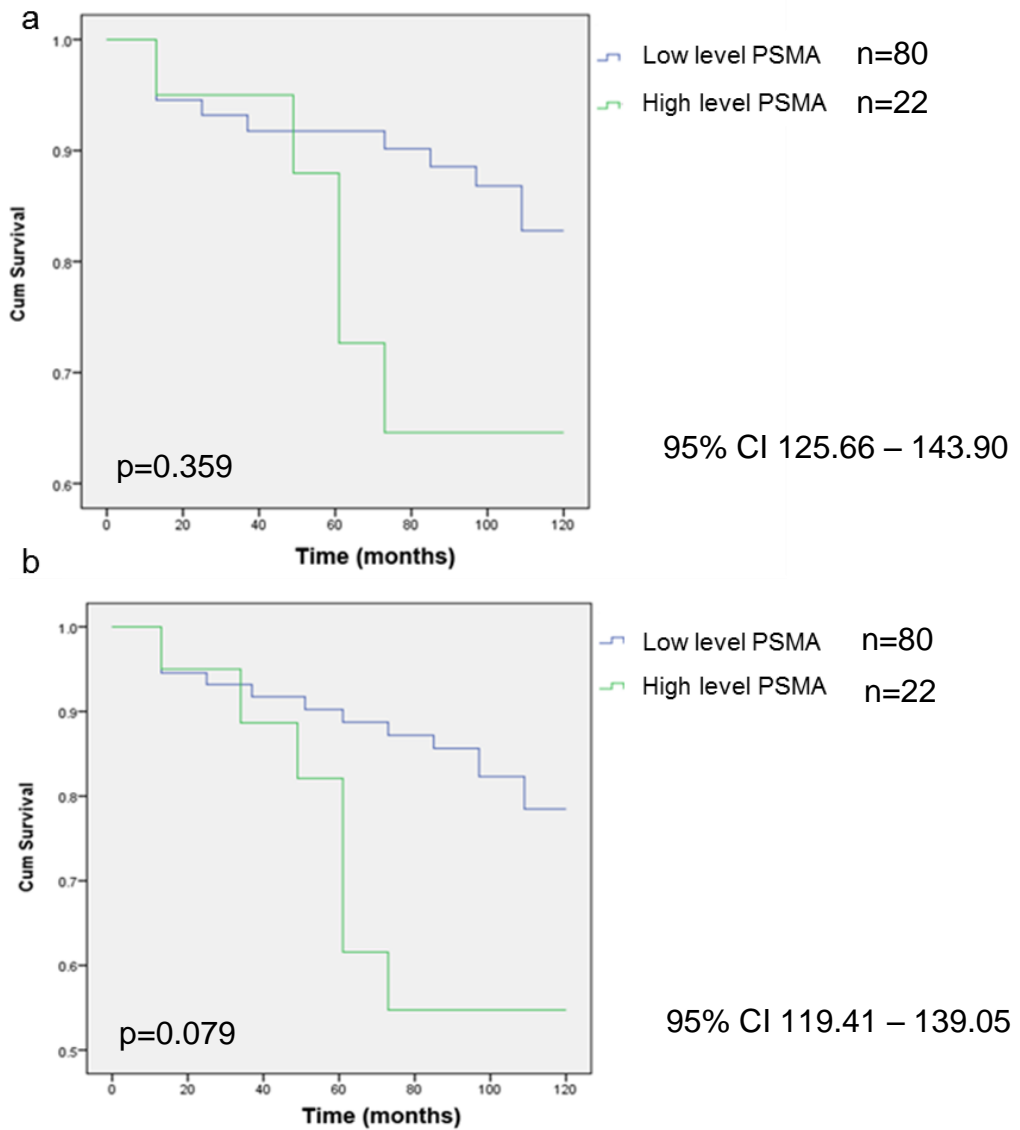


Figure 3.11. Survival analysis of breast cancer patients with low or high PSMA transcript expression. a) Overall survival (high level PSMA median 137.75 and low level PSMA median 106.77). b) Disease-free survival (high level PSMA median 133.84 and low level PSMA median 97.12). (Data dichotomised using NPI2; graphs show cumulative survival against survival time in months).

3.4. Discussion

MDM2 is implicated in the progressive properties and is overexpression in many types of cancer (Rayburn et al., 2005, Shangary et al., 2008, Wade et al., 2013, Onel and Cordon-Cardo, 2004), including breast cancer (Turbin et al., 2006, McCann et al., 1995, Brekman et al., 2011, Onel and Cordon-Cardo, 2004).

PSMA was originally thought to be solely overexpressed in prostate cancer (Horoszewicz et al., 1987, Chang and Heston, 2002, Chang et al., 1999, Bostwick, 1998, Bostwick et al., 1998, Sweat et al., 1998), however has been more recently found to be expressed in other types of cancers, including breast (Wernicke et al., 2014, Nomura et al., 2014, Ross et al., 2003, Haffner et al., 2009).

A relatively recent study showed that in the prostate cancer cell line, LNCaP, PSMA knockdown led to a decrease in *MDM2*, amongst other gene expression changes (Xu et al., 2013). In addition, many pathways in which each of the proteins are implicated are the same, including: folate metabolism (Pinto et al., 1996, Yao et al., 2010, Maguire et al., 2008); PI3K/AKT (Guo et al., 2014, Ogawara et al., 2002, Milne et al., 2004, Mayo and Donner, 2001); and the MMPs (Conway et al., 2006, Syed et al., 2012, Chen et al., 2013, Zhang et al., 2014).

Therefore, this study was intended to assess if there was an interplay between MDM2 and PSMA in breast cancer cells, a line of study which has been, thus far, not explored.

As an initial step, all available breast cancer cell lines were screened for their transcript levels of *MDM2* and *PSMA*. Although this study was aiming to look at the activity of MDM2 independent to p53, the p53 status of the cell lines being used in a study must be taken into account. Therefore, the intention was to choose one cell line which was p53 wild-type and one which was p53 mutant, in order for it to be possible to assess whether functional and signalling changes we were seeing through MDM2 knockdown were through p53 or another mechanism. In addition we attempted to choose one TNBC cell line and one non-TNBC in order to cover a wider variety of breast cancer types. Finally, the *MDM2* and *PSMA* gene expression levels were assessed in order to choose correct cell lines. It was seen that the highest expressing cell line of *MDM2* transcript was ZR-75.1, followed by MCF-7, SK-Br-3 and then MDA-MB-231. *PSMA* transcript, on the other hand, showed highest expression in the SK-Br-3 cell line, followed by ZR-75.1, MCF-7 and MDA-MB-231. When assessed *in vitro*, SK-Br-3 cells were extremely hard to culture, and with the types of functional experiments and transfections we had in mind for this project, we needed cell lines which proliferated well and were amenable to a reasonable level of manipulation. Therefore, with this in mind and our ideal breast cancer cell lines, as stipulated above, ZR-75.1 (p53 wild-type, ER(+), high *MDM2* and high *PSMA* expression) and MDA-MB-231 (p53 mutant, TNBC, average *MDM2* and average *PSMA* expression) were chosen for this study.

One potential problem with using ZR-75.1 is that they are classed as having a low invasive capacity, with invasion being something we hoped to address following knockdown in this study. However, other reports do indicate that they were able to gain results from ZR-75.1 in terms of changes to the invasive capacity of cells (Wang et al., 2015, Kato et al., 2005).

MDA-MB-231 cells, on the other hand, are known to be highly invasive. They are also known to express high levels of p53 although this protein is mutated (Hui et al., 2006). This mutation is known as R280K and is seen in MDA-MB-231 to affect the DNA-binding domain of the molecule and occurs in 1.3% of breast tumours (Walerych et al., 2012, Bull et al., 2004). Unlike many tumour suppressors genes whose inactivation occurs when they are deleted or truncated, the majority of the mutations which occur in the *TP53* gene are missense mutations. This means that the mutation is a simple base-pair substitution which results in the translation of a different amino acid in the protein. It is known that many of these mutations can lead to a dominant-negative effect being exerted on the remaining wild-type allele, which allows an abrogation of the ability of p53 to inhibit transformation of a cell, especially when this mutant protein is expressed at much higher levels than its wild-type counterpart, which is often the case (Brosh and Rotter, 2009, Oren and Rotter, 2010, Freed-Pastor et al., 2012). It is well established that the loss-of-function leads to an inability of wild type p53 to bind to responsive elements on DNA but it is also thought that these

missense mutations may cause a gain-of-function, with strong selection for these types of mutations suggesting a positive role for certain p53 mutants in tumorigenesis (Yeudall et al., 2012, Bae et al., 2013, Freed-Pastor and Prives, 2012). In particular, reports claim that mutant p53 may have the ability to promote the migration and metastasis of cells (Terzian et al., 2008, Adorno et al., 2009, Caulin et al., 2007, Muller et al., 2009).

Though the use of cell lines is appropriate and requisite for this study, it is important to remember throughout the limitations of using cell lines to model the *in vivo* environment of tumour formation. Establishment of a new breast cancer cell line involves a pattern of growth which is characterised by an initially slow proliferation of cells which is then followed by an exponential expansion of a few cells, implying a clonal selection for cells which are particularly proliferative and amenable to cell culture (Vincent et al., 2015). Cells are prone to genotypic and phenotypic drift through their continuous culture, where subpopulations with more rapid growth, differing hormone receptor content, karyotype and clonogenicity arise, leading to selection of clones within a population. These variances lead to a high level of discrepancies between the same cell line used by different laboratories (Burdall et al., 2003).

Another weakness of cell culture is the lack of the environment surrounding the cells. *In vivo* cells are growing in a highly complex, partially hypoxic, 3D microenvironment. However, in culture, the cells are supplemented with growth factors, maintained in nutrient-

rich media and passaged indefinitely at relatively high atmospheric pressure (Vincent et al., 2015). Culture of cells in conditions which are incorrect can also lead to a dramatic change in the cell morphology, cell-cell and cell-matrix interactions, cell polarity and differentiation (Holliday and Speirs, 2011, Yamada and Cukierman, 2007, Streuli et al., 1991). Therefore, it is highly feasible that different cells will thrive in this environment and the cells may differ substantially from the tumours from which they came (Vincent et al., 2015).

However, despite these downfalls, cell lines have many advantages: they are easy to handle; they allow scientists an unlimited source of self-replicating cells which can be grown in huge quantities; they can be frozen and rethawed; and they are relatively homogeneous (Burdall et al., 2003). In addition, cell lines are the current way in which it is possible to model the tumour environment to some extent in a cost- and time-effective manner, before experiments are moved on to the *in vivo* stages in promising studies.

When selecting methods to be undertaken in order to achieve knockdown of MDM2 and PSMA, there were a variety of different method choices. However, due to siRNA being cheap and quick to optimise, this transient form of knockdown was selected for use over the more expensive, time-consuming stable method of lentiviral knockdown. The transient nature of siRNA knockdown was not a limitation for this study, since all of the assays undertaken were short-term and were not be affected by this aspect of the knockdown

method. Therefore, our chosen cell lines: MDA-MB-231 and ZR-751, were used to optimise and decide on dose and time points to be used.

Firstly, it is important to note that the same dose of siRNA was hoped to be used for both knockdowns, allowing the same concentration of NT siRNA to be used in each experiment, so that this could be used as a control for both MDM2 and PSMA siRNA. In addition, it was hoped that choosing the same dose of siRNA for both knockdowns would allow for a more direct comparison, without having to take into account how the varying siRNA concentrations lead to a differing amount of off-target effects. In addition, the same logic was used when choosing the time-points at which to undertake assays and take RNA and protein. Moreover, at gene expression levels, we aimed for a >50% knockdown to be achieved, since knockdown is usually less apparent at protein level and in order to have the best chance of seeing significant results, a significant level of protein knockdown is needed. A final important note is that, although the MDM2 protein half-life is extremely short, with a number of reports claiming this is around 30 minutes (Pan and Haines, 1999, Peng et al., 2001, Finlay, 1993), the PSMA half-life has been proved to be much longer. Differing reports have claimed the protein has a half-life of two days (Schulke et al., 2003) or 55 hours (Ghosh and Heston, 2004) and it is important to bear this in mind when assessing protein knockdown.

With all this in mind, in MDA-MB-231 a dose of 100 nM of siRNA was selected following gene knockdown, and transcript levels were seen to significantly decrease following both siRNA treatments compared to the NT control. Time-course studies at this concentration then showed a significant knockdown in transcript expression through both siRNAs from 24, 48 and 72 hours onwards. Due to the long half-life of PSMA, protein levels were assessed at 72 hours to show a greater level of knockdown, at this point, levels were decreased to around 50% when cells were treated with PSMA siRNA, which is what would be expected. MDM2 protein levels were also seen to be significantly decreased following MDM2 siRNA.

Similar results were seen in ZR-75.1 cells, although 50 nM of siRNA was highlighted to be enough to induce effective knockdown of both siRNAs. Time-course studies showed similar results, with onwards of 24 hours of treatment showing a significant decrease in gene expression for both siRNAs. Protein analysis also showed a significant knockdown at 72 hours of both siRNAs, with PSMA protein expression showing, again, a decrease of around 50% following PSMA siRNA treatment. In addition, MDM2 knockdown was highly significant.

Interestingly, assessment of the levels of *MDM2* transcript following PSMA siRNA treatment in each cell line showed a significant decrease in expression compared to the NT control, which is in line with those results seen in LNCaP (Xu et al., 2013). Additionally, assessment of *PSMA* transcript levels following MDM2 siRNA led to

a similar decrease in both cell lines. However, this decrease, although highly significant at gene level, was not replicated at protein level. This is a highly interesting phenomenon which is not unheard of. In fact it is now well known that often mRNA and protein levels do not correlate well and only around 40% of time are cellular protein levels correctly predicted through mRNA measurements (Kendrick, 2014). Many groups have attempted to quantify this correlation through the use of the coefficient of determination (R^2) and found surprisingly low values when mRNA and protein expression are compared. R^2 values of 0.29 (Vogel and Marcotte, 2008), 0.35 (Tian et al., 2004) and 0.3 (Schwanhausser et al., 2011) have been reported. Moreover Schwanhausser *et al.*, (2011) found that the most important cellular regulators have the lowest correlation between mRNA and protein, due to their unstable mRNA and protein. On the other hand, they showed that it is the housekeeping proteins which have a relatively good correlation. It is well known that a multitude of post-translational mechanisms exist in order to control protein turnover. Given this, it is not wholly unreasonable that we may only see a 40% correlation.

Dual siRNA treatments were also undertaken in both cell lines and it was seen that both *MDM2* and *PSMA* transcript expression is significantly decreased following treatment with 50 nM of each MDM2/PSMA, MDM2/NT or PSMA/NT, compared to 100nM NT siRNA alone.

Finally, *MDM2* and *PSMA* transcript levels were assessed in a breast tissue cohort. Comparison of normal and tumour breast tissue showed no significance in the transcript expression levels of either *MDM2* or *PSMA*. In terms of *MDM2* transcript expression, there are varying reports on the amplification of gene expression in cancer. Some studies claim that amplification of the *MDM2* gene is common in liposarcomas (Teodoro et al., 2007, Marino-Enriquez et al., 2014); however, it has been stated that amplification of *MDM2* gene is very rare in primary breast cancer (Yu et al., 2014). In addition, assessment of GEO datasets showed similar results, with no difference between normal and tumour transcript expression of *MDM2*, or between normal lobular tissue and invasive lobular carcinoma, or normal ductal tissue and invasive ductal (GEO dataset GDS3139 & GDS2635) *PSMA* mRNA, on the other hand, has been seen to be overexpressed in prostate cancer (Schmittgen et al., 2003). However, no significance was seen when the same GEO data sets as analysed for *MDM2*, were assessed for *PSMA* transcript.

The lack of significance in the difference in transcript expression levels between normal and tumour, although both proteins are known to be overexpressed in various cancer types. This implies that the increased expression of both *MDM2* and *PSMA* occurs post-transcriptionally.

Interestingly, in the cohort study, both *MDM2* and *PSMA* transcript levels were seen to be significantly altered in relation to ER. *MDM2*

transcript levels were significantly higher in ER α negative tumours, compared to ER α positive tumours. On the other hand, *PSMA* transcript levels were significantly higher in those patients expressing ER β .

ER α and ER β belong to a superfamily of nuclear receptors that regulate the transcription of multiple target genes upon binding to oestrogen response elements (ERE) present within the regulatory region of the genes (Green et al., 1986). Expression of ER α in breast cancer is closely associated with tumour biology (Jensen et al., 2001). The presence of ER α indicates a phenotype of a less aggressive nature and a more favourable prognosis (Nomura et al., 1988). The role of ER β is much less well-characterised and its exact role remains elusive (Haldosen et al., 2014).

MDM2 has been previously linked to oestrogen receptor, with a significant correlation between levels of MDM2 and ER α being seen in both breast cancer tissue and cell lines (Hideshima et al., 1997, Marchetti et al., 1995, Gudas et al., 1995). It was previously observed that all ER α -positive breast cancer cell lines studied show an increased level of *MDM2* transcript, with the opposite seen in those negative for ER α (Gudas et al., 1995), indicating some functional relationship between the two proteins, with one group suggesting that MDM2 is a p53-independent, positive regulator of ER α (Saji et al., 2001). In addition, another group claimed that MDM2, through interactions with ER α , plays a role in the enhancement of ER α -mediating gene expression and oestrogen

responsiveness of breast cancer cells (Kim et al., 2011a); whilst another stated that oestrogen increases the protein levels of MDM2 in the breast cancer cell line MCF-7 (Brekman et al., 2011). However, the cohort analysis in our own study showed data with the opposite correlation, with those patient samples lacking ER α showing higher *MDM2* transcript levels than those with the receptor.

On the other hand, PSMA has not been investigated alongside ER, apart from in one study of the neovasculature of breast carcinoma showing higher PSMA expression was seen in those patients who were ER-negative (Wernicke et al., 2014). Again, although this does not specify a type of ER receptor, this does not fit with what was seen in our cohort, with those patients who were negative for ER β showing lower levels of *PSMA* transcript than those who were positive.

MDM2 transcript levels were shown to decrease through TNM stages, whilst increasing through the tumour grade. However, no significance was seen between the NPI scores. This is very interesting, as both TNM staging and NPI take into account the tumour size and spread to lymph nodes, however TNM staging takes into account metastases, whereas NPI takes into account the grade. This insinuates that it is something in the metastasis of the tumour which leads to a lower level of *MDM2* transcript expression. This could be simply that, since the majority of the increase in expression is not reliant on amplification, and MDM2 protein levels are known to increase in more progressive tumours, that the cells are simply

attempting to restabilise MDM2 levels. This feedback loop is, at least, known to occur when wild-type p53 is present (Moll and Petrenko, 2003). However, it must be noted that there were only two patients in TNM stage 1 and a higher number would need to be used in order to draw firm conclusions from this data. The other interesting finding is that there exists a trend between high levels of expression of both MDM2 and PSMA transcripts and shorter survival of the patients. Although these trends do not reach statistical significance, owing largely to the size of the cohort in the present study, the trend does provide some support to the portrayed link between these two molecules and disease progression. A larger cohort blended with analyses on gene transcripts and protein would be highly desirable.

In summary, MDA-MB-231 and ZR-75.1 cells lines were chosen to continue the work throughout the project. Interestingly, *PSMA* transcript levels were significantly decreased following MDM2 siRNA treatment and *vice versa*; however, this was not replicated at protein level.

Chapter IV

Knockdown of MDM2
and PSMA in breast
cancer cell lines leads
to a decrease in
proliferative abilities
and altered apoptotic
ability and cell cycle
progression

4.1. Introduction

There are many facets to the development of cancer from a normal cell and one of these is the ability to proliferate in an uninhibited manner, through both sustained proliferative signalling and the evasion of growth suppressors. Normal tissues carefully control the production and release of growth-promoting signals, but cancer cells are able to deregulate these signals, mostly conveyed through growth factors which bind cell-surface receptors. Cancer cells can produce growth factor ligands; they may send signals into the tumour-associated stroma in order to induce paracrine signalling from normal cells; they can elevate the levels of receptor on the cell surface, causing hypersensitivity to ligand; and they can cause constitutive activation of components working downstream of receptors, meaning no receptor-ligand binding is needed for activation of the proliferative signalling (Hanahan and Weinberg, 2000, Hanahan and Weinberg, 2011).

In normal tissues, many anti-proliferative signals (including soluble growth inhibitors and immobilised inhibitors embedded in the ECM and on the surface of nearby cells) work to maintain cell quiescence and homeostasis. However, in addition to their ability to increase proliferative signalling pathway activation, cancer cells can also gain the ability to evade this growth suppression (Hanahan & Weinberg, 2000).

Previously, an increase in MDM2 has been linked to an increase in cell proliferation (Deb et al., 2014, Brekman et al., 2011) and use of the MDM2 inhibitor nutlin-3a was shown to suppress proliferation (Wang et al., 2012). Similar results were seen in reports of PSMA, with Yao *et al.*, (2006) reporting expression of PSMA leading to an increase in proliferation. This sentiment was echoed in other reports (Yao et al., 2010, Zhang et al., 2013).

The cell cycle is also often altered in cancer, leading to unscheduled proliferation (Massague, 2004, Malumbres and Barbacid, 2009).

This process is controlled by many mechanisms which ensure correct cell division (mitosis). Replication of the DNA occurs in what is known as the S phase, before this cells are in gap 1 phase (G1) where cells can enter a state known as G0, which accounts for the majority of cells which are non-growing and non-proliferating.

Following this, a second gap phase (G2) occurs (Vermeulen et al., 2003, Schafer, 1998). Tumour-associated defects in the cell cycle are often mediated through changes in cyclin-dependent kinase (CDK) activity. Cyclins are produced and then degraded at different points in the cycle in order to regulate the CDKs, which are essential for driving each phase of the cell cycle in a timely manner (Malumbres and Barbacid, 2009).

Despite its known oncogenic ability, MDM2 has been shown to induce an arrest in cell cycle at G0/G1 phase in normal human and mouse cells (Frum and Deb, 2003, Brown et al., 1998). In addition, p53 has been shown to control both the G2/M transition and G1

checkpoints of the cell cycle (Agarwal et al., 1995). Meanwhile, PSMA was shown to play a part in mitosis, with an involvement in interphase (S phase) and an interaction with the anaphase promoting complex (APC) to promote chromosomal instability (Rajasekaran et al., 2008). Studies using short hairpin knockdown of PSMA showed an increased in cells in G1 phase and a decrease in cells at S phase (Zhang et al., 2013).

The ability of the tumour cell population to increase in number is not just dictated by rate of cell proliferation, but also by the rate of programmed cell death (apoptosis). Apoptotic machinery can be broadly divided into two categories – sensors and effectors. Sensors are responsible for monitoring the extracellular environment for normal or abnormal conditions and then regulate the effectors (Hanahan and Weinberg, 2000). The most commonly occurring loss of an apoptotic regulator through mutation involves the *p53* tumour suppressor gene. The mutation results in an inactivation of the p53 protein and it is seen in over 50% of human cancers (Harris, 1996a, Hanahan and Weinberg, 2000). The p53 protein is known to be negatively regulated by MDM2 (Moll and Petrenko, 2003) and MDM2 overexpression is also very common in human cancers (Toi *et al.*, 1997; Baunoch *et al.*, 1996; Deb, 2003), leading to a similar phenotype as seen through a mutation in the *p53* gene – an inability of p53 protein to act as it should. With this, it has been seen that loss of MDM2 in cells leads to an increase in apoptosis (de Rozieres et al., 2000, Ray et al., 2011, Dilla et al., 2000). The same result was

seen by one group from PSMA knockdown in prostate cancer cells (Huang, 2015).

The caspases are a family of endoproteases which are involved in cell homeostasis through regulation of cell death. Caspase-mediated processing of substrates can result in the generation of active signalling molecules which participate in ordered processes such as apoptosis and inflammation (McIlwain et al., 2016). Caspases have been broadly classified into their known roles in apoptosis (caspase-3, -7, -8 and -9) and inflammation (caspase-1, -4, -5 and -12). In apoptosis, initiator caspases (-8 and -9) activate the executioner caspases (-3 and -7), which use their activity to degrade important structural proteins and activate other enzymes (Chang et al., 2003, Riedl and Shi, 2004, McIlwain et al., 2016).

MDM2 has previously been linked to caspase-2 and -3. One report claimed that caspase-2 mediates the cleavage of MDM2 (Oliver et al., 2011, Pochampally et al., 1999). In addition, another report claimed that MDM2 is cleaved by caspase-3 (Pochampally et al., 1998). Thus far, PSMA has not been linked directly to any of the caspases.

Therefore, in this chapter of research we aimed to assess the ability of MDM2 and PSMA knockdown to complete these initial stages during cellular metastasis.

4.2. Materials & Methods

Cell lines and treatments

MDA-MB-231 and ZR-75.1 metastatic breast cancer cell lines, maintained in DMEM media with 10% FBS and antibiotics, were used in this chapter. All cells were maintained at 37°C with 5% CO₂. The breast cancer cell lines were transiently transfected with MDM2-, PSMA- or non-targeting siRNA using Fect4 (for MDA-MB-231) or Fect1 (for ZR-75.1) transfection reagents, respectively. MDA-MB-231 cells were treated with 100nM of each siRNA and ZR-75.1 cells were treated with 50nM, according to the manufacturer's instructions, following our optimisation experiments.

Proliferation assay

5 x 10³ cells were seeded in 100 µl of serum-free medium (no antibiotics) per well in a black 96-well plate. Six replicates were undertaken per condition and four identical plates were produced. Twelve hours later, cells were treated with siRNA and DharmaFECT solutions, as specified in section 2.3.5. Following this, a proliferation assay was carried out as outlined in Section 2.6.1.

Cell imaging

Cells were imaged following 72 hours of MDM2, PSMA, MDM2/PSMA and NT siRNA treatment using Leica DMI1 light microscope (Leica Microsystems, Wetzlar, Germany) at magnification 20x.

Cell cycle assay

Cells were treated with siRNA as detailed above and then the assay was carried out as specified in Section 2.6.6.

Apoptosis assay

Cells were treated with siRNA as detailed above and then the assay was carried out as specified in Section 2.6.7 with annexin V-FITC and propidium iodide (PI).

RNA isolation and RT-PCR

Following treatment of MDA-MB-231 and ZR-75.1 cells with MDM2-, PSMA- and non-targeting siRNA for 72 hours in a 6-well plate, TRI reagent was added to cells. RNA isolation and RT-PCR was then undertaken according to Sections 2.4.1 and 2.4.2.

Quantitative PCR (qPCR)

qPCR was undertaken using cDNA produced in reverse transcription detailed above, using primers for caspase-3, -7, -8 and -9, as well as GAPDH (listed in Table 2.3), following the procedure outlined in 2.4.3. CT values gained from qPCR were analysed using $2^{-\Delta\Delta CT}$ normalisation to GAPDH. Each qPCR sample was set up in triplicate, with the experiment being independently set up three times. Analysis was undertaken using one-way ANOVA of MDM2- and PSMA-targeting siRNA compared to NT.

Western blotting

Following 72 hours of treatment of MDA-MB-231 and ZR-75.1 with MDM2-, PSMA- and non-targeting siRNA, cells were scraped from the 6-well plate into 50 μ l RIPA buffer (with added inhibitors), left on a blood wheel for 1 hour at 4°C, then centrifuged for 15 minutes at 13,000 X G. Following this, an equal amount of 2 x Laemmli was added and SDS-PAGE, western blotting and immune-probing using caspase-3, caspase-8, caspase-9 and GAPDH (antibody list in Table 2.4) was undertaken as outlined in 2.5.1.

Statistical analysis

Data was statistically analysed using either t-test or two-way ANOVA, with a *P*-value of <0.05 considered statistically significant. Asterisk (*) notation was used to signify significances: * *P*<0.05, ** *P*<0.01, *** *P*<0.001 and **** *P*<0.0001.

4.3. Results

The effect of MDM2 and PSMA knockdown on breast cancer cell proliferation

Assessment of proliferation of MDA-MB-231 and ZR-75.1 breast cancer cell lines was undertaken using the Alamar blue proliferation assay. Cell proliferation was assessed at 24 hour intervals following MDM2, PSMA and NT siRNA treatment. MDA-MB-231 cells showed no significant difference between MDM2, PSMA or both siRNAs compared to NT control at either the 24 or 48 hour time points. However, following 72 hours of treatment, the decrease in growth of all targeted treatments compared to the NT control became highly significant (MDM2 siRNA $p=0.0002$; PSMA siRNA $p=0.0001$; MDM2/PSMA siRNAs $p=0.0008$) (Figure 4.1.a).

ZR-75.1 cells also showed no significant difference between the targeted treatments and then NT control at 24 hours, but did show a significance at both 48 (MDM2 siRNA $p=0.002$; PSMA siRNA $p=0.0002$; MDM2/PSMA siRNAs $p=0.0001$) and 72 hours post-treatment (MDM2 siRNA $p<0.0001$; PSMA siRNA $p<0.0001$; MDM2/PSMA siRNAs $p<0.0001$) (Figure 4.1.b).

When siRNA--treated cells were imaged, a significant change in the visible cell morphology was seen. MDA-MB-231 cells seemed unable to form their usual spindle-shape and ZR-75.1 cells were unable to form their typical clusters. PSMA siRNA treatment, on the other hand, conveyed no visible effect on cell morphology and the

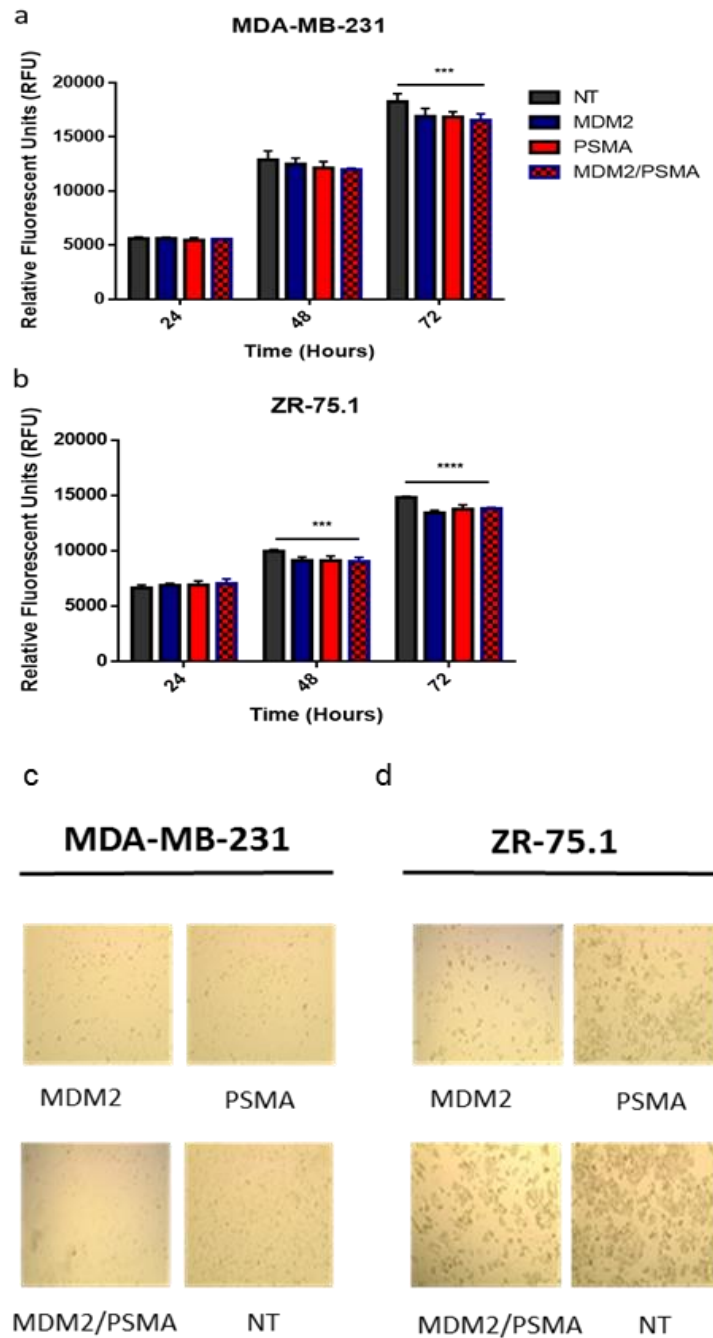


Figure 4.1. Proliferation ability of MDA-MB-231 and ZR-75.1 breast cancer cells following 72 hours of MDM2 or PSMA siRNA treatment. a) Proliferation of MDA-MB-231 cells following 24, 48 and 72 hours of MDM2-, PSMA- or non-targeting siRNA treatment. Graph shows mean RFU+SD (representative data; individual experiments carried out with six repeats; n=3). b) Proliferation of MDA-MB-231 cells following 24, 48 or 72 hours of MDM2-, PSMA- or non-targeting siRNA treatment. Graph shows mean RFU+ SD (representative data; individual experiments carried out with six repeats; n=3). (All data statistically analysed using two-way ANOVA, with *** $p < 0.001$ and **** $p < 0.0001$). c) 72 hour cell images of MDA-MB-231 cells treated with MDM2, PSMA, MDM2/PSMA or NT siRNA. d) 72 hour cell images of ZR-75.1 cells treated with MDM2, PSMA, MDM2/PSMA or NT siRNA.

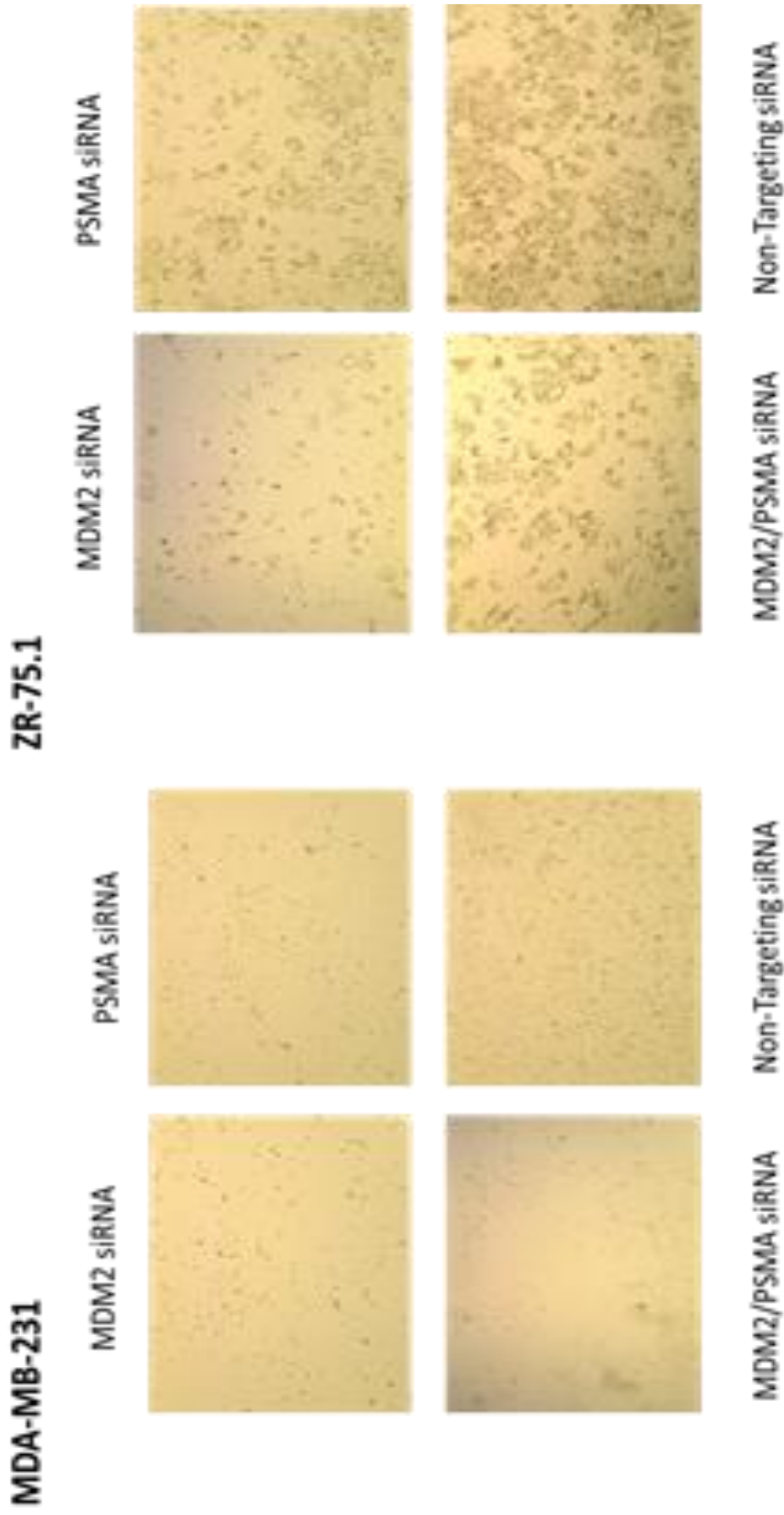


Figure 4.1.1. Zoomed in 72 hour cell images Figure 4.1.c and d.

cells treated with both siRNAs exhibited an intermediate phenotype (Figure 4.1.c and d).

The effect of MDM2 and PSMA siRNA treatment on cell cycle in breast cancer cells

To assess any changes in cell cycle, MDA-MB-231 and ZR-75.1 cells were treated with MDM2, PSMA or NT siRNA for 72 hours and then assessed for their involvement in the various stages using flow cytometry.

Comparing MDM2 siRNA treatment to NT siRNA, MDA-MB-231 cells showed a 3.9% increase in cells in G1 phase ($p=0.0037$), a 2.5% increase in G2 phase ($p=0.0262$) a 4.3% decrease in cells in S phase ($p=0.0003$). On the other hand, PSMA siRNA treatment showed a 3.1% decrease in G1 phase ($p=0.0232$), a 4.2% increase in G2 phase ($p=0.0015$) and a 2.9% increase in S phase ($p=0.023$) (Figure 4.2a-c representative; Figure 4.2d).

In ZR-75.1 cells, MDM2 siRNA treatment led to a 6.6% increase of cells in G1 phase ($p=0.0046$), a 4.3% increase in G2 phase ($p=0.0035$) and a 7.5% decrease in S phase ($p=0.0002$), compared to the NT control. PSMA siRNA led to an increase of 5.2% in G1 phase ($p=0.0058$), 4.1% decrease in G2 phase ($p=0.0058$) but no significant change in the percentage of cells in S phase (Figure 4.3a-c representative; Figure 4.3d).

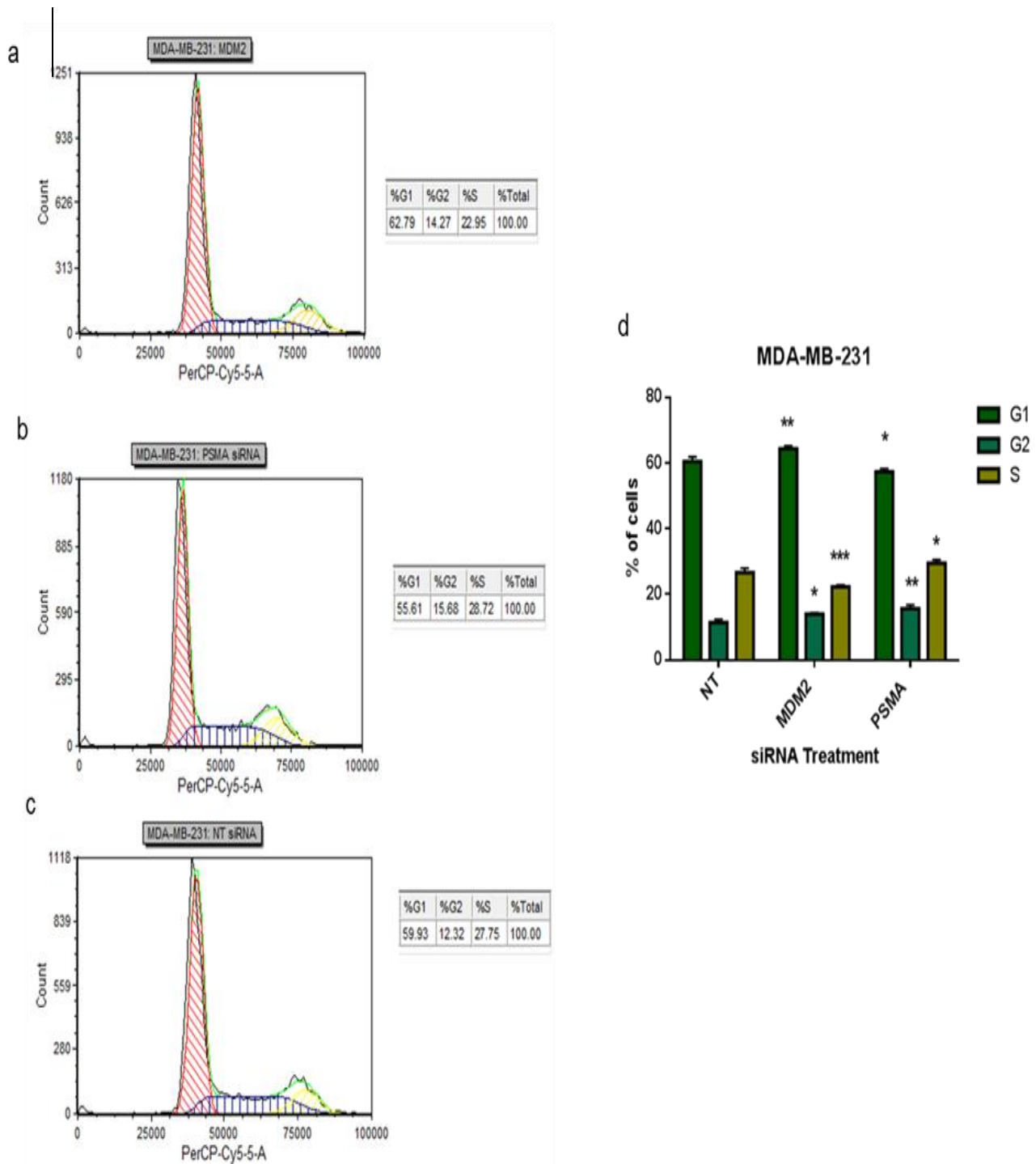


Figure 4.2. The effect of 72 hours of MDM2 and PSMA siRNA on MDA-MB-231 cell cycle. a) % of cells in stages of cell cycle following NT siRNA treatment. b) % of cells in stages of cell cycle following MDM2 siRNA treatment. c) % of cells in stages of cell cycle following PSMA siRNA treatment. d) Percentage of MDA-MB-231 cells in gap 1 (G1), gap 2 (G2) and synthesis (S) phases following NT, MDM2 and PSMA siRNA treatment. (Graph shows % of cells in stage+SD; n=3). (Data statistically analysed using unpaired t-test: * $p < 0.05$, ** $p < 0.01$ and *** $p < 0.001$).

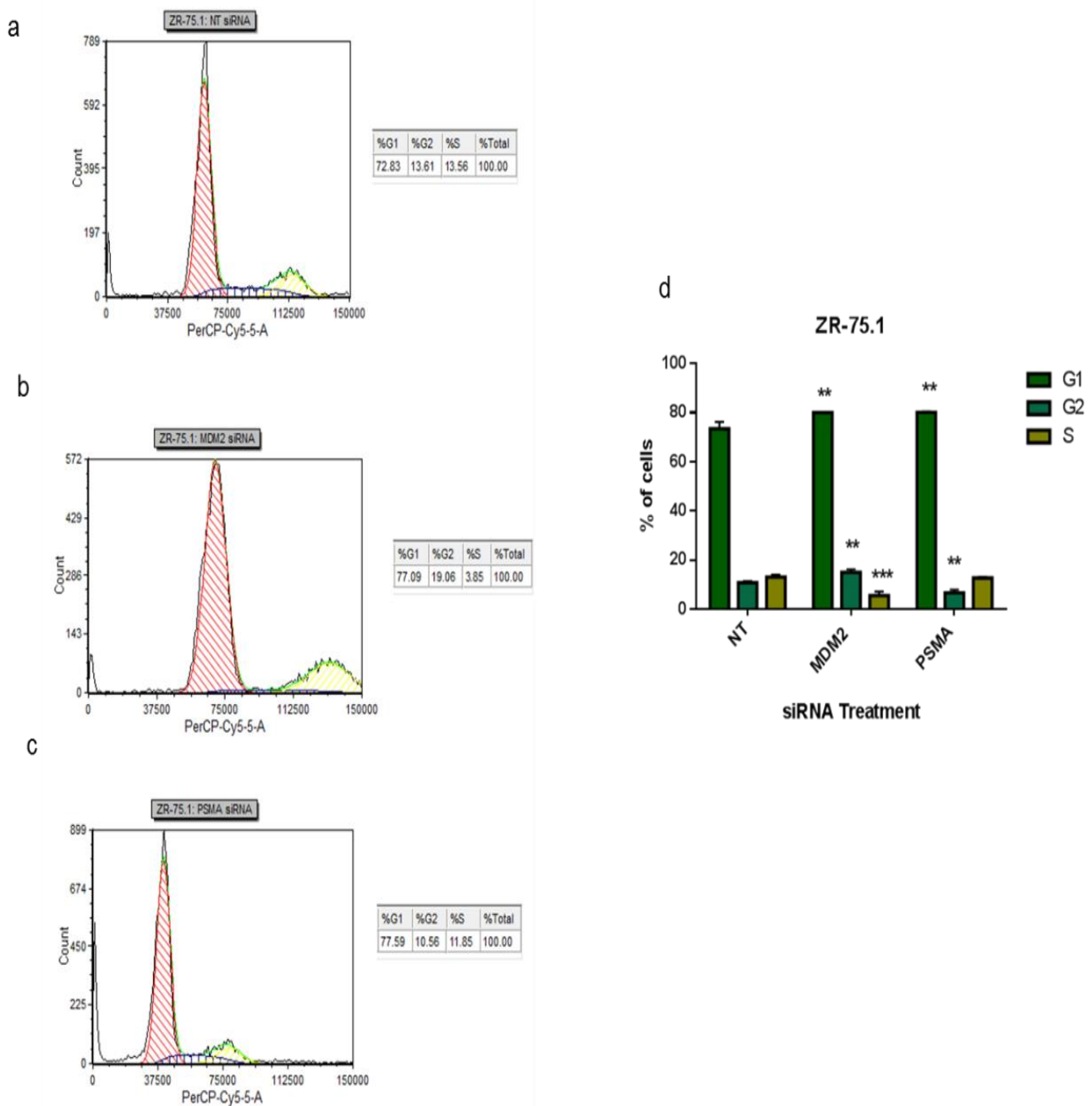


Figure 4.3. The effect of 72 hours of MDM2 and PSMA siRNA ZR-75.1 cell cycle. . a) % of cells in stages of cell cycle following NT siRNA treatment. b) % of cells in stages of cell cycle following MDM2 siRNA treatment. c) % of cells in stages of cell cycle following PSMA siRNA treatment. d) Percentage of ZR-75.1 cells in G1, G2 and S phases following NT, MDM2 and PSMA siRNA treatment. (Graphs show % of cells in stage+SD; n=3). (Data statistically analysed using unpaired t-test: * $p < 0.05$, ** $p < 0.01$ and $p < 0.001$).

The effect of MDM2 and PSMA knockdown on breast cancer apoptosis

MDA-MB-231 and ZR-75.1 breast cancer cells, following treatment with MDM2, PSMA or NT siRNA were assessed for their apoptotic ability, as well as their resistance to an apoptotic agent (staurosporine). MDA-MB-231 cells showed a significant increase ($p=0.0274$) in early stage apoptosis in those cells treated with MDM2 siRNA, compared to those treated with the NT control siRNA. When these cells, treated with MDM2 siRNA, were also subjected to treatment with staurosporine, there was an even more significant increase ($p=0.0055$) (Figure 4.4a shows representative figure; Figure 4.4b shows $n=3$) in the percentage of MDM2 siRNA-treated cells in early stage apoptosis, compared to the NT control (Figure 4.4c).

A similar result was seen in the ZR-75.1 cells (representative data shown in Figure 4.5a), with a significant increase in cells undergoing early stage apoptosis both untreated and treated with staurosporine (Figure 4.5b) (before: $p=0.0101$; after $p=0.0461$) when treated with MDM2 siRNA, compared to the NT control siRNA. In addition, MDM2 siRNA treated ZR-75.1 cells, also showed a significant decrease in live cells when left untreated ($p=0.0155$).

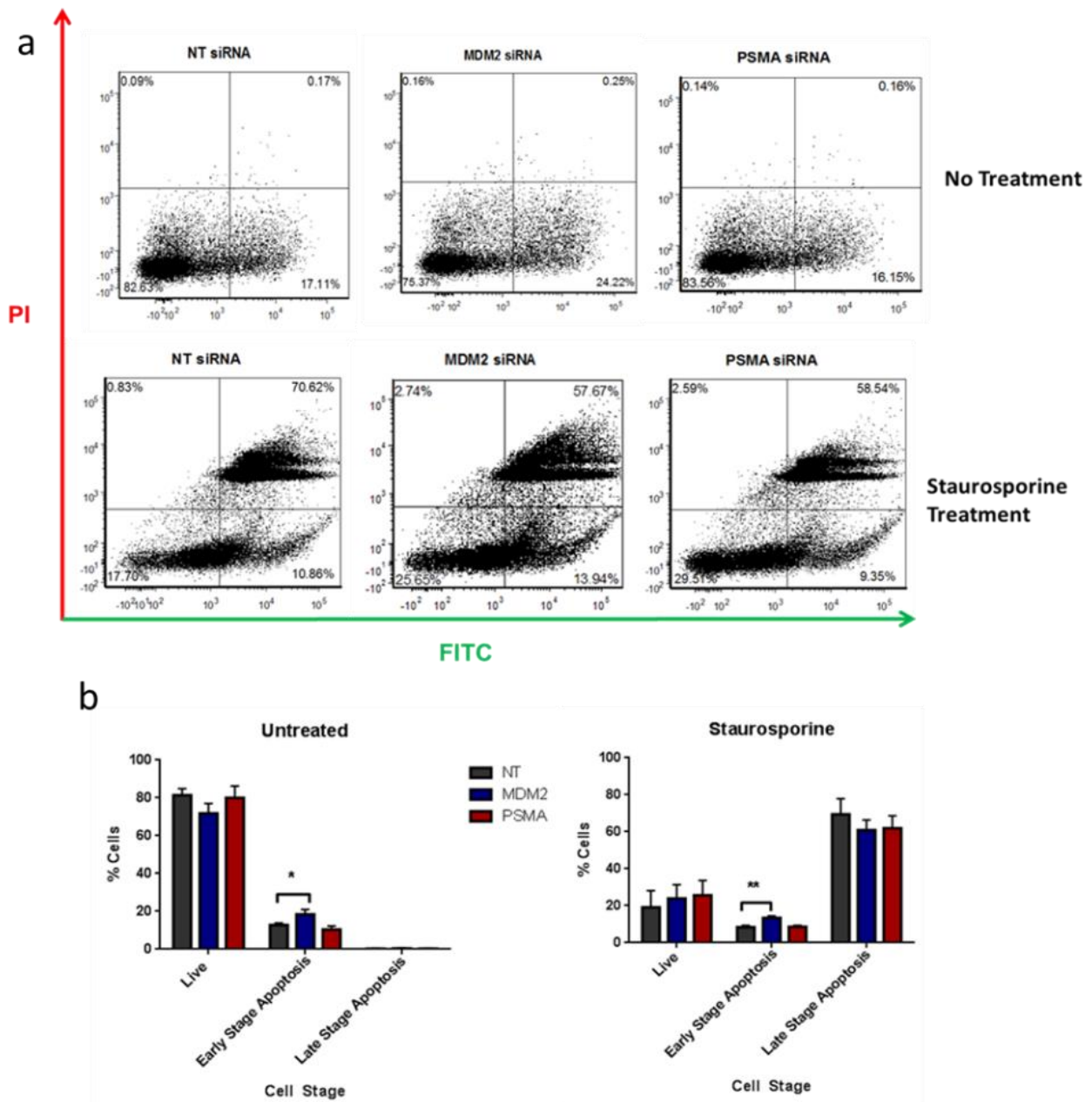


Figure 4.4. Early and late apoptosis of MDA-MB-231 cells treated with MDM2 or PSMA siRNA. a) Percentage of live (bottom left), early apoptotic (bottom right) or late apoptotic (top right) MDA-MB-231 cells following 72 hours of treatment with NT, MDM2 or PSMA siRNA (representative data). b) Percentage of live, early apoptotic or late apoptotic MDA-MB-231 cells following 72 hours of treatment with NT, MDM2 or PSMA siRNA, followed by 1.5 hours of staurosporine treatment (representative data). c) Percentage of cells in each cell stage (live, early apoptosis and late apoptosis following 72 hours of siRNA treatment (graphs show % cells+SD; n=3). d) Percentage of cells in each cell stage (live, early apoptosis and late apoptosis following 72 hours of siRNA treatment and 1.5 hours of staurosporine treatment (graphs show % cells+SD; n=3). (All data statistically analysed using unpaired t-test, with * $p < 0.05$ and ** $p < 0.01$).

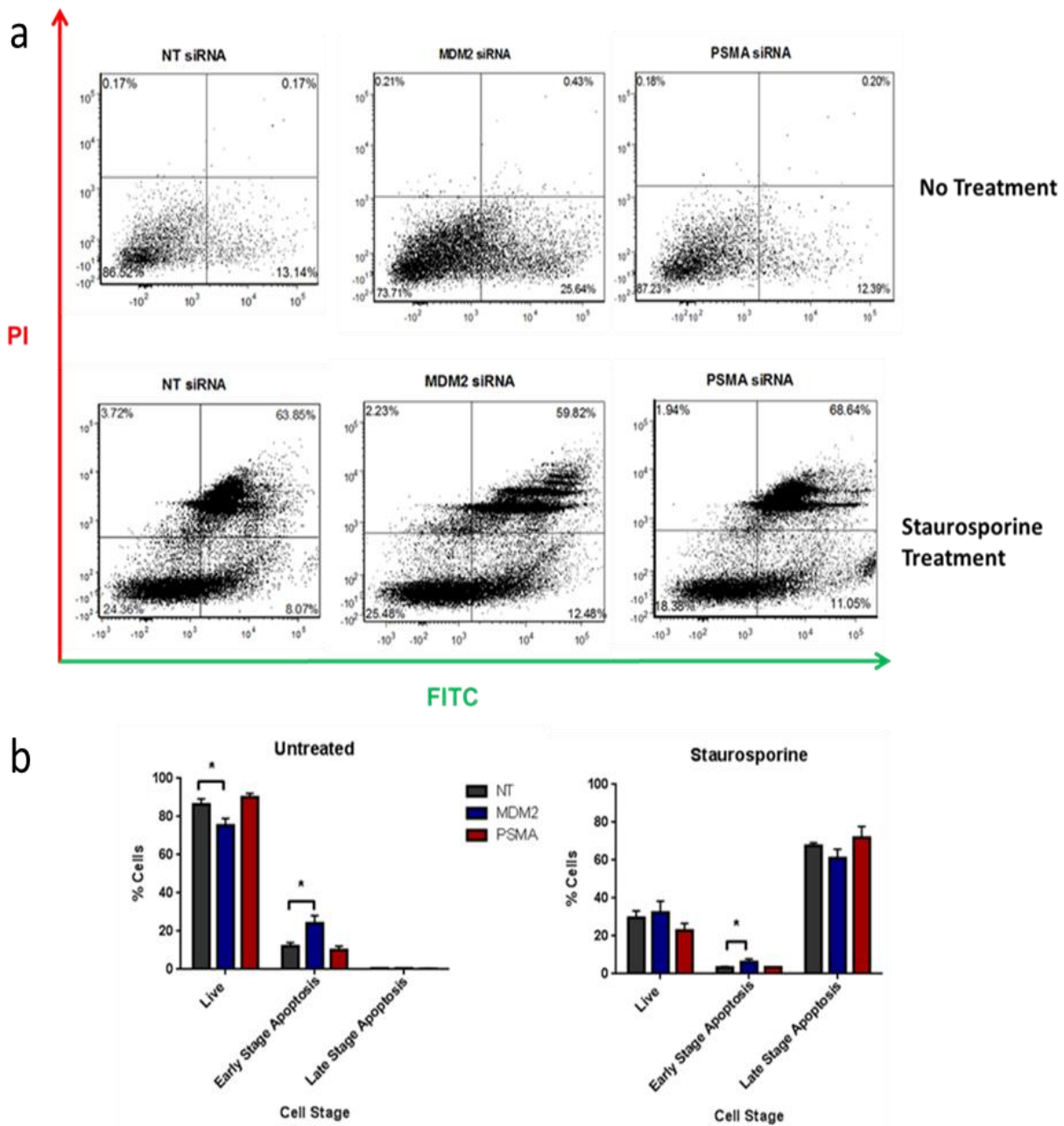


Figure 4.5. Early and late apoptosis of ZR-75.1 cells treated with MDM2 or PSMA siRNA. a) Percentage of live (bottom left), early apoptotic (bottom right) or late apoptotic (top right) ZR-75.1 cells following 72 hours of treatment with NT, MDM2 or PSMA siRNA (representative data). b) Percentage of live, early apoptotic or late apoptotic ZR-75.1 cells following 72 hours of treatment with NT, MDM2 or PSMA siRNA, followed by 1.5 hours of staurosporine treatment (representative data). c) Percentage of cells in each cell stage (live, early apoptosis and late apoptosis) following 72 hours of siRNA treatment (graphs show % cells+SD; n=3). d) Percentage of cells in each cell stage (live, early apoptosis and late apoptosis) following 72 hours of siRNA treatment and 1.5 hours of staurosporine treatment (graphs show % cells+SD; n=3). (All data statistically analysed using unpaired t-test, with * $p < 0.05$ and ** $p < 0.01$).

The effect of MDM2 and PSMA knockdown on caspase levels in breast cancer cells

Following the changes seen in apoptosis in both breast cancer cell lines, caspase levels were assessed for alterations in comparison to the NT control.

Initially, MDA-MB-231 cells were assessed for their caspase gene and protein levels, 72 hours of siRNA treatment of the same time of siRNA treatment as well as 1.5 hours of staurosporine treatment. Caspase-3 gene levels was seen to significantly increase ($p=0.0094$) in those MDA-MB-231 cells with MDM2 siRNA + staurosporine treatment, compared to when cells were untreated (Figure 4.6.a). No significant differences in caspase-7 gene levels were seen compared to NT control, or when comparing no treatment to staurosporine (Figure 4.6.b). Caspase-8 gene levels were seen to significantly increase following PSMA siRNA + staurosporine treatment ($p=0.0048$) (Figure 4.6.c), compared to no staurosporine treatment. Also, PSMA siRNA treated cells showed a significantly higher expression of caspase-8 than NT siRNA following staurosporine treatment ($p=0.0025$) No significant differences in caspase-9 expression were seen following any treatments (Figure 4.6.d).

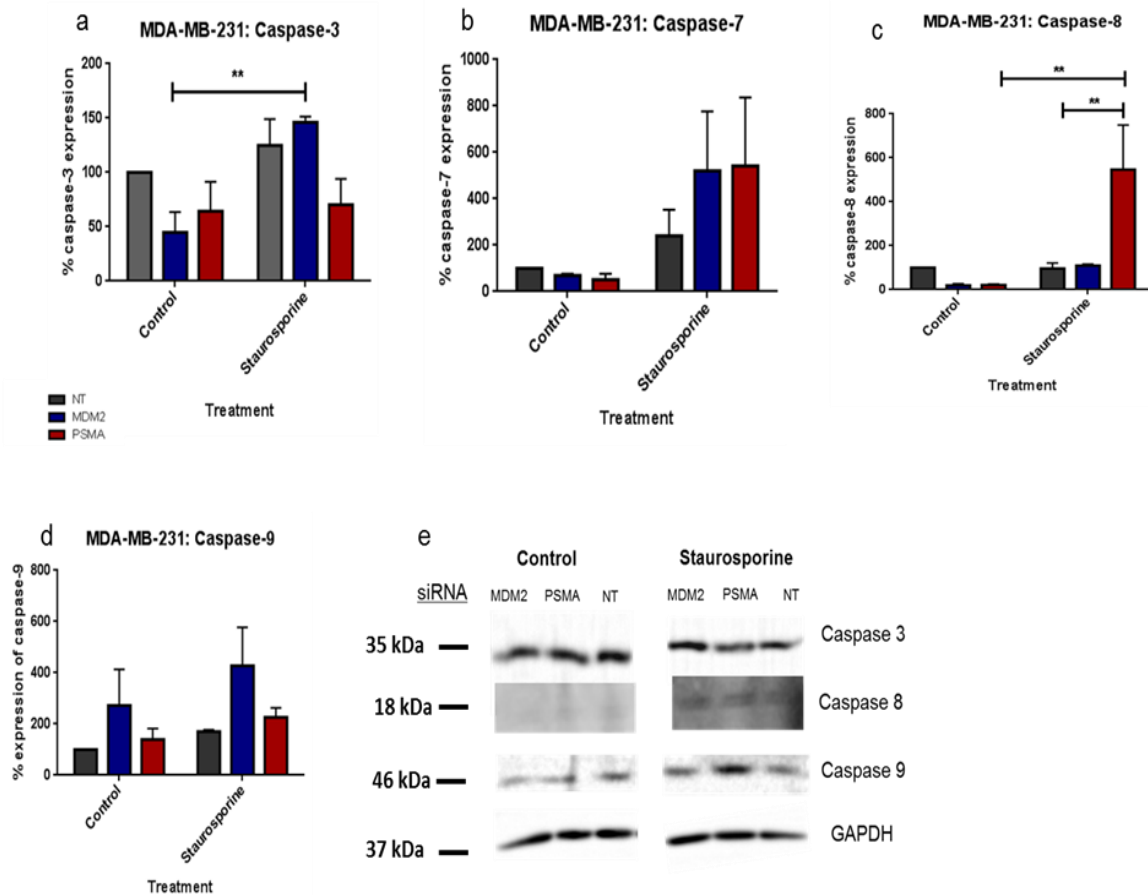


Figure 4.6. Assessment of caspase levels in MDA-MB-231 cells following 72 hours of siRNA treatment and with or without 1.5 hours of staurosporine treatment. a) Caspase-3 gene levels as a percentage of NT siRNA untreated with staurosporine expression. b) Caspase-7 gene levels as a percentage of NT siRNA untreated with staurosporine expression. c) Caspase-8 gene levels as a percentage of NT siRNA untreated with staurosporine expression. d) Caspase-9 gene levels as a percentage of NT siRNA untreated with staurosporine expression. (All graphs show % NT control with no treatment+SD; n=3) (Data statistically analysed using unpaired t-test with ** $p < 0.01$). e) Western blot of caspase -3, -8 and -9 expression following MDM2, PSMA or NT siRNA treatment, with or without staurosporine treatment. (Blots show representative data; n=3).

Assessment of caspase-3, -8 and -9 protein levels showed a similar increase in caspase-3 following MDM2 siRNA + staurosporine treatment compared to those untreated with staurosporine. In addition, caspase-3 levels were shown to increase in those cells treated with MDM2 siRNA + staurosporine, and decrease in cells treated with PSMA siRNA + staurosporine, compared to NT siRNA + staurosporine. Unfortunately, protein assessment of caspase-7 levels was unsuccessful (data not shown). Caspase-8 protein expression increased following staurosporine treatment; however, no differential expression was seen between each siRNA treatment. When caspase-9 protein expression was analysed, PSMA siRNA-treated cells were shown to express the protein at high levels following staurosporine treatment, compared to both PSMA siRNA with no treatment and NT siRNA + staurosporine (Figure 4.6.e).

Following this, ZR-75.1 cells were treated in the same way and gene and protein levels were assessed. Gene expression studies showed no significance between any of the siRNA treatment, with or without staurosporine treatment (Figure 4.7.a, b, c & d). However, assessment of protein levels still showed some differentiation in expression throughout the treatment. MDM2 siRNA + staurosporine treatment showed high levels of caspase-3 expression compared to both MDM2 siRNA with no treatment and NT siRNA + staurosporine.

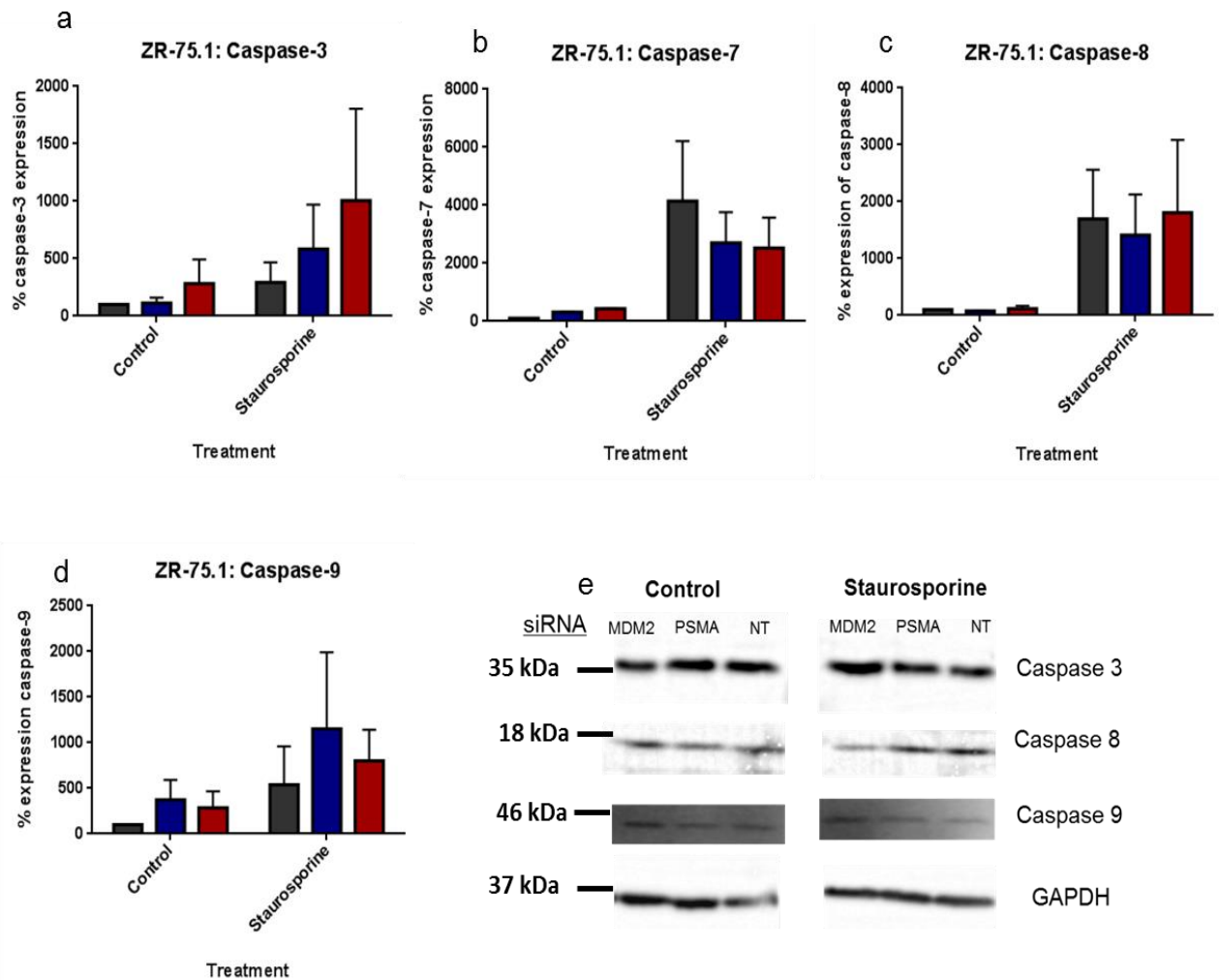


Figure 4.7. Assessment of caspase levels in ZR-75.1 cells following 72 hours of siRNA treatment and with or without 1.5 hours of staurosporine treatment. a) Caspase-3 gene levels as a percentage of NT siRNA untreated with staurosporine expression. b) Caspase-7 gene levels as a percentage of NT siRNA untreated with staurosporine expression. c) Caspase-8 gene levels as a percentage of NT siRNA untreated with staurosporine expression. d) Caspase-9 gene levels as a percentage of NT siRNA untreated with staurosporine expression. (All graphs show % NT control with no treatment+SD; n=3) (Data statistically analysed using unpaired t-test). e) Western blot of caspase -3, -8 and -9 expression following MDM2, PSMA or NT siRNA treatment, with or without staurosporine treatment (Blots show representative data; n=3).

Caspase-8 expression was shown to be decreased in MDM2 siRNA + staurosporine treatment compared to NT control +staurosporine. MDM2 siRNA showed an increase in caspase-9 protein expression in both no treatment and staurosporine treated cells compared to other treatments (Figure 4.7.e).

4.4. Discussion

Within the primary tumour, and subsequent tumours which may form, it is important for cells to gain the ability to proliferate in an uncontrolled manner, as well as to evade apoptosis. This chapter aims to assess these functional abilities of breast cancer cells which harbour MDM2 or PSMA knockdown.

Assessment of proliferation in MDM2 and PSMA treated MDA-MB-231 and ZR-75.1 cells showed a decrease from both knockdowns over a 72 hour period. However, ZR-75.1 showed a significant change in proliferation at an earlier stage post-siRNA treatment, with a highly significant difference being seen between MDM2, PSMA or both siRNAs and the NT control at both 48 and 72 hour time points. On the other hand, MDA-MB-231 cells only showed a significant difference of each treatment compared to the NT control at 72 hours, and the significance was less than the 72 hour time point of ZR-75.1 cells. This may be due to the more significant knockdown of both MDM2 and PSMA in ZR-75.1 compared to MDA-MB-231 cells, leading to a more profound effect on proliferative abilities of the cells. It could also, at least in terms of MDM2 expression, be explained by the fact that ZR-75.1 carry wild-type p53, whereas MDA-MB-231 carry a mutated version of the gene. It has long been known that in cancer cells, MDM2 overexpression leads to an increased proliferative ability of cells (Teoh et al., 1997, Wang et al., 2012). This effect was thought to be due to the negative regulatory role played by MDM2 towards p53 leading to a decrease in the ability of

p53 to halt the cell cycle, and thus an increased cell proliferation.

This hypothesis is supported in many reports by different groups with one group reporting that using nutlin-3a, an inhibitor of the interaction between MDM2 and p53 led to a decrease in the proliferative ability of osteosarcoma cells (Wang et al., 2012). Qi *et al.*, (Qi et al., 2014) suggested a p53-dependent stabilisation of MDM2 through direct binding with the DNAJ/heat shock protein 40, DNAJB1, in MCF7 breast cancer cell proliferation. However, a later study by the same group indicated another way in which MDM2 suppression could inhibit proliferation may be p53-independent via translational regulation in retinoblastoma cells (Qi and Cobrinik, 2016). Another study also supports this hypothesis and claims that MDM2 is also involved in p53-independent activities and plays a role in oestrogen-activated MCF7 breast cancer cell proliferation, with p53 not being the key target of MDM2 in this pathway (Brekman et al., 2011).

Therefore, this could provide reasoning as to why we see a decrease in proliferation in both p53 mutant and wild-type cell lines harbouring MDM2 knockdown. It is also to bear in mind that although the proliferation changes were statistically significant, the actual changes were not very obvious and so perhaps *in vivo* setting, may not be very significant.

In terms of the current view on PSMA involvement in cancer cell proliferation, it is widely believed that the molecule is a positive regulator of proliferation of prostate cancer cells, though currently no data exists in breast cancer cells. Yao *et al.*, (Yao et al., 2010) found

that a PSMA increase in PC3 cell lines increases the folate uptake ability of cells and thus confers a proliferative advantage. In addition, the same group has published multiple papers assessing how PSMA knockdown in prostate cancer LNCaP cells affects them, with a conclusion that PSMA decrease leads to a lowered proliferative ability of cells and a suggestion that PSMA may be a novel regulator of p38 (Guo et al., 2011, Zhang et al., 2013, Guo et al., 2014). Therefore, the results seen in my work are strongly supported by current literature.

Also, interestingly, when MDM2, PSMA, MDM2/PSMA and NT siRNA cells were imaged, a change in morphology could be visualised in those cells treated with MDM2 siRNA. These cells were unable to form their typical spindle shape in MDA-MB-231 and clusters in ZR-75.1. Changes in cellular morphology following MDM2 knockdown have been reported before (Yang et al., 2006), with this group claiming that decreased MDM2 reduces the level of E-cadherin, which leads to the loss of cell-cell contract and changes in cell morphology.

When the differences in cell cycle were assessed in the cell lines treated with MDM2 and PSMA siRNA, it was shown that MDM2 siRNA leads to similar changes in both MDA-MB-231 and ZR-75.1 cell lines, in that each show an increase in the G1 and G2 phases and a decrease in those in S phase. However, the difference is more profound in the ZR-75.1 cell line, with the percentage of cells being almost double that shown in MDA-MB-231. Again, this could be due

to the higher level of knockdown or the p53 state of the cells.

Currently, studies show that MDM2 can induce cell cycle arrest at G1 stage in normal human and murine cells (Brown et al., 1998, Frum and Deb, 2003) and that p53 is involved in the G2 to M transition, as well as the G1 checkpoint (Shaw, 1998; Agarwar *et al.*, 1995). This could explain why MDM2 knockdown shows an increase in the percentage of cells in G1 phase and subsequently why we see a decrease in the percentage of cells at S phase. However, it does not explain why the number of cells in G2 phase also increases. The data imply, however, that the decrease in the number of cells in S-phase may be the reason for the decrease in proliferation we see following MDM2 siRNA treatment. It also implies that MDM2 may cause cell cycle arrest at both G1 and G2 stages of the cell cycle. It is also important to point out that the arrest of cell cycle by MDM2 goes against what we know about the protein. However, it has been reported in previous studies and it could be that the percentage changes are so small, although significant, that the arrests at G1 and G2 are cancelled out by the increase in cells at S-phase, which is why MDM2 leads to a decrease in proliferation of cells overall.

Cell cycle analysis of breast cancer cells following PSMA knockdown showed highly interesting results. The MDA-MB-231 and ZR-75.1 cell lines showed opposing results to one another. PSMA knockdown in MDA-MB-231 led to a decrease in the percentage of cells in G1 phase and an increase in S and G2 phases. However, ZR-75.1 cells showed an increase in the percentage of cells in G1

phase and a decrease in those in G2 phase, with no change in the percentage of cells in S phase. This implies that PSMA may play different roles in different types of breast cancers, in terms of its effect on the cell cycle. Previous reports in the literature have shown differing effects of PSMA on cell cycle. Rajasekaran *et al.*, (2009) identified a role of PSMA in mitosis and showed that ectopic expression of PSMA in PC3 prostate cancer cell lines led to an increase in the exit from mitosis for cells. Later studies showed that inhibition of PSMA increases G1 phase and decreases S and G2 phases (Zhang *et al.*, 2012, Guo *et al.*, 2014). These results are similar to those seen in the ZR-75.1 cell line, although no significant change in S-phase was observed in our data; but oppose those seen in MDA-MB-231.

Since proliferation and the cell cycle are often known to be altered in cancer cells, we also investigated another process which is often circumvented by tumour cells– apoptosis. Annexin V-FITC and PI were used in order to assess the number of cells which were alive, in early stage apoptosis or in late stage apoptosis/undergoing necrosis.

Initially, cells were treated with each siRNA for 72 hours and then either left untreated or treated with the apoptotic agent staurosporine for 1.5 hours. In MDA-MB-231 cells, MDM2 siRNA treatment led to a significant increase in early stage apoptosis from the NT siRNA. A trend of decrease in live cells was also seen following MDM2 siRNA treatment; however, this was not significant over three repeats. The same was seen in ZR-75.1 cells, with MDM2 siRNA treatment again

leading to an increase in early stage apoptosis from NT siRNA in both untreated and staurosporine treated cells. In addition, the number of live cells significantly decreased from NT siRNA in untreated cells with MDM2 siRNA treatment. This implies that cells either just begun to undergo apoptosis, or that cells are maintained in this state, without crossing through to late stage or dying. In addition, it is worth noting that the increase in early stage apoptosis from NT to MDM2 siRNA was of a higher percentage in ZR-75.1 cells. In untreated cells, the increase was over two-fold, compared to MDA-MB-231 where the increase was just 1.25-fold. Following staurosporine treatment, ZR-75.1 again showed an over two-fold increase in early stage apoptotic cells, whilst MDA-MB-231 showed a 1.45-fold change. This is what would be expected since ZR-75.1 is p53 wild-type and when MDM2 is knocked down in these cells, p53 is no longer governed and so cell death may occur. However, MDA-MB-231 following MDM2 siRNA knockdown also showing an increase in early stage apoptosis implicates MDM2 in other, p53-independent, apoptotic regulatory processes.

It is also interesting to note that, although the data did not reach significance over the three repeats, following staurosporine treatment, both MDM2 siRNA and PSMA siRNA treated MDA-MB-231 cells showed a decrease in the number of cells in late stage apoptosis/necrosis. In addition, both of the targeted siRNA cell treatments led to an increase in the number of live cells, although again this was not significant over the three experiments undertaken.

In ZR-75.1 cells, MDM2 siRNA followed by staurosporine treatment showed, although not to significance, a decrease in the number of cells in late stage apoptosis/necrosis; but no difference in the number of live cells compared to the NT control siRNA. However, interestingly, PSMA siRNA followed by staurosporine treatment showed a trend of increase in late stage apoptosis/necrosis and a decrease in the number of live cells. Therefore, opposing effects were seen from PSMA siRNA treatment on the two different cell lines.

In terms of what is reported in the literature, it is well known that a decrease in MDM2 results in p53 tumour suppressor being free to halt cell cycle progression and cause cellular apoptosis (Rozieres *et al.*, 2000), and so data has already been presented showing that MDM2 promotes apoptosis in many reports (Wang *et al.*, 2012, Lai *et al.*, 2012). However, the only study which breaks down the stages of apoptosis is by Daniele *et al.*, (Daniele *et al.*, 2015) and this reports that a significant increase of both early and late stage apoptosis is seen following treatment of Glioblastoma Multiforme cancer stem cells when cells are treated with MDM2 inhibitor ISA27. On the other hand, there are papers which suggest that MDM2 may play a p53-independent role in the promotion of apoptosis (Dilla *et al.*, 2011; Lee *et al.*, 2015; Bouska *et al.*, 2009).

Only one report of the link between PSMA and apoptosis has been published, with Huang *et al.*, (2014) stating that inhibition of PSMA

promotes apoptosis. This falls in line with the trend we have seen in ZR-75.1 cells but is the opposite from what is seen in MDA-MB-231.

Following this, caspase levels were assessed in order to find a possible link between these molecules and what was seen in the apoptosis assays. In MDA-MB-231 cells, caspase-3 gene expression levels were seen to significantly increase in those cells treated with MDM2 siRNA, from untreated to staurosporine treated. This was echoed at protein level. In addition, caspase-3 protein levels in cells treated with MDM2 siRNA were increased and those treated with PSMA siRNA were decreased from NT siRNA, following staurosporine treatment. Caspase-8 gene expression levels were seen to increase from untreated to staurosporine treatment and an increase in protein levels was seen between all of the untreated and treated samples. No differences were seen in caspase-9 gene expression levels but protein levels were shown to be heightened in those cells treated with PSMA siRNA with staurosporine, both over the NT control with staurosporine and the PSMA siRNA untreated cells. This implies that although some protein level increases did agree with their gene expression changes, there is likely to be post-transcriptional regulation of caspase levels following knockdown of MDM2 and PSMA. Thus far, there are no studies connecting PSMA to the caspases and those which link MDM2 to the molecules identify them to be working upstream (Oliver *et al.*, 2011; Pochampally *et al.*, 1998; Pochampally *et al.*, 1999).

In ZR-75.1 cells treated with each of the siRNAs, with or without staurosporine, no significant differences were seen in gene expression although a general trend of increased caspase expression was seen between those cells untreated and treated with staurosporine. However, differences were still seen at protein level, with MDM2 siRNA + staurosporine treatment compared to MDM2 siRNA without treatment and also compared to NT control + staurosporine treatment. In this cell line, caspase-3 protein levels in PSMA siRNA treated cells were unchanged compared to the NT control following staurosporine treatment. Caspase-8 protein levels were decreased and caspase-9 levels increased after MDM2 siRNA treatment compared to NT siRNA following staurosporine treatment.

A difference in expression of caspase protein was seen between the two different cell lines following each treatment and may indicate that MDM2 and PSMA play varying roles in caspase expression regulation between different types of breast cancer.

It is interesting to see that in ZR-75.1 cells, PSMA siRNA treatment results in no changes to caspase protein levels, whereas in MDA-MB-231 caspase-3 levels are lower than in the NT following staurosporine treatment, although caspase-9 levels are increased. Caspase-9 is an initiator caspase and is responsible for the activation of executioner caspases such as caspase-3 (Chang *et al.*, 2003; Riedl & Shi, 2004; McIlwain *et al.*, 2016). Therefore, even though the levels of caspase-9 is increased, if there is no caspase-3 to be activated, the level of caspase-3 degradation will still be lower.

Interestingly, caspase-3 has been linked to the regulation of PS externalisation of erythrocytes (Mandal et al., 2002) and if this were to be the same in cancer cells, the lack of caspase-3 may explain why MDA-MB-231 cells show a decreased level of cell death with PSMA knockdown, but ZR-75.1 show an increase, which is what would be expected from the results of other studies (Huang *et al.*, 2014).

Therefore, in conclusion, it seems that MDM2 and PSMA show similar effects on breast cancer cell proliferation but varying effects in terms of apoptotic ability of cells as well as the part they play in the cell cycle. It is also important to note that PSMA seems to play different roles in the two cell lines which were used, suggesting possible multiple roles for this protein dependent on breast cancer cell type.

Chapter V

Knockdown of MDM2
and PSMA in breast
cancer cell lines leads
to a decrease in their
migratory and invasive
capacity through the
action via matrix
metalloproteinases

5.1. Introduction

The spread of cancers via the movement of tumour cells relies on a number of vital biological processes which allow the cells to break down, migrate and invade the extracellular matrix (ECM) and subsequently metastasise. Cancer cells have many ways in which they can influence this situation, most significantly by altering the expression of components key to these processes (Hanahan & Weinberg, 2011).

A family of molecules heavily implicated in the migration and invasion of cells through the ECM is the matrix metalloproteinases (MMPs). The MMPs are known to break down the components of the ECM, with different family members playing varying roles and targeting different molecules (Page-McCaw *et al.*, 2007).

Studies have linked both MDM2 and PSMA to the MMPs, as well as more generally to migration and invasion of cells. MDM2 has been connected to MMP9 in numerous studies, with immunohistochemical (IHC) staining of IDC showing a significant correlation between the expression of MDM2 and MMP9 (Chen *et al.*, 2013), as well as the expression of the two proteins being linked in the oncogenesis of lung cancer in rats (Zhang *et al.*, 2014). Studies have also linked MDM2 to invasion, both *in vitro* (Yang *et al.*, 2006) and *in vivo* (Rajabi *et al.*, 2012). PSMA has been positively correlated with MMP9 expression in mouse prostate cancer cells (Zhao *et al.*, 2012). In addition, PSMA has been linked to MMP2, through which it is

believed to work to generate small peptides which can augment the invasive and adhesive abilities of endothelial cells (Conway *et al.*, 2013). Moreover, a study was recently published in which PSMA knockdown in the prostate cancer cell line, LNCaP, was linked to the gene expression of *MMP2*, *MMP3* and *MMP13*, as well as *MDM2* (Xu *et al.*, 2013).

Therefore, we aimed to investigate the functional consequences of MDM2 and PSMA knockdown in breast cancer cell lines, and what this means in terms of MMP expression, in order to elucidate a possible interplay between the two proteins under study.

5.2. Materials & Methods

Cell lines and treatments

MDA-MB-231 and ZR-75.1 metastatic breast cancer cell lines, maintained in DMEM media with 10% FBS and antibiotics, were used in this chapter. These cell lines were transiently transfected with MDM2, PSMA or non-targeting (NT) siRNA using Fect4 or Fect1 transfection reagents, respectively. All treatments were undertaken in a 6-well plate and a total volume of 1ml of treatment was used in each case. MDA-MB-231 cells were treated with 100 nM of each siRNA and ZR-75.1 cells were treated with 50 nM, according to the manufacturer's instructions, following optimisation experiments. Treatments were undertaken for 48 or 72 hours, dependent on the experiment.

Transwell migration assay

MDA-MB-231 and ZR-75.1 cells were treated with MDM2, PSMA and NT siRNA for 48 or 72 hours. The experiments were carried out three independent times over a 4 hour period and the individual experiments as outlined in 2.6.3. Data were analysed using unpaired t-test of each MDM2- and PSMA-targeting siRNA compared to NT.

Scratch wound healing assay

MDA-MB-231 and ZR-75.1 cells were treated with MDM2, PSMA and NT siRNA for 72 hours. Following this, cells were scratched using a pipette tip and imaged at time points depending on the healing speed

of the cells. Each experiment was carried out in triplicate, with the full protocol is shown in 2.6.5. Data were analysed using two-way ANOVA of MDM2 and PSMA siRNA compared to NT.

Transwell invasion assay

MDA-MB-231 and ZR-75.1 cells were treated with MDM2, PSMA and NT siRNA for 48 or 72 hours. The experiments were carried out three independent times over a 24 hour period and the individual experiments were undertaken as outlined in 2.6.4. Data were analysed using unpaired t-test with Welch's correction of each MDM2 and PSMA siRNA compared to NT.

Endothelial cell adhesion assay

A HMVEC monolayer was allowed to form in a 24-well plate by seeding 3×10^5 cells/well. Following 72 hours of siRNA treatment, cancer cells were fluorescently stained and 4×10^4 cells/well were allowed to adhere to the monolayer for 30 minutes as Section 2.6.2.

Western blotting

Following 48 and 72 hours of treatment of MDA-MB-231 and ZR-75.1 with MDM2, PSMA and NT siRNA, cells were scraped from the 6-well plate into 50 μ l RIPA buffer (with added inhibitors), left on a blood wheel for 1 hour at 4°C, then centrifuge for 15 minutes at 13,000 X G. Following this an equal amount of 2 x Laemmli and SDS-PAGE, western blotting and immune-probing using MDM2,

phospho-MDM2 (serine 166) and GAPDH (antibody list in Table 2.4) was undertaken as outlined in 2.5.1.

Immunocytochemistry

MDA-MB-231 and ZR-75.1 cells were treated with MDM2, PSMA and NT siRNA for 48 hours and then 20,000 cells in 200 μ l DMEM was added to each well of a chamber slide, before overnight incubation at 37 °C. The following morning the protocol outlined in 2.5.2. was undertaken using MDM2 (serine 166 antibody).

RNA isolation and RT-PCR

Following treatment of MDA-MB-231 and ZR-75.1 cells with MDM2, PSMA and NT siRNA for 72 hours in a 6-well plate, TRI reagent was added to cells. RNA isolation and RT-PCR was then undertaken according to sections 2.4.1 and 2.4.2.

Quantitative PCR (qPCR)

qPCR was undertaken using cDNA produced in reverse transcription detailed above, using primers for MMP1, MMP2, MMP3, MMP7, MMP8, MMP9, MMP10, MMP11, MMP12, MMP13, TIMP1, TIMP2 and GAPDH (listed in Table 2.3), following the procedure outlined in 2.4.3. CT values gained from this processes were analysed using $2^{-\Delta\Delta CT}$ normalisation to GAPDH. Each qPCR sample was set up in triplicate, with the experiment being independently set up three times. Analysis was undertaken using unpaired t-test Welch's correction of MDM2- and PSMA-targeting siRNA compared to NT.

RayBio® C-Series Human Matrix Metalloproteinase Antibody Array

C1

Following MDA-MB-231 and ZR-75.1 treatment with MDM2, PSMA and NT siRNA for 24 hours, serum-free media was added to the cells and this tumour-conditioned media (TCM) was harvested at 72 hours post-treatment. This TCM was the assessed for MMP secretion by cancer cells according to the protocol outlined in section 2.5.4.

Flow cytometric analysis of MMP2 and MMP8 levels

Following treatment of MDA-MB-231 and ZR-75.1 cells with MDM2, PSMA and NT siRNA for 72 hours, intracellular MMP2 and MMP8 expression was assessed as detailed in 2.5.3.

MMP inhibitor studies

To inhibit MMP2 in MDA-MB-231 and ZR-75.1, cells were treated with 6nM ARP100 and 12nM Marimastat. To inhibit MMP8, cells were treated with 4nM MMP8 inhibitor. Following this, proliferation, migration and invasion assays were undertaken as detailed in 2.6.1, 2.6.3 and 2.6.4.

IL-6 and IL-8 ELISA

Following 48 hours of MDM2, PSMA and NT siRNA treatment, cells were washed with PBS and 500 µl serum-free media added to the well. At 72 hours post-treatment, this media was removed from the cells and centrifuged at 1700 X G for 10 minutes to remove cellular debris. The samples from MDA-MB-231 were diluted 1:5 and those

from ZR-75.1 were diluted 1:2. The assays were then carried out as specified in Section 2.5.5.

Statistical analysis

Data was statistically analysed using either unpaired t-test with Welch's correction or two-way ANOVA, with a P -value of <0.05 considered statistically significant. Asterisk (*) notation was used to signify significances: * $P<0.05$, ** $P<0.01$, *** $P<0.001$ and $P<0.0001$.

5.3. Results

The effect of MDM2 and PSMA knockdown on breast cancer cell migration

Following MDM2-, PSMA- and non-targeting (NT) siRNA treatment on MDA-MB-231 and ZR-75.1 breast cancer cells for both 48 and 72 hours, transwell migration assays were undertaken in order to elucidate the change in chemotactic migration, if any, over a 6 hour period, resulting from a decrease in MDM2 and PSMA protein levels. This assay involves the movement of cells towards a chemotactic factor, in this case FCS and aims to partially replicate the *in vivo* migration of cells from a primary tumour site, into the blood stream, which may then result in metastases occurring. MDA-MB-231 cells exhibited a significant decrease in migration following MDM2-targeting siRNA treatment, compared to the NT control at both 48 hours (51.8% decrease, $p=0.0099$) and 72 hours (52.0% decrease, $p=0.0193$) (Figure 5.1a). The same was seen following PSMA-targeting siRNA treatment, with 48 hours of treatment leading to a 64.20% decrease in migratory capacity ($p=0.0005$) and 72 hours causing a 72.4% decrease ($p<0.0001$) (Figure 5.1b).

Similar results were seen in the ZR-75.1 breast cancer cell line, with MDM2-targeting siRNA treatment resulting in a 67.4% decrease in migration through the transwell ($p=0.0132$) after 48 hours and a 72.9% decrease after 72 hours of treatment ($p=0.0072$) (figure 5.1c). Again, PSMA-targeted siRNA led to a decrease in migratory

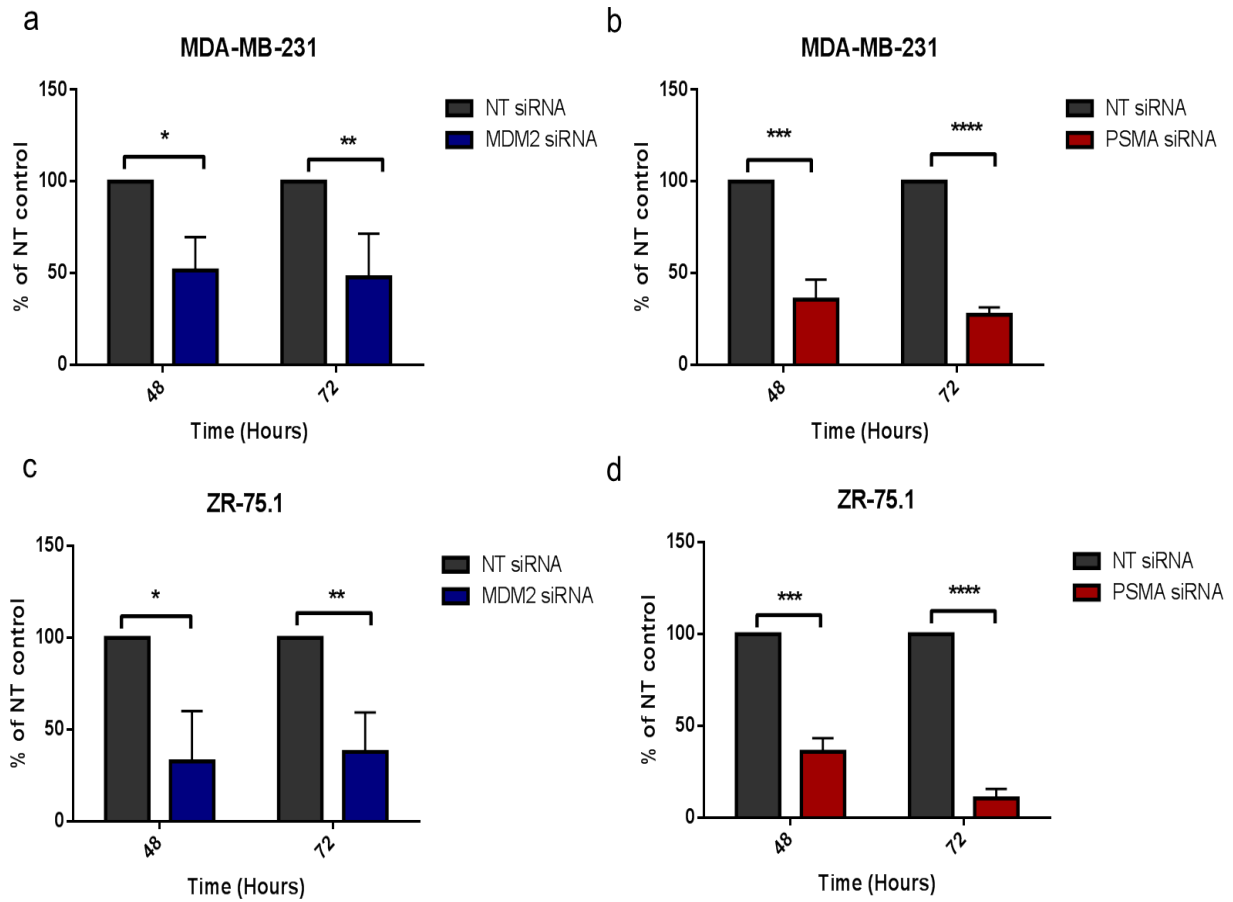


Figure 5.1. Migration capacity of MDA-MB-231 and ZR-75.1, over a 4 hour period, of siRNA treated cells after 48 and 72 hours of treatment. a) Migration of MDA-MB-231 treated with MDM2 siRNA. b) Migration of MDA-MB-231 treated with PSMA siRNA. c) Migration of ZR-75.1 treated with MDM2 siRNA. d) Migration of ZR-75.1 treated with PSMA siRNA. (All graphs are shown as % of NT control siRNA-treated cells +SD; n=3; each experiment undertaken in triplicate; significant differences calculated by unpaired t-test with Welch's correction; * p<0.05, ** p<0.01, **** p<0.0001).

tendencies in ZR-75.1, with 48 hours of treatment leading to a 64.26% decrease in cell movement across the transwell ($p=0.0001$) and 72 hours causing a decrease of 89.6% ($p<0.0001$) (Figure 5.1d).

Similar results were seen in the ZR-75.1 breast cancer cell line, with MDM2-targeting siRNA treatment resulting in a 67.4% decrease in migration through the transwell ($p=0.0132$) after 48 hours and a 72.9% decrease after 72 hours of treatment ($p=0.0072$) (figure 5.1c).

Again, PSMA-targeted siRNA led to a decrease in migratory tendencies in ZR-75.1, with 48 hours of treatment leading to a 64.26% decrease in cell movement across the transwell ($p=0.0001$) and 72 hours causing a decrease of 89.6% ($p<0.0001$) (Figure 5.1d).

In order to support this observation, wound healing (scratch) assays were carried out on both cell lines following treatment with each siRNA. MDA-MB-231 cells completely healed within 3 hours, with a significant difference between the healing capability of the cells, compared to NT siRNA, when treated with MDM2 siRNA at 2 hours ($p<0.0001$). However, the difference between PSMA and NT siRNA almost reaches significance after 1 hour ($p=0.0645$) and then the time to heal is significantly slower in cells treated with PSMA siRNA than NT at the 2 and 4 hour time points (2 hours $p=0.0212$; 4 hours $p=0.0256$) (Figure 5.2a and b). ZR-75.1 cells, on the other hand, took over 24 hours to heal and the NT siRNA-treated cells showed a stark and significantly higher wound healing capacity, compared to both MDM2 and PSMA siRNA treated cells (Figure 5.2c and d).

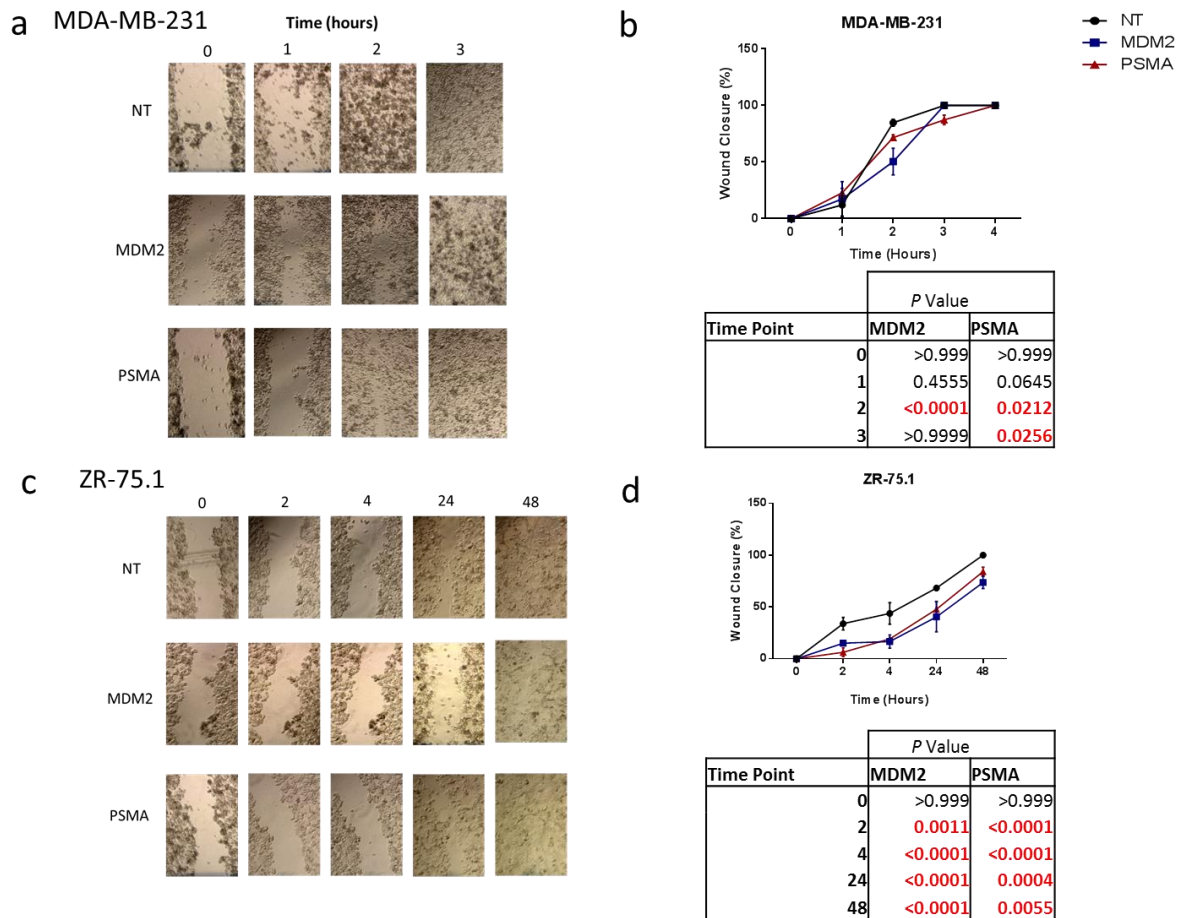


Figure 5.2. Scratch wound healing assay of siRNA-treated MDA-MB-231 and ZR-75.1 cells. a) Representative images of wounded MDA-MB-231 treated with siRNA, over a 4 hour period of healing. b) Assessment of the healing at three points on wounded MDA-MB-231 (% wound coverage \pm SD) with *p* values of MDM2 and PSMA siRNA compared to NT shown in table, with statistically significant time points shown in red. c) Representative images of wounded ZR-75.1 treated with siRNA, over a 48 hour period of healing. d) Assessment of the healing at three points on wounded ZR-75.1 cells (% wound coverage \pm SD) with *p* values of MDM2 and PSMA siRNA compared to non-targeting shown in table, with statistically significant time points shown in red.

The effect of MDM2 and PSMA knockdown on breast cancer cell invasion

In the same way as the transwell migration assays were undertaken, invasion of cells over a 24 hour period, following knockdown of MDM2 and PSMA, was investigated. This involved coating a 0.8 μ pore transwell in Matrigel and allowing the siRNA-treated cells to invade, towards the chemoattractant in the receiver well. It was repeatedly seen that after 48 hours, MDM2 knockdown led to an enhanced invasive capacity of MDA-MB-231 which increased around 36.5% compared to the non-targeting siRNA ($p=0.0012$). However, 72 hours after treatment, this was no longer the case, with a significant decrease in invasion of more than 50.8% being seen in both MDA-MB-231 ($p=0.0004$) (Figure 5.3 a). Cells treated with PSMA siRNA showed no difference at 48 hours in MDA-MB-231 cells. However, the decrease in invasion was highly marked after 72 hours of siRNA treatment, with MDA-MB-231 cells decreasing in their invasive capacity by 55.1% ($p=0.0099$) (Figure 5.3 b).

A similar trend was seen in ZR-75.1 cells following 48 hours treatment with MDM2 siRNA, and the invasive capacity increased by over 100% ($p=0.0004$) (Figure 5.3c). Again, after 72 hours, with cells decreasing in their invasive capability by more than 50.2% ($p=0.0308$). PSMA-targeted siRNA treatment of ZR-75.1 cells led to a 43.3% decrease in invasion ($p=0.0075$) after 48 hours and an almost 90.9% decrease after 72 hours ($p<0.0001$) (Figure 5.3 d).

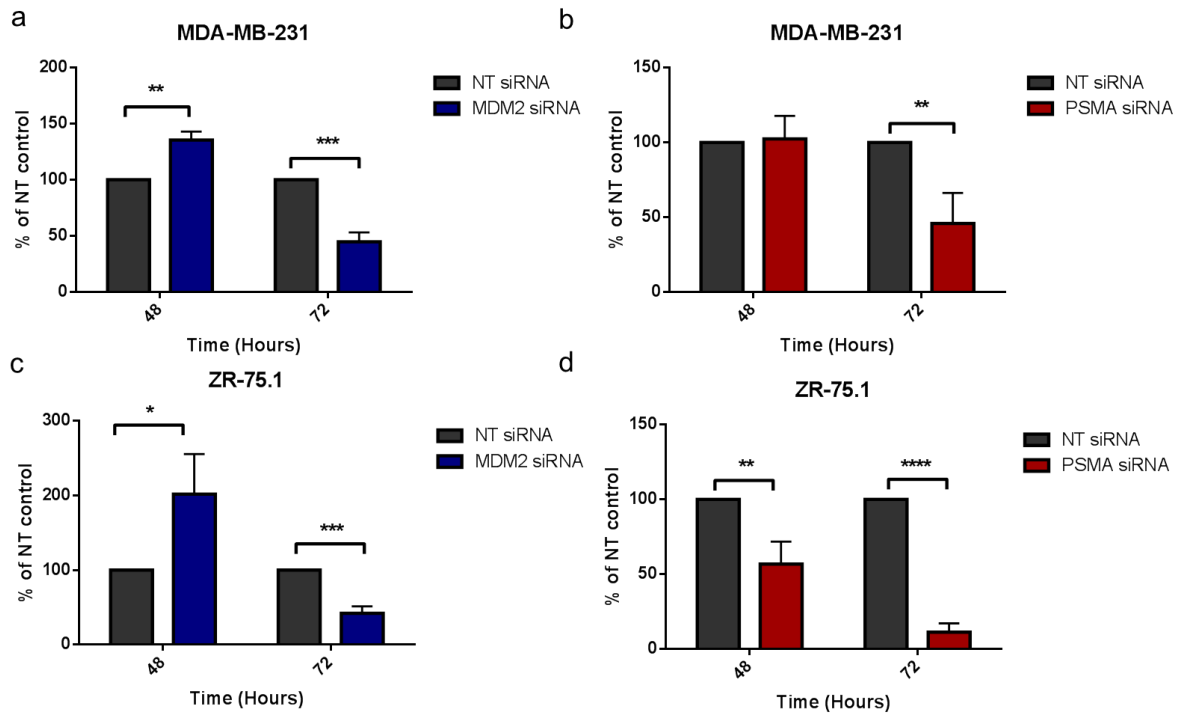


Figure 5.3. Invasion capacity of MDA-MB-231 and ZR-75.1, over a 24 hour period, of siRNA treated cells after 48 and 72 hours of treatment. a) Invasion of MDA-MB-231 treated with MDM2 siRNA. b) Invasion of MDA-MB-231 treated with PSMA siRNA. c) Invasion of ZR-75.1 treated with MDM2 siRNA. d) Invasion of ZR-75.1 treated with PSMA siRNA. (All graphs are shown as % of NT control siRNA-treated cells +SD; n=3; each experiment undertaken in triplicate; significant differences calculated by t-test with Welch's correction; * $p < 0.05$, ** $p < 0.01$).

The effect of MDM2 and PSMA knockdown on breast cancer cell adhesion

Following 72 hours of treatment with siRNA, the ability of fluorescently stained MDA-MB-231 and ZR-75.1 cells to adhere to an endothelial cell monolayer was assessed. Following 30 minutes of time for cells to adhere, the number of cancer cells were assessed using a fluorescent plate reader. The adherence of MDA-MB-231 was seen to be highly effected by each knockdown; with MDM2 siRNA, PSMA siRNA and both siRNAs all showing a highly significant decrease compared to the NT siRNA ($p < 0.0001$) (Figure 5.4a). The effect of ZR-75.1 cell adhesion was less profound, although a significant decrease in the ability of the cells to adhere compared to NT siRNA from MDM2 siRNA ($p = 0.002$), PSMA siRNA ($p = 0.020$) and both siRNAs ($p < 0.0001$) (Figure 5.4b).

Phospho-MDM2 (ser166) levels 48 and 72 hours post-MDM2 siRNA treatment

In an attempt to elucidate why 48 and 72 hours of MDM2-targeted siRNA treatment led to such surprisingly opposing results, phosphorylation levels of MDM2 at ser166 were investigated. It was seen that 48 hours after MDM2 knockdown, phosphorylation of serine 166 on MDM2 was actually increased significantly compared to the non-targeting control in both MDA-MB-231 (Figure 5.5a) and ZR-75.1 (Figure 5.5b). However, at 72 hours post-treatment, these levels have completely diminished (Figure 5.5c and d).

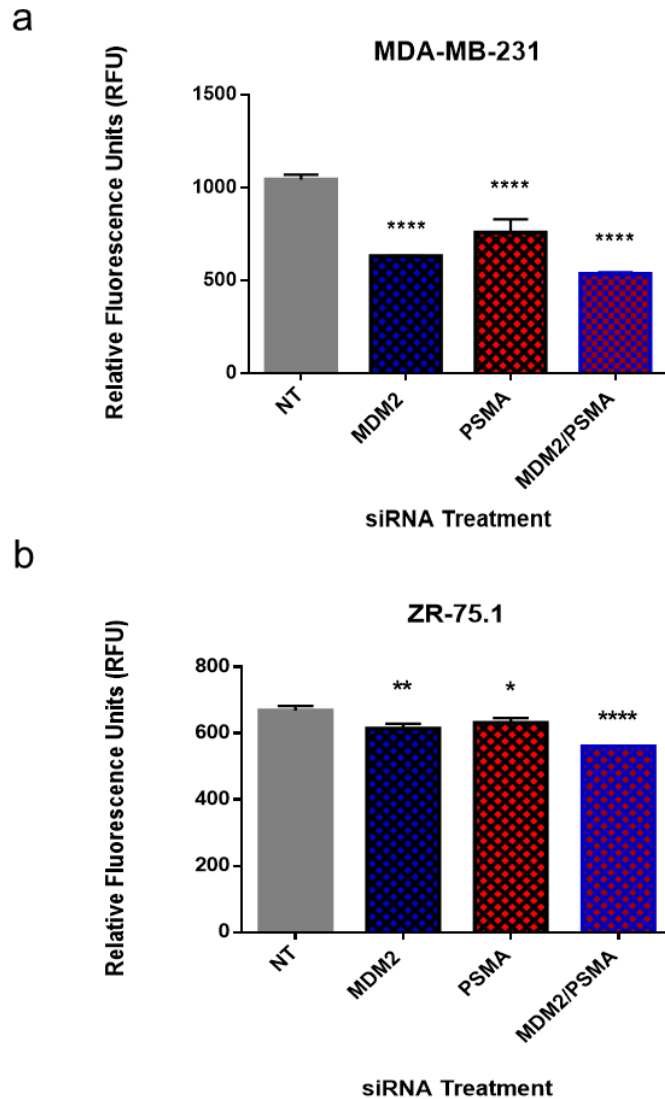


Figure 5.4. Adhesion capability of MDA-MB-231 and ZR-75.1 cells to an endothelial cell monolayer. a) Adhesion of MDA-MB-231 treated with MDM2, PSMA, MDM2/PSMA or NT siRNA. b) Adhesion of ZR-75.1 treated with MDM2, PSMA, MDM2/PSMA or NT siRNA. (All graphs shown as RFU + SD; n=3; each experiment undertaken in triplicate; significant differences assessed using one-way ANOVA; * p<0.05, ** p<0.01 and **** p<0.0001).

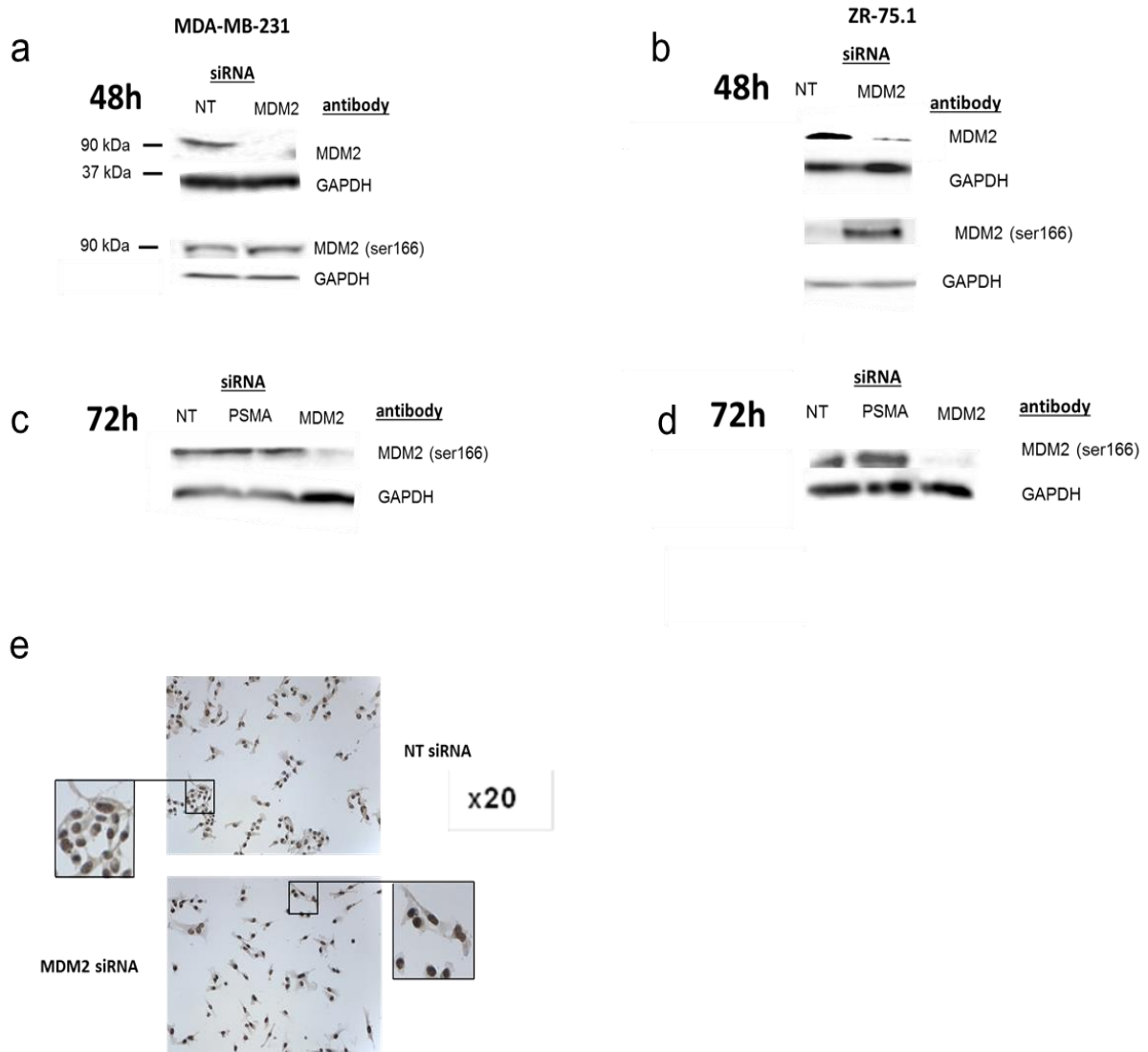


Figure 5.5. MDM2 (serine 166) phosphorylation following MDM2 siRNA treatment. a) MDM2 and MDM2 (serine 166) phosphorylation levels in MDA-MB-231 following 48 hours of MDM2 siRNA treatment. b) MDM2 and MDM2 (serine 166) phosphorylation levels in ZR-75.1 following 48 hours of MDM2 siRNA treatment. c) MDM2 (serine 166) phosphorylation levels in MDA-MB-231 cells following 72 hours of MDM2 siRNA treatment. d) MDM2 (serine 166) phosphorylation levels in ZR-75.1 cells following 72 hours of MDM2 siRNA. (All western blots are representative data; n=3). e) Immunocytochemical staining of MDA-MB-231 cells treated with NT or MDM2 siRNA for 48 hours and stained with MDM2 (serine 166) antibody (representative images).

In addition, immunocytochemical staining was undertaken following treatment of MDA-MB-231 with MDM2 or NT siRNA for 48 hours. These cells were then probed with the phospho-MDM2 (serine 166) antibody. Cells treated with NT siRNA showed medium positive staining of MDM2 phosphorylated at ser166 in both the cytoplasm and the nucleus. However, those cells treated with MDM2 siRNA showed a distinct decrease in cytoplasmic staining and a strongly positive nuclear staining (Figure 5.5e).

The effect of MDM2 and PSMA expression on matrix metalloproteinase (MMP) and tissue inhibitor of matrix metalloproteinase (TIMP) gene expression

Following 72 hours of siRNA treatment, gene expression levels of *MMP* and *TIMP* were assessed in the MDM2 and PSMA siRNA-treated cells compared to those treated with the NT siRNA control. *MMP1* expression was seen to be unchanged following MDM2 siRNA treatment in MDA-MB-231 cells but significantly downregulated following treatment with PSMA siRNA ($p < 0.0001$). ZR-75.1 cells showed a significant decrease in *MMP1* expression following treatment with each of the siRNAs ($p < 0.0001$). *MMP2* expression was seen to be downregulated by each of the treatments in both cell lines (MDM2 siRNA $p = 0.0003$; all others $p < 0.0001$). *MMP3* expression significantly increased following MDM2 siRNA treatment of MDA-MB-231 ($p = 0.0004$) and ZR-75.1 ($p < 0.0001$) cells, and after PSMA siRNA treatment ($p = 0.0482$ and $p < 0.0001$, respectively). *MMP7* expression levels were unchanged in both cells

lines following MDM2 siRNA treatment, but significantly increased following PSMA siRNA treatment (MDA-MB-231 $p < 0.0001$; ZR-75.1 $p = 0.0411$).

There were no significant changes in *MMP8* expression following MDM2 and PSMA siRNA treatment in either cell lines. An *MMP9* expression decrease was seen in both cell lines following MDM2 siRNA treatment (MDA-MB-231 $p < 0.0001$; ZR-75.1 $p = 0.0003$); however, PSMA treatment did not lead to significant change in expression levels. *MMP10* was seen to significantly increase in both cell lines after each treatment (MDA-MB-231: MDM2 siRNA $p = 0.0115$, PSMA siRNA $p = 0.0014$; ZR-75.1: MDM2 siRNA $p < 0.0001$, PSMA siRNA $p = 0.0084$). *MMP11* expression only increased significantly in MDA-MB-231 cells following PSMA siRNA treatment ($p = 0.0039$), whilst the other treatments did not cause significant changes in either cell line. There were no significant changes in *MMP12* expression in either cell lines after any treatment. *MMP13* expression was seen to significantly increase following both MDM2 siRNA (MDA-MB-231 $p = 0.0002$; ZR-75.1 $p < 0.0001$) and PSMA siRNA (MDA-MB-231 $p < 0.0001$; ZR-75.1 $p < 0.0001$). *TIMP1* expression was not significantly changed in MDA-MB-231 cells following MDM2 siRNA treatment; however, treatment with PSMA siRNA led to a significant increase in expression ($p = 0.0008$). ZR-75.1 cells showed a significant increase in expression following treatment with both MDM2 siRNA ($p < 0.0001$) and PSMA siRNA ($p < 0.0001$). Finally, *TIMP2* expression was unchanged through

treatment with MDM2 siRNA and significantly increased following treatment with PSMA siRNA in both cell lines (MDA-MB-231 $p=0.0111$; ZR-75.1 $p<0.0001$) (Figure 5.6).

The effect of MDM2 and PSMA expression on matrix metalloproteinase (MMP) and tissue inhibitor of matrix metalloproteinase (TIMP) protein secretion

To assess the MMP and TIMP secretion from breast cancer cell lines, the tumour-conditioned media was collected from siRNA-treated MDA-MB-231 and ZR-75.1 cell lines and levels assessed using the RayBioTech Human MMP Array C1. MDA-MB-231 cells showed a significant decrease was seen in MMP2 (MDM2 siRNA: $p=0.0021$; PSMA siRNA: $p=0.0081$) and MMP8 (MDM2 siRNA: $p=0.0325$; PSMA siRNA: $p<0.0001$). TIMP4 levels were also decreased to an almost significant level when MDM2 siRNA treated cells were compared to NT control treated cells ($p=0.0597$) (Figure 5.7.b and c). In the ZR-75.1 cell line, again, MMP2 (MDM2 siRNA: $p=0.0324$; PSMA siRNA: $p=0.0242$) and MMP8 (MDM2 siRNA: $p=0.0459$; PSMA siRNA: $p=0.0440$) levels were seen to significantly altered in both cell lines treated with each siRNA. In addition, a significant decrease in MMP9 secretion was seen in this cell line following each siRNA treatment, compared to the NT control (MDM2 siRNA: $p=0.0359$; PSMA siRNA: $p=0.0271$) (Figure 5.7. b and d).

Flow cytometric analysis was then undertaken in order to assess the internal MMP2 and MMP8 levels following 72 hours of treatment.

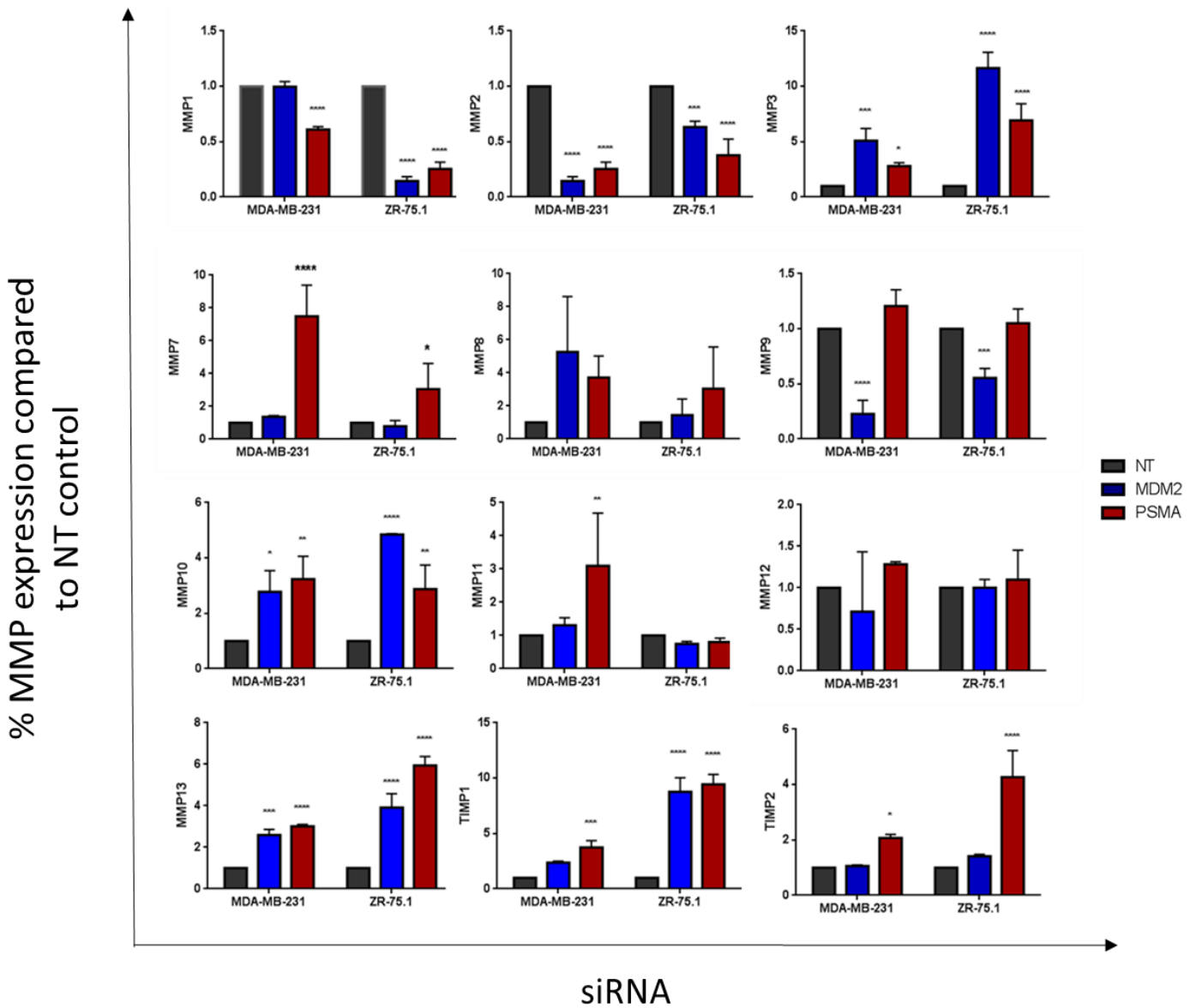


Figure 5.6. Gene expression of matrix metalloproteinases (MMPs) and tissue inhibitors of matrix metalloproteinases (TIMPs) in MDA-MB-231 and ZR-75.1 following siRNA treatment. (Data are mean fold change in expression compared to NT control + SD; n=3; individual experiments carried out in triplicate; significant differences calculated using unpaired t-test with Welch's correction with * $p < 0.05$, ** $p < 0.01$, *** $p < 0.001$ and **** $p < 0.0001$).

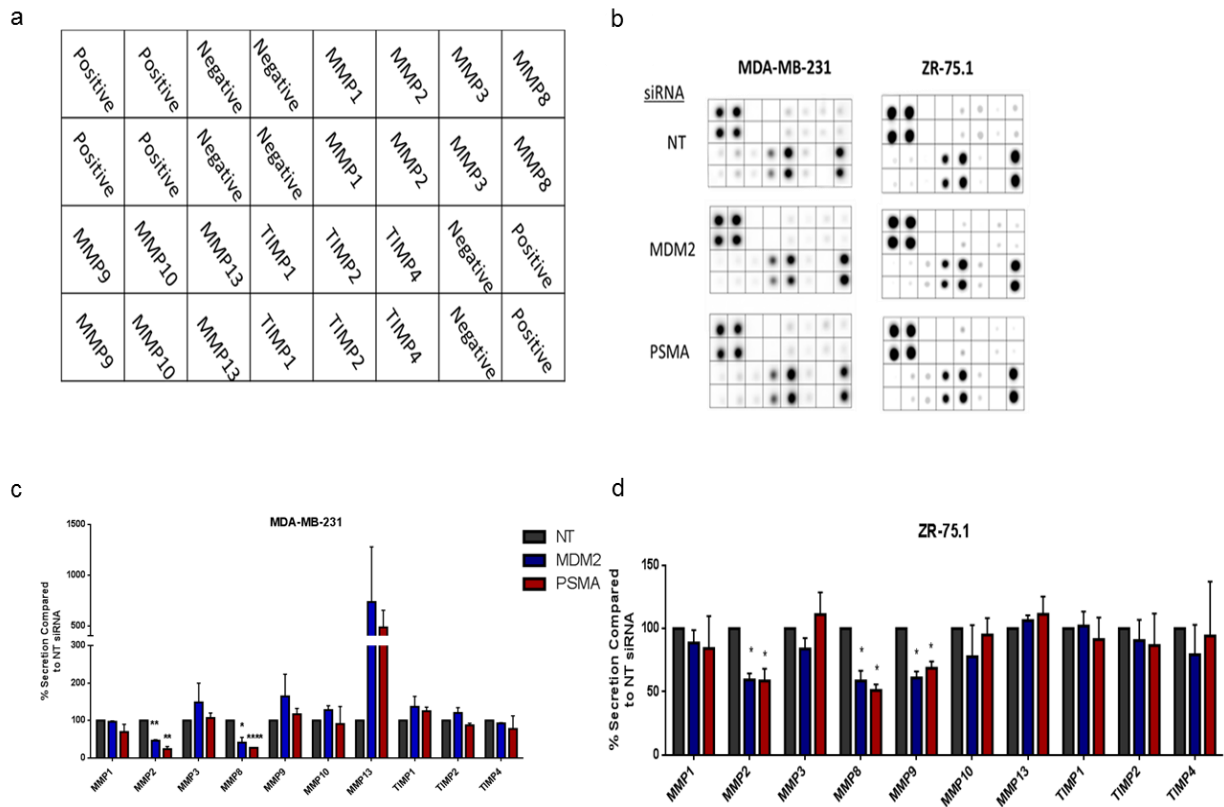


Figure 5.7. Protein expression of MMPs and TIMPs following siRNA treatment in MDA-MB-231 and ZR-75.1. a) Human MMP array blot layout. b) Representative human MMP array blots following treatment with MDM2, PSMA and NT siRNA in MDA-MB-231 and ZR-75.1 cell lines. c) Secretion of MMPs and TIMPs in MDA-MB-231 following MDM2 and PSMA siRNA as a percentage of NT control ($n=2$; each experiment undertaken in duplicate; graphs show % of NT control +SD; significant differences calculated by t-test with Welch's correction, with * $p < 0.05$, ** $p < 0.01$, **** $p < 0.0001$). d) Secretion of MMPs and TIMPs in ZR-75.1 following MDM2 and PSMA siRNA as a percentage of NT control ($n=2$; each experiment undertaken in duplicate; graphs show % of NT control +SD; significant differences calculated by t-test with Welch's correction with * $p < 0.05$, ** $p < 0.01$).

Both cell lines showed a decrease in MMP2 protein levels when treated with MDM2- or PSMA-targeted siRNA, compared to the NT control. In MDA-MB-231 cells, following gating to remove readings from any cellular debris or clusters, it was shown that MDM2 and PSMA siRNA resulted in a significantly lower level of MMP2 protein expression [MDM2 siRNA= 41.11% ($p=0.0010$) of cells and PSMA siRNA=17.83% of cells ($p=0.0001$)] compared to NT siRNA treated cells (72.02% of cells) (Figure 5.8a-d). Similar results were seen in the ZR-75.1 cell line, with 80.88% of cells expressing MMP2 when treated with NT siRNA, but MDM2 and PSMA siRNA-treated cells showing a substantial decrease in expression [MDM2 siRNA=35.47% of cells ($p=0.0003$) and PSMA siRNA=20.23% of cells($p<0.0001$)] (Figure 5.9a-d).

When MMP8 intracellular expression was monitored, it was seen that no differences in protein expression were seen, implying that the differences seen in MMP8 levels were due to a change in secretion of MMP8, not protein levels (Figures 5.10a-d and 5.11a-d).

The effect of MMP2 and MMP8 inhibition on breast cancer cells

In order to validate the hypothesis that matrix metalloproteinase secretion decrease is the reason for the decrease in growth, migration and invasion of breast cancer cell lines, two MMP2 inhibitors were used: ARP100 (specific to MMP2 at 6nM) and Marimastat (specific to MMP2 at 12nM). The proliferative potential of MDA-MB-231 cells following treatment with ARP100 showed a significant decrease in proliferation at all time points using two-way ANOVA (24 hours:

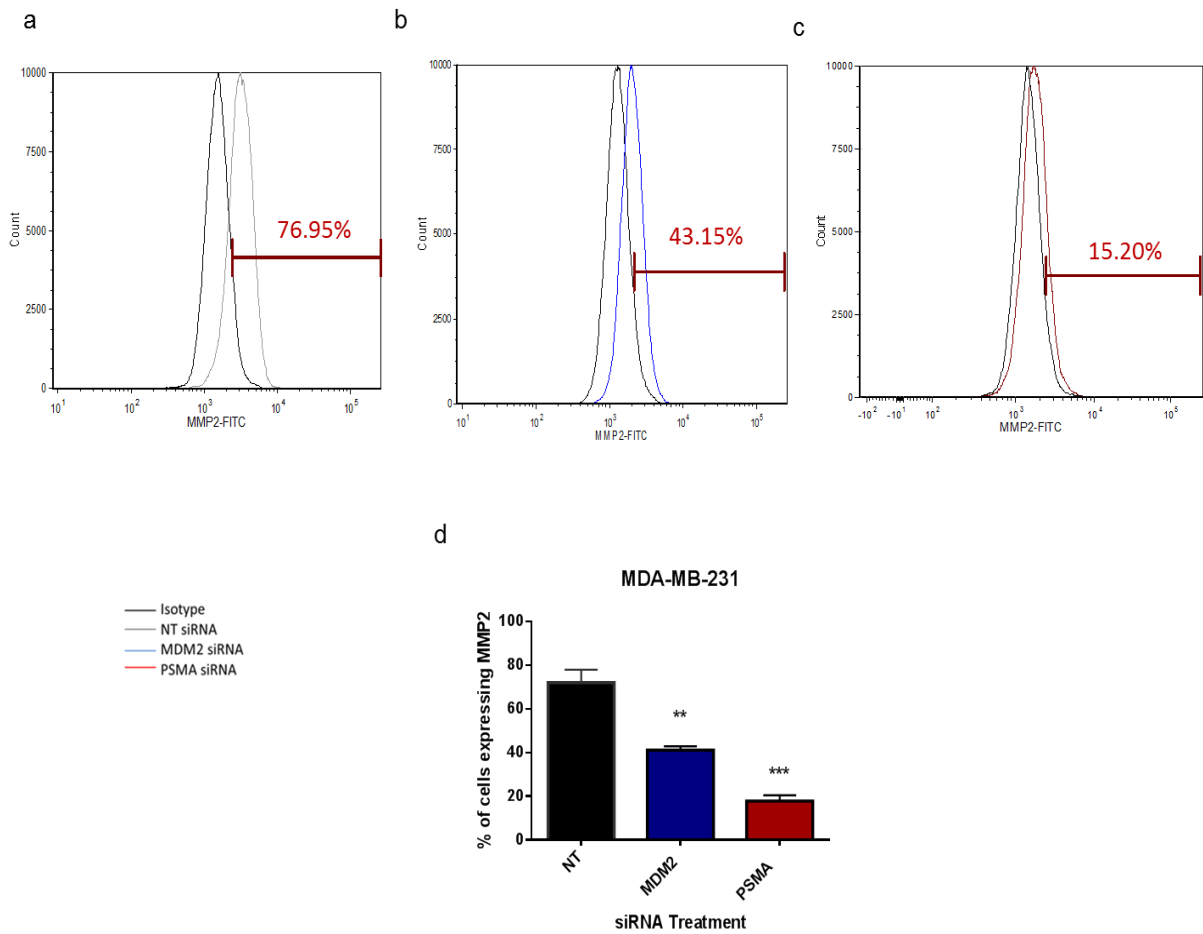


Figure 5.8. Flow cytometric analysis of MMP2 expression in MDA-MB-231. a) MMP2 expression of MDA-MB-231 treated with NT siRNA. b) MMP2 expression of MDA-MB-231 treated with MDM2 siRNA. c) MMP2 expression of MDA-MB-231 treated with PSMA siRNA. (All graphs show representative data of MMP2 protein expression in each siRNA treatment compared to isotype control). d) Summary of MMP2 flow cytometric data (n=3; graph shows mean + SD) (Significance assessed through unpaired t-test: ** $p < 0.01$, *** $p < 0.001$).

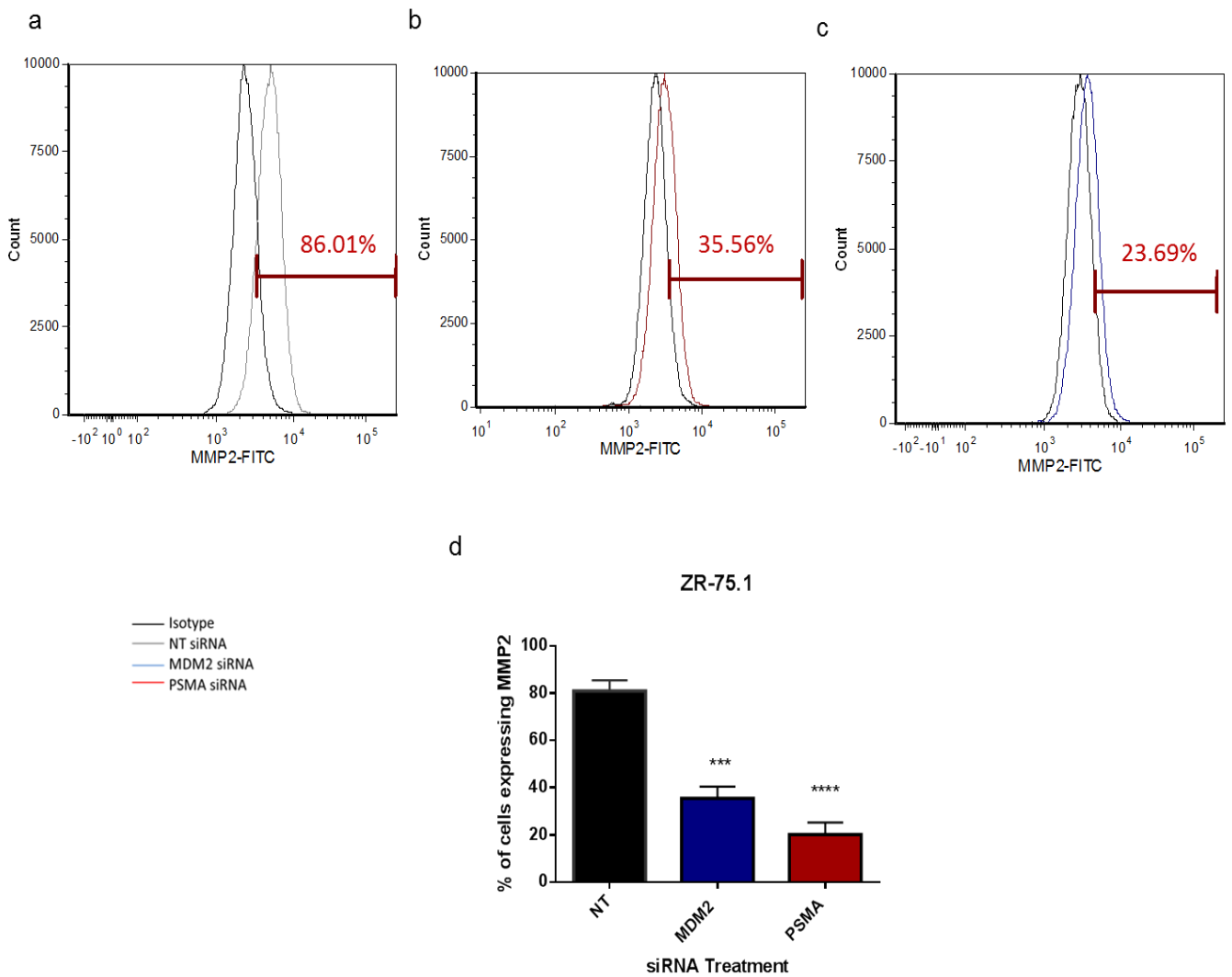


Figure 5.9. Flow cytometric analysis of MMP2 expression in ZR-75.1. a) MMP2 expression of ZR-75.1 treated with NT siRNA. b) MMP2 expression of ZR-75.1 treated with MDM2 siRNA. c) MMP2 expression of ZR-75.1 treated with PSMA siRNA. (All graphs show representative data of MMP2 protein expression in each siRNA treatment compared to isotype control). d) Summary of MMP2 flow cytometric data (n=3; graph shows mean + SD) (Significance assessed through unpaired t-test: ** $p < 0.01$, *** $p < 0.001$).

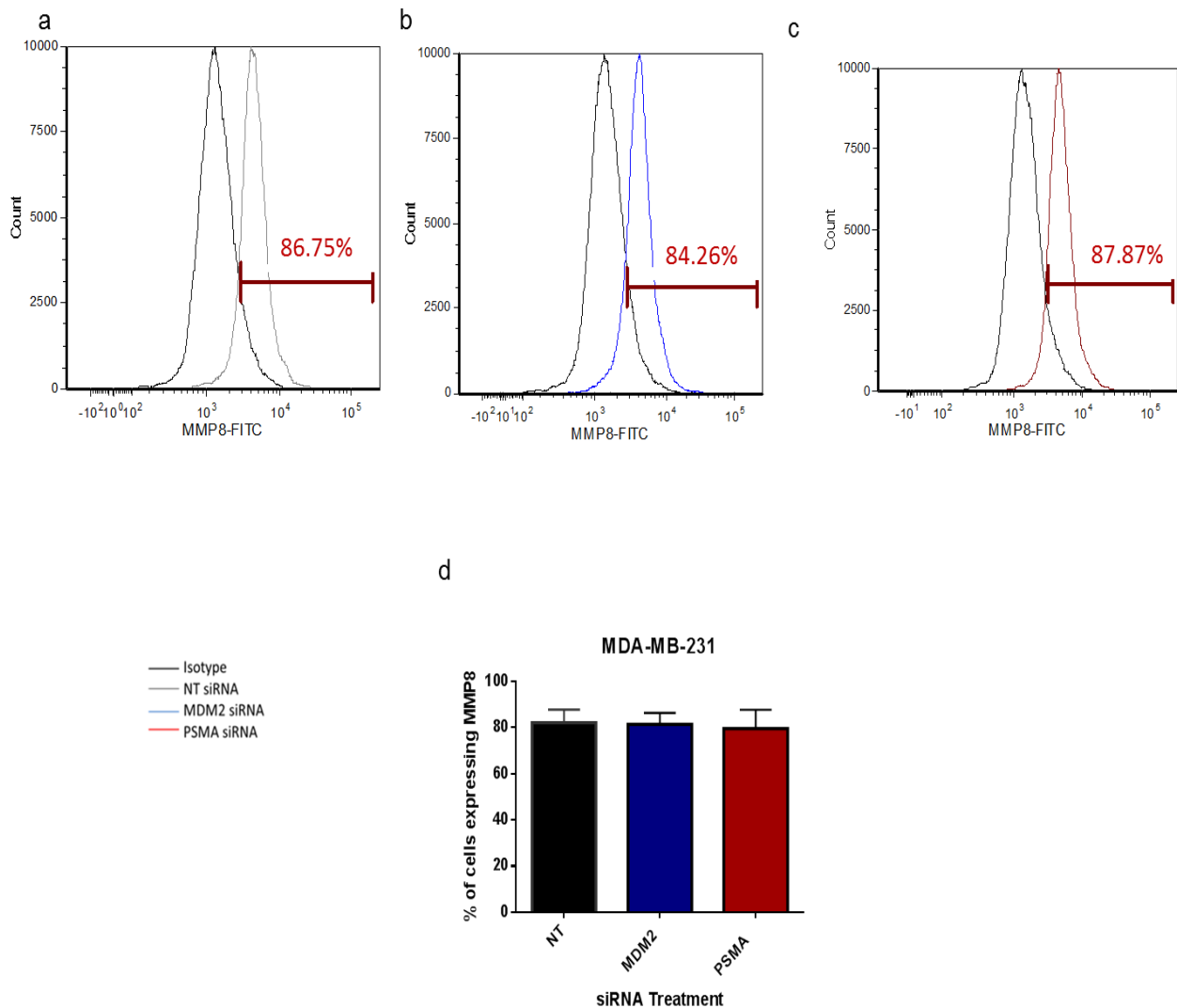


Figure 5.10. Flow cytometric analysis of MMP8 expression in MDA-MB-231. a) MMP8 expression of MDA-MB-231 treated with NT siRNA. b) MMP8 expression of MDA-MB-231 treated with MDM2 siRNA. c) MMP8 expression of MDA-MB-231 treated with PSMA siRNA. (All graphs show representative data of MMP2 protein expression in each siRNA treatment compared to isotype control). d) Summary of MMP8 flow cytometric data (n=3; graph shows mean + SD) (Significance assessed through unpaired t-test).

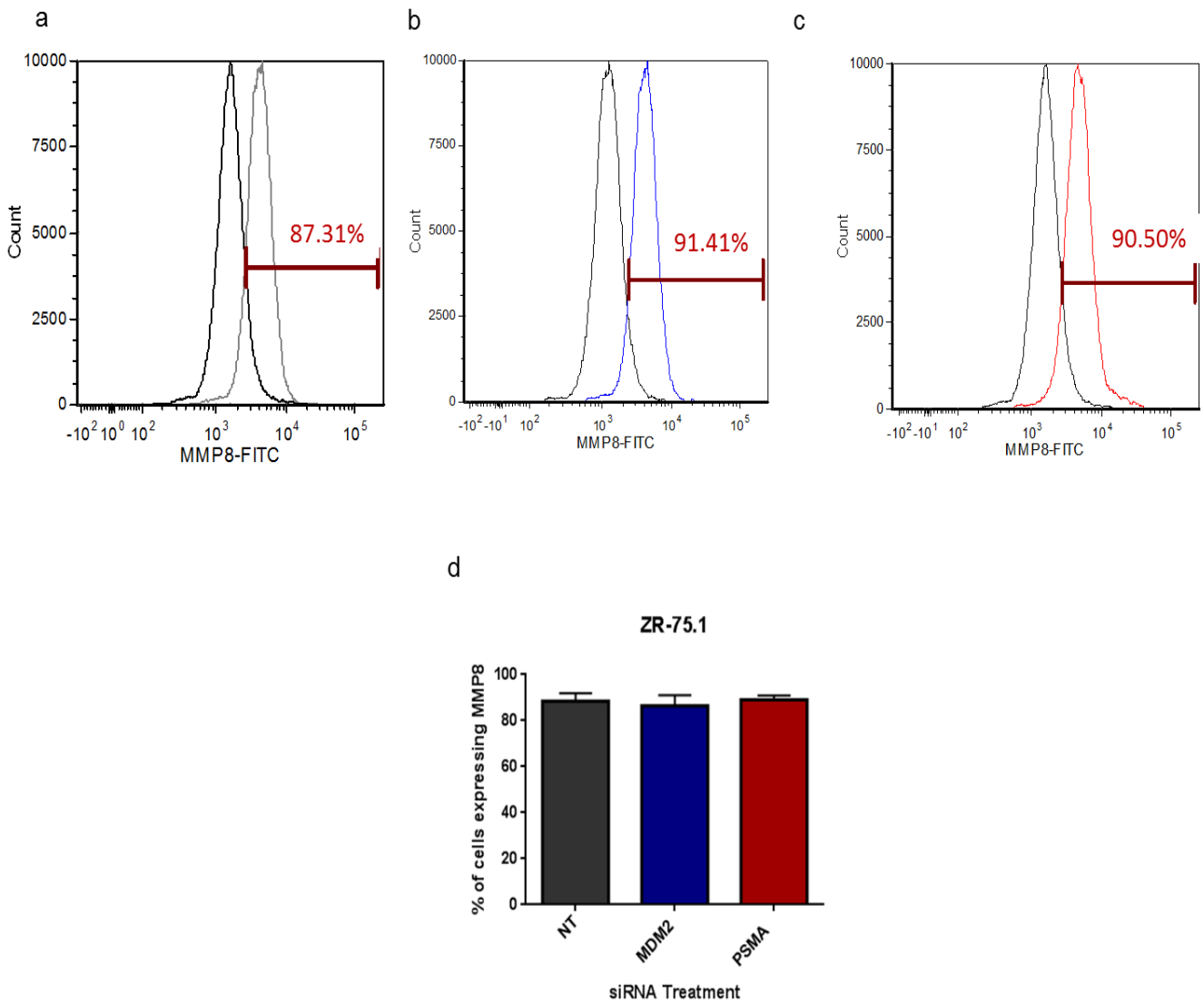


Figure 5.11. Flow cytometric analysis of MMP8 expression in ZR-75.1. a) MMP8 expression of ZR-75.1 treated with NT siRNA. b) MMP8 expression of ZR-75.1 treated with MDM2 siRNA. c) MMP8 expression of ZR-75.1 treated with PSMA siRNA. (All graphs show representative data of MMP2 protein expression in each siRNA treatment compared to isotype control). d) Summary of MMP8 flow cytometric data (n=3; graph shows mean + SD) (Significance assessed through unpaired t-test).

$p=0.0221$; 48 hours: $p=0.0198$; 72 hours: $p<0.0001$) . However, treatment with Marimastat showed less significance, with no significant difference from the DMSO control after 24 or 48 hours ($p=0.0791$ and $p=0.2961$, respectively) but a significant difference at 72 hours ($p=0.0039$) (Figure 5.12a). Following this, migration and invasion with each of the inhibitors were evaluated. Migration was seen to decrease following treatment of both cell line with inhibitor compared to the relevant DMSO control. Moreover, the DMSO control showed no significant difference from the wild-type cells in each case (data not shown) MDA-MB-231 cells showed a 53.4% decrease in migratory capacity when treated with 6nM ARP100 ($p=0.0296$), and a 56.7% decrease with 12nM Marimastat ($p=0.0369$) (Figure 5.12b). A decrease in invasion was also seen following both treatments (6nM ARP100: $p=0.0405$; 12nM Marimastat $p=0.0019$) (Figure 5.12c).

Similarly, ZR-75.1 cells showed a decrease in their ability to proliferate when MMP2 was inhibited. ARP100 treatment resulted in a decrease in proliferation only after 72 hours ($p=0.0069$) (Figure 5.13a), whereas a more obvious result was seen from Marimastat, which showed a growth decrease at 48 ($p=0.0002$) and 72 hours ($p<0.0001$) (Figure 5.13a). Migration (ARP100: 57.3% decrease, $p=0.021$; Marimastat: 48.7%, $p=0.0342$) (Figure 5.13b) and invasion (ARP100: 56.7%, $p=0.0105$; Marimastat: 41.2%, $p=0.0127$) (Figure 5.13c) were also decreased following treatment of ZR-75.1 with both inhibitors.

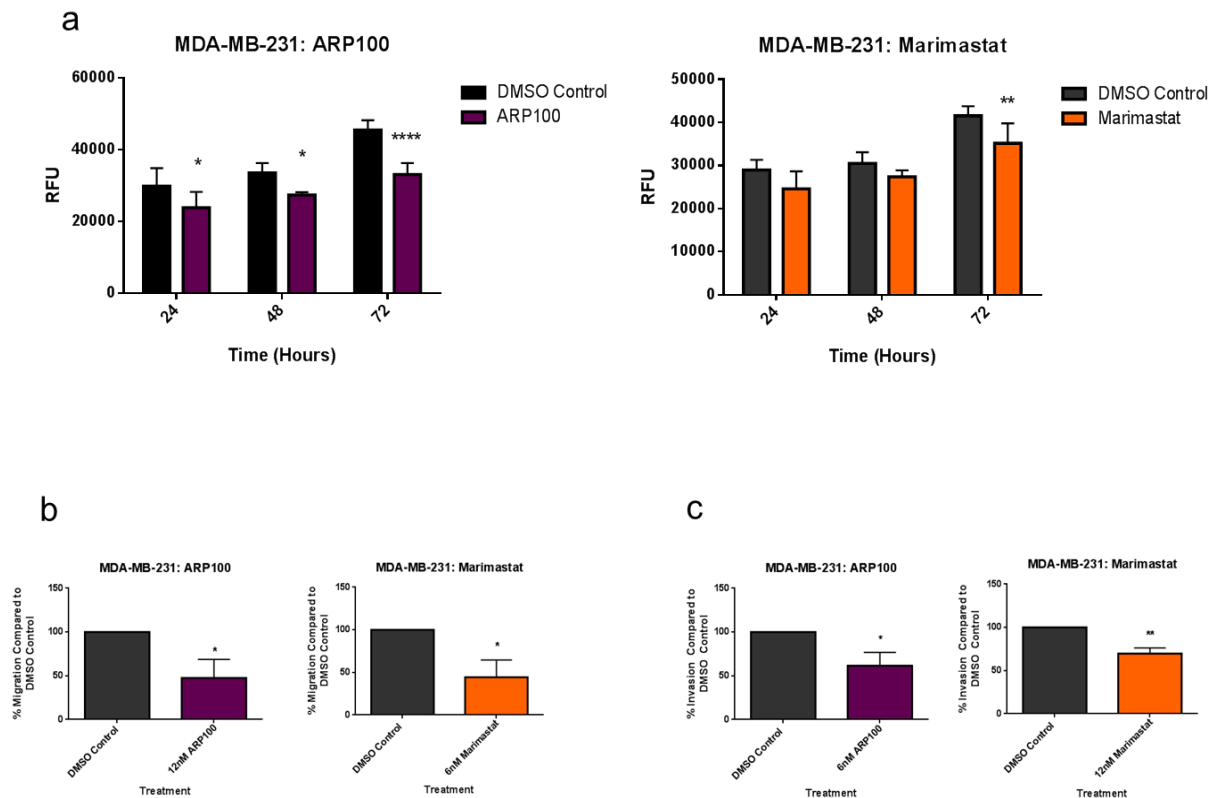


Figure 5.12. Effect of MMP2 inhibitors on MDA-MB-231 cell proliferation, migration and invasion. a) Proliferative capabilities of MDA-MB-231 cells following 24, 48 and 72 hours of MMP-2 inhibitors (6nM ARP100 and 12nM Marimastat) (representative data; graphs show mean RFU+SD; n=3; each individual experiment carried out six times; significances calculated using two-way ANOVA). b) Migratory capacity of MDA-MB-231 cells following treatment with 6nM ARP100 and 12nM Marimastat (graphs are shown as % of NT control siRNA-treated cells +SD; n=3; each experiment undertaken in triplicate; significant differences calculated by unpaired t-test with Welch's correction). c). Invasive capacity of MDA-MB-231 cells following treatment with 6nM ARP100 and 12nM Marimastat (graphs are shown as % of NT control siRNA-treated cells+SD; n=3; each experiment undertaken in triplicate; significant differences calculated by unpaired t-test with Welch's correction). Asterisks show significances: * $p < 0.05$, ** $p < 0.01$, **** $p < 0.0001$.

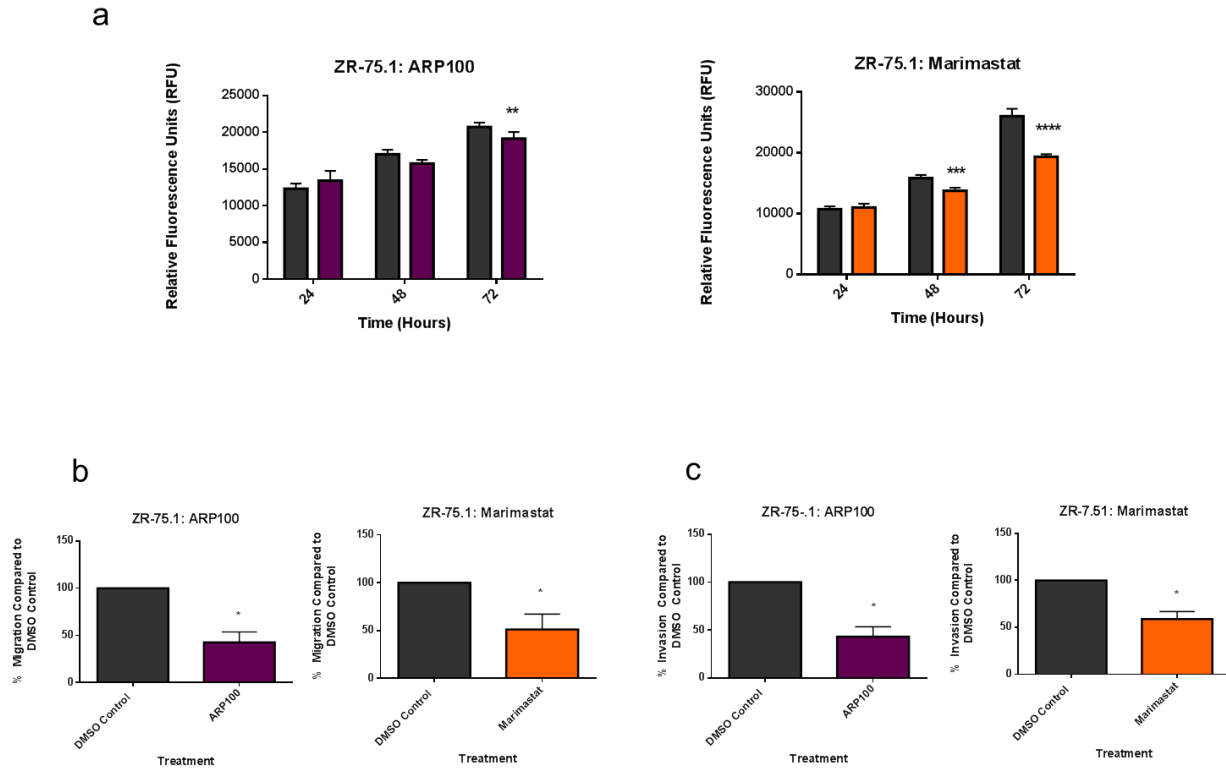


Figure 5.13. Effect of MMP2 inhibitors of ZR-75.1 cell proliferation, migration and invasion. a) Proliferative capabilities of ZR-75.1 cells following 24, 48 and 72 hours of MMP-2 inhibitors (6nM ARP100 and 12nM Marimastat) (representative data; graphs show mean RFU+SD; n=3; each individual experiment carried out six times; significances calculated using two-way ANOVA). b) Migratory capacity of ZR-75.1 cells following treatment with 6nM ARP100 and 12nM Marimastat (graphs are shown as % of NT control siRNA-treated cells +SD; n=3; each experiment undertaken in triplicate; significant differences calculated by unpaired t-test with Welch's correction). c). Invasive capacity of ZR-75.1 cells following treatment with 6nM ARP100 and 12nM Marimastat (graphs are shown as % of NT control siRNA-treated cells+SD; n=3; each experiment undertaken in triplicate; significant differences calculated by unpaired t-test with Welch's correction). Asterisks show significances: * $p < 0.05$, ** $p < 0.01$, *** $p < 0.001$, **** $p < 0.0001$).

As no difference in *MMP8* transcript level was seen at 48 hours, other time points following MDM2 or PSMA siRNA treatment were assessed, with no significant difference in *MMP8* transcript seen, compared to the NT control, at 6, 18 or 24 hours (Figure 5.14a-d). Following this, 4nm of an MMP8 inhibitor was used to assess the result of decreased MMP8 activity and no functional differences were seen upon assessment of growth (Figure 5.14e and f), migratory (Figure 5.11 g and h) and invasive (Figure 5.14i and j) ability of both MDA-MB-231 and ZR-75.1 cells.

IL-6 and IL-8 ELISA

To assess if MMP8 levels were truly changed in the TCM, an ELISA of IL-6 and IL-8 levels were examined, since MMP8 has previously been linked to these two interleukins in breast cancer cells (Thirkettle et al., 2013). Interestingly, it was seen that following both MDM2 and PSMA knockdown, a significant decrease in both IL-6 and IL-8 occurred. IL-6 levels were highly decreased in MDA-MB-231 following PSMA siRNA treatment compared to NT control ($p=0.0006$; decreased by 141 pg/ml), but less decreased after MDM2 siRNA ($p=0.0027$; decreased by 75 pg/ml) (Figure 5.15a). However, in ZR-75.1 cells, MDM2 siRNA treatment led to a greater decrease in secreted IL-6 levels, with a decrease of 60 pg/ml compared to the NT control ($p=0.0019$), whilst PSMA siRNA led to a decrease of 44 pg/ml ($p=0.0415$), just reaching significance (Figure 5.15b). IL-8 levels were also decreased in both cell lines following both siRNA treatments, with levels less significantly decreased in MDA-MB-231

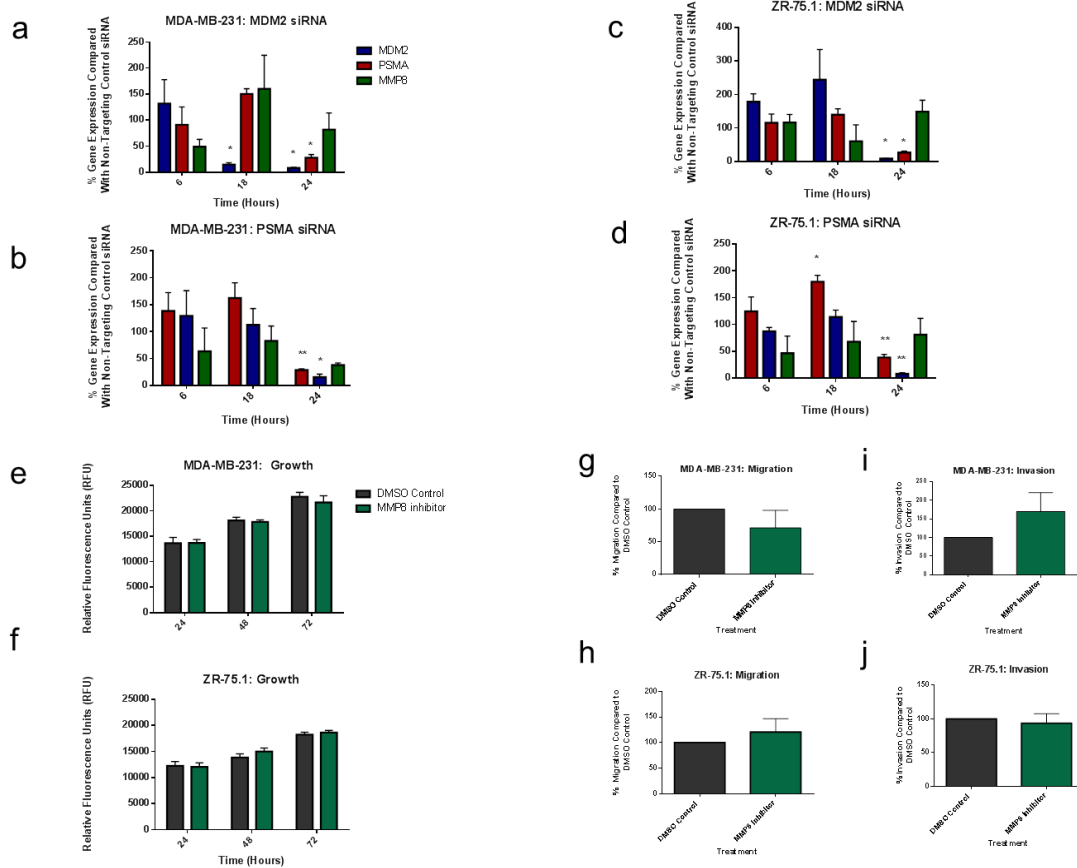
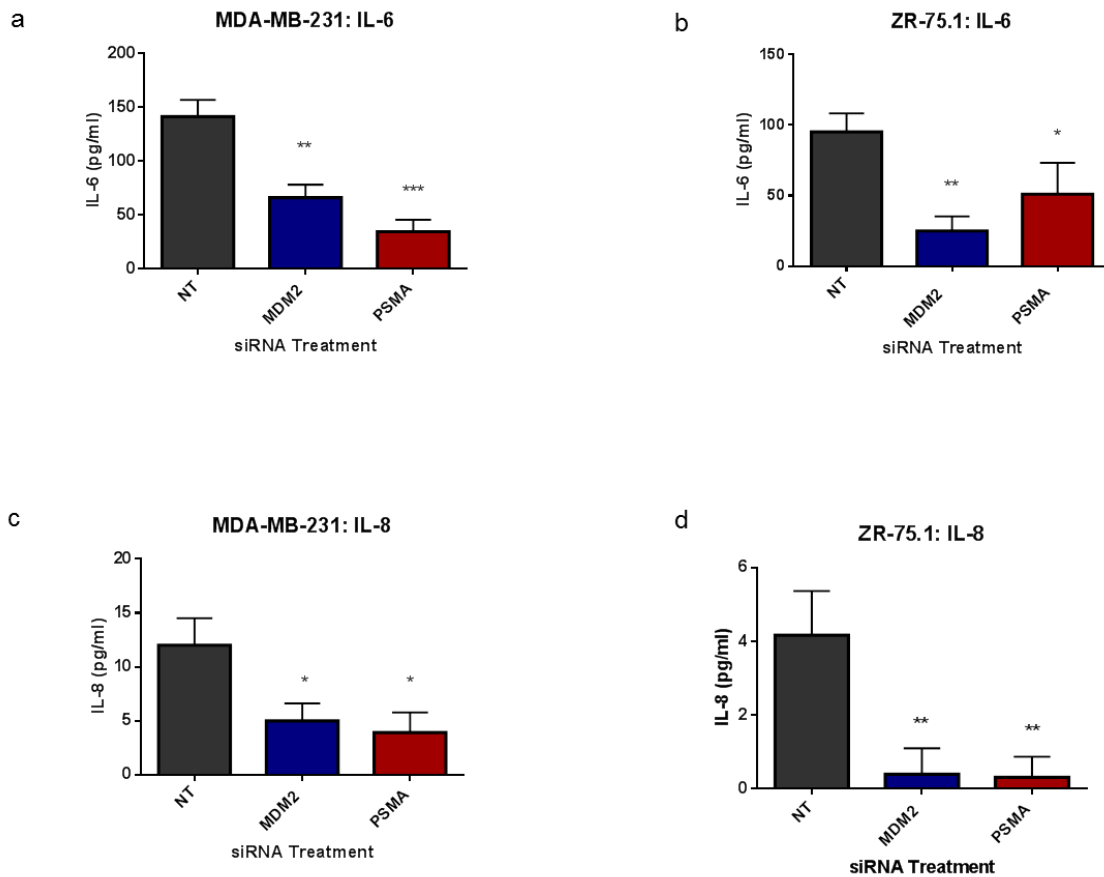


Figure 5.14. Effect of MMP8 inhibitor on MDA-MB-231 and ZR-75.1 cell proliferation, migration and invasion. a) *MMP8*, *MDM2* and *PSMA* gene level in MDA-MB-231 following 6, 18 and 24 hours of *MDM2* siRNA treatment. b) *MMP8*, *MDM2* and *PSMA* gene levels in MDA-MB-231 following 6, 18 and 24 hours of *PSMA* siRNA treatment. c) *MMP8*, *MDM2* and *PSMA* gene levels in ZR-75.1 following 6, 18 and 24 hours of *MDM2* siRNA treatment. d) *MMP8*, *MDM2* and *PSMA* gene levels in ZR-75.1 following 6, 18 and 24 hours of *PSMA* siRNA treatment. e) Proliferative ability of MDA-MB-231 cells following 24 48 and 72 hours of treatment with MMP8 inhibitor (Graphs show RFU+SD; n=3; individual experiments carried out six times; significance tested using two-way ANOVA). f) Proliferative ability of ZR-75.1 cells following 24, 48 and 72 hours of treatment with MMP8 inhibitor (Graphs show RFU+SD; n=3; individual experiments carried out six times; significance tested using two-way ANOVA). g) Migratory capacity of MDA-MB-231 cells treated with MMP8 inhibitor. h) Invasive capacity of ZR-75.1 cells treated with MMP8 inhibitor. i) Migratory capacity of MDA-MB-231 cells treated with MMP8 inhibitor. j) Invasive capacity of ZR-75.1 cells treated with MMP8 inhibitor. (Graphs are shown as % of NT control siRNA-treated cells+SD, unless otherwise stated; n=3; each experiment undertaken in triplicate; significant differences calculated by t-test with Welch's correction). Asterisks show significances: * $p < 0.05$, ** $p < 0.01$.



5.15. Secreted IL-6 and IL-8 levels of MDA-MB-231 and ZR-75.1 following 72 hours of MDM2 or PSMA siRNA treatment, as estimated by ELISA. a) IL-6 secretion in pg/ml from MDA-MB-231 cells following NT, MDM2 or PSMA siRNA treatment. b) IL-6 secretion in pg/ml from ZR-75.1 cells following NT, MDM2 or PSMA siRNA treatment. c) IL-8 secretion in pg/ml from MDA-MB-231 cells following NT, MDM2 or PSMA siRNA treatment. d) b) IL-8 secretion in pg/ml from ZR-75.1 cells following NT, MDM2 or PSMA siRNA treatment. (Graphs show mean pg/ml +SD; n=3; experiments carried out in triplicate; significance assessed using unpaired t-test with * $p < 0.05$, ** $p < 0.01$ and *** $p < 0.001$).

(MDM2 siRNA: $p=0.0146$, decreased by 7pg/ml; PSMA siRNA:
 $p=0.0105$, decreased by 4 pg/ml) (Figure 5.15c) , than ZR-75.1

(MDM2 siRNA: $p=0.0098$, decreased by 3.5 ng/ml; PSMA siRNA:
 $p=0.0071$, 3.8 pg/ml) (Figure 5.15d).

5.4. Discussion

Tumour cell migration and invasion are crucial steps in the spread of cancer through the tissues. These processes are key for the formation of metastases from the primary tumour, which are the main cause of death from cancer. The cells in these metastases are much more resistant, aggressive and efficient than those forming the primary tumour, as these cells have had to migrate and invade to form a colony at a new site (Bozzuto et al., 2010).

Migration assays undertaken following MDM2 and PSMA knockdown using targeting siRNA showed that cells possess a decrease in the migratory capacity through the pores of a transwell and also in the closing of a wound. Yang *et al.*, (2006) already linked MDM2 overexpression to an increase in cell motility and PSMA knockdown has been linked to a decrease in migration (Guo *et al.*, 2014; Zhang *et al.*, 2013).

Interestingly, it can be seen that PSMA knockdown led to a greater decrease in the ability of both breast cancer cell lines to migrate through the transwell, than MDM2 knockdown, despite knockdown only being around 50% efficient. This could indicate that PSMA plays an extremely important role in the migration of cells during the progression of breast cancer and slight changes in protein levels may incur large changes.

It is the general consensus in the literature that MDM2 is positively correlated with the invasion capacity of cancer cells (Chen *et al.*,

2013; Rajabi *et al.*, 2012). However, through the use of MDM2 siRNA, this study showed that 48 hours post-treatment, an increase in invasive capacity was seen, as well as an increase in phosphorylation at serine 166 on MDM2. On the other hand, at 72 hours, invasion was decreased, as was the phosphorylation at serine 166.

This is a very interesting phenomenon and it can be partially explained by the literature, which claims that phosphorylation of sites on MDM2 protein may increase the stability and half-life of the protein (Batuello *et al.*, 2015, Feng *et al.*, 2004b). Due to the important and multifunctional role played by MDM2 in the cell, particularly its regulation of p53 tumour suppressor (Moll & Petrenko, 2003), a sudden drop in MDM2 levels may lead to an attempt at sequestration of the protein in order for the cell to avoid apoptosis through activation of p53. However, it seems that 72 hours is enough for this process to no longer be ongoing and MDM2 levels are seen to drop (both total and serine 166 phosphorylation). These results indicate an increase in MDM2 ser166 phosphorylation correlates with an increased invasive capacity, and vice versa, may link phosphorylation of MDM2 at this site to the ability of cancer cells to invade.

PSMA knockdown resulted in a decrease in invasion at both 48 and 72 hours in ZR-75.1 cells, but only 72 hours showed a significant decrease in MDA-MB-231 cells. This may be due to the higher levels of PSMA expression ZR-75.1 cells, compared to MDA-MB-231 cells,

with a similar percentage decrease resulting in a larger effect functionally. Other studies have been undertaken to assess how PSMA levels affected the invasion capacity of cells and yielded varying results, with Dassie *et al.*, (Dassie et al., 2014) showing that overexpression of PSMA results in an increase in invasion, but Ghosh *et al.* (2005) claiming the opposite. However, results gained in the current study and the increasing expression of PSMA in more progressed cancers (Perner et al., 2007, Kasperzyk et al., 2013) indicate that the former paper was correct.

When the adhesion of cancer cells to an endothelial cell monolayer was assessed, a significant decrease was seen in each of the knockdowns, including the dual knockdown, compared to the NT siRNA. However, the effect on adherence of cells in the MDA-MB-231 cell line was more pronounced than ZR-75.1. This is interesting as through the study, ZR-75.1 has shown more significant effects after knockdown, which is potentially due to their greater level of knockdown compared to the MDA-MB-231 cell line. However, the reason for these results in terms of adhesion may be due to ZR-75.1 cells being less adherent and perhaps the length of time the cells were left was not long enough to show the true extent of the difference between the NT, MDM2 and PSMA siRNA treatment.

Since the MMP family is known to be associated with both migration, invasion and adhesion of cancers, this seemed like an informed place to start. Therefore, gene and secreted protein levels of the MMP and TIMP family members were studied following knockdown

of each of the molecules. Upon analysis of gene expression levels after knockdown, many of the family members were seen to be significantly altered. However, assessment of the secreted levels of MMPs and TIMPs into the tumour-conditioned media showed that only MMP2 and MMP8 in both MDA-MB-231 and ZR-75.1 were seen to be significantly altered, although ZR-75.1 cells showed a significant decrease in MMP9 levels following both knockdowns. In each cell line, MMP2 gene and protein levels were significantly decreased following both MDM2 and PSMA knockdown. This indicates that the changes seen following MDM2 and PSMA protein levels were realised through decreased transcription of the gene. However, although secreted MMP8 secreted protein levels were decreased following both knockdowns, there was no significant changes to gene level or intracellular protein levels, implying that changes to MMP8 levels was undertaken after the transcriptional process, or that secretion of MMP8 from the cell, was affected. It is also important to note that both cell lines do show a gene level decrease in MMP9 following MDM2 siRNA treatment, although a resultant change in MMP9 protein secretion level is only reflected in ZR-75.1 cell lines. However, ZR-75.1 also show a decrease in MMP9 protein secretion following PSMA siRNA treatment, but this is not shown at gene level. This indicates that MMP9 expression in ZR-75.1 is regulated through different pathways after MDM2 and PSMA knockdown.

It is important to note that due to monetary constraints, the MMP blots were undertaken only twice and the results analysed are the averages of two spots per blot. It would be a highly valuable undertaking to repeat this experiment, in order to check the significances and differences seen in secretion levels.

In order to investigate the hypothesis that MMP2 protein levels were decreased due to a decrease in transcript levels, whereas MMP8 protein levels were decreased due to a change after transcription or in secretion of the molecules, flow cytometry was used to assess the intracellular levels of the two proteins. As expected, it was seen that MMP2 intracellular levels were decreased following knockdown of both MDM2 and PSMA, compared to levels seen in those cells treated with NT control siRNA. Although, interestingly, the % of cells which expressed MMP2 was much higher in ZR-75.1 than MDA-MB-231, even though it can be seen from the blots that MDA-MB-231, as a culture, secrete more of the protein. This could mean that a higher number of cells secrete MMP2, but each individual MDA-MB-231 cell which does secrete the molecule, secretes much more. On the other hand, MMP8 levels were seen to remain the same, in spite of their siRNA treatment. This result indicates that MMP8 levels change following MDM2 and PSMA knockdown due to a decrease in secretion of the protein, rather than a change in actual protein levels in the cell.

Therefore, to further link MMP2 and MMP8 to the functionality of the cells following each knockdown, MMP2 inhibitors ARP100 and

Marimastat and MMP8 inhibitor were used in the assessment of growth, migration and invasion following treatment. It was seen that the MMP2 inhibitors show a decrease in growth, migration and invasion capacity following inhibitor treatment, compared to the DMSO control. Therefore, the decrease in MMP2 levels following each knockdown could be the reason for the decrease in migration and invasion seen. On the other hand, MMP8 inhibitor showed no significant change in growth, migration or invasion capacity. This data suggests that MMP2, but not MMP8, may be, in part, responsible for the decrease in growth, migration and invasion seen following MDM2 and PSMA knockdown.

Interestingly, in cancer studies, neither MDM2 nor PSMA have been directly linked to MMP2 or MMP8 protein levels in previous literature; however, both have been linked to MMP9. MDM2 has been linked to MMP9 levels in clinical samples of IDC (Chen *et al.*, 2013) and further work in breast cancer cell lines, including MDA-MB-231 showed a significant decrease in gene expression levels of MMP9 through RT-PCR, which correlates with the current study. A significant correlation in expression was also seen between the two molecules in the oncogenesis of lung cancer in rats (Zhang *et al.*, 2014). PSMA expression has been linked to MMP9 levels following induced overexpression of PSMA in prostate cancer cell line, RM-1; with immunohistochemistry indicating MMP9 levels were distinctly higher in mice injected with the cells overexpressing PSMA. The group also backed this up *in vitro*, showing an increase in protein

levels using western blotting (Zhao *et al.*, 2012). Therefore, it is interesting that MDA-MB-231 and ZR-75.1 show differing expression patterns of MMP9 protein following MDM2 or PSMA knockdown. However, this could be due to the vast difference in the cell types used. This decrease in MMP9, as well as MMP2, could go some way in explaining the heightened decrease in migration and invasion showed by ZR-75.1 cells following MDM2 and PSMA knockdown.

In terms of roles of MMP2 and MMP8 in cancer, it may be expected that a decrease in MMP2 levels may occur following the knockdowns, taking into account the decrease in the progressive properties of the cells, as the literature clearly states that MMP2 is correlated with the migration and invasion of tumour cells (Jeziarska and Motyl, 2009). On the other hand, MMP8 has also been shown to be a metastasis-suppressor, though its expression is deleterious to long-term growth (20 days), as well as inducing IL-6 and IL-8 factors which promote malignancy in breast cancer cells (Thirkettle *et al.*, 2013). Moreover, MMP8 has been said to have a protective role against lymph node metastasis, following a study of inflammatory breast cancer patients (Decock *et al.*, 2008).

Finally, we assessed the levels of IL-6 and IL-8 in breast cancer cells, since MMP8 has previously been linked to their expression. Thirkettle *et al.*, (2013) previously identified MMP8 as an inducer of IL-6 and IL-8 expression in breast cancer cells. Our data showed the same result, with MMP8 decrease due to MDM2 and PSMA siRNA leading to a decrease in both IL-6 and IL-8. This indicates that, since

MMP8 levels are only changed outside the cells, that MMP8 somehow regulates the levels of IL-6 and IL-8 outside the cells, perhaps through proteolytic cleavage. Interestingly, PSMA has previously been linked to regulation of IL-6 expression through activation of the MAPK pathway in prostate cancer cells (Colombatti et al., 2009, Ben Jemaa et al., 2013) and it has been claimed that IL-6 can downregulate p53 expression (Brighenti et al., 2014). IL-6 has been seen to play a role in regulation of the tumour microenvironment (Fisher et al., 2014), stem-cell-like cell production in breast cancer (Xie et al., 2012), metastasis (Miao et al., 2014) and DNA methylation alterations (Gasche et al., 2011). In addition, patients with advanced cancers show high IL-6 blood levels (Hussein et al., 2004, Salgado et al., 2003). IL-8 has been suggested to promote angiogenic response in endothelial cells, increase proliferation and survival of endothelial and cancer cells and increase the migration of cancer cells and endothelial cells (Waugh and Wilson, 2008).

In conclusion, it seems that MDM2 and PSMA knockdown result in a similar functional response of breast cancer cells and this could be executed through their ability to decrease the levels of MMPs in the tumour-conditioned media. This decrease could also result in a decrease in the secretion of IL-6 and IL-8 from breast cancer cells.

Chapter VI

Knockdown of MDM2
and PSMA in breast
cancer cell lines leads
to changes in AKT and
c-JUN phosphorylation
levels

6.1. Introduction

The online tool www.genemania.com lists genes with potential interactions by searching large, publicly available datasets to find related genes. This relationship may be protein-protein, protein-DNA and genetic interactions, pathways, reactions, gene and protein expression data, protein domains and phenotypic screening profiles.

Through this, the database can suggest possible links and potential pathways of a large number of genes. Using the search terms 'MDM2', 'PSMA', 'MMP2' and 'MMP8' led to the discovery of a potential interaction of these molecules with c-JUN.

c-JUN, when activated, is thought to play an important role in cancer progression and malignancy. This activation occurs when extra- or intracellular signalling such as growth factors, UV radiation or transforming oncoproteins stimulate the phosphorylation of c-JUN at serines 63 and 73 (Vleugel et al., 2006). Studies have linked c-JUN expression to an increase in the progressive properties of breast cancer (Zhang et al., 2007, Vleugel et al., 2006).

In addition, the literature shows that there may be a link between both MDM2 and PSMA with AKT. It has been shown that knockdown of PSMA leads to a decrease in the levels of serine 473 phosphorylation, whilst total levels of AKT remain the same (Guo *et al.*, 2002). In addition, AKT is heavily implicated in the phosphorylation of MDM2 at multiple sites, although different groups report a number of findings. There are varying reports on the involvement of AKT phosphorylation

on MDM2 nuclear entry. For instance, Mayo & Donner (2001) claiming that serine 166 and 186 phosphorylation promote nuclear entry. However, Ogawara *et al.*, (2002) disputed this, claiming that phosphorylation of MDM2 sites showed no effect on subcellular localisation. Feng *et al.*, (2004) claimed that serine 166 and 186 are phosphorylated by AKT serine 473 and this inhibits MDM2 self-ubiquitination and thus its stability, but serine 186 is reported to be unphosphorylated. Moreover, p53 tumour suppressor is consistently linked to AKT signalling. The molecules play opposing roles in the transduction of apoptosis and it seems that conflicting signals governed by each of the molecules are integrated into each of the two pathways involved (Sabbatini & McCormick, 1999; Yamaguchi *et al.*, 2001; Hong *et al.*, 1999; Mazzoni *et al.*, 1999; Gottlieb *et al.*, 2002).

Therefore, in this chapter we aimed to assess the roles of both c-JUN and AKT phosphorylation in the interaction of MDM2 and PSMA in breast cancer cells.

6.2. Materials & Methods

Cell lines and treatment

MDA-MB-231 and ZR-75.1 metastatic breast cancer cell lines were maintained in DMEM media with 10% FBS and antibiotics. These cell lines were transiently transfected with MDM2, PSMA or non-targeting (NT) siRNA using Fect4 or Fect1 transfection reagent, respectively. All treatments were undertaken in a 6-well plate and a total volume of 1ml per well was used in each case. MDA-MB-231 cells were treated with 100 nM of each siRNA and ZR-75.1 cells were treated with 50 nM, according to manufacturer's instructions, following optimisation experiments. Treatments were undertaken for 24, 48 or 72 hours, dependent on the experiment.

RNA isolation and RT-PCR

Following treatment of MDA-MB-231 and ZR-75.1 cells with MDM2, PSMA and NT siRNA in a 6-well plate, TRI reagent was added to cells. RNA isolation and RT-PCR were then undertaken according to sections 2.4.1 and 2.4.2.

Quantitative PCR (qPCR)

qPCR was carried out using cDNA produced in reverse transcription detailed above, using primers for *JUN*, *AKT* and *GAPDH* (listed in Table 2.3), following the procedure outlined in 2.4.3. CT values gained from this were analysed using $2^{-\Delta\Delta CT}$ normalisation to *GAPDH*.

Each qPCR sample was set up in triplicate, with the experiment being independently set up three times. Each reading was expressed as a percentage of NT control and statistical analysis was undertaken using unpaired t-test with Welch's correction, comparing each MDM2 and PSMA siRNA to NT control.

Western blotting

Following 72 hours of treatment of MDA-MB-231 and ZR-75.1 with MDM2, PSMA and NT siRNA, cells were scraped from the 6-well plate into 50 µl RIPA buffer (with added inhibitors), left on a blood wheel for 1 hour at 4°C, then centrifuged for 15 minutes at 12,000 X G. Following this protein was quantified and a standard concentration decided upon. Then an equal amount of 2 x Laemmli was added and SDS-PAGE, western blotting and immuno-probing using anti-AKT, anti-phospho-AKT (serine 473), anti-phospho-MDM2 (serine 186/188), anti-phospho-MDM2 (serine 186) and anti-GAPDH (antibody list in Table 2.4) was undertaken as outlined in 2.5.1.

Flow cytometric analysis of c-JUN and AKT levels

Following treatment of MDA-MB-231 and ZR-75.1 cells with MDM2, PSMA and NT siRNA for 72 hours, intracellular c-JUN, phospho-c-JUN (serine 63) and phospho-AKT (serine 473) were assessed as detailed in 2.5.3.

AKT inhibitor studies

To inhibit AKT in MDA-MB-231 and ZR-75.1, cells were treated with 5 μ M of AKT inhibitor (124005). Following this, RNA isolation, reverse transcription and qPCR were carried out as detailed above.

Statistical analysis

Data were statistically analysed using either unpaired t-test or unpaired t-test with Welch's correction, with a p -value of <0.05 considered statistically significant. Asterisk (*) was used to signify p -values:

* $p<0.05$, ** $p<0.01$, *** $p<0.001$ and **** $p<0.0001$.

6.3. Results

The proteins which may link MDM2 and PSMA

Using Genemania (www.genemania.com), a plug in of Cytoscape, to assess which proteins may be involved in the interplay between MDM2, PSMA and MMP2 and MMP8 led to the discovery of an interaction of these molecules with c-JUN (Figure 6.1a). Additionally, searching the literature revealed that both MDM2 and PSMA have been linked to AKT and its phosphorylation at site 473. Moreover, both c-JUN and AKT have previously been linked to a possible regulation of the MMPs (Figure 6.1b), and so their study may indicate a way in which MDM2 and PSMA proteins interplay to regulate MMP secretion.

c-JUN gene and protein expression following MDM2 and PSMA knockdown in breast cancer cells

Following MDM2, PSMA or NT siRNA treatment, *JUN* gene, as well as c-JUN protein and phosphorylation levels were assessed through RT-qPCR and flow cytometry, respectively. Assessment of *JUN* gene levels at 24, 48 and 72 hours revealed no significant changes in transcript expression following either of the knockdowns, compared to the *JUN* expression of the NT control treated MDA-MB-231 breast cancer cells (Figure 6.2a) and this was also shown using flow cytometry upon assessment of total c-JUN expression levels (Figure 6.2b-d). However, observation of the phosphorylation levels of c-JUN at serine 63, following each of the knockdown showed a

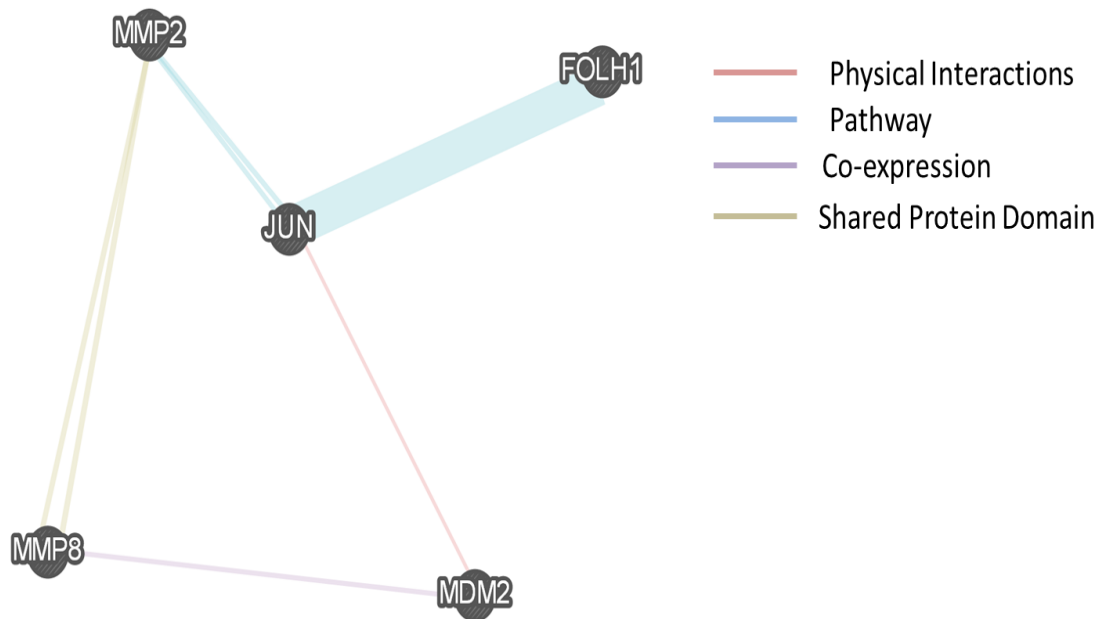


Figure 6.1. Results of GeneMANIA search with 'MDM2', 'FOLH1/PSMA', 'MMP2' and 'MMP8' outlined as search terms. GeneMANIA searches online databases to show potential interactions between genes. The database lists physical interactions, pathways, co-expression and shared protein domain links between genes. Use of this database enables the prediction of interactions between a number of genes and how these interactions may fall into a pathway or a set of interactions.

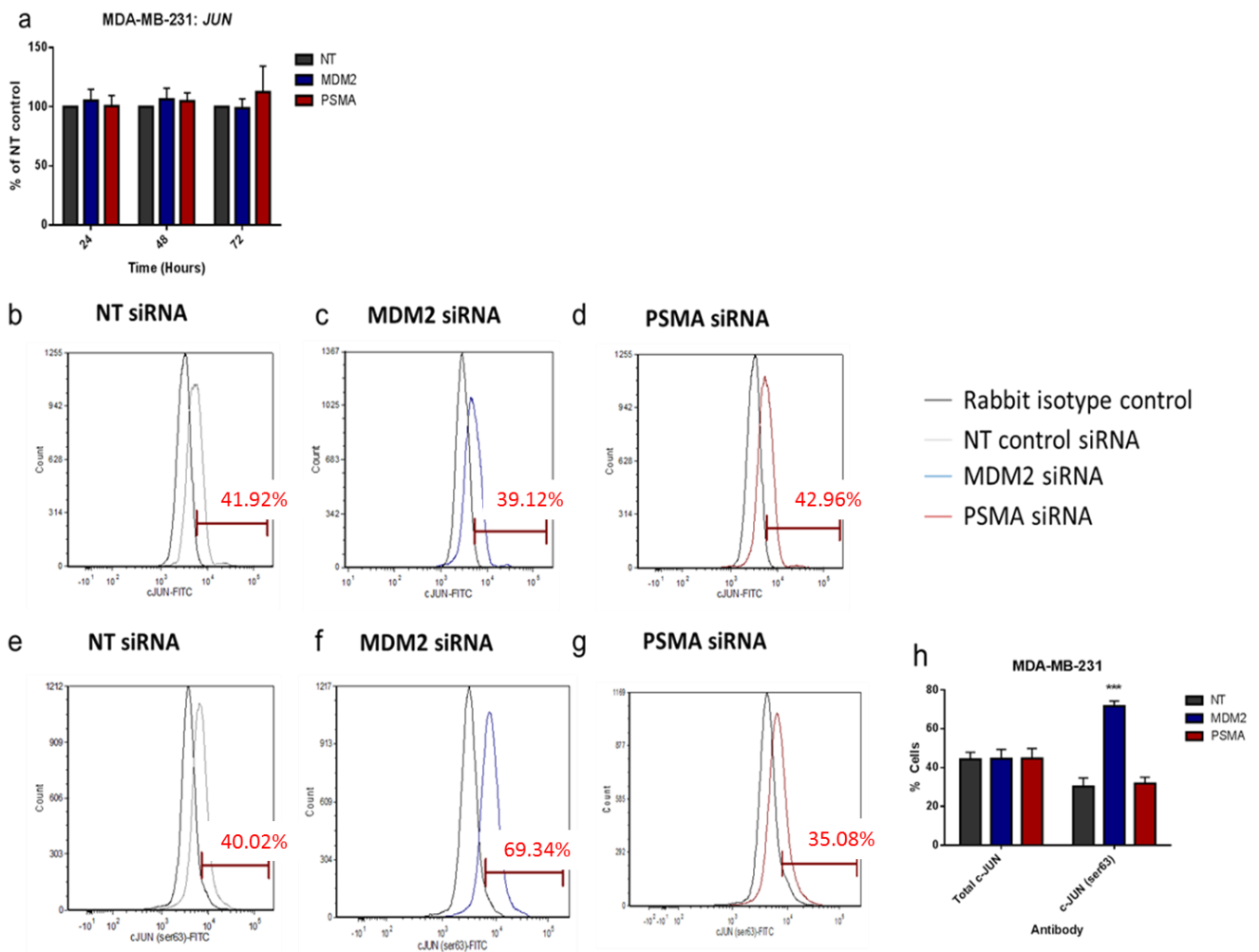


Figure 6.2. JUN gene and c-JUN protein expression and phosphorylation levels following 72 hours of MDM2 and PSMA siRNA treatment MDA-MB-231 cells. a) Gene expression levels of JUN following MDM2, PSMA and NT siRNA treatment (Graph shows % of NT control siRNA-treated cells +SD; each experiment undertaken in triplicate; significant difference calculated by t-test with Welch's correction). b) Flow cytometric analysis of NT control siRNA-treated cell expression of cJUN total protein. c) Flow cytometric analysis of MDM2 siRNA-treated cell expression of cJUN total protein. d) Flow cytometric analysis of PSMA control siRNA-treated cell expression of cJUN total protein. e) Flow cytometric analysis of NT siRNA-treated cell expression of cJUN phosphorylation at ser63. f) Flow cytometric analysis of MDM2 siRNA-treated cell expression of cJUN phosphorylation at serine 63. g) Flow cytometric analysis of PSMA siRNA-treated cell expression of cJUN phosphorylation at serine 63. (All flow cytometry graphs show representative data; percentages show cells expressing the protein being assessed). h) Summary of total and phosphorylation (serine 63) cJUN levels following NT, MDM2 and PSMA siRNA treatment (n=3; Graph shows % of cells expressing cJUN/p-cJUN (serine 63)+SD; significant difference against NT control calculated by t-test; *** $p < 0.001$).

significant increase in phosphorylation of this serine when MDM2 knockdown was carried out ($p=0.0005$) (Figure 6.2e-h).

Similarly, in the ZR-75.1 breast cancer cell line, qPCR assessment of *JUN* transcript levels showed no significant change after any knockdown, at any time-point (Figure 6.3a), as well as no change of total c-JUN protein levels shown through flow cytometry (Figure 6.3b,c and d). Assessment of serine 63 phosphorylation following each knockdown bore similar results in terms of MDM2 siRNA treatment, with a significant increase in phosphorylation of this site being seen, compared to the NT control ($p=0.0015$) (Figure 6.3e and f). However, this cell line also exhibited an increase in phosphorylation at this site following PSMA knockdown ($p=0.0015$) (Figure 6.3e and g) (all data summarised in Figure 6.3h).

AKT gene and protein expression following MDM2 and PSMA knockdown in breast cancer cells

AKT levels were also assessed following treatment with MDM2 and PSMA siRNA. It can be seen that transcript levels of AKT were significantly increased following 72 hours of PSMA siRNA treatment in MDA-MB-231 cells ($p=0.0049$; Figure 6.4a) and this was also seen at protein level (Figure 6.4b). In addition, MDM2 siRNA treatment also seemed to increase the levels of total AKT protein.

Phosphorylation of AKT at serine 473 is highly important for the activity of the protein, as well as being implicated in possible interaction with both MDM2 (Ogawara *et al.*,2002; Singh *et al.*,2013)

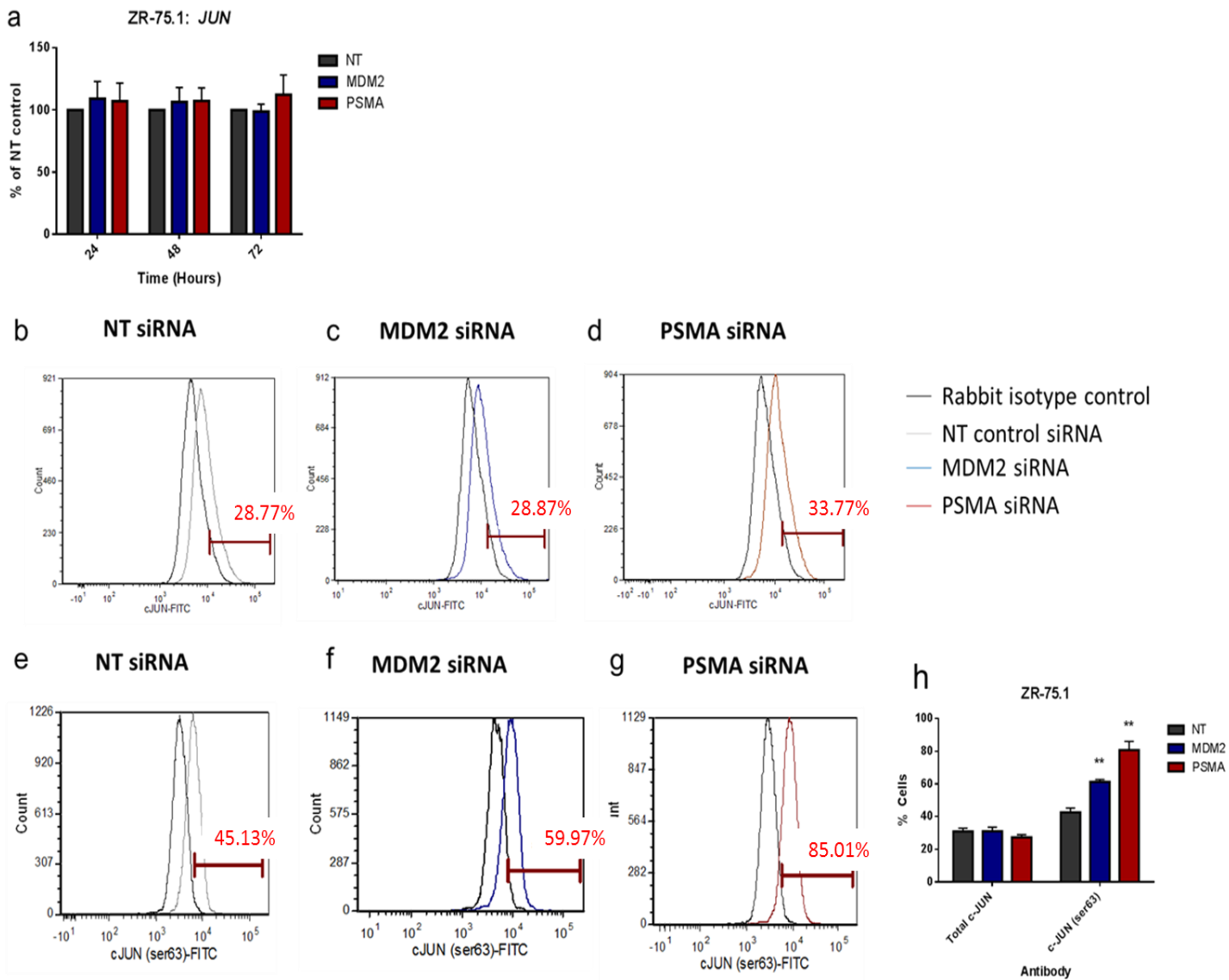


Figure 6.3. JUN gene and c-JUN protein expression and phosphorylation levels following 72 hours of MDM2 and PSMA siRNA treatment ZR-75.1 cells.

a) Gene expression levels of JUN following MDM2, PSMA and NT siRNA treatment (Graph shows % of NT control siRNA-treated cells +SD; each experiment undertaken in triplicate; significant difference calculated by t-test with Welch's correction). b) Flow cytometric analysis of NT control siRNA-treated cell expression of c-JUN total protein. c) Flow cytometric analysis of MDM2 siRNA-treated cell expression of c-JUN total protein. d) Flow cytometric analysis of PSMA siRNA-treated cell expression of cJUN total protein. e) Flow cytometric analysis of NT siRNA-treated cell expression of cJUN phosphorylation at serine 63. f) Flow cytometric analysis of MDM2 siRNA-treated cell expression of cJUN phosphorylation at serine 63. g) Flow cytometric analysis of PSMA siRNA-treated cell expression of cJUN phosphorylation at serine 63. (All flow cytometry graphs show representative data; percentages show cells expressing the protein being assessed). h) Summary of total and phosphorylation (serine 63) c-JUN levels in cells following NT, MDM2 and PSMA siRNA treatment (n=3; Graph shows % of cells expressing cJUN/phosphorylated cJUN (serine 63)+SD; significant difference against NT control calculated by t-test; ** $p < 0.01$).

and PSMA (Guo *et al.*, 2014). Therefore, phosphorylation levels at this site were assessed following knockdown of both MDM2 and PSMA, compared to NT control. Interestingly, western blots of MDA-MB-231 cells treated with the siRNAs showed a modest, yet consistent, decrease in the phosphorylation of AKT at this site following both MDM2 and PSMA siRNA treatment (Figure 6.4b). As the decrease was small when visualised through western blotting, the phosphorylation levels in MDA-MB-231 were also assessed using flow cytometry. This showed that there was indeed a decrease in the percentage of cells with serine 473 phosphorylation after both MDM2 siRNA (15.2%; figure 6.4.c and d) and PSMA siRNA (20.11%; figure 6.4.c and e), compared to the NT control siRNA. When all data were accumulated from $n=3$ experiments, it was seen that the decrease in phosphorylation levels was significant for both MDM2 ($p=0.0162$) and PSMA siRNA ($p=0.0008$) (Figure 6.4f).

When ZR-75.1 cells were treated with MDM2, PSMA or NT siRNA, similar results were seen, with a significant increase in *AKT* transcript levels in cells treated with PSMA siRNA at both 48 ($p=0.0391$) and 72 hours ($p=0.0009$) (Figure 6.5a) and again this increase was seen at protein level through western blotting (Figure 6.5b). As in the MDA-MB-231 cells, levels of phosphorylation at serine 473 were significantly decreased following PSMA siRNA compared to NT control. However, in this cell line it seems that MDM2 siRNA did not have an effect on the phosphorylation levels of this site (Figure 6.5b).

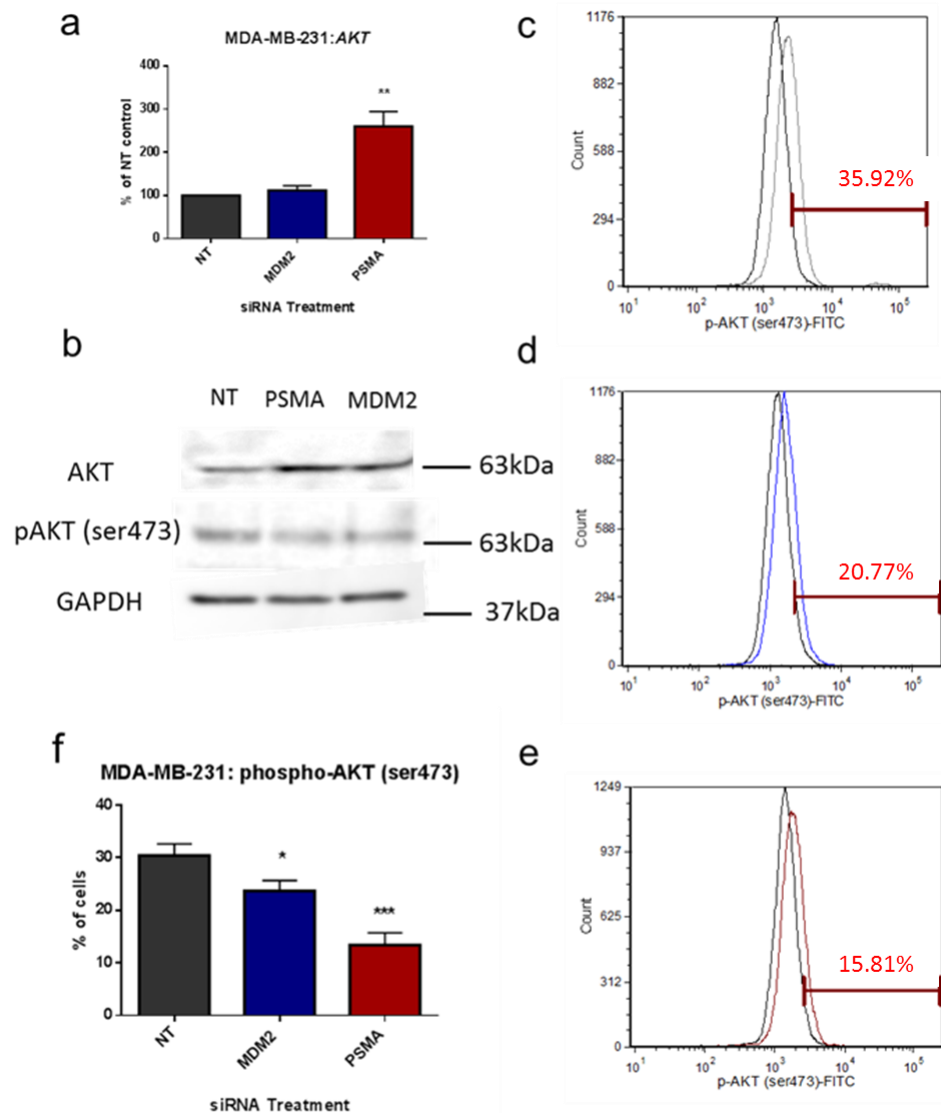


Figure 6.4. AKT gene, protein and phosphorylation levels following 72 hours of MDM2 and PSMA siRNA treatment in MDA-MB-231 cells. a) Gene expression of AKT following MDM2, PSMA and NT siRNA treatment (Graphs show % expression of NT control+SD; each experiment carried out in triplicate; significant difference from NT control calculated by t-test with Welch's correction). b) Western blot of total AKT and phosphorylation levels of AKT at serine 473 following PSMA, MDM2 and NT control siRNA treatment (representative data; n=3). c) Flow cytometric analysis of NT control siRNA-treated cell AKT phosphorylation (serine 473). d) Flow cytometric analysis of MDM2 control siRNA-treated cell AKT phosphorylation (serine 473). e) Flow cytometric analysis of PSMA control siRNA-treated cell AKT phosphorylation (serine 473). (All flow cytometry graphs show representative data; percentages show cells expressing the protein being assessed). f) Summary of phosphorylated (serine 473) AKT levels following NT, MDM2 and PSMA siRNA treatment of cells (n=3; graph shows % of cells expressing phosphorylated AKT (serine 473) +SD; significant difference against NT control calculated by unpaired t-test; * $p < 0.05$; ** $p < 0.01$ and *** $p < 0.001$).

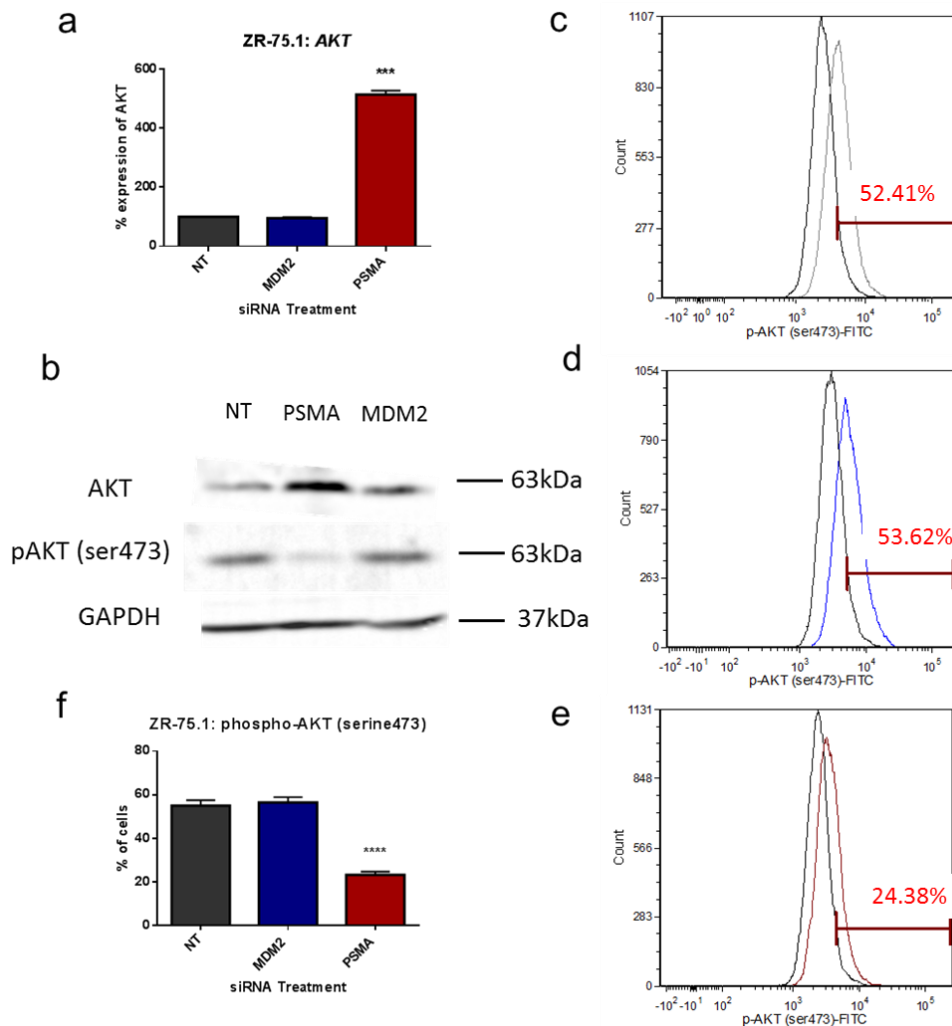


Figure 6.5. AKT gene, protein and phosphorylation levels following 72 hours of MDM2 and PSMA siRNA treatment in ZR-75.1 cells. a) Gene expression of AKT following MDM2, PSMA and NT siRNA treatment (Graphs show % expression of NT control+SD; each experiment carried out in triplicate; significant difference from NT control calculated by t-test with Welch's correction). b) Western blot of total AKT and phosphorylation levels of AKT at serine 473 following PSMA, MDM2 and NT control siRNA treatment (representative data; n=3). c) Flow cytometric analysis of NT control siRNA-treated cell AKT phosphorylation (serine 473). d) Flow cytometric analysis of MDM2 control siRNA-treated cell AKT phosphorylation (serine 473). e) Flow cytometric analysis of PSMA control siRNA-treated cell AKT phosphorylation (serine 473). (All flow cytometry graphs show representative data; percentages show cells expressing the protein being assessed). f) Summary of phosphorylated (serine 473) AKT levels following NT, MDM2 and PSMA siRNA treatment of cells (n=3; graph shows % of cells expressing p-AKT (serine 473) +SD; significant difference against NT control calculated by unpaired t-test; *** $p < 0.001$ and **** $p < 0.0001$).

These levels were checked using flow cytometry and, interestingly, it was seen that MDM2 siRNA shows no difference in phosphorylation of AKT at serine 473 compared to NT siRNA in the ZR-75.1 cell line (Figure 6.5c and d). However, PSMA siRNA treatment was confirmed to show a significant decrease in phosphorylation levels compared to the NT siRNA (28%; Figure 6.5c and e). When three repeats of this experiment were analysed, the decrease in phosphorylation at serine 473 on AKT was seen to be highly significant in ZR-75.1 harbouring PSMA knockdown ($p < 0.0001$).

Phosphorylation of MDM2 at serines 186 and 188 following MDM2 and PSMA knockdown in breast cancer cell lines

Due to recent advancement in the literature showing that AKT may be involved in the phosphorylation of MDM2 at serines 186 and 188, western blots were undertaken in order to ascertain whether any difference in the phosphorylation levels of these sites following each of the siRNA treatment. Also, a specific serine 188 antibody does not exist and so a process of elimination had to be undertaken by using an antibody which recognises both serine 186 and 188 and one which recognises serine 186 alone.

As expected, MDM2 siRNA treatment of both cell lines leads to a decrease in the level of phosphorylation at both sites. However, strikingly, probing of cell lysates with the serine186/188 antibody showed a decrease in phosphorylation following PSMA siRNA treatment, but with the serine 186 antibody showed no decrease

(Figure 6.6a and b). This leads to the surmising that PSMA is involved in the phosphorylation of MDM2 at site 188, possibly through its effect on AKT phosphorylation at serine 473 (Figure 6.6c).

The effect of a PI3K inhibitor on gene levels of MDM2, PSMA and the MMPs in breast cancer cell lines

Since PI3K is known to be important in the phosphorylation of AKT at serine 473 (Scheid *et al.*, 2002), a PI3K inhibitor (LY 294002) was used in order to indirectly also inhibit phosphorylation at this site. Transcript levels were assessed following 24 hours of treatment with either LY 294002 or its control (LY 303511), in both MDA-MB-231 or ZR-75.1 cells. As expected, since the inhibitor works at protein level, transcript levels of *AKT* were unchanged between the inhibitor and control treated cells (Figure 6.7a). Interestingly, a significant decrease in *MDM2* (MDA-MB-231: $p=0.0111$; ZR-75.1: $p=0.0036$) and *PSMA* gene expression (MDA-MB-231: $p=0.0042$; ZR-75.1: $p=0.0082$) (Figure 6.7b and c). Assessment of *MMP2* levels showed a significant decrease following treatment with the inhibitor, compared to control (MDA-MD-231: $p=0.0129$; ZR-75.1 $p=0.0262$) (Figure 6.7d), whereas *MMP8* transcript was unchanged compared to the control (Figure 6.7e).

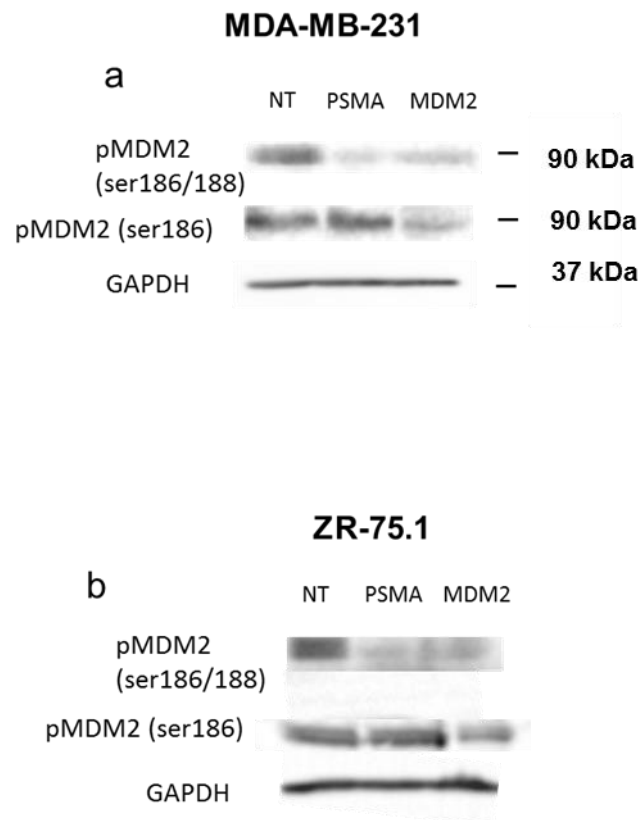


Figure 6.6. Phosphorylation of MDM2 at serines 186 and 188 following 72 hours of MDM2 and PSMA siRNA treatment in MDA-MB-231 and ZR-75.1 cells. a) Western blot showing phosphorylation of MDM2 at serine 186/188 and serine 186 alone following NT, PSMA and MDM2 siRNA treatment in MDA-MB-231 cells . b) Western blot showing phosphorylation of MDM2 at serine 186/188 and serine 186 alone following NT, PSMA and MDM2 siRNA treatment in ZR-75.1 cells. (All data representative; n=3).

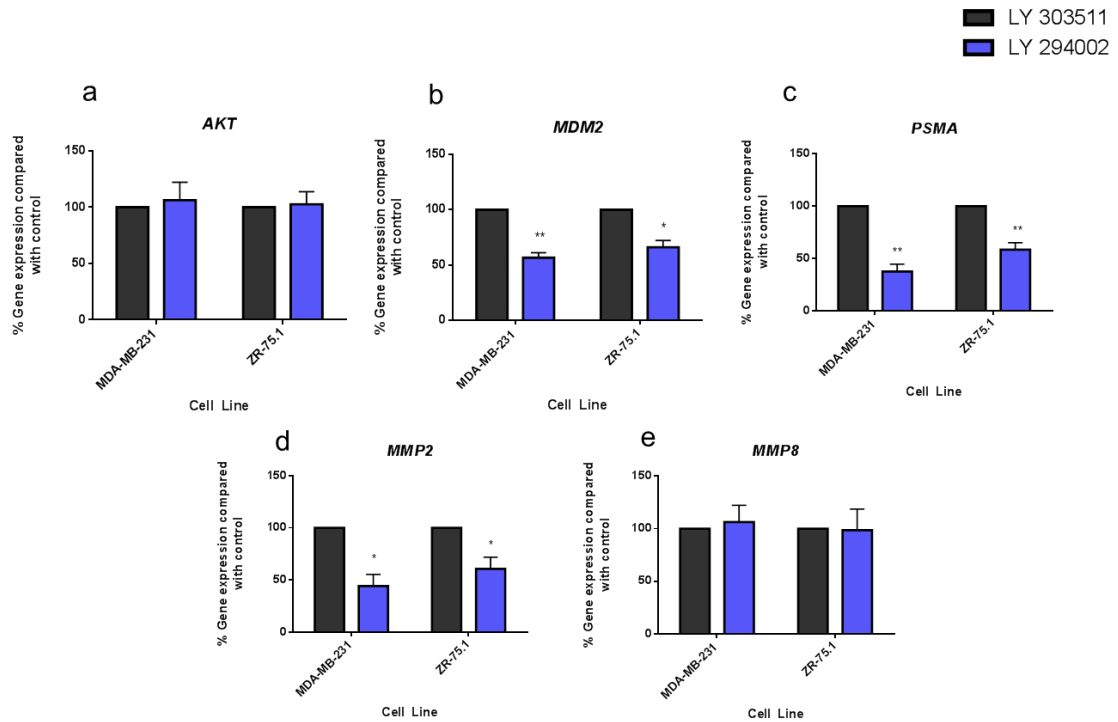


Figure 6.7. The effect of 50 μ M LY 294002 hydrochloride or LY 303511 on gene levels of MDM2, PSMA and the MMPs in MDA-MB-231 and ZR-75.1 cells. Transcript levels following 24 hour 50 μ M AKT inhibitor (LY 294002) treatment: a) *AKT*. b) *MDM2*. c) *PSMA*. d) *MMP2*. e) *MMP8*. f. (All graphs show % of LY 303511 control + SD; n=3) (Statistical significance assessed using unpaired t-test with Welch's correction, with * $p \leq 0.05$ and ** $p \leq 0.01$).

6.4. Discussion

Whilst an understanding of the functionality of cells and how particular molecules affect this is important in the study of cancer, the real purpose of cancer studies is to disentangle the molecular mechanisms involved which result in this functionality. In this way, therapeutics can be specifically designed for the targeting of different types of molecular dysregulation.

Following a Genemania search of MDM2, PSMA and the MMPs which were shown to be downregulated following MDM2 and PSMA siRNA treatment (MMP2 and MMP8), c-JUN was highlighted as a possible checkpoint between each of the molecules. Therefore, gene and protein levels were assessed in MDA-MB-231 and ZR-75.1 cells following MDM2 and PSMA knockdown. Gene levels were seen to be unchanged after each of the treatment, compared to the NT control siRNA treatment. Flow cytometry was then used to assess the protein levels of c-JUN, as well as phosphorylation levels at serine 63.

c-JUN

c-JUN

Both cell lines showed no difference in total c-JUN levels; however, varying results were seen between the two cell lines concerning phosphorylation levels of c-JUN at serine 63. MDA-MB-231 cells

showed that, following MDM2 siRNA knockdown, c-JUN serine 63 phosphorylation levels were significantly increased but PSMA knockdown showed no difference in phosphorylation levels. However, ZR-75.1 cells showed that both MDM2 and PSMA knockdown led to a significant increase in serine 63 phosphorylation of c-JUN. These results are interesting for a number of reasons. Firstly, c-JUN was previously reported to work in a p53-dependent manner in its regulation of the cell cycle (Dunn et al., 2002), as well as c-JUN being known to play a direct role in regulation of p53 stability and transcriptional activity (Fuchs et al., 1998a, Fuchs et al., 1998b), with one group finding that c-JUN regulates transcription of *p53* negatively through binding to a variant of the AP-1 site in the promoter of *p53* (Schreiber et al., 1999). Moreover, studies have shown that c-JUN null fibroblasts express elevated levels of p53 and their cell cycle defects can be reverted by simultaneous deletion of p53 (Hilberg et al., 1993, Schreiber et al., 1999). The increase in c-JUN serine 63 phosphorylation was seen in cell lines which were both p53 wild-type and mutant, indicating that this upregulation of c-JUN phosphorylation by MDM2 is p53-independent. Since it is known that both c-JUN and MDM2 negatively regulate p53, the decrease in MDM2 levels may lead to an increase in the phosphorylation and thus activation of c-JUN in an attempt to continue the negative regulation of p53, in an attempt to keep the cells alive.

PSMA has previously only been linked to c-JUN N-terminal kinase (JNK) in the prostate cancer cell line LNCaP, with a group reporting

that a decrease in PSMA protein levels in these cells led to a decrease in phosphorylation of JNKs (Huang, 2015). JNKs are proteins which bind to the c-JUN transactivation domain and phosphorylate serine 63 and 73 (Ip and Davies, 1998). Beyond this, however, the topic of a possible interaction of PSMA and c-JUN has not been broached, apart from when the two were suggested for potential interplay in a human functional protein interaction network (Wu et al., 2012). If the fact that these kinases phosphorylate c-JUN is taken into account with the fact that it was reported that PSMA knockdown led to a decrease in phosphorylation of JNK, it would be expected that PSMA decrease would lead to a decrease in the phosphorylation of serine 63 at c-JUN. However, in both breast cell lines studied, this was not seen. MDA-MB-231 cells showed no significant change in phosphorylation at this site and ZR-75.1 showed a significant increase in serine 63 phosphorylation.

It is important to remember that the work linking PSMA and JNKs was undertaken in prostate cancer and, more importantly, LNCaP cells which are hormone-dependent, meaning that they are still sensitive to androgen treatment. c-JUN has been shown to interact with androgen receptor (AR) (Bubulya et al., 1996, Bubulya et al., 2000, Chen et al., 2006, Tinzl et al., 2013) and JNKs interact with androgens (Lozena and Saatcioglu, 2008). Moreover, PSMA and AR have been shown to be concomitantly downregulated following androgen deprivation by one group studying LNCaP cells (Liu et al., 2012b), while in other cells lines (VCaP and derived forms) PSMA levels

were seen to increase following androgen deprivation therapy.

Therefore, applying this study in an androgen-dependent cell line to the wider field of cancer, especially when it concerns molecules which have previously been linked to the androgen receptor and shown sensitivity to androgen therapy in the past, is something we must be careful of.

Another reason the upregulation seen in c-JUN phosphorylation following the knockdown of MDM2 and PSMA in breast cancer cell lines is interesting, is that c-JUN is known to have an involvement in the progression of cancers (Vleugel et al., 2006; Zhang et al., 2007), with its overexpression being reported in human cancers, as well as *in vitro* cell studies correlating c-JUN with a more tumourigenic, invasive phenotype (Smith et al, 1999). With this, it may be sensible to infer that the phosphorylation of serine 63, which causes activation of c-JUN protein, would also lead to this more aggressive phenotype. However, we have seen that this increased phosphorylation of serine 63 of c-JUN occurs following knockdown of two pro-oncogenes, MDM2 and PSMA, which are both known to be involved in the progressive properties of cancer (Bradbury et al., 2016, Dassie et al, 2014, Guo et al., 2014, Chen et al, 2013, Yang et al., 2006). This seems like a paradoxical state of events, when it may be natural, with all the evidence to hand, to assume that knockdown of MDM2 and PSMA would lead to a decrease in the phosphorylation of c-JUN at serine 63. This could indicate that serine 63 phosphorylation does not play an important role in this scenario, with other effectors of

MDM2 and PSMA playing a more significant role and dampening the phenotypic effect of this activation, or that serine 63 phosphorylation may play an anti-cancer role which is, as of yet, undiscovered. The latter theory is not wholly far-fetched as, although most reports show c-JUN in a tumour contributory role, there are some which show that it may have alternative roles working against tumour formation. One study highlighted the role of c-JUN in preventing promoter methylation of p16INK4a, a tumour suppressor, leading to a prevention of gene silencing (Kollmann et al., 2011). Another report claimed that tylophorine, a plant-derived alkaloid with anti-tumoural activity, may act through c-JUN (Yang et al., 2013).

One point to take into consideration in terms of this phosphorylation at serine 63 on c-JUN, is that, since siRNA was used for the knockdown of MDM2 and PSMA, it is unknown for how long this phosphorylation occurs. Phosphorylation can be transient or longer sustained and it is important to remember that the increase observed could, in fact, be a highly transient increase seen around the 72 hour mark, perhaps in an attempt to rebalance cellular signalling following knockdown of an important molecule to cellular homeostasis.

To further understand the increased phosphorylation of c-JUN, it would also be interesting to assess the role of serine 73, another important phosphorylation site of c-JUN (Ip & Davis, 1998), following each knockdown.

AKT

Another potential interactor of both MDM2 and PSMA is AKT. One study reported that, through its effect on the phosphorylation of MDM2 at serine 166 and 186, the PI3K/AKT pathway is able to promote nuclear entry of MDM2, leading to diminished levels of p53. Furthermore, they found that mutants of these phosphorylation sites in MDM2 are unable to enter the nuclear and therefore increase p53 activity (Mayo & Donner, 2001). However, this was contested by another group, who claimed that AKT phosphorylation of serine 186 showed no effect on subcellular localisation of MDM2 but did increase the ubiquitination and therefore degradation of p53. Using immunoprecipitation, this group found that MDM2 and AKT directly associate in MCF-7 cells under serum-free conditions (Ogawara *et al.*, 2002). This could imply that it is the phosphorylation by AKT at serine 166 which is the important site for localisation of MDM2 to the nucleus. Another group suggested that AKT can be destructed in a p53-dependent manner suggesting, with reports of AKT negatively regulating p53 levels through MDM2 phosphorylation taken into account, that AKT may be involved in a feedback loop involving MDM2 and p53.

Most importantly for this study, however, other groups have found that AKT phosphorylates serine 188 of MDM2. The first study claims that AKT inhibits MDM2 self-ubiquitination through phosphorylation of serine 166 and 188, implying that phosphorylated AKT (serine 473) plays an important role in regulating MDM2 stability in mouse

embryonic fibroblasts (MEFs) (Feng *et al.*, 2004). A slightly later study highlighted the same phosphorylation sites as interacting with AKT in cancer cell lines MCF-7, OSA and U2OS (Milne *et al.*, 2004). This link between AKT phosphorylation at serine 473 and MDM2 serine 188 is something which has been confirmed within this study.

PSMA has also previously been linked to AKT, with knockdown of PSMA in prostate cancer cell line LNCaP, resulting in a decrease in the phosphorylation of AKT at serine 473, implicating these proteins in a signalling pathway concerning the tumourigenicity of cells, with a decrease in proliferation, migration and cell survival being seen by the group (Guo *et al.*, 2014). Another later study showed the same results (Perico *et al.*, 2016). Again, this link of PSMA knockdown and phosphorylation at AKT serine 473 was exhibited in my own work.

In terms of my own results, in both breast cancer cell lines studied, I found that PSMA knockdown leads to a decrease in phosphorylation of AKT at serine 473. In addition MDA-MB-231 cells also showed a decrease in phosphorylation of this site following MDM2 siRNA treatment, whereas ZR-75.1 cells showed no difference.

In line with previously undertaken studies reported in the literature, MDM2 serine 186/188 phosphorylation was assessed, as well as just serine 186 (MDM2 serine 166 had already been studied in earlier work) and it was seen that PSMA knockdown also led to a decrease in the phosphorylation of serine 186/188, but showed no change when cell lysates were probed with an antibody specific for serine

186, implicating PSMA in the phosphorylation of MDM2 serine 188. This directly links PSMA knockdown to phosphorylation of MDM2 at serine 188, possibly through phosphorylation of AKT at serine 473, and a schematic was drawn up to illustrate the potential link between the proteins, as shown in the literature and my own work (Figure 6.8).

Interestingly, when total AKT levels were assessed through western blotting, MDA-MB-231 cell showed an increase in protein levels in both MDM2 and PSMA siRNA treated cells. However, ZR-75.1 showed an increase in total AKT levels following just PSMA knockdown. This increase in total AKT falls in line with the decrease in phosphorylated AKT in each cell line. This increase in total protein could be an attempt by the cell to restabilise AKT levels when activity of the molecule through phosphorylation of serine 473 is decreased.

To further link AKT to MDM2, PSMA and MMPs, an inhibitor of PI3K was used in order to indirectly inhibit the phosphorylation of AKT at serine 473 (Scheid et al., 2002). Gene expression was assessed following treatment of MDA-MB-231 and ZR-75.1 cell with either this inhibitor of PI3K or its control. Interestingly, it was seen that both MDM2 and PSMA levels were decreased following inhibitor treatment. This, again, links the gene expression levels of MDM2 and PSMA, showing that when one is knocked down, so is the other. This could go some way towards explaining why PSMA siRNA decreased *MDM2* transcript levels, when our own data are taken into consideration. However, it does not explain why both cell lines tested would show a decrease in *PSMA* following MDM2 siRNA

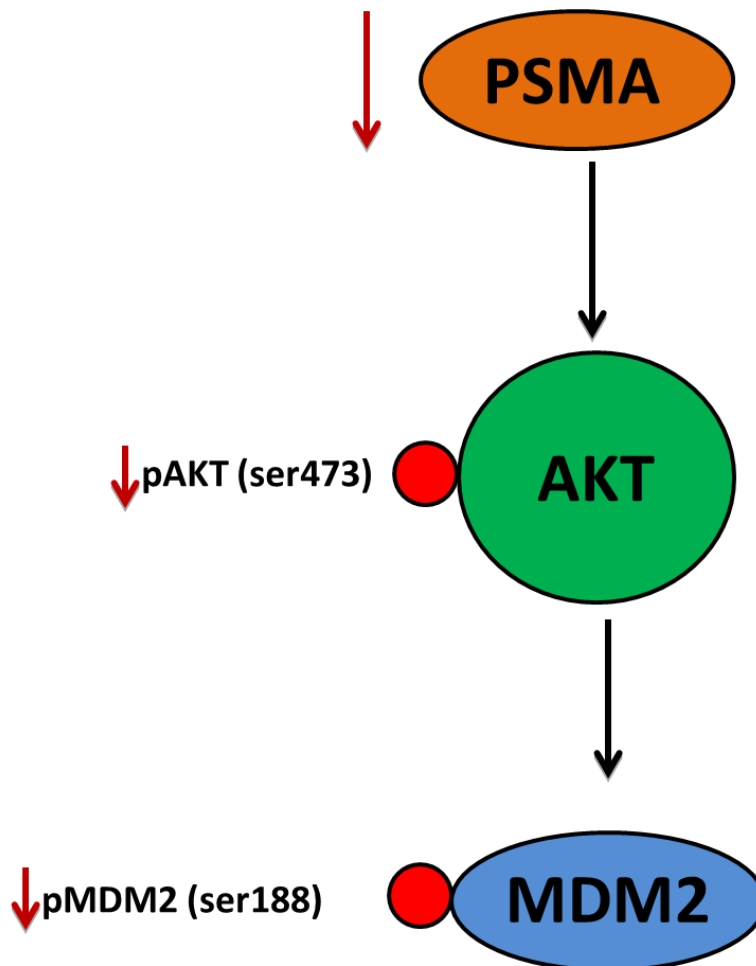


Figure 6.8. Schematic diagram showing the possible interplay between PSMA, phosphorylated AKT (serine 473) and phosphorylated MDM2 (serine 188). Illustrates the potential interplay between the molecules, as indicates by my own data and that in the literature. It may be that PSMA knockdown leads to a decrease in the phosphorylation of AKT at serine 473 (Guo *et al.*, 2014) and decreased phosphorylation of this residue on AKT leads to a decrease in phosphorylation of serine 188 on MDM2 (Feng *et al.*, 2004; Milne *et al.*, 2004).

treatment, since only MDA-MB-231 cells show a decrease in serine 473 phosphorylation following MDM2 knockdown.

In addition, assessment of *MMP2* and *MMP8* gene expression levels following this inhibitor treatment showed the same as was seen from both knockdowns at transcript level, with *MMP2* showing a significant decrease compared to the control, but *MMP8* levels showing no difference. This similar gene pattern could link AKT to the differences seen in MMP protein levels following MDM2 and PSMA siRNA treatment.

It is important to remember that the inhibitor used was not specific to the phosphorylation site serine 473, it inhibited the activity of PI3K, and so results are showing the effects on gene level from inhibiting this kinase, not solely the inhibition of phosphorylation at serine 473. As a start point, however, it is an interesting study and linked phosphorylation inhibition of AKT to a decrease in *MDM2*, *PSMA* and *MMP2* gene expression.

Therefore, this chapter shows that PSMA knockdown leads to a decrease in serine 473 phosphorylation on AKT and with this a decrease in MDM2 serine 188 phosphorylation. In addition, c-JUN phosphorylation at serine 63 was shown to increase following MDM2 knockdown in both cell lines and following PSMA knockdown in ZR-75.1 cells.

Chapter VII

Final Discussion

PSMA overexpression is observed in the neovasculature of solid tumours but not in that of normal tissues (Kasperzyk *et al.*, 2013). In addition, increased PSMA expression is positively associated with tumour stage and grade, although its function in cancer remains unclear (Chang *et al.*, 2004). MDM2 is a negative regulator of tumour suppressor p53 (Lahav, 2008) but also plays p53-independent roles in the cell (Ganguli and Wasyluk, 2003, Thomasova *et al.*, 2012). Both proteins have been considered as biomarkers and therapeutic targets for advanced solid tumours. Additionally, MDM2 and PSMA have been shown to play an important role in the progression of breast cancer (Turbin *et al.*, 2005; Jiang *et al.*, 1997; Ross *et al.*, 2003; Perner *et al.*, 2007).

A recent study showed that knockdown of PSMA led to a decrease in *MDM2* gene expression levels, as well as changes to *MMP2*, *MMP3* and *MMP13* transcript levels (Xu *et al.*, 2013). Both MDM2 and PSMA have also been linked to the regulation of MMPs (Conway *et al.*, 2013; Zhao *et al.*, 2012; Yang *et al.*, 2006; Rajabi *et al.*, 2012; Chen *et al.*, 2013; Cheng *et al.*, 2014). In addition, the PI3K-AKT pathway has been linked to the MDM2, PSMA and the MMPs (Parks *et al.*, 2001; Thant *et al.*, 2001; Zhang *et al.*, 2003; Kim *et al.*, 2001; Liotta & Kohn, 2000; Suzuki *et al.*, 2004). Notably, it has been shown that PSMA knockdown in prostate cancer cell lines leads to a decrease of phosphorylation at serine 473 on AKT (Guo *et al.*, 2014), whilst the phosphorylation state of MDM2 is known to be regulated by AKT phosphorylation, although the site on MDM2 which is

phosphorylated by AKT is still unclear, as different reports suggest varying sites (Ogawara *et al.*, 2002; Feng *et al.*, 2004; Ashcroft *et al.*, 2002; Mayo & Donner, 2001; Zhou *et al.*, 2001). Therefore, we hypothesised that MDM2, PSMA and AKT form a pathway which results in regulation of the MMPs in breast cancer cell lines.

Following the choice of MDA-MB-231 and ZR-75.1 cell lines, MDM2 and PSMA were effectively knocked down in both cell lines. In these breast cancer cell lines, transcript levels of *MDM2* were seen to decrease following PSMA siRNA treatment, which echoes what Xu *et al.*, (2013) observed in the prostate cancer cell line, LNCaP.

Interestingly, we also found that the *PSMA* transcript level was decreased following MDM2 siRNA treatment, which has not before been reported. However, this decrease was not replicated at protein level. Interestingly, transcript levels of *MDM2* were seen to decrease following PSMA siRNA and *PSMA* transcript levels were decreased following MDM2 siRNA treatment. This falls in line with what Xu *et al.* (2013) saw in the prostate cancer cell line, LNCaP. However, this decrease was not replicated at protein level.

A decrease was seen in proliferative, adhesive, migratory and invasive capacity, following each knockdown in both cell lines. In addition, a decrease in serine 473 phosphorylation of AKT was seen when PSMA was knocked down, shown through both western blotting and flow cytometric analysis. This is similar to what has already been seen in prostate cancer cells by two groups, with each claiming that PSMA is able to activate AKT through phosphorylation

at serine 473 (Perico *et al.*, 2016; Guo *et al.*, 2014). Interestingly, the decrease in phosphorylation at this site was linked to an increase in the total levels of AKT in the cells. To gain a better understanding of this and why it occurs, further work would need to be undertaken. Following this, assessment of MDM2 phosphorylation sites following knockdown of both MDM2 and PSMA showed a decrease in phosphorylation at serine 188 after both knockdowns, but no change at serine 166 or 186. A decrease in phosphorylation at this site following PSMA knockdown was very interesting and implicated the two proteins in a pathway, with AKT phosphorylation being a possible link between them. Phosphorylation of MDM2 at serine 188 by AKT has already been shown in mouse embryonic fibroblasts (MEFs) (Feng *et al.*, 2004) and a range of cancer cell lines (Milne *et al.*, 2004). Now our work has highlighted this link in two metastatic breast cancer cell lines, whilst also showing that PSMA knockdown can cause a decrease in phosphorylation at serine 473 on AKT.

As already mentioned, AKT has been linked to the regulation and production of MMP2, MMP9 and MT1-MMP (Parks *et al.*, 2001; Thant *et al.*, 2001; Zhang *et al.*, 2003; Kim *et al.*, 2001; Liotta & Kohn, 2000; Suzuki *et al.*, 2004). Assessment of MMP secretion from breast cancer cells with MDM2 or PSMA knockdown showed a decrease in MMP2 and MMP8, with ZR-75.1 also showing a decrease in MMP9. This could implicate this pathway in the regulation, production and secretion of MMPs by MDM2, PSMA and AKT seen in previous

literature (Chen *et al.*, 2013; Zhang *et al.*, 2014; Rajabi *et al.*, 2012; Zhao *et al.*, 2012; Conway *et al.*, 2013).

This change in MMP levels, especially MMP2, explains why a decrease in migration, invasion and adhesion was seen in cells with knockdown of MDM2 and PSMA (Bauvois, 2012, Jezierska and Motyl, 2009).

Additionally, c-JUN may link MDM2 and PSMA activity as predicted by the search tool GeneMANIA. Interestingly, knockdown of MDM2 led to an increase in c-JUN phosphorylation at serine 63, but conveyed no effect on total protein levels. PSMA knockdown also showed an increase in c-JUN phosphorylation at serine 63, but only in one of the cell lines tested. This is against what would be expected from cells with knockdown of known pro-angiogenic proteins since c-JUN phosphorylation at serine 63 activates the molecule (Li *et al.*, 2004). This leads to a cellular ability to promote proliferation and decrease angiogenesis (Vleugel *et al.*, 2006).

AKT is also implicated in cell proliferation and survival (Lawlor and Alessi, 2001), with the protein driving cell proliferation and inhibiting apoptosis.

Proliferation of cells was seen to decrease following a knockdown of both MDM2 and PSMA proteins, which is what we would expect from AKT serine 473 phosphorylation decrease, but not from c-JUN serine 63 increase. Apoptosis data showed a significant increase in only the early stages of apoptosis following MDM2 knockdown. However,

late stage apoptosis may also be expected to increase and live cells decrease. The increase in c-JUN phosphorylation may account for this, leading to less of a dramatic change than would be expected. In addition, the results gained from the cell cycle assay are varied between cell lines after PSMA knockdown and this may be due to the difference in an increase in serine 63 phosphorylation of c-JUN between the two cell lines. It may be important to also assess the phosphorylation levels of serine 73, which is also implicated in the activation of c-JUN (Li *et al.*, 2004).

Clinically, since both MDM2 and PSMA are implicated as therapeutic targets, this signalling data could be highly important and may highlight why clinical trials involving these proteins have so far not been hugely successful.

A link between these two proteins is an important step forward in this area of research, as a more exact understanding of the interplay between them, AKT and MMPs, which are all therapeutic targets, could lead to a dual targeting with drugs which hadn't before been considered.

In conclusion, the main and novel finding of this study was that, in metastatic breast cancer cell lines, PSMA knockdown leads to a decrease in AKT phosphorylation at serine 473, and also a decrease in MDM2 phosphorylation at serine 188. Knockdown of both MDM2 and PSMA leads to similar phenotypes in terms of growth, migration, invasion and adhesion which may be due to this pathway. In

addition, each of the knockdowns leads to a decrease of MMP2 and MMP8 in both cell lines tested, which could also be due to both of the protein's involvement in this pathway. This work could also implicate MDM2 serine 188 as an important phosphorylation site on the protein and this must be further investigated.

Future work

Since it seems that PSMA knockdown leads to a decrease in AKT serine 473 phosphorylation, it is important that future work addresses how this occurs. It is not known currently if PSMA holds kinase activity and so it may act through a kinase which is known to work upstream of AKT.

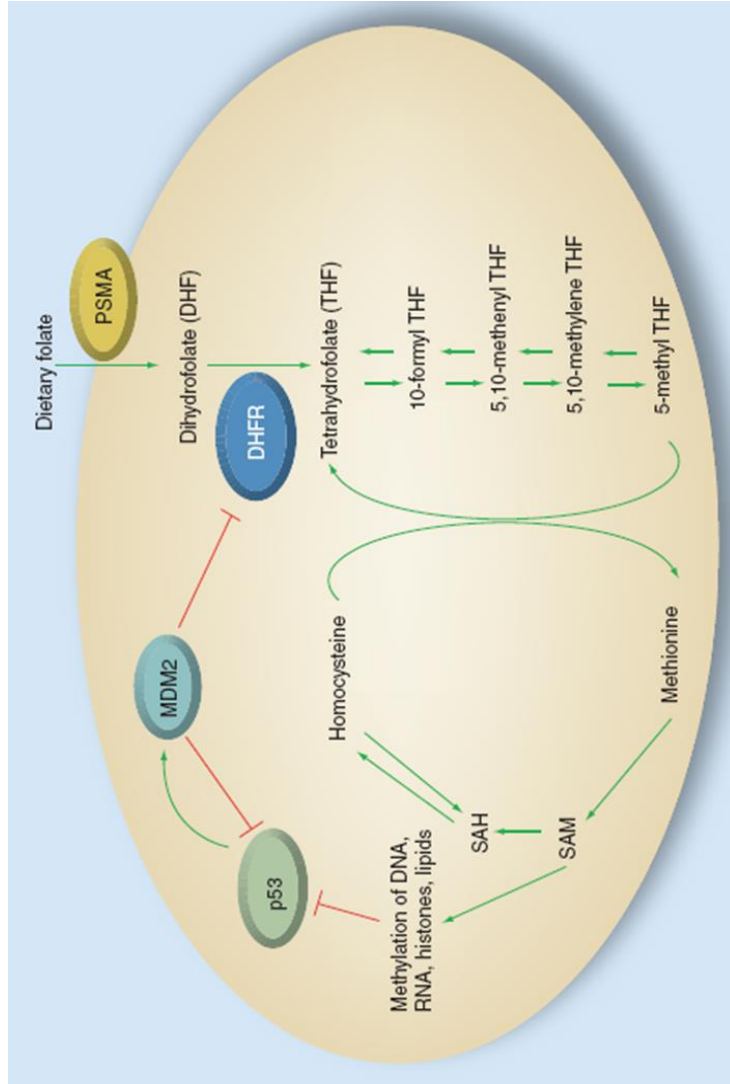
It would also be important to assess the levels of MDM2 serine 188 following a decrease in serine 473 phosphorylation of AKT, perhaps through use of an inhibitor, allowing us to assess if there is a true link between phosphorylation statuses of each of the proteins.

In addition, since this work has suggested that MDM2 serine 188 may play a role in a pathway downstream of AKT and the importance of phosphorylation of MDM2 at serine 188 in terms of functionality of cells could be investigated using cells harbouring MDM2 with a mutation at this site, leading to no phosphorylation of serine 188 being able to occur. This would allow us to investigate how important phosphorylation of this site is to the functionality of cells and secretion of MMPs.

It may also be interesting to investigate how MDM2 and PSMA may further interplay in folate metabolism, via their interactions with DHFR (Samplaski et al., 2011, Pinto et al., 1996) (Figure 7.1) and how they may fit into the schematic including VEGF and HIF1 (Figure 7.2).

In terms of a wider clinical implication, the potential use of PSMA-targeting drugs in breast cancer could be a highly useful as these drugs have already been developed and undergone clinical trials for prostate cancer. Additionally, the functional implications of PSMA in breast cancer cell shows that it is an important molecule in the malignancy of breast cancer, and further investigation of this may lead to the use of PSMA as a biomarker or a therapy in breast cancer.

Thus far, the targeting of MDM2 and AKT in cancer cells has not yielded as significant results as we may have expected and the discovery of this pathway and the subsequent targeting of one or more of the molecules within it, may lead to more encouraging results.



7.1. Hypothesised MDM2 and PSMA interaction through folate metabolism in aggressive tumours.

PSMA metabolises dietary folate to produce dihydrofolate (DHF), which is then converted to tetrahydrofolate (THF) by dihydrofolate reductase (DHFR). DHFR is regulated by MDM2 through its RING-finger dependent E3 ubiquitin ligase activity, which is known to also regulate the p53 tumour suppressor. p53 is regulated by methylation of DNA, RNA, histone and lipids, which is governed by folate metabolism. Therefore, we hypothesise that in cancer cells, PSMA may be involved in the expression of activity of MDM2 through aberrant regulation of p53 methylation via folate metabolism. (Taken from Bradbury *et al.*, 2015.)

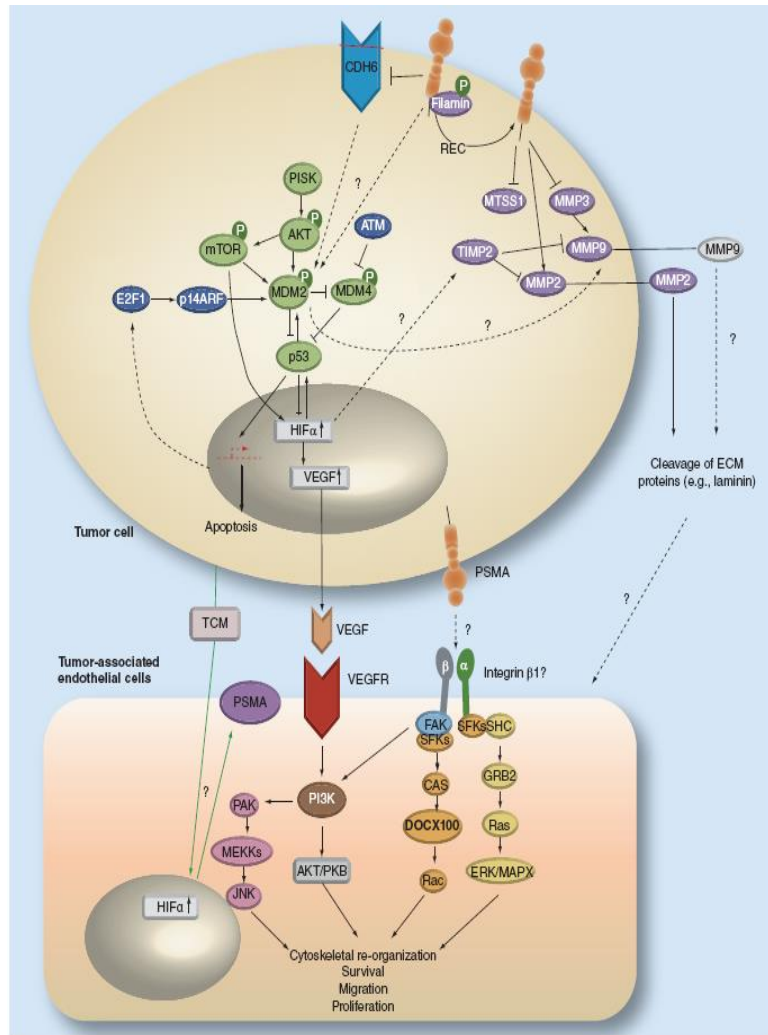


Figure 7.2. Proposed interplay roles of MDM2 and PSMA in tumour invasion and metastasis through multiple signalling pathways. MDM2 and PSMA have both been linked to MMP2 and MMP9. HIF-1 α is known to regulate the MMP inhibitor, TIMP-1. Since MDM2 activates HIF-1 α , both PSMA and MDM2 may play a role in MMP regulation in hypoxia. MDM2 inactivates p53 which is known to suppression transcription of VEGF. The PI3K and PAK pathways in endothelial cells can be activated directly by VEGF and indirectly by PSMA through binding with integrin. Therefore, MDM2 and PSMA may mediate angiogenesis which could permit the exertion of a synergetic pro-angiogenic effect between the proteins. (Taken from Bradbury *et al.*, 2015).

Reference List

- ADORNO, M., CORDENONSI, M., MONTAGNER, M., DUPONT, S., WONG, C., HANN, B., SOLARI, A., BOBISSE, S., RONDINA, M. B., GUZZARDO, V., PARENTI, A. R., ROSATO, A., BICCIATO, S., BALMAIN, A. & PICCOLO, S. 2009. A Mutant-p53/Smad complex opposes p63 to empower TGFbeta-induced metastasis. *Cell*, 137, 87-98.
- AGARWAL, M. L., AGARWAL, A., TAYLOR, W. R. & STARK, G. R. 1995. p53 controls both the G2/M and the G1 cell cycle checkpoints and mediates reversible growth arrest in human fibroblasts. *Proc Natl Acad Sci U S A*, 92, 8493-7.
- AKHTAR, N. H., PAIL, O., SARAN, A., TYRELL, L. & TAGAWA, S. T. 2012. Prostate-specific membrane antigen-based therapeutics. *Adv Urol*, 2012, 973820.
- AL-KURAYA, K., SCHRAML, P., TORHORST, J., TAPIA, C., ZAHARIEVA, B., NOVOTNY, H., SPICHTIN, H., MAURER, R., MIRLACHER, M., KOCHLI, O., ZUBER, M., DIETERICH, H., MROSS, F., WILBER, K., SIMON, R. & SAUTER, G. 2004. Prognostic relevance of gene amplifications and coamplifications in breast cancer. *Cancer Res*, 64, 8534-40.
- ALBERGARIA, A., RICARDO, S., MILANEZI, F., CARNEIRO, V., AMENDOEIRA, I., VIEIRA, D., CAMESELLE-TEIJEIRO, J. & SCHMITT, F. 2011. Nottingham Prognostic Index in triple-negative breast cancer: a reliable prognostic tool? *BMC Cancer*, 11, 299.
- ALT, J. R., GREINER, T. C., CLEVELAND, J. L. & EISCHEN, C. M. 2003. Mdm2 haplo-insufficiency profoundly inhibits Myc-induced lymphomagenesis. *EMBO J*, 22, 1442-50.
- ALTOMARE, D. A. & TESTA, J. R. 2005. Perturbations of the AKT signaling pathway in human cancer. *Oncogene*, 24, 7455-64.
- APOLO, A. B., PANDIT-TASKAR, N. & MORRIS, M. J. 2008. Novel tracers and their development for the imaging of metastatic prostate cancer. *J Nucl Med*, 49, 2031-41.
- ASHCROFT, M., LUDWIG, R. L., WOODS, D. B., COPELAND, T. D., WEBER, H. O., MACRAE, E. J. & VOUSDEN, K. H. 2002. Phosphorylation of HDM2 by Akt. *Oncogene*, 21, 1955-62.
- BACIU, P. C., SULEIMAN, E. A., DERYUGINA, E. I. & STRONGIN, A. Y. 2003. Membrane type-1 matrix metalloproteinase (MT1-MMP) processing of pro-alpha v integrin regulates cross-talk between alpha v beta 3 and alpha 2 beta 1 integrins in breast carcinoma cells. *Exp Cell Res*, 291, 167-75.
- BAE, Y. H., RYU, J. H., PARK, H. J., KIM, K. R., WEE, H. J., LEE, O. H., JANG, H. O., BAE, M. K., KIM, K. W. & BAE, S. K. 2013.

- Mutant p53-Notch1 Signaling Axis Is Involved in Curcumin-Induced Apoptosis of Breast Cancer Cells. *Korean J Physiol Pharmacol*, 17, 291-7.
- BANDER, N. H., MILOWSKY, M. I., NANUS, D. M., KOSTAKOGLU, L., VALLABHAJOSULA, S. & GOLDSMITH, S. J. 2005. Phase I trial of ¹⁷⁷lutetium-labeled J591, a monoclonal antibody to prostate-specific membrane antigen, in patients with androgen-independent prostate cancer. *J Clin Oncol*, 23, 4591-601.
- BARKER, C. A. 2015. Radiation Therapy for Cutaneous Melanoma: Clonogenic Assays to Clinical Trials. *Oncology (Williston Park)*, 29, 752, 754.
- BARTEL, F., TAUBERT, H. & HARRIS, L. C. 2002. Alternative and aberrant splicing of MDM2 mRNA in human cancer. *Cancer Cell*, 2, 9-15.
- BATUELLO, C. N., HAUCK, P. M., GENDRON, J. M., LEHMAN, J. A. & MAYO, L. D. 2015. Src phosphorylation converts Mdm2 from a ubiquitinating to a neddylation E3 ligase. *Proc Natl Acad Sci U S A*, 112, 1749-54.
- BAUVOIS, B. 2012. New facets of matrix metalloproteinases MMP2 and MMP9 as cell surface transducers: outside-in signaling and relationship to tumor progression. *Biochim Biophys Acta*, 1825, 29-36.
- BELLACOSA, A., KUMAR, C. C., DI CRISTOFANO, A. & TESTA, J. R. 2005. Activation of AKT kinases in cancer: implications for therapeutic targeting. *Adv Cancer Res*, 94, 29-86.
- BEN JEMAA, A., SALLAMI, S., RAMARLI, D., COLOMBATTI, M. & OUESLATI, R. 2013. The proinflammatory cytokine, IL-6, and its interference with bFGF signaling and PSMA in prostate cancer cells. *Inflammation*, 36, 643-50.
- BERNACKI, K. D., FIELDS, K. L. & ROH, M. H. 2014. The utility of PSMA and PSA immunohistochemistry in the cytologic diagnosis of metastatic prostate carcinoma. *Diagn Cytopathol*, 42, 570-5.
- BERNARD, D., ZHAO, Y. & WANG, S. 2012. AM-8553: a novel MDM2 inhibitor with a promising outlook for potential clinical development. *J Med Chem*, 55, 4934-5.
- BHOWMICK, N. A., NEILSON, E. G. & MOSES, H. L. 2004. Stromal fibroblasts in cancer initiation and progression. *Nature*, 432, 332-7.
- BINDER, B. R. 2007. A novel application for murine double minute 2 antagonists: the p53 tumor suppressor network also controls angiogenesis. *Circ Res*, 100, 13-4.
- BOICE, J. D., JR., PRESTON, D., DAVIS, F. G. & MONSON, R. R. 1991. Frequent chest X-ray fluoroscopy and breast cancer incidence among tuberculosis patients in Massachusetts. *Radiat Res*, 125, 214-22.
- BOS, R., VAN DIEST, P. J., DE JONG, J. S., VAN DER GROEP, P., VAN DER VALK, P. & VAN DER WALL, E. 2005. Hypoxia-inducible factor-1alpha is associated with angiogenesis, and

- expression of bFGF, PDGF-BB, and EGFR in invasive breast cancer. *Histopathology*, 46, 31-6.
- BOSTWICK, D. G. 1998. Practical clinical application of predictive factors in prostate cancer. A review with an emphasis on quantitative methods in tissue specimens. *Anal Quant Cytol Histol*, 20, 323-42.
- BOSTWICK, D. G., PACELLI, A., BLUTE, M., ROCHE, P. & MURPHY, G. P. 1998. Prostate specific membrane antigen expression in prostatic intraepithelial neoplasia and adenocarcinoma: a study of 184 cases. *Cancer*, 82, 2256-61.
- BOUCK, N. 1996. P53 and angiogenesis. *Biochim Biophys Acta*, 1287, 63-6.
- BOUSKA, A. & EISCHEN, C. M. 2009. Mdm2 affects genome stability independent of p53. *Cancer Res*, 69, 1697-701.
- BOZZUTO, G., RUGGIERI, P. & MOLINARI, A. 2010. Molecular aspects of tumor cell migration and invasion. *Ann Ist Super Sanita*, 46, 66-80.
- BRADBURY, R., JIANG, W. G. & CUI, Y. X. 2015. The clinical and therapeutic uses of MDM2 and PSMA and their potential interaction in aggressive cancers. *Biomark Med*, 9, 1353-70.
- BRADBURY, R., JIANG, W. G. & CUI, Y. X. 2016. MDM2 and PSMA Play Inhibitory Roles in Metastatic Breast Cancer Cells Through Regulation of Matrix Metalloproteinases. *Anticancer Res*, 36, 1143-51.
- BREKMAN, A., SINGH, K. E., POLOTSKAIA, A., KUNDU, N. & BARGONETTI, J. 2011. A p53-independent role of Mdm2 in estrogen-mediated activation of breast cancer cell proliferation. *Breast Cancer Res*, 13, R3.
- BRIGHENTI, E., CALABRESE, C., LIGUORI, G., GIANNONE, F. A., TRERE, D., MONTANARO, L. & DERENZINI, M. 2014. Interleukin 6 downregulates p53 expression and activity by stimulating ribosome biogenesis: a new pathway connecting inflammation to cancer. *Oncogene*, 33, 4396-406.
- BRINTON, L. A., HOOVER, R. & FRAUMENI, J. F., JR. 1983. Reproductive factors in the aetiology of breast cancer. *Br J Cancer*, 47, 757-62.
- BRINTON, L. A., SCHAIRER, C., HOOVER, R. N. & FRAUMENI, J. F., JR. 1988. Menstrual factors and risk of breast cancer. *Cancer Invest*, 6, 245-54.
- BROOKS, C. L. & GU, W. 2003. Ubiquitination, phosphorylation and acetylation: the molecular basis for p53 regulation. *Curr Opin Cell Biol*, 15, 164-71.
- BROSH, R. & ROTTER, V. 2009. When mutants gain new powers: news from the mutant p53 field. *Nat Rev Cancer*, 9, 701-13.
- BROWN, D. R., THOMAS, C. A. & DEB, S. P. 1998. The human oncoprotein MDM2 arrests the cell cycle: elimination of its cell-cycle-inhibitory function induces tumorigenesis. *EMBO J*, 17, 2513-25.
- BRUNET, A., DATTA, S. R. & GREENBERG, M. E. 2001. Transcription-dependent and -independent control of neuronal

- survival by the PI3K-Akt signaling pathway. *Curr Opin Neurobiol*, 11, 297-305.
- BRYAN, T. M. & CECH, T. R. 1999. Telomerase and the maintenance of chromosome ends. *Curr Opin Cell Biol*, 11, 318-24.
- BRYAN, T. M., ENGLEZOU, A., GUPTA, J., BACCHETTI, S. & REDDEL, R. R. 1995. Telomere elongation in immortal human cells without detectable telomerase activity. *EMBO J*, 14, 4240-8.
- BUBULYA, A., WISE, S. C., SHEN, X. Q., BURMEISTER, L. A. & SHEMSHEDINI, L. 1996. c-Jun can mediate androgen receptor-induced transactivation. *J Biol Chem*, 271, 24583-9.
- BUBULYA, A., ZHOU, X. F., SHEN, X. Q., FISHER, C. J. & SHEMSHEDINI, L. 2000. c-Jun targets amino terminus of androgen receptor in regulating androgen-responsive transcription. *Endocrine*, 13, 55-62.
- BUESO-RAMOS, C. E., YANG, Y., DELEON, E., MCCOWN, P., STASS, S. A. & ALBITAR, M. 1993. The human MDM-2 oncogene is overexpressed in leukemias. *Blood*, 82, 2617-23.
- BULL, H. A., BRICKELL, P. M. & DOWD, P. M. 1994. Src-related protein tyrosine kinases are physically associated with the surface antigen CD36 in human dermal microvascular endothelial cells. *FEBS Lett*, 351, 41-4.
- BULL, S. B., OZCELIK, H., PINNADUWAGE, D., BLACKSTEIN, M. E., SUTHERLAND, D. A., PRITCHARD, K. I., TZONTCHEVA, A. T., SIDLOFSKY, S., HANNA, W. M., QIZILBASH, A. H., TWEEDDALE, M. E., FINE, S., MCCREADY, D. R. & ANDRULIS, I. L. 2004. The combination of p53 mutation and neu/erbB-2 amplification is associated with poor survival in node-negative breast cancer. *J Clin Oncol*, 22, 86-96.
- BURDALL, S. E., HANBY, A. M., LANSDOWN, M. R. & SPEIRS, V. 2003. Breast cancer cell lines: friend or foe? *Breast Cancer Res*, 5, 89-95.
- BURGER, M. J., TEBAY, M. A., KEITH, P. A., SAMARATUNGA, H. M., CLEMENTS, J., LAVIN, M. F. & GARDINER, R. A. 2002. Expression analysis of delta-catenin and prostate-specific membrane antigen: their potential as diagnostic markers for prostate cancer. *Int J Cancer*, 100, 228-37.
- CAHILLY-SNYDER, L., YANG-FENG, T., FRANCKE, U. & GEORGE, D. L. 1987. Molecular analysis and chromosomal mapping of amplified genes isolated from a transformed mouse 3T3 cell line. *Somat Cell Mol Genet*, 13, 235-44.
- CARTHEW, R. W. & SONTHEIMER, E. J. 2009. Origins and Mechanisms of miRNAs and siRNAs. *Cell*, 136, 642-55.
- CAULIN, C., NGUYEN, T., LANG, G. A., GOEPFERT, T. M., BRINKLEY, B. R., CAI, W. W., LOZANO, G. & ROOP, D. R. 2007. An inducible mouse model for skin cancer reveals distinct roles for gain- and loss-of-function p53 mutations. *J Clin Invest*, 117, 1893-901.

- CHABNER, B. A. & MURPHY, M. J., JR. 2005. Breast cancer: a tale of two centuries: with implications for understanding cancer metastasis and cancer stem cell biology. *Oncologist*, 10, 369.
- CHABNER, B. A. & ROBERTS, T. G., JR. 2005. Timeline: Chemotherapy and the war on cancer. *Nat Rev Cancer*, 5, 65-72.
- CHAKRABORTI, S., MANDAL, M., DAS, S., MANDAL, A. & CHAKRABORTI, T. 2003. Regulation of matrix metalloproteinases: an overview. *Mol Cell Biochem*, 253, 269-85.
- CHAMBERS, A. F. & MATRISIAN, L. M. 1997. Changing views of the role of matrix metalloproteinases in metastasis. *J Natl Cancer Inst*, 89, 1260-70.
- CHANG, H. C., HSU, C., HSU, H. K. & YANG, R. C. 2003. Functional role of caspases in sphingosine-induced apoptosis in human hepatoma cells. *IUBMB Life*, 55, 403-7.
- CHANG, S. S. 2004. Overview of prostate-specific membrane antigen. *Rev Urol*, 6 Suppl 10, S13-8.
- CHANG, S. S., GAUDIN, P. B., REUTER, V. E., O'KEEFE, D. S., BACICH, D. J. & HESTON, W. D. 1999. Prostate-Specific Membrane Antigen: Much More Than a Prostate Cancer Marker. *Mol Urol*, 3, 313-320.
- CHANG, S. S. & HESTON, W. D. 2002. The clinical role of prostate-specific membrane antigen (PSMA). *Urol Oncol*, 7, 7-12.
- CHEN, S. Y., CAI, C., FISHER, C. J., ZHENG, Z., OMWANCHA, J., HSIEH, C. L. & SHEMSHEDINI, L. 2006. c-Jun enhancement of androgen receptor transactivation is associated with prostate cancer cell proliferation. *Oncogene*, 25, 7212-23.
- CHEN, X., QIU, J., YANG, D., LU, J., YAN, C., ZHA, X. & YIN, Y. 2013. MDM2 promotes invasion and metastasis in invasive ductal breast carcinoma by inducing matrix metalloproteinase-9. *PLoS One*, 8, e78794.
- CHEN, Y., DHARA, S., BANERJEE, S. R., BYUN, Y., PULLAMBHATLA, M., MEASE, R. C. & POMPER, M. G. 2009. A low molecular weight PSMA-based fluorescent imaging agent for cancer. *Biochem Biophys Res Commun*, 390, 624-9.
- CHENG, N., CHYTIL, A., SHYR, Y., JOLY, A. & MOSES, H. L. 2008. Transforming growth factor-beta signaling-deficient fibroblasts enhance hepatocyte growth factor signaling in mammary carcinoma cells to promote scattering and invasion. *Mol Cancer Res*, 6, 1521-33.
- CHRISTOFORI, G. & SEMB, H. 1999. The role of the cell-adhesion molecule E-cadherin as a tumour-suppressor gene. *Trends Biochem Sci*, 24, 73-6.
- CIRIELLO, G., SINHA, R., HOADLEY, K. A., JACOBSEN, A. S., REVA, B., PEROU, C. M., SANDER, C. & SCHULTZ, N. 2013. The molecular diversity of Luminal A breast tumours. *Breast Cancer Res and Treat*, 141(3), 409-420

- CLARK, I. M., SWINGLER, T. E., SAMPIERI, C. L. & EDWARDS, D. R. 2008. The regulation of matrix metalloproteinases and their inhibitors. *Int J Biochem Cell Biol*, 40, 1362-78.
- CLEMONS, M., LOIJENS, L. & GOSS, P. 2000. Breast cancer risk following irradiation for Hodgkin's disease. *Cancer Treat Rev*, 26, 291-302.
- COLOMBATTI, M., GRASSO, S., PORZIA, A., FRACASSO, G., SCUPOLI, M. T., CINGARLINI, S., POFPE, O., NAIM, H. Y., HEINE, M., TRIDENTE, G., MAINIERO, F. & RAMARLI, D. 2009. The prostate specific membrane antigen regulates the expression of IL-6 and CCL5 in prostate tumour cells by activating the MAPK pathways. *PLoS One*, 4, e4608.
- CONWAY, R. E., PETROVIC, N., LI, Z., HESTON, W., WU, D. & SHAPIRO, L. H. 2006. Prostate-specific membrane antigen regulates angiogenesis by modulating integrin signal transduction. *Mol Cell Biol*, 26, 5310-24.
- CORDON-CARDO, C., LATRES, E., DROBNJAK, M., OLIVA, M. R., POLLACK, D., WOODRUFF, J. M., MARECHAL, V., CHEN, J., BRENNAN, M. F. & LEVINE, A. J. 1994. Molecular abnormalities of mdm2 and p53 genes in adult soft tissue sarcomas. *Cancer Res*, 54, 794-9.
- COUNTER, C. M., AVILION, A. A., LEFEUVRE, C. E., STEWART, N. G., GREIDER, C. W., HARLEY, C. B. & BACCHETTI, S. 1992. Telomere shortening associated with chromosome instability is arrested in immortal cells which express telomerase activity. *EMBO J*, 11, 1921-9.
- COUSSENS, L. M. & WERB, Z. 1996. Matrix metalloproteinases and the development of cancer. *Chem Biol*, 3, 895-904.
- COWELL, C. F., WEIGELT, B., SAKR, R. A., NG, C. K., HICKS, J., KING, T. A. & REIS-FILHO, J. S. 2013. Progression from ductal carcinoma in situ to invasive breast cancer: revisited. *Mol Oncol*, 7, 859-69.
- DANIELE, S., COSTA, B., ZAPPELLI, E., DA POZZO, E., SESTITO, S., NESI, G., CAMPIGLIA, P., MARINELLI, L., NOVELLINO, E., RAPPOSELLI, S. & MARTINI, C. 2015. Combined inhibition of AKT/mTOR and MDM2 enhances Glioblastoma Multiforme cell apoptosis and differentiation of cancer stem cells. *Sci Rep*, 5, 9956.
- DASSIE, J. P., HERNANDEZ, L. I., THOMAS, G. S., LONG, M. E., ROCKEY, W. M., HOWELL, C. A., CHEN, Y., HERNANDEZ, F. J., LIU, X. Y., WILSON, M. E., ALLEN, L. A., VAENA, D. A., MEYERHOLZ, D. K. & GIANGRANDE, P. H. 2014. Targeted inhibition of prostate cancer metastases with an RNA aptamer to prostate-specific membrane antigen. *Mol Ther*, 22, 1910-22.
- DE ROZIERES, S., MAYA, R., OREN, M. & LOZANO, G. 2000. The loss of mdm2 induces p53-mediated apoptosis. *Oncogene*, 19, 1691-7.
- DEB, S. P., SINGH, S. & DEB, S. 2014. MDM2 overexpression, activation of signaling networks, and cell proliferation. *Subcell Biochem*, 85, 215-34.

- DECOCK, J., HENDRICKX, W., VANLEEuw, U., VAN BELLE, V., VAN HUFFEL, S., CHRISTIAENS, M. R., YE, S. & PARIDAENS, R. 2008. Plasma MMP1 and MMP8 expression in breast cancer: protective role of MMP8 against lymph node metastasis. *BMC Cancer*, 8, 77.
- DENMEADE, S. R., MHAKA, A. M., ROSEN, D. M., BRENNEN, W. N., DALRYMPLE, S., DACH, I., OLESEN, C., GUREL, B., DEMARZO, A. M., WILDING, G., CARDUCCI, M. A., DIONNE, C. A., MOLLER, J. V., NISSEN, P., CHRISTENSEN, S. B. & ISAACS, J. T. 2012. Engineering a prostate-specific membrane antigen-activated tumor endothelial cell prodrug for cancer therapy. *Sci Transl Med*, 4, 140ra86.
- DILLA, T., VELASCO, J. A., MEDINA, D. L., GONZALEZ-PALACIOS, J. F. & SANTISTEBAN, P. 2000. The MDM2 oncoprotein promotes apoptosis in p53-deficient human medullary thyroid carcinoma cells. *Endocrinology*, 141, 420-9.
- DING, Q., ZHANG, Z., LIU, J. J., JIANG, N., ZHANG, J., ROSS, T. M., CHU, X. J., BARTKOVITZ, D., PODLASKI, F., JANSON, C., TOVAR, C., FILIPOVIC, Z. M., HIGGINS, B., GLENN, K., PACKMAN, K., VASSILEV, L. T. & GRAVES, B. 2013. Discovery of RG7388, a potent and selective p53-MDM2 inhibitor in clinical development. *J Med Chem*, 56, 5979-83.
- DISCHER, D. E., JANMEY, P. & WANG, Y. L. 2005. Tissue cells feel and respond to the stiffness of their substrate. *Science*, 310, 1139-43.
- DUNN, C., WILTSHIRE, C., MACLAREN, A. & GILLESPIE, D. A. 2002. Molecular mechanism and biological functions of c-Jun N-terminal kinase signalling via the c-Jun transcription factor. *Cell Signal*, 14, 585-93.
- DUPONT, W. D., PARL, F. F., HARTMANN, W. H., BRINTON, L. A., WINFIELD, A. C., WORRELL, J. A., SCHUYLER, P. A. & PLUMMER, W. D. 1993. Breast cancer risk associated with proliferative breast disease and atypical hyperplasia. *Cancer*, 71, 1258-65.
- EASTON, D. 1999a. Familial risks of cancer. *Eur J Cancer*, 35, 1043-5.
- EASTON, D. F. 1999b. How many more breast cancer predisposition genes are there? *Breast Cancer Res*, 1, 14-7.
- EASTON, D. F. 2002. Familial risks of breast cancer. *Breast Cancer Res*, 4, 179-81.
- EASTON, D. F., BISHOP, D. T., FORD, D. & CROCKFORD, G. P. 1993. Genetic linkage analysis in familial breast and ovarian cancer: results from 214 families. The Breast Cancer Linkage Consortium. *Am J Hum Genet*, 52, 678-701.
- ECKES, B., NISCHT, R. & KRIEG, T. 2010. Cell-matrix interactions in dermal repair and scarring. *Fibrogenesis Tissue Repair*, 3, 4.
- EISCHEN, C. M., WEBER, J. D., ROUSSEL, M. F., SHERR, C. J. & CLEVELAND, J. L. 1999. Disruption of the ARF-Mdm2-p53

- tumor suppressor pathway in Myc-induced lymphomagenesis. *Genes Dev*, 13, 2658-69.
- ELBASHIR, S. M., HARBORTH, J., LENDECKEL, W., YALCIN, A., WEBER, K. & TUSCHL, T. 2001. Duplexes of 21-nucleotide RNAs mediate RNA interference in cultured mammalian cells. *Nature*, 411, 494-8.
- ELLISON, R. C., ZHANG, Y., MCLENNAN, C. E. & ROTHMAN, K. J. 2001. Exploring the relation of alcohol consumption to risk of breast cancer. *Am J Epidemiol*, 154, 740-7.
- ELSASSER-BEILE, U., BUHLER, P. & WOLF, P. 2009. Targeted therapies for prostate cancer against the prostate specific membrane antigen. *Curr Drug Targets*, 10, 118-25.
- ELSTON, C. W. & ELLIS, I. O. 1991. Pathological prognostic factors in breast cancer. I. The value of histological grade in breast cancer: experience from a large study with long-term follow-up. *Histopathology*, 19, 403-10.
- FAKHARZADEH, S. S., TRUSKO, S. P. & GEORGE, D. L. 1991. Tumorigenic potential associated with enhanced expression of a gene that is amplified in a mouse tumor cell line. *EMBO J*, 10, 1565-9.
- FALATO, C., TOBIN, N. P., LORENT, J., LINDSTROM, L. S., BERGH, J. & FOUKAKIS, T. 2016. Intrinsic subtypes and genomic signatures of primary breast cancer and prognosis after systemic relapse. *Mol Oncol*, 10, 517-25.
- FAN, C., OH, D. S., WESSELS, L., WEIGELT, B., NUYTEN, D. S., NOBEL, A. B., VAN'T VEER, L. J. & PEROU, C. M. 2006. Concordance among gene-expression-based predictors for breast cancer. *N Engl J Med*, 355, 560-9.
- FANG, S., JENSEN, J. P., LUDWIG, R. L., VOUSDEN, K. H. & WEISSMAN, A. M. 2000. Mdm2 is a RING finger-dependent ubiquitin protein ligase for itself and p53. *J Biol Chem*, 275, 8945-51.
- FANJUL-FERNANDEZ, M., FOLGUERAS, A. R., CABRERA, S. & LOPEZ-OTIN, C. 2010. Matrix metalloproteinases: evolution, gene regulation and functional analysis in mouse models. *Biochim Biophys Acta*, 1803, 3-19.
- FENG, J., PARK, J., CRON, P., HESS, D. & HEMMINGS, B. A. 2004a. Identification of a PKB/Akt hydrophobic motif Ser-473 kinase as DNA-dependent protein kinase. *J Biol Chem*, 279, 41189-96.
- FENG, J., TAMASKOVIC, R., YANG, Z., BRAZIL, D. P., MERLO, A., HESS, D. & HEMMINGS, B. A. 2004b. Stabilization of Mdm2 via decreased ubiquitination is mediated by protein kinase B/Akt-dependent phosphorylation. *J Biol Chem*, 279, 35510-7.
- FERLAY, J., FORMAN, D., MATHERS, C. D. & BRAY, F. 2012. Breast and cervical cancer in 187 countries between 1980 and 2010. *Lancet*, 379, 1390-1.
- FINLAY, C. A. 1993. The mdm-2 oncogene can overcome wild-type p53 suppression of transformed cell growth. *Mol Cell Biol*, 13, 301-6.

- FISHER, D. T., APPENHEIMER, M. M. & EVANS, S. S. 2014. The two faces of IL-6 in the tumor microenvironment. *Semin Immunol*, 26, 38-47.
- FOLKMAN, J. & HANAHAN, D. 1991. Switch to the angiogenic phenotype during tumorigenesis. *Princess Takamatsu Symp*, 22, 339-47.
- FOSS, C. A., MEASE, R. C., FAN, H., WANG, Y., RAVERT, H. T., DANNALS, R. F., OLSZEWSKI, R. T., HESTON, W. D., KOZIKOWSKI, A. P. & POMPER, M. G. 2005. Radiolabeled small-molecule ligands for prostate-specific membrane antigen: in vivo imaging in experimental models of prostate cancer. *Clin Cancer Res*, 11, 4022-8.
- FRANTZ, C., STEWART, K. M. & WEAVER, V. M. 2010. The extracellular matrix at a glance. *J Cell Sci*, 123, 4195-200.
- FREED-PASTOR, W. A., MIZUNO, H., ZHAO, X., LANGEROD, A., MOON, S. H., RODRIGUEZ-BARRUECO, R., BARSOTTI, A., CHICAS, A., LI, W., POLOTSKAIA, A., BISSELL, M. J., OSBORNE, T. F., TIAN, B., LOWE, S. W., SILVA, J. M., BORRESEN-DALE, A. L., LEVINE, A. J., BARGONETTI, J. & PRIVES, C. 2012. Mutant p53 disrupts mammary tissue architecture via the mevalonate pathway. *Cell*, 148, 244-58.
- FREED-PASTOR, W. A. & PRIVES, C. 2012. Mutant p53: one name, many proteins. *Genes Dev*, 26, 1268-86.
- FREEDMAN, D. A., EPSTEIN, C. B., ROTH, J. C. & LEVINE, A. J. 1997. A genetic approach to mapping the p53 binding site in the MDM2 protein. *Mol Med*, 3, 248-59.
- FRUM, R. & DEB, S. P. 2003. Flow cytometric analysis of MDM2-mediated growth arrest. *Methods Mol Biol*, 234, 257-67.
- FUCHS, S. Y., ADLER, V., BUSCHMANN, T., YIN, Z., WU, X., JONES, S. N. & RONAI, Z. 1998a. JNK targets p53 ubiquitination and degradation in nonstressed cells. *Genes Dev*, 12, 2658-63.
- FUCHS, S. Y., ADLER, V., PINCUS, M. R. & RONAI, Z. 1998b. MEKK1/JNK signaling stabilizes and activates p53. *Proc Natl Acad Sci U S A*, 95, 10541-6.
- FYNAN, T. M. & REISS, M. 1993. Resistance to inhibition of cell growth by transforming growth factor-beta and its role in oncogenesis. *Crit Rev Oncog*, 4, 493-540.
- GALSKY, M. D., EISENBERGER, M., MOORE-COOPER, S., KELLY, W. K., SLOVIN, S. F., DELACRUZ, A., LEE, Y., WEBB, I. J. & SCHER, H. I. 2008. Phase I trial of the prostate-specific membrane antigen-directed immunoconjugate MLN2704 in patients with progressive metastatic castration-resistant prostate cancer. *J Clin Oncol*, 26, 2147-54.
- GANGULI, G. & WASYLYK, B. 2003. p53-independent functions of MDM2. *Mol Cancer Res*, 1, 1027-35.
- GASCHE, J. A., HOFFMANN, J., BOLAND, C. R. & GOEL, A. 2011. Interleukin-6 promotes tumorigenesis by altering DNA methylation in oral cancer cells. *International Journal of Cancer*, 129, 1053-1063.

- GHOSH, A. & HESTON, W. D. 2004. Tumor target prostate specific membrane antigen (PSMA) and its regulation in prostate cancer. *J Cell Biochem*, 91, 528-39.
- GHOSH, A., WANG, X., KLEIN, E. & HESTON, W. D. 2005. Novel role of prostate-specific membrane antigen in suppressing prostate cancer invasiveness. *Cancer Res*, 65, 727-31.
- GIALELI, C., THEOCHARIS, A. D. & KARAMANOS, N. K. 2011. Roles of matrix metalloproteinases in cancer progression and their pharmacological targeting. *FEBS J*, 278, 16-27.
- GIANCOTTI, F. G. & RUOSLAHTI, E. 1999. Integrin signaling. *Science*, 285, 1028-32.
- GOTTLIEB, T. M., LEAL, J. F., SEGER, R., TAYA, Y. & OREN, M. 2002. Cross-talk between Akt, p53 and Mdm2: possible implications for the regulation of apoptosis. *Oncogene*, 21, 1299-303.
- GRAEBER, T. G., OSMANIAN, C., JACKS, T., HOUSMAN, D. E., KOCH, C. J., LOWE, S. W. & GIACCIA, A. J. 1996. Hypoxia-mediated selection of cells with diminished apoptotic potential in solid tumours. *Nature*, 379, 88-91.
- GRANT, C. L., CAROMILE, L. A., HO, V., DURRANI, K., RAHMAN, M. M., CLAFFEY, K. P., FONG, G. H. & SHAPIRO, L. H. 2012. Prostate specific membrane antigen (PSMA) regulates angiogenesis independently of VEGF during ocular neovascularization. *PLoS One*, 7, e41285.
- GRASBERGER, B. L., LU, T., SCHUBERT, C., PARKS, D. J., CARVER, T. E., KOBLISH, H. K., CUMMINGS, M. D., LAFRANCE, L. V., MILKIEWICZ, K. L., CALVO, R. R., MAGUIRE, D., LATTANZE, J., FRANKS, C. F., ZHAO, S., RAMACHANDREN, K., BYLEBYL, G. R., ZHANG, M., MANTHEY, C. L., PETRELLA, E. C., PANTOLIANO, M. W., DECKMAN, I. C., SPURLINO, J. C., MARONEY, A. C., TOMCZUK, B. E., MOLLOY, C. J. & BONE, R. F. 2005. Discovery and cocrystal structure of benzodiazepinedione HDM2 antagonists that activate p53 in cells. *J Med Chem*, 48, 909-12.
- GREEN, S., WALTER, P., GREENE, G., KRUST, A., GOFFIN, C., JENSEN, E., SCRACE, G., WATERFIELD, M. & CHAMBON, P. 1986. Cloning of the human oestrogen receptor cDNA. *J Steroid Biochem*, 24, 77-83.
- GUDAS, J. M., NGUYEN, H., KLEIN, R. C., KATAYOSE, D., SETH, P. & COWAN, K. H. 1995. Differential expression of multiple MDM2 messenger RNAs and proteins in normal and tumorigenic breast epithelial cells. *Clin Cancer Res*, 1, 71-80.
- GUDKOV, A. V. & KOMAROVA, E. A. 2003. The role of p53 in determining sensitivity to radiotherapy. *Nat Rev Cancer*, 3, 117-29.
- GUO, Z., HUANG, H., ZENG, L., DU, T., XU, K., LIN, T., JIANG, C., DONG, W., CAO, Y., CHEN, J., ZHONG, W. & HUANG, J. 2011. Lentivirus-mediated RNAi knockdown of prostate-specific membrane antigen suppresses growth, reduces

- migration ability and the invasiveness of prostate cancer cells. *Med Oncol*, 28, 878-87.
- GUO, Z., LAI, Y., DU, T., ZHANG, Y., CHEN, J., BI, L., LIN, T., LIU, H., WANG, W., XU, K., JIANG, C., HAN, J., ZHANG, C., DONG, W., HUANG, J. & HUANG, H. 2014. Prostate specific membrane antigen knockdown impairs the tumorigenicity of LNCaP prostate cancer cells by inhibiting the phosphatidylinositol 3-kinase/Akt signaling pathway. *Chin Med J (Engl)*, 127, 929-36.
- GUSTERSON, B. A. & STEIN, T. 2012. Human breast development. *Semin Cell Dev Biol*, 23, 567-73.
- GUTH, U., HUANG, D. J., DIRNHOFER, S., ROCHLITZ, C. & WIGHT, E. 2009. Distant metastatic breast cancer as an incurable disease: a tenet with a need for revision. *Cancer J*, 15, 81-6.
- HAFFNER, M. C., KRONBERGER, I. E., ROSS, J. S., SHEEHAN, C. E., ZITT, M., MUHLMANN, G., OFNER, D., ZELGER, B., ENSINGER, C., YANG, X. J., GELEY, S., MARGREITER, R. & BANDER, N. H. 2009. Prostate-specific membrane antigen expression in the neovasculature of gastric and colorectal cancers. *Hum Pathol*, 40, 1754-61.
- HALDOSEN, L. A., ZHAO, C. & DAHLMAN-WRIGHT, K. 2014. Estrogen receptor beta in breast cancer. *Mol Cell Endocrinol*, 382, 665-72.
- HALSTED, C. H., LING, E. H., LUTHI-CARTER, R., VILLANUEVA, J. A., GARDNER, J. M. & COYLE, J. T. 1998. Folylpoly-gamma-glutamate carboxypeptidase from pig jejunum. Molecular characterization and relation to glutamate carboxypeptidase II. *J Biol Chem*, 273, 20417-24.
- HANAHAN, D. & FOLKMAN, J. 1996. Patterns and emerging mechanisms of the angiogenic switch during tumorigenesis. *Cell*, 86, 353-64.
- HANAHAN, D. & WEINBERG, R. A. 2000. The hallmarks of cancer. *Cell*, 100, 57-70.
- HANAHAN, D. & WEINBERG, R. A. 2011. Hallmarks of cancer: the next generation. *Cell*, 144, 646-74.
- HARRIS, C. C. 1996a. p53 tumor suppressor gene: at the crossroads of molecular carcinogenesis, molecular epidemiology, and cancer risk assessment. *Environ Health Perspect*, 104 Suppl 3, 435-9.
- HARRIS, C. C. 1996b. p53 tumor suppressor gene: from the basic research laboratory to the clinic--an abridged historical perspective. *Carcinogenesis*, 17, 1187-98.
- HARRIS, C. C. 1996c. Structure and function of the p53 tumor suppressor gene: clues for rational cancer therapeutic strategies. *J Natl Cancer Inst*, 88, 1442-55.
- HAUPT, Y., MAYA, R., KAZAZ, A. & OREN, M. 1997. Mdm2 promotes the rapid degradation of p53. *Nature*, 387, 296-9.

- HAY, T. J. & MEEK, D. W. 2000. Multiple sites of in vivo phosphorylation in the MDM2 oncoprotein cluster within two important functional domains. *FEBS Lett*, 478, 183-6.
- HAYFLICK, L. 1997. Mortality and immortality at the cellular level. A review. *Biochemistry (Mosc)*, 62, 1180-90.
- HEARNE, B. J., TEARE, M. D., BUTT, M. & DONALDSON, L. 2015. Comparison of Nottingham Prognostic Index and Adjuvant Online prognostic tools in young women with breast cancer: review of a single-institution experience. *BMJ Open*, 5, e005576.
- HEMMINGS, B. A. & RESTUCCIA, D. F. 2015. The PI3K-PKB/Akt pathway. *Cold Spring Harb Perspect Biol*, 7.
- HIDESHIMA, T., SHINOHARA, T., BABA, M. & SHIRAKUSA, T. 1997. The expression of MDM2 and p53 protein breast carcinoma. *Oncol Rep*, 4, 297-300.
- HILBERG, F., AGUZZI, A., HOWELLS, N. & WAGNER, E. F. 1993. c-jun is essential for normal mouse development and hepatogenesis. *Nature*, 365, 179-81.
- HILLIER, S. M., MARESCA, K. P., FEMIA, F. J., MARQUIS, J. C., FOSS, C. A., NGUYEN, N., ZIMMERMAN, C. N., BARRETT, J. A., ECKELMAN, W. C., POMPER, M. G., JOYAL, J. L. & BABICH, J. W. 2009. Preclinical evaluation of novel glutamate-urea-lysine analogues that target prostate-specific membrane antigen as molecular imaging pharmaceuticals for prostate cancer. *Cancer Res*, 69, 6932-40.
- HOLLIDAY, D. L. & SPEIRS, V. 2011. Choosing the right cell line for breast cancer research. *Breast Cancer Res*, 13, 215.
- HONDA, R., TANAKA, H. & YASUDA, H. 1997. Oncoprotein MDM2 is a ubiquitin ligase E3 for tumor suppressor p53. *FEBS Lett*, 420, 25-7.
- HONDA, R. & YASUDA, H. 1999. Association of p19(ARF) with Mdm2 inhibits ubiquitin ligase activity of Mdm2 for tumor suppressor p53. *EMBO J*, 18, 22-7.
- HONG, M., LAI, M. D., LIN, Y. S. & LAI, M. Z. 1999. Antagonism of p53-dependent apoptosis by mitogen signals. *Cancer Res*, 59, 2847-52.
- HORI, M., SHIMAZAKI, J., INAGAWA, S., ITABASHI, M. & HORI, M. 2002. Overexpression of MDM2 oncoprotein correlates with possession of estrogen receptor alpha and lack of MDM2 mRNA splice variants in human breast cancer. *Breast Cancer Res Treat*, 71, 77-83.
- HOROSZEWICZ, J. S., KAWINSKI, E. & MURPHY, G. P. 1987. Monoclonal antibodies to a new antigenic marker in epithelial prostatic cells and serum of prostatic cancer patients. *Anticancer Res*, 7, 927-35.
- HOWLADER, N., ALTEKRUSE, S. F., LI, C. I., CHEN, V. W., CLARKE, C. A., RIES, L. A. & CRONIN, K. A. 2014. US incidence of breast cancer subtypes defined by joint hormone receptor and HER2 status. *J Natl Cancer Inst*, 106.

- HUANG, H., WANG, H.E., LAI, Y., ZHANG, Y., DONG, W., GUO, Z., LIN, T., HUANG, J & DU, T. 2015. Study of PI3K/AKT Pathway on Prostate Cancer Cell Proliferation, Apoptosis and Migration Regulated by PSMA. *Sun Yat-Sen University*.
- HUI, L., ZHENG, Y., YAN, Y., BARGONETTI, J. & FOSTER, D. A. 2006. Mutant p53 in MDA-MB-231 breast cancer cells is stabilized by elevated phospholipase D activity and contributes to survival signals generated by phospholipase D. *Oncogene*, 25, 7305-10.
- HUSSEIN, M. Z., AL FIKKY, A., ABDEL BAR, I. & ATTIA, O. 2004. Serum IL-6 and IL-12 levels in breast cancer patients. *Egypt J Immunol*, 11, 165-70.
- HYNES, R. O. 2009. The extracellular matrix: not just pretty fibrils. *Science*, 326, 1216-9.
- HYNES, R. O. & WAGNER, D. D. 1996. Genetic manipulation of vascular adhesion molecules in mice. *J Clin Invest*, 98, 2193-5.
- IOZZO, R. V., ZOELLER, J. J. & NYSTROM, A. 2009. Basement membrane proteoglycans: modulators Par Excellence of cancer growth and angiogenesis. *Mol Cells*, 27, 503-13.
- IP, Y. T. & DAVIS, R. J. 1998. Signal transduction by the c-Jun N-terminal kinase (JNK)--from inflammation to development. *Curr Opin Cell Biol*, 10, 205-19.
- IVAN, M., KONDO, K., YANG, H., KIM, W., VALIANDO, J., OHH, M., SALIC, A., ASARA, J. M., LANE, W. S. & KAELIN, W. G., JR. 2001. HIFalpha targeted for VHL-mediated destruction by proline hydroxylation: implications for O₂ sensing. *Science*, 292, 464-8.
- IWAKUMA, T. & LOZANO, G. 2003. MDM2, an introduction. *Mol Cancer Res*, 1, 993-1000.
- JAAKKOLA, P., MOLE, D. R., TIAN, Y. M., WILSON, M. I., GIELBERT, J., GASKELL, S. J., VON KRIEGSHEIM, A., HEBESTREIT, H. F., MUKHERJI, M., SCHOFIELD, C. J., MAXWELL, P. H., PUGH, C. W. & RATCLIFFE, P. J. 2001. Targeting of HIF-alpha to the von Hippel-Lindau ubiquitylation complex by O₂-regulated prolyl hydroxylation. *Science*, 292, 468-72.
- JACKSON, M. W. & BERBERICH, S. J. 2000. MdmX protects p53 from Mdm2-mediated degradation. *Mol Cell Biol*, 20, 1001-7.
- JAVED, A. & LTEIF, A. 2013. Development of the human breast. *Semin Plast Surg*, 27, 5-12.
- JEMAL, A., BRAY, F., CENTER, M. M., FERLAY, J., WARD, E. & FORMAN, D. 2011. Global cancer statistics. *CA Cancer J Clin*, 61, 69-90.
- JENSEN, E. V., CHENG, G., PALMIERI, C., SAJI, S., MAKELA, S., VAN NOORDEN, S., WAHLSTROM, T., WARNER, M., COOMBES, R. C. & GUSTAFSSON, J. A. 2001. Estrogen receptors and proliferation markers in primary and recurrent breast cancer. *Proc Natl Acad Sci U S A*, 98, 15197-202.

- JESINGER, R. A. 2014. Breast anatomy for the interventionalist. *Tech Vasc Interv Radiol*, 17, 3-9.
- JEZIERSKA, A. & MOTYL, T. 2009. Matrix metalloproteinase-2 involvement in breast cancer progression: a mini-review. *Med Sci Monit*, 15, RA32-40.
- JIANG, M., SHAO, Z. & ZHANG, Y. 1997. [Study on p53, mdm-2 and p21WAF1 protein expression in ER-positive and ER-negative human breast cancer cell lines and its relation to biological features]. *Zhonghua Bing Li Xue Za Zhi*, 26, 327-30.
- JOENSUU, K., LEIDENIUS, M., KERO, M., ANDERSSON, L. C., HORWITZ, K. B. & HEIKKILA, P. 2013. ER, PR, HER2, Ki-67 and CK5 in Early and Late Relapsing Breast Cancer-Reduced CK5 Expression in Metastases. *Breast Cancer (Auckl)*, 7, 23-34.
- JONES, R. G. & THOMPSON, C. B. 2009. Tumor suppressors and cell metabolism: a recipe for cancer growth. *Genes Dev*, 23, 537-48.
- JONES, S. N., ROE, A. E., DONEHOWER, L. A. & BRADLEY, A. 1995. Rescue of embryonic lethality in Mdm2-deficient mice by absence of p53. *Nature*, 378, 206-8.
- JOSHI, S., SINGH, A. R. & DURDEN, D. L. 2014. MDM2 regulates hypoxic hypoxia-inducible factor 1alpha stability in an E3 ligase, proteasome, and PTEN-phosphatidylinositol 3-kinase-AKT-dependent manner. *J Biol Chem*, 289, 22785-97.
- KASPERZYK, J. L., FINN, S. P., FLAVIN, R., FIORENTINO, M., LIS, R., HENDRICKSON, W. K., CLINTON, S. K., SESSO, H. D., GIOVANNUCCI, E. L., STAMPFER, M. J., LODA, M. & MUCCI, L. A. 2013. Prostate-specific membrane antigen protein expression in tumor tissue and risk of lethal prostate cancer. *Cancer Epidemiol Biomarkers Prev*, 22, 2354-63.
- KATO, S., PINTO, M., CARVAJAL, A., ESPINOZA, N., MONSO, C., SADARANGANI, A., VILLALON, M., BROSENS, J. J., WHITE, J. O., RICHER, J. K., HORWITZ, K. B. & OWEN, G. I. 2005. Progesterone increases tissue factor gene expression, procoagulant activity, and invasion in the breast cancer cell line ZR-75-1. *J Clin Endocrinol Metab*, 90, 1181-8.
- KENNECKE, H., YERUSHALMI, R., WOODS, R., CHEANG, M. C., VODUC, D., SPEERS, C. H., NIELSEN, T. O. & GELMON, K. 2010. Metastatic behavior of breast cancer subtypes. *J Clin Oncol*, 28, 3271-7.
- KESSENBROCK, K., PLAKS, V. & WERB, Z. 2010. Matrix metalloproteinases: regulators of the tumor microenvironment. *Cell*, 141, 52-67.
- KIM, K., BURGHARDT, R., BARHOUMI, R., LEE, S. O., LIU, X. & SAFE, S. 2011a. MDM2 regulates estrogen receptor alpha and estrogen responsiveness in breast cancer cells. *J Mol Endocrinol*, 46, 67-79.
- KIM, S. H., TURNBULL, J. & GUIMOND, S. 2011b. Extracellular matrix and cell signalling: the dynamic cooperation of integrin,

- proteoglycan and growth factor receptor. *J Endocrinol*, 209, 139-51.
- KIMBUNG, S., LOMAN, N. & HEDENFALK, I. 2015. Clinical and molecular complexity of breast cancer metastases. *Semin Cancer Biol*, 35, 85-95.
- KIRKIN, V., CAHUZAC, N., GUARDIOLA-SERRANO, F., HUAULT, S., LUCKERATH, K., FRIEDMANN, E., NOVAC, N., WELS, W. S., MARTOGLIO, B., HUEBER, A. O. & ZORNIG, M. 2007. The Fas ligand intracellular domain is released by ADAM10 and SPPL2a cleavage in T-cells. *Cell Death Differ*, 14, 1678-87.
- KOHN, E. C. & LIOTTA, L. A. 1995. Molecular insights into cancer invasion: strategies for prevention and intervention. *Cancer Res*, 55, 1856-62.
- KOLLMANN, K., HELLER, G. & SEXL, V. 2011. c-JUN prevents methylation of p16(INK4a) (and Cdk6): the villain turned bodyguard. *Oncotarget*, 2, 422-7.
- KONECNY, G. E., WILSON, C. A. & SLAMON, D. J. 2003. Is there a role for epidermal growth factor receptor inhibitors in breast cancer prevention? *J Natl Cancer Inst*, 95, 1813-5.
- KOSHIKAWA, N., GIANNELLI, G., CIRULLI, V., MIYAZAKI, K. & QUARANTA, V. 2000. Role of cell surface metalloprotease MT1-MMP in epithelial cell migration over laminin-5. *J Cell Biol*, 148, 615-24.
- KULAR, J. K., BASU, S. & SHARMA, R. I. 2014. The extracellular matrix: Structure, composition, age-related differences, tools for analysis and applications for tissue engineering. *J Tissue Eng*, 5, 2041731414557112.
- KULIK, G., KLIPPEL, A. & WEBER, M. J. 1997. Antiapoptotic signalling by the insulin-like growth factor I receptor, phosphatidylinositol 3-kinase, and Akt. *Mol Cell Biol*, 17, 1595-606.
- LAHAV, G. 2008. Oscillations by the p53-Mdm2 feedback loop. *Adv Exp Med Biol*, 641, 28-38.
- LAI, C. Y., TSAI, A. C., CHEN, M. C., CHANG, L. H., SUN, H. L., CHANG, Y. L., CHEN, C. C., TENG, C. M. & PAN, S. L. 2012. Aciculin induces p53-dependent apoptosis via MDM2 depletion in human cancer cells in vitro and in vivo. *PLoS One*, 7, e42192.
- LANDO, D., PEET, D. J., GORMAN, J. J., WHELAN, D. A., WHITELOW, M. L. & BRUICK, R. K. 2002. FIH-1 is an asparaginyl hydroxylase enzyme that regulates the transcriptional activity of hypoxia-inducible factor. *Genes Dev*, 16, 1466-71.
- LAPIDUS, R. G., TIFFANY, C. W., ISAACS, J. T. & SLUSHER, B. S. 2000. Prostate-specific membrane antigen (PSMA) enzyme activity is elevated in prostate cancer cells. *Prostate*, 45, 350-4.
- LARUSCH, G. A., JACKSON, M. W., DUNBAR, J. D., WARREN, R. S., DONNER, D. B. & MAYO, L. D. 2007. Nutlin3 blocks

- vascular endothelial growth factor induction by preventing the interaction between hypoxia inducible factor 1alpha and Hdm2. *Cancer Res*, 67, 450-4.
- LAU, C. K., YANG, Z. F., LAM, C. T., TAM, K. H., POON, R. T. & FAN, S. T. 2006. Suppression of hypoxia inducible factor-1alpha (HIF-1alpha) by YC-1 is dependent on murine double minute 2 (Mdm2). *Biochem Biophys Res Commun*, 348, 1443-8.
- LAWLOR, M. A. & ALESSI, D. R. 2001. PKB/Akt: a key mediator of cell proliferation, survival and insulin responses? *Journal of Cell Science*, 114, 2903-2910.
- LEE, H. R., TOTH, Z., SHIN, Y. C., LEE, J. S., CHANG, H., GU, W., OH, T. K., KIM, M. H. & JUNG, J. U. 2009. Kaposi's sarcoma-associated herpesvirus viral interferon regulatory factor 4 targets MDM2 to deregulate the p53 tumor suppressor pathway. *J Virol*, 83, 6739-47.
- LEEK, J., LENCH, N., MARAJ, B., BAILEY, A., CARR, I. M., ANDERSEN, S., CROSS, J., WHELAN, P., MACLENNAN, K. A., MEREDITH, D. M. & ET AL. 1995. Prostate-specific membrane antigen: evidence for the existence of a second related human gene. *Br J Cancer*, 72, 583-8.
- LEVINE, A. J. 1997. p53, the cellular gatekeeper for growth and division. *Cell*, 88, 323-31.
- LEVY, A. P., LEVY, N. S. & GOLDBERG, M. A. 1996. Post-transcriptional regulation of vascular endothelial growth factor by hypoxia. *J Biol Chem*, 271, 2746-53.
- LIANG, J. & SLINGERLAND, J. M. 2003. Multiple roles of the PI3K/PKB (Akt) pathway in cell cycle progression. *Cell Cycle*, 2, 339-45.
- LIM, E., METZGER-FILHO, O. & WINER, E. P. 2012. The natural history of hormone receptor-positive breast cancer. *Oncology (Williston Park)*, 26, 688-94, 696.
- LIOTTA, L. A. & KOHN, E. C. 2001. The microenvironment of the tumour-host interface. *Nature*, 411, 375-9.
- LIU, R., SUN, J., ZHANG, Z. & XU, Y. 2012a. Cell-selective gene silencing in prostate cancer LNCap cells using prostate-specific membrane antigen promoter and enhancer in vitro and in vivo. *Cell Biol Int*, 36, 863-72.
- LIU, T., JABBES, M., NEDROW-BYERS, J. R., WU, L. Y., BRYAN, J. N. & BERKMAN, C. E. 2011. Detection of prostate-specific membrane antigen on HUVECs in response to breast tumor-conditioned medium. *Int J Oncol*, 38, 1349-55.
- LIU, T., WU, L. Y., FULTON, M. D., JOHNSON, J. M. & BERKMAN, C. E. 2012b. Prolonged androgen deprivation leads to downregulation of androgen receptor and prostate-specific membrane antigen in prostate cancer cells. *Int J Oncol*, 41, 2087-92.
- LIVAK, K. J. & SCHMITTGEN, T. D. 2001. Analysis of relative gene expression data using real-time quantitative PCR and the 2(-Delta Delta C(T)) Method. *Methods*, 25, 402-8.

- LOFFEK, S., SCHILLING, O. & FRANZKE, C. W. 2011. Series "matrix metalloproteinases in lung health and disease": Biological role of matrix metalloproteinases: a critical balance. *Eur Respir J*, 38, 191-208.
- LOPEZ-OTIN, C. & MATRISIAN, L. M. 2007. Emerging roles of proteases in tumour suppression. *Nat Rev Cancer*, 7, 800-8.
- LORENZO, P. I. & SAATCIOGLU, F. 2008. Inhibition of apoptosis in prostate cancer cells by androgens is mediated through downregulation of c-Jun N-terminal kinase activation. *Neoplasia*, 10, 418-428.
- LU, P., WEAVER, V. M. & WERB, Z. 2012. The extracellular matrix: a dynamic niche in cancer progression. *J Cell Biol*, 196, 395-406.
- LUBET, R., WANG, Y., ZHANG, Z. & YOU, M. 2005. Mouse models incorporating alterations in the major tumor suppressor genes P53 and P16: their use in screening for potential carcinogens, developing further relevant mouse models, and screening for potential chemopreventive and chemotherapeutic agents. *Exp Lung Res*, 31, 117-33.
- LUND, M. J., BUTLER, E. N., HAIR, B. Y., WARD, K. C., ANDREWS, J. H., OPREA-ILIES, G., BAYAKLY, A. R., O'REGAN, R. M., VERTINO, P. M. & ELEY, J. W. 2010. Age/race differences in HER2 testing and in incidence rates for breast cancer triple subtypes: a population-based study and first report. *Cancer*, 116, 2549-59.
- MA, D., HOPF, C. E., MALEWICZ, A. D., DONOVAN, G. P., SENTER, P. D., GOECKELER, W. F., MADDON, P. J. & OLSON, W. C. 2006. Potent antitumor activity of an auristatin-conjugated, fully human monoclonal antibody to prostate-specific membrane antigen. *Clin Cancer Res*, 12, 2591-6.
- MAGUIRE, M., NIELD, P. C., DEVLING, T., JENKINS, R. E., PARK, B. K., POLANSKI, R., VLATKOVIC, N. & BOYD, M. T. 2008. MDM2 regulates dihydrofolate reductase activity through monoubiquitination. *Cancer Res*, 68, 3232-42.
- MAHON, P. C., HIROTA, K. & SEMENZA, G. L. 2001. FIH-1: a novel protein that interacts with HIF-1alpha and VHL to mediate repression of HIF-1 transcriptional activity. *Genes Dev*, 15, 2675-86.
- MALUMBRES, M. & BARBACID, M. 2009. Cell cycle, CDKs and cancer: a changing paradigm. *Nat Rev Cancer*, 9, 153-66.
- MANDAL, D., MOITRA, P. K., SAHA, S. & BASU, J. 2002. Caspase 3 regulates phosphatidylserine externalization and phagocytosis of oxidatively stressed erythrocytes. *FEBS Lett*, 513, 184-8.
- MANFREDI, J. J. 2010. The Mdm2-p53 relationship evolves: Mdm2 swings both ways as an oncogene and a tumor suppressor. *Genes Dev*, 24, 1580-9.
- MANNING, B. D. & CANTLEY, L. C. 2007. AKT/PKB signaling: navigating downstream. *Cell*, 129, 1261-74.

- MARCHETTI, A., BUTTITTA, F., GIRLANDO, S., DALLA PALMA, P., PELLEGRINI, S., FINA, P., DOGLIONI, C., BEVILACQUA, G. & BARBARESCHI, M. 1995. mdm2 gene alterations and mdm2 protein expression in breast carcinomas. *J Pathol*, 175, 31-8.
- MARINO-ENRIQUEZ, A., HORNICK, J. L., DAL CIN, P., CIBAS, E. S. & QIAN, X. 2014. Dedifferentiated liposarcoma and pleomorphic liposarcoma: a comparative study of cytomorphology and MDM2/CDK4 expression on fine-needle aspiration. *Cancer Cytopathol*, 122, 128-37.
- MARKOWITZ, S., WANG, J., MYEROFF, L., PARSONS, R., SUN, L., LUTTERBAUGH, J., FAN, R. S., ZBOROWSKA, E., KINZLER, K. W., VOGELSTEIN, B. & ET AL. 1995. Inactivation of the type II TGF-beta receptor in colon cancer cells with microsatellite instability. *Science*, 268, 1336-8.
- MARTINI, M., DE SANTIS, M. C., BRACCINI, L., GULLUNI, F. & HIRSCH, E. 2014. PI3K/AKT signaling pathway and cancer: an updated review. *Ann Med*, 46, 372-83.
- MASSAGUE, J. 2004. G1 cell-cycle control and cancer. *Nature*, 432, 298-306.
- MAYO, L. D. & DONNER, D. B. 2001. A phosphatidylinositol 3-kinase/Akt pathway promotes translocation of Mdm2 from the cytoplasm to the nucleus. *Proc Natl Acad Sci U S A*, 98, 11598-603.
- MAZZONI, I. E., SAID, F. A., ALOYZ, R., MILLER, F. D. & KAPLAN, D. 1999. Ras regulates sympathetic neuron survival by suppressing the p53-mediated cell death pathway. *J Neurosci*, 19, 9716-27.
- MCCANN, A. H., KIRLEY, A., CARNEY, D. N., CORBALLY, N., MAGEE, H. M., KEATING, G. & DERVAN, P. A. 1995. Amplification of the MDM2 gene in human breast cancer and its association with MDM2 and p53 protein status. *Br J Cancer*, 71, 981-5.
- MCILWAIN, D. W., ZOETEMELK, M., MYERS, J. D., EDWARDS, M. T., SNIDER, B. M. & JERDE, T. J. 2016. Coordinated induction of cell survival signaling in the inflamed microenvironment of the prostate. *Prostate*, 76, 722-34.
- MEASE, R. C., DUSICH, C. L., FOSS, C. A., RAVERT, H. T., DANNALS, R. F., SEIDEL, J., PRIDEAUX, A., FOX, J. J., SGOUROS, G., KOZIKOWSKI, A. P. & POMPER, M. G. 2008. N-[N-[(S)-1,3-Dicarboxypropyl]carbamoyl]-4-[18F]fluorobenzyl-L-cysteine, [18F]DCFBC: a new imaging probe for prostate cancer. *Clin Cancer Res*, 14, 3036-43.
- MEEK, D. W. & KNIPPSCHILD, U. 2003. Posttranslational modification of MDM2. *Mol Cancer Res*, 1, 1017-26.
- MENDRYSA, S. M., MCELWEE, M. K., MICHALOWSKI, J., O'LEARY, K. A., YOUNG, K. M. & PERRY, M. E. 2003. mdm2 is critical for inhibition of p53 during lymphopoiesis and the response to ionizing irradiation. *Mol Cell Biol*, 23, 462-72.

- METZGER-FILHO, O., CATTEAU, A., MICHIELS, S., BUYSE, M., IGNATIADIS, M., SAINI, K. S., DE AZAMBUJA, E., FASOLO, V., NAJI, S., CANON, J. L., DELREE, P., COIBION, M., CUSUMANO, P., JOSSA, V., KAINS, J. P., LARSIMONT, D., RICHARD, V., FAVERLY, D., CORNEZ, N., VUYLSTEKE, P., VANDERSCHUEREN, B., PEYRO-SAINT-PAUL, H., PICCART, M. & SOTIRIOU, C. 2013a. Genomic Grade Index (GGI): feasibility in routine practice and impact on treatment decisions in early breast cancer. *PLoS One*, 8, e66848.
- METZGER-FILHO, O., MICHIELS, S., BERTUCCI, F., CATTEAU, A., SALGADO, R., GALANT, C., FUMAGALLI, D., SINGHAL, S. K., DESMEDT, C., IGNATIADIS, M., HAUSSY, S., FINETTI, P., BIRNBAUM, D., SAINI, K. S., BERLIERE, M., VEYS, I., DE AZAMBUJA, E., BOZOVIC, I., PEYRO-SAINT-PAUL, H., LARSIMONT, D., PICCART, M. & SOTIRIOU, C. 2013b. Genomic grade adds prognostic value in invasive lobular carcinoma. *Ann Oncol*, 24, 377-84.
- MHAWECH-FAUCEGLIA, P., ZHANG, S., TERRACCIANO, L., SAUTER, G., CHADHURI, A., HERRMANN, F. R. & PENETRANTE, R. 2007. Prostate-specific membrane antigen (PSMA) protein expression in normal and neoplastic tissues and its sensitivity and specificity in prostate adenocarcinoma: an immunohistochemical study using multiple tumour tissue microarray technique. *Histopathology*, 50, 472-83.
- MIAO, J. W., LIU, L. J. & HUANG, J. 2014. Interleukin-6-induced epithelial-mesenchymal transition through signal transducer and activator of transcription 3 in human cervical carcinoma. *International Journal of Oncology*, 45, 165-176.
- MILNE, D., KAMPANIS, P., NICOL, S., DIAS, S., CAMPBELL, D. G., FULLER-PACE, F. & MEEK, D. 2004. A novel site of AKT-mediated phosphorylation in the human MDM2 onco-protein. *FEBS Lett*, 577, 270-6.
- MITSIADES, N., POULAKI, V., MITSIADES, C. S. & ANDERSON, K. C. 2001. Induction of tumour cell apoptosis by matrix metalloproteinase inhibitors: new tricks from a (not so) old drug. *Expert Opin Investig Drugs*, 10, 1075-84.
- MOLL, U. M. & PETRENKO, O. 2003. The MDM2-p53 interaction. *Mol Cancer Res*, 1, 1001-8.
- MOMAND, J., ZAMBETTI, G. P., OLSON, D. C., GEORGE, D. & LEVINE, A. J. 1992. The mdm-2 oncogene product forms a complex with the p53 protein and inhibits p53-mediated transactivation. *Cell*, 69, 1237-45.
- MUISE-HELMERICKS, R. C., GRIMES, H. L., BELLACOSA, A., MALSTROM, S. E., TSICHLIS, P. N. & ROSEN, N. 1998. Cyclin D expression is controlled post-transcriptionally via a phosphatidylinositol 3-kinase/Akt-dependent pathway. *J Biol Chem*, 273, 29864-72.
- MULLER, P. A., CASWELL, P. T., DOYLE, B., IWANICKI, M. P., TAN, E. H., KARIM, S., LUKASHCHUK, N., GILLESPIE, D. A., LUDWIG, R. L., GOSSELIN, P., CROMER, A., BRUGGE, J.

- S., SANSOM, O. J., NORMAN, J. C. & VOUSDEN, K. H. 2009. Mutant p53 drives invasion by promoting integrin recycling. *Cell*, 139, 1327-41.
- MURPHY, G. & NAGASE, H. 2008. Progress in matrix metalloproteinase research. *Mol Aspects Med*, 29, 290-308.
- MUTHUMANI, P., ALAGARSAMY, K., DHANDAYUTHAPANI, S., VENKATESAN, T. & RATHINAVELU, A. 2014. Pro-angiogenic effects of MDM2 through HIF-1alpha and NF-kappaB mediated mechanisms in LNCaP prostate cancer cells. *Mol Biol Rep*, 41, 5533-41.
- NAKAMURA, M., MIYAMOTO, S., MAEDA, H., ISHII, G., HASEBE, T., CHIBA, T., ASAKA, M. & OCHIAI, A. 2005. Matrix metalloproteinase-7 degrades all insulin-like growth factor binding proteins and facilitates insulin-like growth factor bioavailability. *Biochem Biophys Res Commun*, 333, 1011-6.
- NAKANISHI, K., HIROI, S., TOMINAGA, S., AIDA, S., KASAMATSU, H., MATSUYAMA, S., MATSUYAMA, T. & KAWAI, T. 2005. Expression of hypoxia-inducible factor-1alpha protein predicts survival in patients with transitional cell carcinoma of the upper urinary tract. *Clin Cancer Res*, 11, 2583-90.
- NARASIMHAN, M., ROSE, R., KARTHIKEYAN, M. & RATHINAVELU, A. 2007. Detection of HDM2 and VEGF co-expression in cancer cell lines: novel effect of HDM2 antisense treatment on VEGF expression. *Life Sci*, 81, 1362-72.
- NARASIMHAN, M., ROSE, R., RAMAKRISHNAN, R., ZELL, J. A. & RATHINAVELU, A. 2008. Identification of HDM2 as a regulator of VEGF expression in cancer cells. *Life Sci*, 82, 1231-41.
- NARGUND, V., AL HASHMI, D., KUMAR, P., GORDON, S., OTITIE, U., ELLISON, D., CARROLL, M., BAITHUN, S. & BRITTON, K. E. 2005. Imaging with radiolabelled monoclonal antibody (MUJ591) to prostate-specific membrane antigen in staging of clinically localized prostatic carcinoma: comparison with clinical, surgical and histological staging. *BJU Int*, 95, 1232-6.
- NAVIN, N., KRASNITZ, A., RODGERS, L., COOK, K., METH, J., KENDALL, J., RIGGS, M., EBERLING, Y., TROGE, J., GRUBOR, V., LEVY, D., LUNDIN, P., MANER, S., ZETTERBERG, A., HICKS, J. & WIGLER, M. 2010. Inferring tumor progression from genomic heterogeneity. *Genome Res*, 20, 68-80.
- NEALE, J. H., BZDEGA, T. & WROBLEWSKA, B. 2000. N-Acetylaspartylglutamate: the most abundant peptide neurotransmitter in the mammalian central nervous system. *J Neurochem*, 75, 443-52.
- NELSON, H. D., HUMPHREY, L. L., NYGREN, P., TEUTSCH, S. M. & ALLAN, J. D. 2002. Postmenopausal hormone replacement therapy: scientific review. *JAMA*, 288, 872-81.

- NIEMINEN, A. L., QANUNGO, S., SCHNEIDER, E. A., JIANG, B. H. & AGANI, F. H. 2005. Mdm2 and HIF-1 α interaction in tumor cells during hypoxia. *J Cell Physiol*, 204, 364-9.
- NOEL, A., JOST, M. & MAQUOI, E. 2008. Matrix metalloproteinases at cancer tumor-host interface. *Semin Cell Dev Biol*, 19, 52-60.
- NOMURA, N., PASTORINO, S., JIANG, P., LAMBERT, G., CRAWFORD, J. R., GYMNPOULOS, M., PICCIONI, D., JUAREZ, T., PINGLE, S. C., MAKALE, M. & KESARI, S. 2014. Prostate specific membrane antigen (PSMA) expression in primary gliomas and breast cancer brain metastases. *Cancer Cell Int*, 14, 26.
- NOMURA, Y., TASHIRO, H. & HISAMATSU, K. 1988. [Clinical values of estrogen receptor (ER) as a prognostic factor in breast cancer]. *Nihon Gan Chiryō Gakkai Shi*, 23, 844-58.
- NORBURY, C. J. & ZHIVOTOVSKY, B. 2004. DNA damage-induced apoptosis. *Oncogene*, 23, 2797-808.
- OFIA, G., BRENNAN, K. & Hopkins, A. M. 2011. Junctional Adhesion Molecules (JAMs) - New Players in Breast cancer. *Breast Cancer - Focusing on Tumor Microenvironment, Stem cells and Metastasis*. DOI: 10.5772/22110
- O'KEEFE, D. S., SU, S. L., BACICH, D. J., HORIGUCHI, Y., LUO, Y., POWELL, C. T., ZANDVLIET, D., RUSSELL, P. J., MOLLOY, P. L., NOWAK, N. J., SHOWS, T. B., MULLINS, C., VONDER HAAR, R. A., FAIR, W. R. & HESTON, W. D. 1998. Mapping, genomic organization and promoter analysis of the human prostate-specific membrane antigen gene. *Biochim Biophys Acta*, 1443, 113-27.
- OGAWARA, Y., KISHISHITA, S., OBATA, T., ISAZAWA, Y., SUZUKI, T., TANAKA, K., MASUYAMA, N. & GOTOH, Y. 2002. Akt enhances Mdm2-mediated ubiquitination and degradation of p53. *J Biol Chem*, 277, 21843-50.
- OLIVER, T. G., MEYLAN, E., CHANG, G. P., XUE, W., BURKE, J. R., HUMPTON, T. J., HUBBARD, D., BHUTKAR, A. & JACKS, T. 2011. Caspase-2-mediated cleavage of Mdm2 creates a p53-induced positive feedback loop. *Mol Cell*, 43, 57-71.
- ONEL, K. & CORDON-CARDO, C. 2004. MDM2 and prognosis. *Mol Cancer Res*, 2, 1-8.
- OREN, M. & ROTTER, V. 2010. Mutant p53 gain-of-function in cancer. *Cold Spring Harb Perspect Biol*, 2, a001107.
- OSBORNE, J. R., AKHTAR, N. H., VALLABHAJOSULA, S., ANAND, A., DEH, K. & TAGAWA, S. T. 2013. Prostate-specific membrane antigen-based imaging. *Urol Oncol*, 31, 144-54.
- OVERALL, C. M. & LOPEZ-OTIN, C. 2002. Strategies for MMP inhibition in cancer: innovations for the post-trial era. *Nat Rev Cancer*, 2, 657-72.
- PAGE-MCCAW, A. 2008. Remodeling the model organism: matrix metalloproteinase functions in invertebrates. *Semin Cell Dev Biol*, 19, 14-23.

- PAGE-MCCAW, A., EWALD, A. J. & WERB, Z. 2007. Matrix metalloproteinases and the regulation of tissue remodelling. *Nat Rev Mol Cell Biol*, 8, 221-33.
- PAGE, D. L., DUPONT, W. D., ROGERS, L. W. & LANDENBERGER, M. 1982. Intraductal carcinoma of the breast: follow-up after biopsy only. *Cancer*, 49, 751-8.
- PAN, Y. & HAINES, D. S. 1999. The pathway regulating MDM2 protein degradation can be altered in human leukemic cells. *Cancer Res*, 59, 2064-7.
- PARISE, C. & CAGGIANO, V. 2014a. Disparities in the risk of the ER/PR/HER2 breast cancer subtypes among Asian Americans in California. *Cancer Epidemiol*, 38, 556-62.
- PARISE, C. A. & CAGGIANO, V. 2014b. Breast Cancer Survival Defined by the ER/PR/HER2 Subtypes and a Surrogate Classification according to Tumor Grade and Immunohistochemical Biomarkers. *J Cancer Epidemiol*, 2014, 469251.
- PARK, C. M., PARK, M. J., KWAK, H. J., LEE, H. C., KIM, M. S., LEE, S. H., PARK, I. C., RHEE, C. H. & HONG, S. I. 2006. Ionizing radiation enhances matrix metalloproteinase-2 secretion and invasion of glioma cells through Src/epidermal growth factor receptor-mediated p38/Akt and phosphatidylinositol 3-kinase/Akt signaling pathways. *Cancer Res*, 66, 8511-9.
- PARKS, D. J., LAFRANCE, L. V., CALVO, R. R., MILKIEWICZ, K. L., GUPTA, V., LATTANZE, J., RAMACHANDREN, K., CARVER, T. E., PETRELLA, E. C., CUMMINGS, M. D., MAGUIRE, D., GRASBERGER, B. L. & LU, T. 2005. 1,4-Benzodiazepine-2,5-diones as small molecule antagonists of the HDM2-p53 interaction: discovery and SAR. *Bioorg Med Chem Lett*, 15, 765-70.
- PELHAM, R. J., JR. & WANG, Y. 1997. Cell locomotion and focal adhesions are regulated by substrate flexibility. *Proc Natl Acad Sci U S A*, 94, 13661-5.
- PENG, Y., CHEN, L., LI, C., LU, W., AGRAWAL, S. & CHEN, J. 2001. Stabilization of the MDM2 oncoprotein by mutant p53. *J Biol Chem*, 276, 6874-8.
- PERICO, M. E., GRASSO, S., BRUNELLI, M., MARTIGNONI, G., MUNARI, E., MOISO, E., FRACASSO, G., CESTARI, T., NAIM, H. Y., BRONTE, V., COLOMBATTI, M. & RAMARLI, D. 2016. Prostate-specific membrane antigen (PSMA) assembles a macromolecular complex regulating growth and survival of prostate cancer cells "in vitro" and correlating with progression "in vivo". *Oncotarget*.
- PERNER, S., HOFER, M. D., KIM, R., SHAH, R. B., LI, H., MOLLER, P., HAUTMANN, R. E., GSCHWEND, J. E., KUEFER, R. & RUBIN, M. A. 2007. Prostate-specific membrane antigen expression as a predictor of prostate cancer progression. *Hum Pathol*, 38, 696-701.

- PHAROAH, P. D., DAY, N. E., DUFFY, S., EASTON, D. F. & PONDER, B. A. 1997. Family history and the risk of breast cancer: a systematic review and meta-analysis. *Int J Cancer*, 71, 800-9.
- PINTO, J. T., SUFFOLETTO, B. P., BERZIN, T. M., QIAO, C. H., LIN, S., TONG, W. P., MAY, F., MUKHERJEE, B. & HESTON, W. D. 1996. Prostate-specific membrane antigen: a novel folate hydrolase in human prostatic carcinoma cells. *Clin Cancer Res*, 2, 1445-51.
- PLAS, D. R. & THOMPSON, C. B. 2005. Akt-dependent transformation: there is more to growth than just surviving. *Oncogene*, 24, 7435-42.
- POCHAMPALLY, R., FODERA, B., CHEN, L., LU, W. & CHEN, J. 1999. Activation of an MDM2-specific caspase by p53 in the absence of apoptosis. *J Biol Chem*, 274, 15271-7.
- POCHAMPALLY, R., FODERA, B., CHEN, L., SHAO, W., LEVINE, E. A. & CHEN, J. 1998. A 60 kd MDM2 isoform is produced by caspase cleavage in non-apoptotic tumor cells. *Oncogene*, 17, 2629-36.
- POMMIER, Y., SORDET, O., ANTONY, S., HAYWARD, R. L. & KOHN, K. W. 2004. Apoptosis defects and chemotherapy resistance: molecular interaction maps and networks. *Oncogene*, 23, 2934-49.
- QI, D. L. & COBRINIK, D. 2016. MDM2 but not MDM4 promotes retinoblastoma cell proliferation through p53-independent regulation of MYCN translation. *Oncogene*.
- QI, M., ZHANG, J., ZENG, W. & CHEN, X. 2014. DNAB1 stabilizes MDM2 and contributes to cancer cell proliferation in a p53-dependent manner. *Biochim Biophys Acta*, 1839, 62-9.
- RA, H. J. & PARKS, W. C. 2007. Control of matrix metalloproteinase catalytic activity. *Matrix Biol*, 26, 587-96.
- RAJABI, P., KARIMIAN, P. & HEIDARPOUR, M. 2012. The relationship between MDM2 expression and tumor thickness and invasion in primary cutaneous malignant melanoma. *J Res Med Sci*, 17, 452-5.
- RAJASEKARAN, A. K., ANILKUMAR, G. & CHRISTIANSEN, J. J. 2005. Is prostate-specific membrane antigen a multifunctional protein? *Am J Physiol Cell Physiol*, 288, C975-81.
- RAJASEKARAN, S. A., CHRISTIANSEN, J. J., SCHMID, I., OSHIMA, E., RYAZANTSEV, S., SAKAMOTO, K., WEINSTEIN, J., RAO, N. P. & RAJASEKARAN, A. K. 2008. Prostate-specific membrane antigen associates with anaphase-promoting complex and induces chromosomal instability. *Mol Cancer Ther*, 7, 2142-51.
- RAVI, R., MOOKERJEE, B., BHUJWALLA, Z. M., SUTTER, C. H., ARTEMOV, D., ZENG, Q., DILLEHAY, L. E., MADAN, A., SEMENZA, G. L. & BEDI, A. 2000. Regulation of tumor angiogenesis by p53-induced degradation of hypoxia-inducible factor 1alpha. *Genes Dev*, 14, 34-44.

- RAY, R. M., BHATTACHARYA, S. & JOHNSON, L. R. 2011. Mdm2 inhibition induces apoptosis in p53 deficient human colon cancer cells by activating p73- and E2F1-mediated expression of PUMA and Siva-1. *Apoptosis*, 16, 35-44.
- RAYBURN, E., ZHANG, R., HE, J. & WANG, H. 2005. MDM2 and human malignancies: expression, clinical pathology, prognostic markers, and implications for chemotherapy. *Curr Cancer Drug Targets*, 5, 27-41.
- REGINO, C. A., WONG, K. J., MILENIC, D. E., HOLMES, E. H., GARMESTANI, K., CHOYKE, P. L. & BRECHBIEL, M. W. 2009. Preclinical evaluation of a monoclonal antibody (3C6) specific for prostate-specific membrane antigen. *Curr Radiopharm*, 2, 9-17.
- REYNOLDS, A., LEAKE, D., BOESE, Q., SCARINGE, S., MARSHALL, W. S. & KHVOROVA, A. 2004. Rational siRNA design for RNA interference. *Nat Biotechnol*, 22, 326-30.
- RIBELLES, N., PEREZ-VILLA, L., JEREZ, J.M., PAJARES, B., VICIOSA, L., JIMENEZ, B., DE LUC, V., FRANCO, L., GALLEGO, E., MARQUES, A., ALVAREZ, M., SANCHES-MUNOZ, A., PEREZ-RIVAS, L. & ALBA, E. 2013. Pattern of recurrence of early breast cancer is different according to intrinsic subtype and proliferation index. *Breast Cancer Res*, 15(R98), doi: 10.1186/bcr3559.
- RIEDL, S. J. & SHI, Y. 2004. Molecular mechanisms of caspase regulation during apoptosis. *Nat Rev Mol Cell Biol*, 5, 897-907.
- RIEMENSCHNEIDER, M. J., BUSCHGES, R., WOLTER, M., REIFENBERGER, J., BOSTROM, J., KRAUS, J. A., SCHLEGEL, U. & REIFENBERGER, G. 1999. Amplification and overexpression of the MDM4 (MDMX) gene from 1q32 in a subset of malignant gliomas without TP53 mutation or MDM2 amplification. *Cancer Res*, 59, 6091-6.
- RIEMENSCHNEIDER, M. J., KNOBBE, C. B. & REIFENBERGER, G. 2003. Refined mapping of 1q32 amplicons in malignant gliomas confirms MDM4 as the main amplification target. *Int J Cancer*, 104, 752-7.
- RISTAU, B. T., O'KEEFE, D. S. & BACICH, D. J. 2014. The prostate-specific membrane antigen: lessons and current clinical implications from 20 years of research. *Urol Oncol*, 32, 272-9.
- ROLFE, K. J. & GROBBELAAR, A. O. 2012. A review of fetal scarless healing. *ISRN Dermatol*, 2012, 698034.
- ROSENTHAL, S. A., HASEMAN, M. K. & POLASCIK, T. J. 2001. Utility of capromab pendetide (ProstaScint) imaging in the management of prostate cancer. *Tech Urol*, 7, 27-37.
- ROSS, J. S., SHEEHAN, C. E., FISHER, H. A., KAUFMAN, R. P., JR., KAUR, P., GRAY, K., WEBB, I., GRAY, G. S., MOSHER, R. & KALLAKURY, B. V. 2003. Correlation of primary tumor prostate-specific membrane antigen expression with disease recurrence in prostate cancer. *Clin Cancer Res*, 9, 6357-62.
- ROTH, J., DOBBELSTEIN, M., FREEDMAN, D. A., SHENK, T. & LEVINE, A. J. 1998. Nucleo-cytoplasmic shuttling of the hdm2

- oncoprotein regulates the levels of the p53 protein via a pathway used by the human immunodeficiency virus rev protein. *EMBO J*, 17, 554-64.
- ROY, R., YANG, J. & MOSES, M. A. 2009. Matrix metalloproteinases as novel biomarkers and potential therapeutic targets in human cancer. *J Clin Oncol*, 27, 5287-97.
- RUGGERO, D. & SONENBERG, N. 2005. The Akt of translational control. *Oncogene*, 24, 7426-34.
- RUNDHAUG, J. E. 2003. Matrix metalloproteinases, angiogenesis, and cancer: commentary re: A. C. Lockhart et al., Reduction of wound angiogenesis in patients treated with BMS-275291, a broad spectrum matrix metalloproteinase inhibitor. *Clin. Cancer Res.*, 9: 00-00, 2003. *Clin Cancer Res*, 9, 551-4.
- RUSSELL, P. J., HEWISH, D., CARTER, T., STERLING-LEVIS, K., OW, K., HATTARKI, M., DOUGHTY, L., GUTHRIE, R., SHAPIRA, D., MOLLOY, P. L., WERKMEISTER, J. A. & KORTT, A. A. 2004. Cytotoxic properties of immunoconjugates containing melittin-like peptide 101 against prostate cancer: in vitro and in vivo studies. *Cancer Immunol Immunother*, 53, 411-21.
- SABBATINI, P. & MCCORMICK, F. 1999. Phosphoinositide 3-OH kinase (PI3K) and PKB/Akt delay the onset of p53-mediated, transcriptionally dependent apoptosis. *J Biol Chem*, 274, 24263-9.
- SACHA, P., ZAMECNIK, J., BARINKA, C., HLOUCHOVA, K., VICHA, A., MLCOCHOVA, P., HILGERT, I., ECKSCHLAGER, T. & KONVALINKA, J. 2007. Expression of glutamate carboxypeptidase II in human brain. *Neuroscience*, 144, 1361-72.
- SAJI, S., OKUMURA, N., EGUCHI, H., NAKASHIMA, S., SUZUKI, A., TOI, M., NOZAWA, Y., SAJI, S. & HAYASHI, S. 2001. MDM2 enhances the function of estrogen receptor alpha in human breast cancer cells. *Biochem Biophys Res Commun*, 281, 259-65.
- SALGADO, R., JUNIUS, S., BENOY, I., VAN DAM, P., VERMEULEN, P., VAN MARCK, E., HUGET, P. & DIRIX, L. Y. 2003. Circulating interleukin-6 predicts survival in patients with metastatic breast cancer. *Int J Cancer*, 103, 642-6.
- SAMPLASKI, M. K., HESTON, W., ELSON, P., MAGI-GALLUZZI, C. & HANSEL, D. E. 2011. Folate hydrolase (prostate-specific antigen) 1 expression in bladder cancer subtypes and associated tumor neovasculature. *Modern Pathology*, 24, 1521-1529.
- SCHAFFER, K. A. 1998. The cell cycle: a review. *Vet Pathol*, 35, 461-78.
- SCHEID, M. P., MARIGNANI, P. A. & WOODGETT, J. R. 2002. Multiple phosphoinositide 3-kinase-dependent steps in activation of protein kinase B. *Molecular and Cellular Biology*, 22, 6247-6260.

- SCHMITTGEN, T. D., TESKE, S., VESSELLA, R. L., TRUE, L. D. & ZAKRAJSEK, B. A. 2003. Expression of prostate specific membrane antigen and three alternatively spliced variants of PSMA in prostate cancer patients. *Int J Cancer*, 107, 323-9.
- SCHREIBER, M., KOLBUS, A., PIU, F., SZABOWSKI, A., MOHLE-STEINLEIN, U., TIAN, J., KARIN, M., ANGEL, P. & WAGNER, E. F. 1999. Control of cell cycle progression by c-Jun is p53 dependent. *Genes Dev*, 13, 607-19.
- SCHULKE, N., VARLAMOVA, O. A., DONOVAN, G. P., MA, D., GARDNER, J. P., MORRISSEY, D. M., ARRIGALE, R. R., ZHAN, C., CHODERA, A. J., SUROWITZ, K. G., MADDON, P. J., HESTON, W. D. & OLSON, W. C. 2003. The homodimer of prostate-specific membrane antigen is a functional target for cancer therapy. *Proc Natl Acad Sci U S A*, 100, 12590-5.
- SCHWANHAUSSER, B., BUSSE, D., LI, N., DITTMAR, G., SCHUCHHARDT, J., WOLF, J., CHEN, W. & SELBACH, M. 2011. Global quantification of mammalian gene expression control. *Nature*, 473, 337-42.
- SECCHIERO, P., CORALLINI, F., GONELLI, A., DELL'IVA, R., VITALE, M., CAPITANI, S., ALBINI, A. & ZAULI, G. 2007. Antiangiogenic activity of the MDM2 antagonist nutlin-3. *Circ Res*, 100, 61-9.
- SELA-PASSWELL, N., ROSENBLUM, G., SHOHAM, T. & SAGI, I. 2010. Structural and functional bases for allosteric control of MMP activities: can it pave the path for selective inhibition? *Biochim Biophys Acta*, 1803, 29-38.
- SHANGARY, S., QIN, D., MCEACHERN, D., LIU, M., MILLER, R. S., QIU, S., NIKOLOVSKA-COLESKA, Z., DING, K., WANG, G., CHEN, J., BERNARD, D., ZHANG, J., LU, Y., GU, Q., SHAH, R. B., PIENTA, K. J., LING, X., KANG, S., GUO, M., SUN, Y., YANG, D. & WANG, S. 2008. Temporal activation of p53 by a specific MDM2 inhibitor is selectively toxic to tumors and leads to complete tumor growth inhibition. *Proc Natl Acad Sci U S A*, 105, 3933-8.
- SHARP, D. A., KRATOWICZ, S. A., SANK, M. J. & GEORGE, D. L. 1999. Stabilization of the MDM2 oncoprotein by interaction with the structurally related MDMX protein. *J Biol Chem*, 274, 38189-96.
- SHAY, J. W. & BACCHETTI, S. 1997. A survey of telomerase activity in human cancer. *Eur J Cancer*, 33, 787-91.
- SHEIKH, M. S., SHAO, Z. M., HUSSAIN, A. & FONTANA, J. A. 1993. The p53-binding protein MDM2 gene is differentially expressed in human breast carcinoma. *Cancer Res*, 53, 3226-8.
- SHI, D. & GU, W. 2012. Dual Roles of MDM2 in the Regulation of p53: Ubiquitination Dependent and Ubiquitination Independent Mechanisms of MDM2 Repression of p53 Activity. *Genes Cancer*, 3, 240-8.
- SIGALAS, I., CALVERT, A. H., ANDERSON, J. J., NEAL, D. E. & LUNEC, J. 1996. Alternatively spliced mdm2 transcripts with

- loss of p53 binding domain sequences: transforming ability and frequent detection in human cancer. *Nat Med*, 2, 912-7.
- SILVER, D. A., PELLICER, I., FAIR, W. R., HESTON, W. D. & CORDON-CARDO, C. 1997a. Prostate-specific membrane antigen expression in normal and malignant human tissues. *Clin Cancer Res*, 3, 81-5.
- SILVER, R. I., PARTIN, A. W., EPSTEIN, J. I., CHAN, D. W., CARTER, H. B., JEFFS, R. D. & GEARHART, J. P. 1997b. Prostate-specific antigen in men born with bladder exstrophy. *Urology*, 49, 253-6.
- SINGLETERY, S. E. 2003. Rating the risk factors for breast cancer. *Ann Surg*, 237, 474-82.
- SOKOLOFF, R. L., NORTON, K. C., GASIOR, C. L., MARKER, K. M. & GRAUER, L. S. 2000. A dual-monoclonal sandwich assay for prostate-specific membrane antigen: levels in tissues, seminal fluid and urine. *Prostate*, 43, 150-7.
- SPORN, M. B. 1996. The war on cancer. *Lancet*, 347, 1377-81.
- STAD, R., LITTLE, N. A., XIRODIMAS, D. P., FRENK, R., VAN DER EB, A. J., LANE, D. P., SAVILLE, M. K. & JOCHEMSEN, A. G. 2001. Mdmx stabilizes p53 and Mdm2 via two distinct mechanisms. *EMBO Rep*, 2, 1029-34.
- STRAND, S., VOLLMER, P., VAN DEN ABEELLEN, L., GOTTFRIED, D., ALLA, V., HEID, H., KUBALL, J., THEOBALD, M., GALLE, P. R. & STRAND, D. 2004. Cleavage of CD95 by matrix metalloproteinase-7 induces apoptosis resistance in tumour cells. *Oncogene*, 23, 3732-6.
- STREULI, C. 1999. Extracellular matrix remodelling and cellular differentiation. *Curr Opin Cell Biol*, 11, 634-40.
- STREULI, C. H., BAILEY, N. & BISSELL, M. J. 1991. Control of mammary epithelial differentiation: basement membrane induces tissue-specific gene expression in the absence of cell-cell interaction and morphological polarity. *J Cell Biol*, 115, 1383-95.
- SUN, D., LI, Z., REW, Y., GRIBBLE, M., BARTBERGER, M. D., BECK, H. P., CANON, J., CHEN, A., CHEN, X., CHOW, D., DEIGNAN, J., DUQUETTE, J., EKSTEROWICZ, J., FISHER, B., FOX, B. M., FU, J., GONZALEZ, A. Z., GONZALEZ-LOPEZ DE TURISO, F., HOUZE, J. B., HUANG, X., JIANG, M., JIN, L., KAYSER, F., LIU, J. J., LO, M. C., LONG, A. M., LUCAS, B., MCGEE, L. R., MCINTOSH, J., MIHALIC, J., OLINER, J. D., OSGOOD, T., PETERSON, M. L., ROVETO, P., SAIKI, A. Y., SHAFFER, P., TOTEVA, M., WANG, Y., WANG, Y. C., WORTMAN, S., YAKOWEC, P., YAN, X., YE, Q., YU, D., YU, M., ZHAO, X., ZHOU, J., ZHU, J., OLSON, S. H. & MEDINA, J. C. 2014. Discovery of AMG 232, a potent, selective, and orally bioavailable MDM2-p53 inhibitor in clinical development. *J Med Chem*, 57, 1454-72.
- SUZUKI, A., LU, J., KUSAKAI, G., KISHIMOTO, A., OGURA, T. & ESUMI, H. 2004. ARK5 is a tumor invasion-associated factor downstream of Akt signaling. *Mol Cell Biol*, 24, 3526-35.

- SWANTON, C., BURRELL, R. A. & FUTREAL, P. A. 2011. Breast cancer genome heterogeneity: a challenge to personalised medicine? *Breast Cancer Res*, 13, 104.
- SWEAT, S. D., PACELLI, A., MURPHY, G. P. & BOSTWICK, D. G. 1998. Prostate-specific membrane antigen expression is greatest in prostate adenocarcinoma and lymph node metastases. *Urology*, 52, 637-40.
- SYED, I., RATHOD, J., PARMAR, M., CORCORAN, G. B. & RAY, S. D. 2012. Matrix metalloproteinase-9, -10, and -12, MDM2 and p53 expression in mouse liver during dimethylnitrosamine-induced oxidative stress and genomic injury. *Mol Cell Biochem*, 365, 351-61.
- SYMPSON, C. J., TALHOUK, R. S., ALEXANDER, C. M., CHIN, J. R., CLIFT, S. M., BISSELL, M. J. & WERB, Z. 1994. Targeted expression of stromelysin-1 in mammary gland provides evidence for a role of proteinases in branching morphogenesis and the requirement for an intact basement membrane for tissue-specific gene expression. *J Cell Biol*, 125, 681-93.
- TAGAWA, S. T., MILOWSKY, M. I., MORRIS, M., VALLABHAJOSULA, S., CHRISTOS, P., AKHTAR, N. H., OSBORNE, J., GOLDSMITH, S. J., LARSON, S., TASKAR, N. P., SCHER, H. I., BANDER, N. H. & NANUS, D. M. 2013. Phase II study of Lutetium-177-labeled anti-prostate-specific membrane antigen monoclonal antibody J591 for metastatic castration-resistant prostate cancer. *Clin Cancer Res*, 19, 5182-91.
- TANIMURA, S., OHTSUKA, S., MITSUI, K., SHIROUZU, K., YOSHIMURA, A. & OHTSUBO, M. 1999. MDM2 interacts with MDMX through their RING finger domains. *FEBS Lett*, 447, 5-9.
- TANZER, M. L. 2006. Current concepts of extracellular matrix. *J Orthop Sci*, 11, 326-31.
- TEODORO, J. G., EVANS, S. K. & GREEN, M. R. 2007. Inhibition of tumor angiogenesis by p53: a new role for the guardian of the genome. *J Mol Med (Berl)*, 85, 1175-86.
- TEOH, G., URASHIMA, M., OGATA, A., CHAUHAN, D., DECAPRIO, J. A., TREON, S. P., SCHLOSSMAN, R. L. & ANDERSON, K. C. 1997. MDM2 protein overexpression promotes proliferation and survival of multiple myeloma cells. *Blood*, 90, 1982-92.
- TERZIAN, T., SUH, Y. A., IWAKUMA, T., POST, S. M., NEUMANN, M., LANG, G. A., VAN PELT, C. S. & LOZANO, G. 2008. The inherent instability of mutant p53 is alleviated by Mdm2 or p16INK4a loss. *Genes Dev*, 22, 1337-44.
- TESTA, J. R. & BELLACOSA, A. 2001. AKT plays a central role in tumorigenesis. *Proc Natl Acad Sci U S A*, 98, 10983-5.
- TESTA, J. R. & TSICHLIS, P. N. 2005. AKT signaling in normal and malignant cells. *Oncogene*, 24, 7391-3.
- THANT, A. A., NAWA, A., KIKKAWA, F., ICHIGOTANI, Y., ZHANG, Y., SEIN, T. T., AMIN, A. R. & HAMAGUCHI, M. 2000. Fibronectin activates matrix metalloproteinase-9 secretion via

- the MEK1-MAPK and the PI3K-Akt pathways in ovarian cancer cells. *Clin Exp Metastasis*, 18, 423-8.
- THEODOROPOULOS, V. E., LAZARIS, A., SOFRAS, F., GERZELIS, I., TSOUKALA, V., GHIKONTI, I., MANIKAS, K. & KASTRIOTIS, I. 2004. Hypoxia-inducible factor 1 alpha expression correlates with angiogenesis and unfavorable prognosis in bladder cancer. *Eur Urol*, 46, 200-8.
- THIRKETTLE, S., DECOCK, J., ARNOLD, H., PENNINGTON, C. J., JAWORSKI, D. M. & EDWARDS, D. R. 2013. Matrix metalloproteinase 8 (collagenase 2) induces the expression of interleukins 6 and 8 in breast cancer cells. *J Biol Chem*, 288, 16282-94.
- THOMASOVA, D., MULAY, S. R., BRUNS, H. & ANDERS, H. J. 2012. p53-independent roles of MDM2 in NF-kappaB signaling: implications for cancer therapy, wound healing, and autoimmune diseases. *Neoplasia*, 14, 1097-101.
- THURLIMANN, B. & SENN, H. J. 2005. [Consensus Meeting of the 9th International Conference on Primary Therapy of Early Breast Cancer (St. Gall, January 26-29, 2005)]. *Gynakol Geburtshilfliche Rundsch*, 45, 143-6.
- TIAN, Q., STEPANIANTS, S. B., MAO, M., WENG, L., FEETHAM, M. C., DOYLE, M. J., YI, E. C., DAI, H., THORSSON, V., ENG, J., GOODLETT, D., BERGER, J. P., GUNTER, B., LINSELEY, P. S., STOUGHTON, R. B., AEBERSOLD, R., COLLINS, S. J., HANLON, W. A. & HOOD, L. E. 2004. Integrated genomic and proteomic analyses of gene expression in Mammalian cells. *Mol Cell Proteomics*, 3, 960-9.
- TINZL, M., CHEN, B., CHEN, S. Y., SEMENAS, J., ABRAHAMSSON, P. A. & DIZEYI, N. 2013. Interaction between c-jun and androgen receptor determines the outcome of taxane therapy in castration resistant prostate cancer. *PLoS One*, 8, e79573.
- TOFT, D. J. & CRYNS, V. L. 2011. Minireview: Basal-like breast cancer: from molecular profiles to targeted therapies. *Mol Endocrinol*, 25, 199-211.
- TOI, M., SAJI, S., SUZUKI, A., YAMAMOTO, Y. & TOMINAGA, T. 1997. MDM2 in Breast Cancer. *Breast Cancer*, 4, 264-268.
- TOVAR, C., GRAVES, B., PACKMAN, K., FILIPOVIC, Z., HIGGINS, B., XIA, M., TARDELL, C., GARRIDO, R., LEE, E., KOLINSKY, K., TO, K. H., LINN, M., PODLASKI, F., WOVKULICH, P., VU, B. & VASSILEV, L. T. 2013. MDM2 small-molecule antagonist RG7112 activates p53 signaling and regresses human tumors in preclinical cancer models. *Cancer Res*, 73, 2587-97.
- TOVAR, C., ROSINSKI, J., FILIPOVIC, Z., HIGGINS, B., KOLINSKY, K., HILTON, H., ZHAO, X., VU, B. T., QING, W., PACKMAN, K., MYKLEBOST, O., HEIMBROOK, D. C. & VASSILEV, L. T. 2006. Small-molecule MDM2 antagonists reveal aberrant p53 signaling in cancer: implications for therapy. *Proc Natl Acad Sci U S A*, 103, 1888-93.

- TRETLI, S. 1989. Height and weight in relation to breast cancer morbidity and mortality. A prospective study of 570,000 women in Norway. *Int J Cancer*, 44, 23-30.
- TRICHOPOULOS, D., MACMAHON, B. & COLE, P. 1972. Menopause and breast cancer risk. *J Natl Cancer Inst*, 48, 605-13.
- TROYER, J. K., BECKETT, M. L. & WRIGHT, G. L., JR. 1995. Detection and characterization of the prostate-specific membrane antigen (PSMA) in tissue extracts and body fluids. *Int J Cancer*, 62, 552-8.
- TSUI, P., RUBENSTEIN, M. & GUINAN, P. 2005. Correlation between PSMA and VEGF expression as markers for LNCaP tumor angiogenesis. *J Biomed Biotechnol*, 2005, 287-90.
- TURBIN, D. A., CHEANG, M. C., BAJDIK, C. D., GELMON, K. A., YORIDA, E., DE LUCA, A., NIELSEN, T. O., HUNTSMAN, D. G. & GILKS, C. B. 2006. MDM2 protein expression is a negative prognostic marker in breast carcinoma. *Mod Pathol*, 19, 69-74.
- VAN WART, H. E. & BIRKEDAL-HANSEN, H. 1990. The cysteine switch: a principle of regulation of metalloproteinase activity with potential applicability to the entire matrix metalloproteinase gene family. *Proc Natl Acad Sci U S A*, 87, 5578-82.
- VASSILEV, L. T. 2007. MDM2 inhibitors for cancer therapy. *Trends Mol Med*, 13, 23-31.
- VEIKKOLA, T. & ALITALO, K. 1999. VEGFs, receptors and angiogenesis. *Semin Cancer Biol*, 9, 211-20.
- VERMEULEN, K., VAN BOCKSTAELE, D. R. & BERNEMAN, Z. N. 2003. The cell cycle: a review of regulation, deregulation and therapeutic targets in cancer. *Cell Prolif*, 36, 131-49.
- VINCENT, K. M., FINDLAY, S. D. & POSTOVIT, L. M. 2015. Assessing breast cancer cell lines as tumour models by comparison of mRNA expression profiles. *Breast Cancer Res*, 17, 114.
- VINCENTI, M. P. & BRINCKERHOFF, C. E. 2007. Signal transduction and cell-type specific regulation of matrix metalloproteinase gene expression: can MMPs be good for you? *J Cell Physiol*, 213, 355-64.
- VLEUGEL, M. M., GREIJER, A. E., BOS, R., VAN DER WALL, E. & VAN DIEST, P. J. 2006. c-Jun activation is associated with proliferation and angiogenesis in invasive breast cancer. *Hum Pathol*, 37, 668-74.
- VODUC, K. D., CHEANG, M. C., TYLDESLEY, S., GELMON, K., NIELSEN, T. O. & KENNECKE, H. 2010. Breast cancer subtypes and the risk of local and regional relapse. *J Clin Oncol*, 28, 1684-91.
- VOGEL, C. & MARCOTTE, E. M. 2008. Calculating absolute and relative protein abundance from mass spectrometry-based protein expression data. *Nat Protoc*, 3, 1444-51.

- VOLPERT, O. V., DAMERON, K. M. & BOUCK, N. 1997. Sequential development of an angiogenic phenotype by human fibroblasts progressing to tumorigenicity. *Oncogene*, 14, 1495-502.
- VU, B., WOVKULICH, P., PIZZOLATO, G., LOVEY, A., DING, Q., JIANG, N., LIU, J. J., ZHAO, C., GLENN, K., WEN, Y., TOVAR, C., PACKMAN, K., VASSILEV, L. & GRAVES, B. 2013. Discovery of RG7112: A Small-Molecule MDM2 Inhibitor in Clinical Development. *ACS Med Chem Lett*, 4, 466-9.
- WADE, M., LI, Y. C. & WAHL, G. M. 2013. MDM2, MDMX and p53 in oncogenesis and cancer therapy. *Nat Rev Cancer*, 13, 83-96.
- WALERYCH, D., NAPOLI, M., COLLAVIN, L. & DEL SAL, G. 2012. The rebel angel: mutant p53 as the driving oncogene in breast cancer. *Carcinogenesis*, 33, 2007-17.
- WANG, B., FANG, L., ZHAO, H., XIANG, T. & WANG, D. 2012. MDM2 inhibitor Nutlin-3a suppresses proliferation and promotes apoptosis in osteosarcoma cells. *Acta Biochim Biophys Sin (Shanghai)*, 44, 685-91.
- WANG, L. N., CUI, Y. X., RUGE, F. & JIANG, W. G. 2015. Interleukin 21 and Its Receptor Play a Role in Proliferation, Migration and Invasion of Breast Cancer Cells. *Cancer Genomics Proteomics*, 12, 211-21.
- WANG, S., SUN, W., ZHAO, Y., MCEACHERN, D., MEAUX, I., BARRIERE, C., STUCKEY, J. A., MEAGHER, J. L., BAI, L., LIU, L., HOFFMAN-LUCA, C. G., LU, J., SHANGARY, S., YU, S., BERNARD, D., AGUILAR, A., DOS-SANTOS, O., BESRET, L., GUERIF, S., PANNIER, P., GORGE-BERNAT, D. & DEBUSSCHE, L. 2014. SAR405838: an optimized inhibitor of MDM2-p53 interaction that induces complete and durable tumor regression. *Cancer Res*, 74, 5855-65.
- WAUGH, D. J. & WILSON, C. 2008. The interleukin-8 pathway in cancer. *Clin Cancer Res*, 14, 6735-41.
- WEAVER, M. S., SAGE, E. H. & YAN, Q. 2006. Absence of SPARC in lens epithelial cells results in altered adhesion and extracellular matrix production in vitro. *J Cell Biochem*, 97, 423-32.
- WEBER, J. D., KUO, M. L., BOTHNER, B., DIGIAMMARINO, E. L., KRIWACKI, R. W., ROUSSEL, M. F. & SHERR, C. J. 2000. Cooperative signals governing ARF-mdm2 interaction and nucleolar localization of the complex. *Mol Cell Biol*, 20, 2517-28.
- WEISS, L. K., BURKMAN, R. T., CUSHING-HAUGEN, K. L., VOIGT, L. F., SIMON, M. S., DALING, J. R., NORMAN, S. A., BERNSTEIN, L., URSIN, G., MARCHBANKS, P. A., STROM, B. L., BERLIN, J. A., WEBER, A. L., DOODY, D. R., WINGO, P. A., MCDONALD, J. A., MALONE, K. E., FOLGER, S. G. & SPIRTAS, R. 2002. Hormone replacement therapy regimens and breast cancer risk(1). *Obstet Gynecol*, 100, 1148-58.
- WERNICKE, A. G., VARMA, S., GREENWOOD, E. A., CHRISTOS, P. J., CHAO, K. S., LIU, H., BANDER, N. H. & SHIN, S. J.

2014. Prostate-specific membrane antigen expression in tumor-associated vasculature of breast cancers. *APMIS*, 122, 482-9.
- WHITE, E. 1987. Projected changes in breast cancer incidence due to the trend toward delayed childbearing. *Am J Public Health*, 77, 495-7.
- WILLIAMS, G. H. & STOEBER, K. 2012. The cell cycle and cancer. *J Pathol*, 226, 352-64.
- WILSON, R. C. & DOUDNA, J. A. 2013. Molecular mechanisms of RNA interference. *Annu Rev Biophys*, 42, 217-39.
- WITTEKIND, C., COMPTON, C. C., GREENE, F. L. & SOBIN, L. H. 2002. TNM residual tumor classification revisited. *Cancer*, 94, 2511-6.
- WU, G., FENG, X. & STEIN, L. 2010. A human functional protein interaction network and its application to cancer data analysis. *Genome Biol*, 11, R53.
- WYNANT, G. E., MURPHY, G. P., HOROSZEWICZ, J. S., NEAL, C. E., COLLIER, B. D., MITCHELL, E., PURNELL, G., TYSON, I., HEAL, A., ABDEL-NABI, H. & ET AL. 1991. Immunoscintigraphy of prostatic cancer: preliminary results with 111In-labeled monoclonal antibody 7E11-C5.3 (CYT-356). *Prostate*, 18, 229-41.
- XIE, G., YAO, Q., LIU, Y., DU, S., LIU, A., GUO, Z., SUN, A., RUAN, J., CHEN, L., YE, C. & YUAN, Y. 2012. IL-6-induced epithelial-mesenchymal transition promotes the generation of breast cancer stem-like cells analogous to mammosphere cultures. *Int J Oncol*, 40, 1171-9.
- XIONG, J., YANG, Q., LI, J. & ZHOU, S. 2014. Effects of MDM2 inhibitors on vascular endothelial growth factor-mediated tumor angiogenesis in human breast cancer. *Angiogenesis*, 17, 37-50.
- XU, J., RODRIGUEZ, D., PETITCLERC, E., KIM, J. J., HANGAI, M., MOON, Y. S., DAVIS, G. E. & BROOKS, P. C. 2001. Proteolytic exposure of a cryptic site within collagen type IV is required for angiogenesis and tumor growth in vivo. *J Cell Biol*, 154, 1069-79.
- XU, L., WANG, Z., LI, X. F., HE, X., GUAN, L. L., TUO, J. L., WANG, Y., LUO, Y., ZHONG, H. L., QIU, S. P. & CAO, K. Y. 2013. Screening and identification of significant genes related to tumor metastasis and PSMA in prostate cancer using microarray analysis. *Oncol Rep*, 30, 1920-8.
- YAMADA, K. M. & CUKIERMAN, E. 2007. Modeling tissue morphogenesis and cancer in 3D. *Cell*, 130, 601-10.
- YAMAGUCHI, A., TAMATANI, M., MATSUZAKI, H., NAMIKAWA, K., KIYAMA, H., VITEK, M. P., MITSUDA, N. & TOHYAMA, M. 2001. Akt activation protects hippocampal neurons from apoptosis by inhibiting transcriptional activity of p53. *J Biol Chem*, 276, 5256-64.
- YAN, C. & BOYD, D. D. 2007. Regulation of matrix metalloproteinase gene expression. *J Cell Physiol*, 211, 19-26.

- YANG, C. W., LEE, Y. Z., HSU, H. Y., WU, C. M., CHANG, H. Y., CHAO, Y. S. & LEE, S. J. 2013. c-Jun-mediated anticancer mechanisms of tylophorine. *Carcinogenesis*, 34, 1304-14.
- YANG, J. Y., ZONG, C. S., XIA, W., WEI, Y., ALI-SEYED, M., LI, Z., BROGLIO, K., BERRY, D. A. & HUNG, M. C. 2006. MDM2 promotes cell motility and invasiveness by regulating E-cadherin degradation. *Mol Cell Biol*, 26, 7269-82.
- YANG, S. C., CHANG, S. S. & CHEN, C. Y. 2011. Identifying HER2 inhibitors from natural products database. *PLoS One*, 6, e28793.
- YANG, Y., LUDWIG, R. L., JENSEN, J. P., PIERRE, S. A., MEDAGLIA, M. V., DAVYDOV, I. V., SAFIRAN, Y. J., OBEROI, P., KENTEN, J. H., PHILLIPS, A. C., WEISSMAN, A. M. & VOUSDEN, K. H. 2005. Small molecule inhibitors of HDM2 ubiquitin ligase activity stabilize and activate p53 in cells. *Cancer Cell*, 7, 547-59.
- YAO, V., BERKMAN, C. E., CHOI, J. K., O'KEEFE, D. S. & BACICH, D. J. 2010. Expression of prostate-specific membrane antigen (PSMA), increases cell folate uptake and proliferation and suggests a novel role for PSMA in the uptake of the non-polyglutamated folate, folic acid. *Prostate*, 70, 305-16.
- YARDEN, R. I. & PAPA, M. Z. 2006. BRCA1 at the crossroad of multiple cellular pathways: approaches for therapeutic interventions. *Mol Cancer Ther*, 5, 1396-404.
- YERUSHALMI, R., HAYES, M. M. & GELMON, K. A. 2009. Breast carcinoma--rare types: review of the literature. *Ann Oncol*, 20, 1763-70.
- YEUDALL, W. A., VAUGHAN, C. A., MIYAZAKI, H., RAMAMOORTHY, M., CHOI, M. Y., CHAPMAN, C. G., WANG, H., BLACK, E., BULYSHEVA, A. A., DEB, S. P., WINDLE, B. & DEB, S. 2012. Gain-of-function mutant p53 upregulates CXCL chemokines and enhances cell migration. *Carcinogenesis*, 33, 442-51.
- YU, Q., LI, Y., MU, K., LI, Z., MENG, Q., WU, X., WANG, Y. & LI, L. 2014. Amplification of Mdmx and overexpression of MDM2 contribute to mammary carcinogenesis by substituting for p53 mutations. *Diagn Pathol*, 9, 71.
- ZAGZAG, D., ZHONG, H., SCALZITTI, J. M., LAUGHNER, E., SIMONS, J. W. & SEMENZA, G. L. 2000. Expression of hypoxia-inducible factor 1alpha in brain tumors: association with angiogenesis, invasion, and progression. *Cancer*, 88, 2606-18.
- ZHANG, D. & BRODT, P. 2003. Type 1 insulin-like growth factor regulates MT1-MMP synthesis and tumor invasion via PI 3-kinase/Akt signaling. *Oncogene*, 22, 974-82.
- ZHANG, D. H., ZHANG, L. Y., LIU, D. J., YANG, F. & ZHAO, J. Z. 2014. Expression and significance of MMP9 and MDM2 in the oncogenesis of lung cancer in rats. *Asian Pac J Trop Med*, 7, 585-8.

- ZHANG, L., WANG, C. Y., YANG, R., SHI, J., FU, R., CHEN, L., KLOCKER, H. & ZHANG, J. 2008. Real-time quantitative RT-PCR assay of prostate-specific antigen and prostate-specific membrane antigen in peripheral blood for detection of prostate cancer micrometastasis. *Urol Oncol*, 26, 634-40.
- ZHANG, Y., GUO, Z., DU, T., CHEN, J., WANG, W., XU, K., LIN, T. & HUANG, H. 2013. Prostate specific membrane antigen (PSMA): a novel modulator of p38 for proliferation, migration, and survival in prostate cancer cells. *Prostate*, 73, 835-41.
- ZHANG, Y., KREGER, B. E., DORGAN, J. F., SPLANSKY, G. L., CUPPLES, L. A. & ELLISON, R. C. 1999. Alcohol consumption and risk of breast cancer: the Framingham Study revisited. *Am J Epidemiol*, 149, 93-101.
- ZHANG, Y., PU, X., SHI, M., CHEN, L., QIAN, L., SONG, Y., YUAN, G., ZHANG, H., YU, M., HU, M., SHEN, B. & GUO, N. 2007. c-Jun, a crucial molecule in metastasis of breast cancer and potential target for biotherapy. *Oncol Rep*, 18, 1207-12.
- ZHANG, Z., WANG, H., LI, M., AGRAWAL, S., CHEN, X. & ZHANG, R. 2004. MDM2 is a negative regulator of p21WAF1/CIP1, independent of p53. *J Biol Chem*, 279, 16000-6.
- ZHAO, Y., AGUILAR, A., BERNARD, D. & WANG, S. 2015. Small-molecule inhibitors of the MDM2-p53 protein-protein interaction (MDM2 Inhibitors) in clinical trials for cancer treatment. *J Med Chem*, 58, 1038-52.
- ZHAO, Y., DUAN, S., ZENG, X., LIU, C., DAVIES, N. M., LI, B. & FORREST, M. L. 2012. Prodrug strategy for PSMA-targeted delivery of TGX-221 to prostate cancer cells. *Mol Pharm*, 9, 1705-16.
- ZHOU, B. P., LIAO, Y., XIA, W., ZOU, Y., SPOHN, B. & HUNG, M. C. 2001. HER-2/neu induces p53 ubiquitination via Akt-mediated MDM2 phosphorylation. *Nat Cell Biol*, 3, 973-82.
- ZHOU, S., GU, L., HE, J., ZHANG, H. & ZHOU, M. 2011. MDM2 regulates vascular endothelial growth factor mRNA stabilization in hypoxia. *Mol Cell Biol*, 31, 4928-37.

Appendix

